CONDITION ASSESSMENT OF POLYETHYLENE PIPELINE SYSTEMS

A thesis submitted for the degree of Doctor of Philosophy

by

HAYDAR JAAFAR

Department of Materials Engineering, Brunel University

November 1997

ACKNOWLEDGMENTS

I would like to express my profound gratitude and thanks to Dr. G. F. Fernando for his supervision of this project. The continuous encouragement and guidance he showed throughout my Ph.D. programme in the Department of Materials Engineering are greatly appreciated.

I am very grateful to British Gas for their financial support of this project. I would also like to thank my industrial supervisors Dr. M. Greig and Mr. T. Hill for the many helpful discussions.

I would like to express my appreciation to Professor B. Ralph for his expert advise and encouragement throughout the period of this research.

It gives me great pleasure to acknowledge the departmental secretaries Margaret and Kathy for their co-operation in administrative matters. Special thanks go to the technical staff; Dr. S. Woodisse, Miss P. Robinson, Mr. D. Adams, Mr. G. Ragbir, Mr. P. Dodia, Mr. J. Felgate and Mr. K. Dutta for their technical support and easing the frustration caused by the equipment.

I would like to thank all my colleagues; Fahad, Haroon, Niaz, Peter, Rod, Anthony, Graham, Dave, Crispin, Tongyu and Keivan for their support.

Finally, I wish to thank my mother for her faithful prayers and many thanks to all members of my family; Neda, Zeki, Maha, Raad, Jaafar, Linda, Luma and Mohammed for the endless moral support and for being patient with me. I would like to dedicate this thesis to my family.

ABSTRACT

This study is an industrial project commissioned by British Gas plc. (UK) to investigate the state of in-service naturally aged polyethylene (PE) buried pipes and to define procedures or techniques available to facilitate the condition assessment programme of PE pipelines systems. The primary goal of this study was to establish a better understanding of the ageing process in commercial piping materials and to understand its effect on long term integrity of PE pipeline systems.

Eltex, Rigidex and Aldyl A are trade names of the PE gas grade resins used in this study and they represent the range of pipe materials used in the transport of potable water and gas in the UK. Sections of pipes used in this project were supplied by British Gas plc. in the form of unaged pipes and pipes which were aged in-service. Laboratory based accelerated ageing of the pipe resin samples was also carried out. The ageing regimes considered were water ageing at 23°C, air-oven ageing at 80°C, water ageing at 80°C, vacuum ageing at 80°C and in-service aged samples. Compression moulded plaques were produced as reference material.

By utilising specific instrumentation and designs, several reliable procedures were developed to produce specimens directly from pipes. The feasibility of using micro-samples instead of large samples was demonstrated. A methodology was developed to retrieve disk samples using electrofusion "tapping-tee" saddles. Appropriate test specimens were designed for chemical and physical evaluations. This sampling method negates the need for excavating large sections of pipe material for the purpose of condition assessment.

Reliable micro and macro-sampling test methods were developed and established as techniques for the condition assessment programme. Characterisation techniques included: (i) differential scanning calorimetry (DSC) to measure (from the same specimen) both the degree of crystallinity and the oxidation induction time (OIT), (ii) HPLC analysis was used to quantify additives concentrations, (iii) Fourier transform infrared spectroscopy was used to monitor the carbonyl index and to identify a pipe resin type from site, (iv) micro- and macro-tensile and fatigue tests to assess the changes in the mechanical properties as function of ageing. The fatigue test procedure was developed to produce brittle fracture at laboratory scale within a shorter period of time as compared to existing procedures such as the hydrostatic test.

A reference data-base was created using the above identified tools and the criteria and methodology for carrying out site condition assessment inspection was compiled. The fundamental mechanisms of chemical and physical ageing were studied along with the possibility of their effect on the mechanical properties of PE pipes.

ACKNOWLEDGMENTS

ABSTRACT

CONTENTS **PAGE**

CHAPTER ONE

CHAPTER ONE

INTRODUCTION

1.1. Background

The creation of national high pressure gas distribution grids and the conversion of customers from town gas to natural gas supplied by service pipes was a huge commercial success for the gas industries around the world [Stafford, 1994]. Another decision that has had an equally revolutionary impact on the market sector was the decision to utilise polymeric pipes for low pressure distribution systems. The use of thermoplastic pipeline systems has increased rapidly since they were first introduced in the 1950's. In the UK, about 80% of all mains and 90% of all services are made from polyethylene (PE) material [Greig, 1994]. Globally, more than 85% of all pipes installed for natural gas distribution are made of PE, and this percentage has been reported to be increasing annually [Mamoun, 1995]. PE has replaced metallic materials for gas distribution networks with operating pressures up to 4 bar [Trankner, 1997]. Ease of installation is one of the primary reasons for the switch from metal pipes as their fittings may be thermally fused together to form secure joints [Bjorklund, 1996]. In addition to this, PE material is relatively cheap, lightweight and flexible [Bowman, 1995]. Significant installation cost reduction can also be achieved by reducing the number of pipe joints making the pipes some hundred of meters long [ElLaithy, 1997]. PE pipes can be made with smoother interior surfaces than pipes of cast iron which reduces surface roughness. This allows greater flow rates at equivalent operating pressure because of the reduction of turbulence [Welker, 1996].

The production of a reliable PE gas pipe system has many requirements. The pipeline systems must be designed and constructed to address the limitations of pipe and

fittings in order to ensure acceptable long term performance. While the construction of new pipeline systems will continue to be important, major efforts will need to be taken in relation to the existing pipeline infrastructure. At present, there are no defined procedures or techniques available to facilitate a condition assessment of PE pipes [Jaafar and Fernando, 1995]. This is because once a pipe is buried, there are no means of determining its integrity and/or criteria to assess its residual properties as a function of service life. This can have implications to aspects of safety and economy; for example, should the pipeline or component in question be repaired, renovated, replaced, or abandoned. It is also possible that a particular pipeline system with a 50 year design life may well have residual life in excess of its design assumptions. Thus, it is important that specified procedures/techniques for a condition assessment for PE pipeline systems are developed now for areas of critical applications such as Gas, Water and Chemical Industries.

There is very little information in the public domain on the topic of condition assessment of PE pipeline systems. However, it is well documented that pressurised PE pipelines can, under severe conditions, fail by brittle slow crack growth (SCG) [Lustiger, 1995]. The SCG is the dominant mode of field failures for PE piping systems [Brown, 1994]. This failure generally occurs under long term and low stress level conditions [Bradley, 1995]. There are also very few published reports on the influence of the chemical and physical states of PE pipeline resins on both their short and long term performance. Furthermore, there are no micro-sampling techniques currently available to facilitate the condition assessment of PE pipelines. The term micro-sampling is used to describe a procedure whereby very small section samples are obtained and characterised via a number of mechanical, chemical, spectroscopic and

microscopic techniques. This means that whole sections of the pipeline in question will not need to be exhumed every time a condition assessment needs to be made. However, prior to arriving at this position, it is very important to establish that the micro-sample is indicative of the quality of the bulk material [Jaafar and Fernando, 1996].

1.2. Objectives

(i) To gain an understanding of the ageing characteristics of PE pipeline materials.

(ii) To develop micro and macro-sampling test methods to facilitate the condition assessment programme.

(iii) To create a reference data-base for the PE pipeline material.

These objectives will facilitate the criteria and methodology for carrying out sites condition assessment for buried PE pipeline systems.

1.3. Outline of Thesis

The thesis consist of eight chapters, including this chapter. Chapter two surveys the current literature which covers aspects of PE resins production, additive packages, the phenomena of ageing in PE material and the techniques that are available to detect the ageing process. In chapter three, a description of the material and the test specimens used is given along with details of experimental techniques and procedures which were used during the course of this study. The experimental results are presented and discussed in chapters four to seven. Issues relating to the oxidative stability of PE pipe resins are covered in chapter four. The degree of crystallinity data as a function of ageing and the concept of physical ageing are discussed in chapter five. Static mechanical properties which included micro- and

macro-tensile testing of specimens are dealt with in chapter six. Chapter seven reports on the fatigue and fracture behaviour of gas-grade PE resins. Finally, chapter eight presents the conclusions of this study and discusses suggestions for future work.

CHAPTER TWO

CHAPTER TWO

LITERATURE REVIEW

2.1. Introduction

The aim of this literature survey is to provide a summary of the current literature concerning the condition assessment and ageing of polyethylene (PE) pipe material.

The field of PE engineering and technology is broad, diverse and continuously evolving and the techniques which can be utilised to investigate the ageing characteristics of this material include chemical, physical and mechanical properties evaluation.

2.2. PE Resin Preparation

In general, PE resin is produced by four methods: (i) Phillips [Hogan, 1983], (ii) Ziegler-Natta [Kryzhanovskii and Pvanchev, 1990], (iii) Standard Oil [Saunders, 1988] and (iv) Union Carbide [Christison, 1977] processes. The first three involve solution or slurry methods and differ primarily in the nature of the catalyst used. The fourth process involves a gas phase. All of these processes are exothermic in nature and require careful control of the temperature and pressure.

The production of PE resins usually involves the use of a comonomer [Platzer, 1983]. The comonomer is incorporated into the PE as short chain branches as shown in Figure 2.1. Their incorporation into the main chain and the frequency of insertion was demonstrated by means of Carbon-13 Nuclear Magnetic Resonance (NMR) [Maddams and Parker, 1989]. These branches can affect the microstructure and the crystallisation behaviour and the ultimate morphology of the copolymer [Sehanobish et al., 1994]. In terms of chain configuration, short chain branching is an irregularity imposed on the linear PE

chain. Although its frequency is small, 2-5 branch/per main chain carbon atom, these branches act partly to reduce crystallinity by limiting the extent of crystallisation. Consequently, this can lead to changes in many physical properties, such as density [Brady and Thomas, 1988], hardness [Egan and Delatycki, 1995], permeability [Dimov and Islam, 1990] and environmental stress cracking resistance [Bubeck and Baker, 1982].

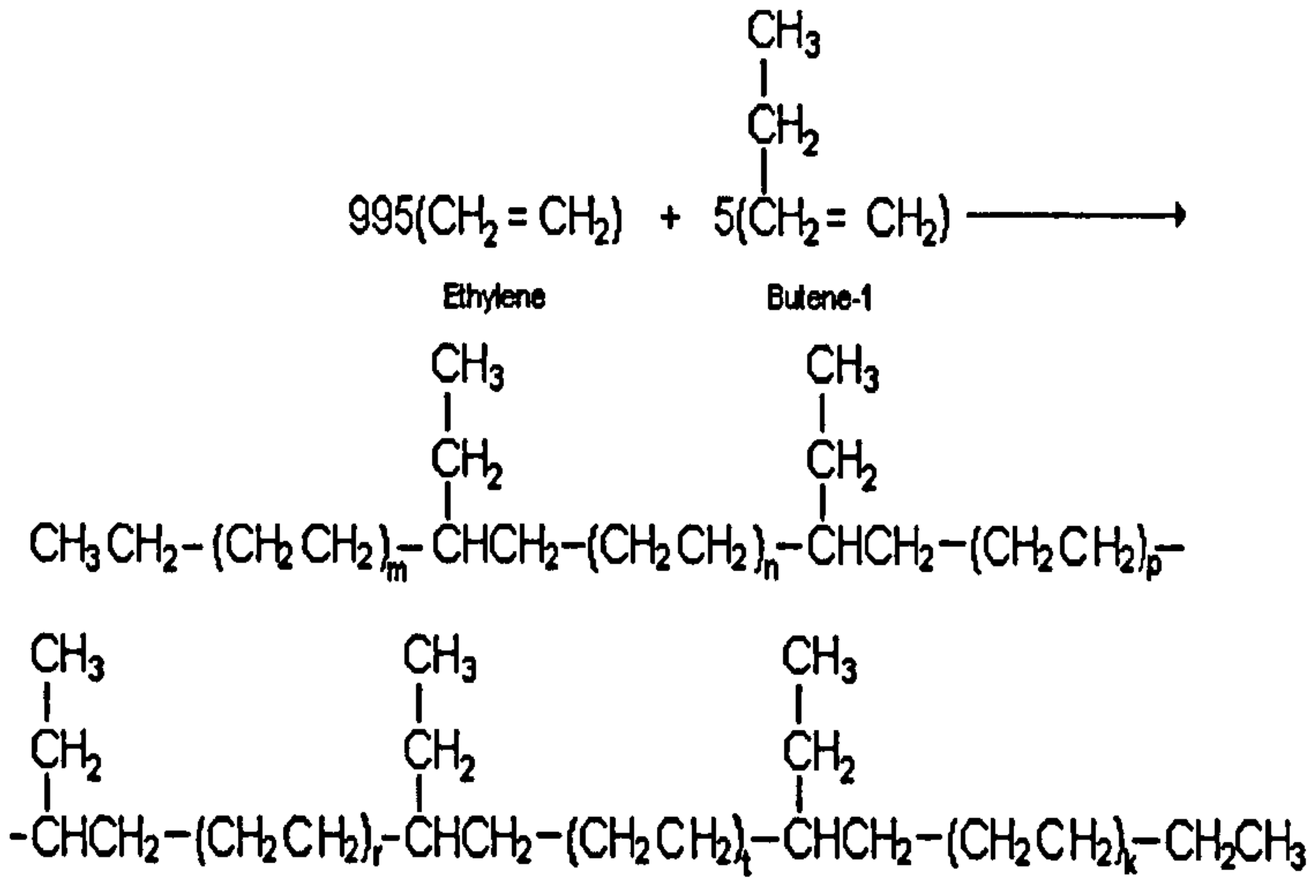

Figure 2.1. Schematic illustration of polymerisation reaction for ethylene/butene copolymer reaction (m+n+p+r+t+k=995).

2.3. Additives for PE

A stabilised PE resin is a multicomponent system which includes mixtures of different additives. The additives are used to provide protection against the influence of light, heat and ageing [Chirinos-Padron et al., 1987]. The level of additives addition is usually 0.01% to 1% weight percent [Han et al., 1987; Malik, 1995].

PE pipe resins are supplied to the extruders as compounded pellets which contain the following additives [Cowie, 1973]:

(i) lubricants to aid in the processing of PE;
(ii) antistatic agents to decrease surface electric resistivity;

(iii) pigments (yellow for gas pipes);
(iv) antioxidants and stabilisers to minimise degradation while fabrication, storage and jointing; and
(v) UV stabilisers to reduce the rate of photo-oxidation.

The effectiveness and durability of the additives in PE resins are influenced by several factors: (i) intrinsic additive behaviour which is determined primarily by the physical structure of the polymer [Ranby and Rabek, 1975]; (ii) the chemical structure of the additive which affects its compatibility with the polymer [Gedde, 1981]; and (iii) permanence of the additive in the polymer [Malik, 1992].

2.3.1. Distribution of Additives

According to Frank [1977], the distribution of additives is uniform in amorphous polymers and is said to form a micro-heterogeneous phase which is dispersed uniformly according to its compatibility with the polymer. Scheirs et al. [1991], used a staining technique to detect localised oxidation. They found that in semi-crystalline polymers, the distribution of additives was not completely uniform owing to the presence of crystalline and amorphous phases in PE. They argued that the additives were rejected from the growing crystallites during cooling and accumulated in the amorphous region. Although no direct evidence was provided it may be possible to explore this hypothesis by using a technique which was recently reported by Mackay et al. [deVries, 1994]. They determined the spatial distribution of additives using a time-of-flight secondary ion mass spectroscopy. The results of the study directly indicated that the distribution of additives in semi-crystalline polymers was heterogeneous.

The plastic processing industry is well aware that the quality of plastic products is related to the pattern of distribution of additives but, at the same time also

accepted that a homogenous distribution of additives in the final product may not be the optimum desired distribution [Hall et al., 1978].

2.3.2. Compatibility of Additives

Compatibility of the additives is subject to their degrees of solubility in the polymer whether an additive is in a solid or molten sate [Grassie and Scott, 1985]. But more importantly, an additive could be totally dissolved in the polymer at the processing temperature but is only partially soluble at ambient temperatures. This may lead to 'blooming' of the additive with time on to the polymer surface [Sugiura et al., 1996]. An additive also could 'bleed' into an adjacent medium if the additive has a degree of solubility in the polymer into which it is incorporated as well as the adjacent medium [Munteanu et al., 1981]. For example, bleeding can be in the form of leaching out of an additive from a PE pipe to the surrounding water due to its solubility in the water [Calvert and Billingham, 1979]. This plays a part wherever the PE pipes come into contact with water especially in the surface layers which are the most sensitive to degradation during ageing [Allen et al., 1990].

2.3.3. Volatility of Additives

Luston et al. [1993] reported that the volatility of an additive from polypropylene was governed by evaporation from the surface. The evaporation process was investigated by means of Thermogravimetric analysis (TGA) at different isothermal temperatures and additive concentrations. Hayashi et al. [Hayashi, 1993] also studied the vaporisation behaviour of an antioxidant at elevated temperatures under the stream of air and nitrogen for 3000 min using Gas Chromatography (GC). They found a similar trend for the experments carried out in air and nitrogen. The percentage recoveries of the antioxidant loss increased linearly up to a certain

temperature and the relationship deviated above this temperature. They related this behaviour to the melting point of the additive and explained how above this temperature the volatility behaviour was influenced by the additive change of phase. However, in both studies the possibility of additives decomposition was not taken into account. Shlyapnikov et al. [1992] used GC-Mass Spectrometer at moderate and high temperatures. They noticed that when the latter conditions were introduced it resulted in additives decomposition. They concluded that when designing high temperature antioxidants for the use in polymers at elevated temperatures, both vaporisation and decomposition processes should be taken into consideration.

2.3.4. Diffusion of Additives

Many important ageing processes such as oxidation, hydrolysis and ozonolysis involve a reaction of the polymer with O_2, H_2O, O_3 [Audouin, 1994]. In many cases, these reactions take place at the outer surfaces causing severe degradation [Moller, 1994]. Hence, an important factor associated with use of additives to protect the polymers is their ability to migrate to these regions where they are most needed. The migration of an additive within a polymer can be influenced by the compatibility of the additive with the polymer [Malaika, 1991]. Several studies have been performed concerning the loss of additives due to diffusion [Norman, 1990; Foldes, 1993]. Detailed mathematical models have been developed for antioxidant loss from thin films in connection with food packaging materials [Gandek, 1989], power cables [McMahon, 1981] and from hot-water pipes [Viebke, 1996]. These models predicted the concentration of antioxidants that were leached into various extractants. However, few of these studies [Billinham, 1980; Gedde, 1992; Gugumus, 1994] determined the additive concentration profiles in the specimens. They were only useful in certain cases like thin films. They were also of limited use for the

determination of actual concentration profiles of more than one additive type. Furthermore, the consumption rates differ in different ageing environments which was not taken into consideration nor are these models applicable to cases with non-symmetrical boundary conditions for example, crystallinity gradients which exist in PE pipe materials.

2.4. Ageing of Polyethylene

There are two processes which could lead a PE material to age, either by a chemical or a physical process. Both processes changes the initial design status of a PE material and, therefore, could impair the useful mechanical properties [Alferink, 1991].

There are a number of ways that could bring about chemical changes. For example, oxidation, cross-linking and chain scission of PE material could take place as a result of production, storage and use of pipes [Broutman, 1986]. Manifestations of these reactions are changes in the chemical structure of the PE materials.

Physical ageing of PE materials was first reported in the literature by Struik [Struik, 1987]. He described that changes in a property of a semi-crystalline polymer as a function of ageing at constant temperature, zero stresses and under no influence from any other external conditions is a result of a physical ageing phenomenon.

2.4.1. Chemical Ageing

A major drawback associated with PE is its susceptibility to oxidative degradation. Once the antioxidant system has been depleted, the PE will deteriorate through a complex sequence of chemical reactions [Bharel, 1992], oxidation becomes autocatalytic [Moison, 1985], and the materials' lifetime is severely reduced [Maddams, 1989]. Usually, there are significant changes in the basic chemical structure of the polymer [Fisch, 1991] such as cross-

linking, chain scission and formation of functional groups e.g., unsaturation, hydroxyl, carbonyl and hydroperoxides. These chemical reactions may be brought about by: (i) the reaction of atmospheric oxygen which attacks the basic structure causing oxidation [Allen et al., 1988], (ii) biological organisms which produce corrosive chemical substance [Weiland et al., 1995] (this type of chemical ageing was not included in this study) and (iii) on exposure to sunlight (UV light) resulting in photo-oxidation [Tidjani and Arnaud, 1993] but, buried PE pipes are not expected to suffer from photo-oxidation after being laid under ground in-service.

Atmospheric oxidation at ambient temperatures away from sun light is of great interest in this study but, there is very little information published in the literature concerning this matter. In contrast, there are many published reports that deal with thermal oxidation of PE material [Gedde et al., 1981; Mathot and Pijpers, 1983; Allen et al., 1990; Scheirs, 1991; Weiland et al., 1995; Ahlstrand, 1995] which are considered more relevant to the manufacturing process of PE pipes.

Thermal oxidation of PE was assumed by Allen et al. [1990] to produce a carbon-centred polymer radical (P•) which undergoes a fast reaction with oxygen. Both cross-linking and chain scission are possible paths as shown in Figure 2.2. The resulting alkylperoxy radicals (POO•) in the second path consume hydrogen atoms from the polymer backbone to form hydroperoxides (POOH). This leads to the production of further radicals via decomposition of the hydroperoxides. This in turn can trigger various types of detrimental reactions in the polymer chain. The hydroperoxides are usually considered to be the key intermediate in the oxidation of PE initiated thermally and photo-chemically [Gugumus, 1995].

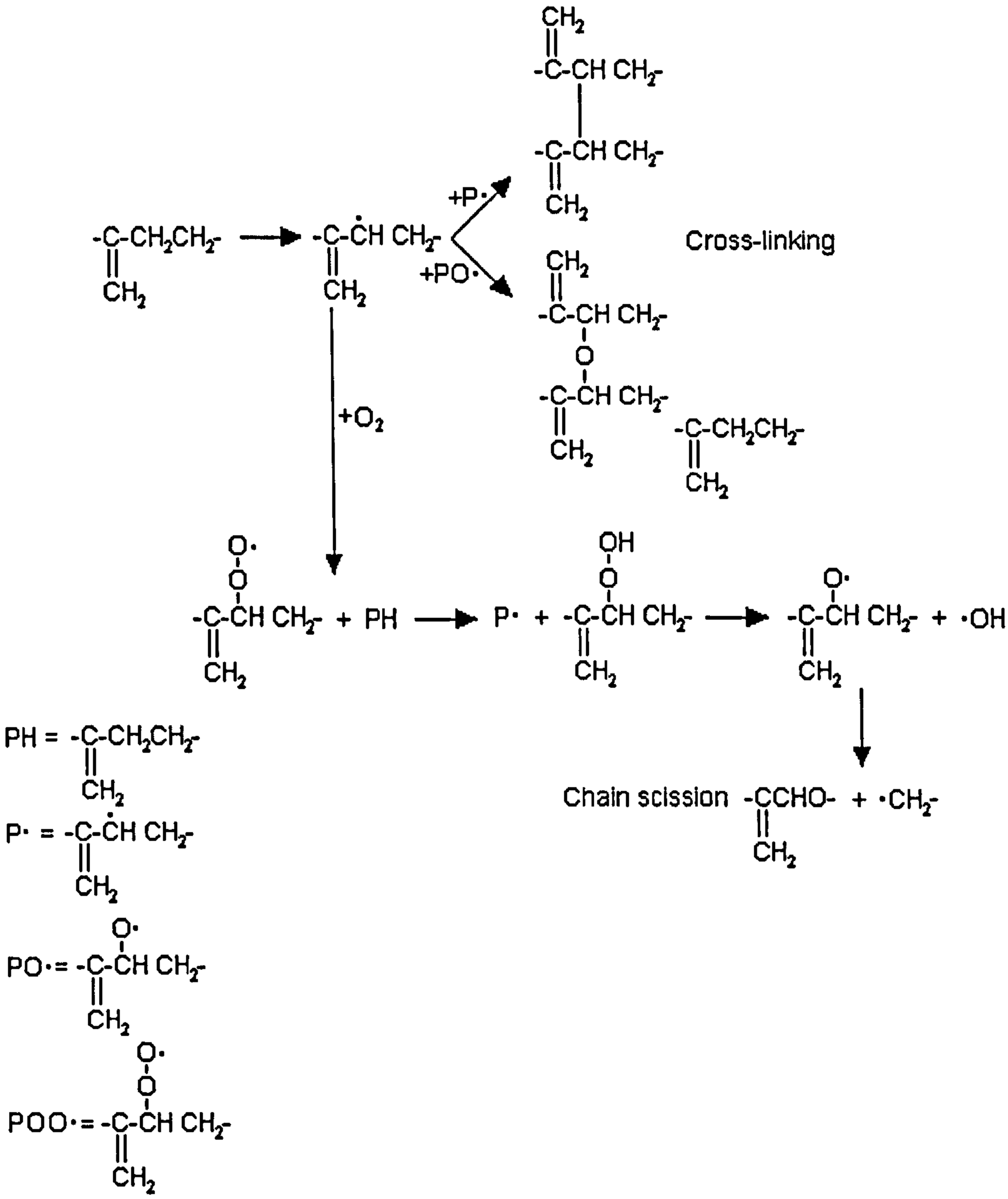

Figure 2.2. Possible PE thermal oxidation mechanisms proposed by Allen et al. [1990].

The actual compounds used as antioxidants can take part in all steps of the oxidation reaction to prevent degradation [Tatarenko, 1992]. For a particular antioxidant, its effectiveness is dependent on a number of factors mentioned earlier. Its concentration in the host polymer could decrease during long-term use [Gugumus, 1994]. Concentration changes could be as a consequence of two processes: (i) chemical reactions of the antioxidant, and (ii) physical loss of the

stabilisers from polymers. Both these processes can eventually lead to changes in the chemical structure of PE pipe material and, therefore, they are considered factors which can contribute towards chemical ageing.

2.4.2. Physical Ageing

The term "physical" is included in order to distinguish this phenomenon from chemical ageing. Chemical changes in PE material structure are irreversible changes. In contrast, physical ageing involves only reversible changes in the material structure and, thus, in its properties. This distinction is fundamental in the understanding of the phenomenon.

The most common situation in which physical ageing is observed is when an amorphous polymer is cooled from above to below its glass transition temperature, Tg, the ageing is then manifest as, for example, a reduction in the specific volume and an apparent shift of the creep response to longer times [Hendra et al., 1991]. Struik [Struik, 1987(a)] suggested that the driving force for the changes in properties arise as a result of the non-equilibrium state of the material. Semi-crystalline polymers contain an amorphous phase, therefore, physical ageing is not confined to only amorphous polymers. One of the first reports of the effects of physical ageing on the properties of semi-crystalline polymers was the study by Yue and Msuysa [1990] of polypropylene films. They reported on an increase in the modulus and a decrease in impact strength with increasing ageing time at a temperature above room temperature. The important aspect of this was that the physical ageing phenomenon occurred at a temperature above the glass transition temperature of polypropylene. It was expected that the amorphous phase would be in equilibrium at temperatures above room temperature. This finding led Struik to justify these results in terms of an "extending glass transition temperature" in semi-crystalline polymers. They argued

that the constrained amorphous regions located in the interfacial interlamellar regions of the spherulites have a higher Tg than the unconstrained amorphous regions. The unconstrained amorphous regions are relatively distant from the crystalline lamellae. Therefore, there will be a range of Tgs extending above the normal Tg of the semi-crystalline polymer. Thus, physical ageing should be anticipated at temperatures above the conventional Tg as structural rearrangement and reduction in free volume occur in these constrained amorphous regions.

Prior to Struik's work on semi-crystalline polymers, Vile and co-workers [1984] suggested that the side branches in PE became squeezed together along the backbone chain as a function of ageing. Most of these branches were said to be concentrated at the edges of the amorphous regions and in the interfacial zones. Their model for the incorporation of branches into the PE crystallite is given in Figure 2.3.

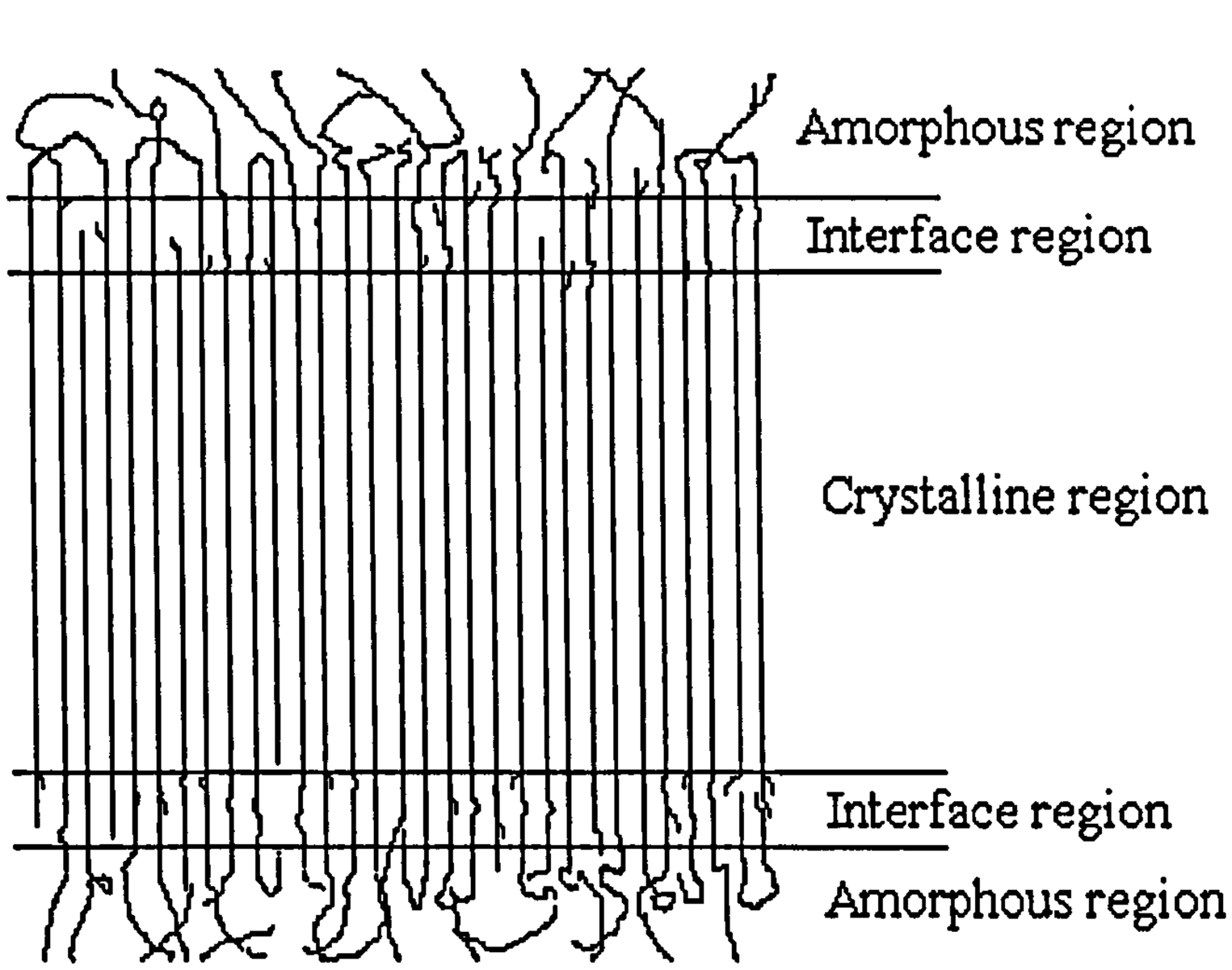

Figure 2.3. Vile's model showing some order at the amorphous-crystalline interface [Vile et al., 1984].

Phillips et al. [1989] observed similar behaviour and explained that this rearrangement arose largely from

differences in the perfection of crystals or in the character of the amorphous phase in the vicinity of the crystal. It is reasonable to suggest that a small increase in the ordering occurring in the very diffuse interfacial phase could result in the effective length of the highly ordered crystalline phase extending into the more disordered interfacial zone as in Figure 2.3. The consequence of this would be expected to be a slight increase in the density which can lead to changes in the physical properties of the material [Msuya and Yue, 1989]. Grzybowski et al. [1986] described the increase in the density of the crystalline region would also increase the separation of spherulites. This type of structural change associated with the physical ageing of PE can have a marked effect on the mechanical properties [Read et al., 1990] and the long term performance of PE pipes as a function of ageing.

2.5. Detection Of Ageing In PE Pipes

A number of techniques can be used as tools to determine the extent of ageing in PE pipe materials for the condition assessment programme.

2.5.1. Differential Scanning Calorimetry (DSC)

For many years the DSC technique between used in the thermal analysis of polymers. One primary use of this technique for PE pipes is to determine the oxidation induction time (OIT). OIT is the time, in minutes, from the start of oxygen purge to the onset of oxidation at a constant temperature [Ahlstrand, 1995]. The simplicity of the test method, makes it attractive as a tool to study thermo-oxidative degradation in polymers. The DSC technique is also used for the determination of enthalpy of melting and crystallisation in polymers [Mandelkern, 1986].

OIT:

In recent years many researchers have used the OIT test as a tool to assess the deterioration of additive concentrations in polymers. For example, the OIT test was used to diagnose aged high voltage polymeric cable [Bulinski et al., 1995], it was used to characterise irradiated polymers for medical applications [Woo et al., 1991] and to estimate the depletion of additives in hot water polymer pipes [Groff et al., 1996]. The measured OIT value for a polymer is a representation of the effective resistance of the material to thermal oxidation measured in the molten state.

Gebler [1989] carried out a set of OIT experiments on PE pipe material. Two experimental pipe resin system compounds were made, one containing 0.05% of (A) undeclared antioxidant, and the other 0.05% of (B) undeclared antioxidant. Pipes extruded from these materials were stored in water at 80°C and the OIT measured on 1 mm layers taken from bore of the pipes after various times up to 5000 hours. The initial values of OIT showed that for the same concentration of antioxidant, the OIT differed by a factor of about two. However, antioxidant (A) was shown to migrate substantially faster than antioxidant (B). Therefore, after 1000 hours storage in water at 80°C, the OITs were approximately the same. He concluded that the OIT of a PE compound depends on a number of factors including the following; the quantity of stabiliser present, the structure of the antioxidant and the solubility of the antioxidants in the polymer. He concluded that the OIT test can not permit conclusions to be drawn about the long term stabilisation performance of pipes at typical service temperatures but, it can be used as an index of quality.

Most of the reported studies using the OIT test on additive combinations were done by the so-called one

variable at a time experimental strategy, which means that only one studied parameter is changed while the remaining parameters are kept constant for a given set of experiments. For example, varying the total concentration, or varying the ratios of the additives at constant level of their total concentration, or varying only test temperatures. This experimental strategy certainly provides valuable information, but it does not allow a more precise description of the whole complexity of polymers stabilisation process. Perhaps one of the most interesting studies reported in the literature on antioxidant performance in PE using an OIT test was carried out by Boast and Latoszynski [1985]. They compared the OIT results with high performance liquid chromatography (HPLC), to examine the long term effectiveness of a non-migratory antioxidant both in the presence and absence of a metal deactivator. The interchangeability of information from both analytical techniques assisted in the understanding of the antioxidant behaviour as a function of ageing.

Enthalpy of Melting:

Pages et al. [1996] used DSC to measure the crystallinity of weathered PE sheets. The degree of crystallinity (C) was calculated from the heat of melting (ΔH_m) traces as follows:

$$C=(\Delta H_m) \ /(\Delta H_{mo}) \qquad (2.1)$$

where (ΔH_{mo}) is the heat of melting of a 100% crystalline PE which is equal to 293 J/gm [Mathot and Pijpers M, 1983]. They reported loss in the degree of crystallinity due to photodegradation. There was no attempt to explain how the photodegradation process resulted in more than one melting peak in their results. Monserrat et al. [1995] observed the same behaviour when working on annealed poly(ethylene terephthalate). They found that by increasing the annealing temperature one peak became more

prominent and the overall crystallinity increased. In another study carried out by Sebaa et al. [1992], thermal and UV ageing was investigated separately on two commercial PEs. Their observations focused on the shape of the DSC traces. They found that more information could be obtained by studying the DSC traces. They realised that the shape and size of the melting peak varied significantly with thermal ageing and sometimes resulting in a doublet. They also noticed that this behaviour was not observed for the photodegraded samples and the melting point remained steady. For all exposed samples, in both the ageing regimes, the mechanical properties changed drastically. They attempted to determine whether oxidation contributed to these changes using infrared spectroscopy. This confirmed that the UV aged samples suffered from severe oxidation but, the thermal ageing induced very little oxidation. They concluded that in the latter case rearrangement of molecular chains occurred while annealing which led to the changes observed in the materials physical properties.

2.5.2. Infrared (IR) Spectroscopy

The value of IR spectroscopy for characterising the carbonyl compounds formed during oxidation processes in PE has been known for 40 years. The work of Rugg, Smith, and Bacon [1954] showed that the broad carbonyl stretching band present in the spectrum of thermally and photochemically oxidised samples consists of three overlapping components. They were assigned as saturated aldehydes (1733 cm^{-1}), ketones (1721 cm^{-1}) and acids (1712 cm^{-1}) [Maddams and Parker, 1989]. According to Gugumus [1995], hydroperoxides are also present in the degradation process but, they are generally believed to be intermediate and their decomposition is very rapid and can not be monitored. Gedde et al. [1981] suggested that the ketonic carbonyl absorbtion peak is the most prominent of the board carbonyl band and it can be used to follow oxidative degradation as it formation is fairly

constant. Similar results have been reported by Terselius et al. [1982]. They studied the carbonyl index of extruded PE pipes which were thermally oxidised. They noted that the carbonyl index was seen to increase in the non-spherulitic region of the inner surfaces of pipes and was observed to fall rapidly away from the pipe surfaces. They concluded that the carbonyl concentration gradient indicated a diffusion-related oxidation process within the amorphous region.

The use of, for example, the methylene rocking band 1460 cm^{-1} as an internal standard in the carbonyl index determination has the advantage that the uncertainty in the thickness determination does not affect the carbonyl index determination significantly [Allen et al., 1990]. This method is simply ratio the absorbance of the band to be monitored with respect to one which remains unchanged during the ageing process. In this study the internal standard peak used was a combination of a Raman active twisting mode and an IR active rocking mode at 2020 cm^{-1} representing both crystalline and amorphous phases [Wedgewood and Seferis, 1983].

2.5.3. Standard Tensile Testing

PE is one of the most widely studied polymers and yet the relationships between molecular and morphological structures and the mechanical behaviour are just beginning to be understood. In a simple tensile experiment the use of a high loading for a short period of time will prompt PE structure, spherulites, to stretch in the loading direction as illustrated in Figure 2.4.

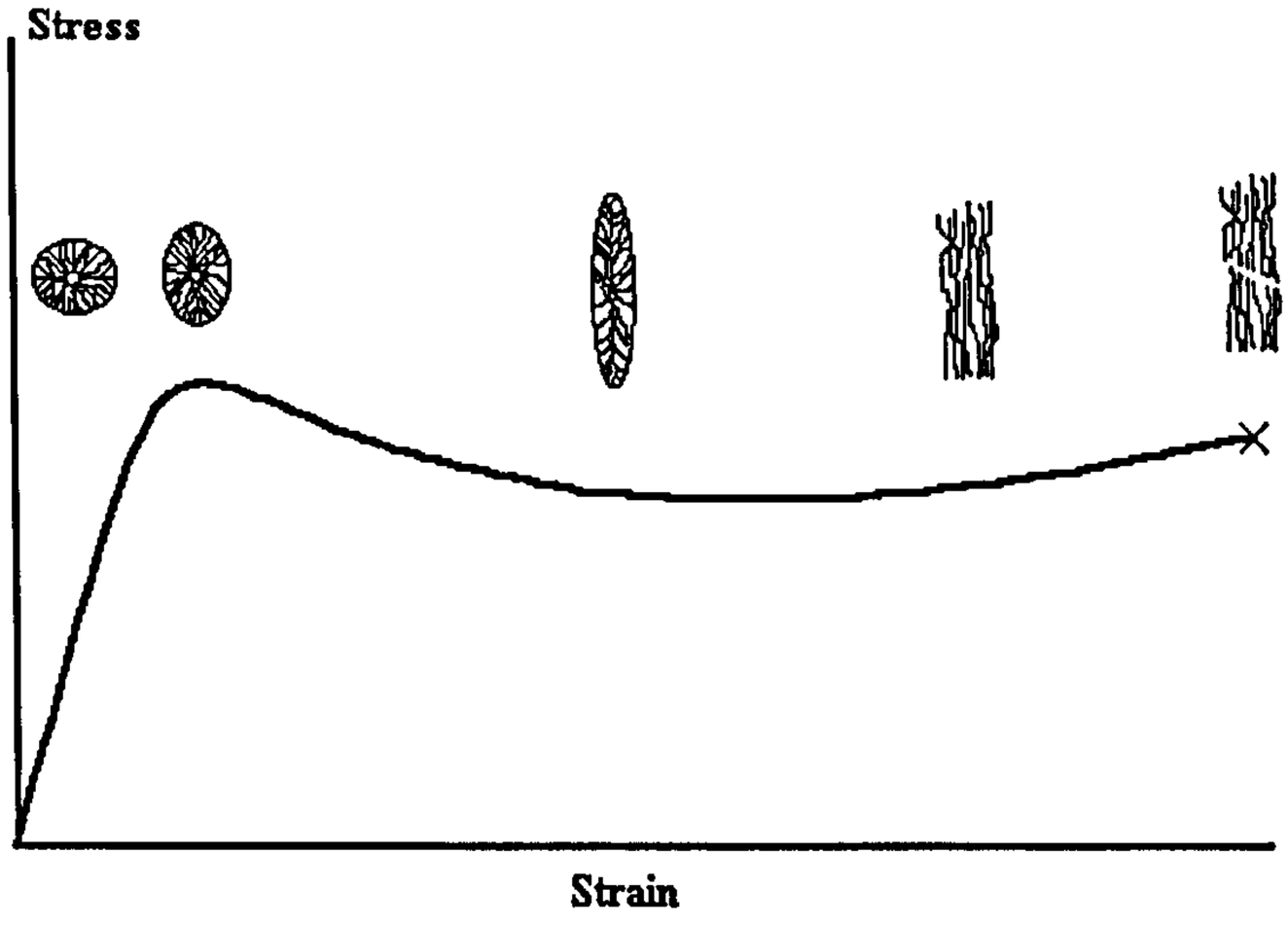

Figure 2.4. A typical stress-strain curve showing spherulitic distortion causing specimen failure after excessive elongation [Young, 1989].

The spherulites begin to distort upon further extension and the molecules slide past each other resulting in dislocations. With further extension, the crystals break and the stretched molecules (fibrils) will align. The ultimate tensile load, specimen failure, is a result of fibrils slipping past each other.

Prasad and Grubb [1989] reported that chains that inter-link the lamellae structure, tie molecules, reach their maximum extension at low loading over a prolonged period of time, resulting in the breaking-up of the lamellae structure into smaller units, consequently to result in a brittle failure of PE. Further extension will result in the spherulites breakage into fibre-like and at maximum extension extensive pull out will result in specimen failure. The low loading type of failure differs significantly when compared to the previously discussed high-loading fracture case.

Brown et al. [1983] examined the tensile properties of PE pipe materials and compared the behaviour of various other types of PE over a wide range of temperatures. The

samples of PE varied in molecular structure, molecular weight and morphology. Their results showed that the strength and stiffness of flexible chain semi-crystalline polymers was related to the degree of crystallinity of the material. They argued that the amorphous phase of flexible chain polymers is rubbery or leathery at room temperature, so they proposed that it was logical that the Young's modulus and yield stress be directly associated with the volume fraction of the hard crystalline phase. The evidence presented by Brooks et al. [1992] showed that for a semi-crystalline polymer like PE, the mechanical properties become less defined as the testing temperature was increased. This implied that even the crystalline portion is affected by the test temperature.

As discussed earlier, when PE is exposed to heat and UV light structural changes can occur. The direct consequences of these changes is the dramatic deterioration of mechanical properties [Lassiaz et al., 1994]. It was believed [Battiste et al., 1981] that the loss of mechanical properties can be easily assessed by the build-up of carbonyl groups by monitoring through IR spectroscopy. Torikai et al. [1986] indicated that the change in mechanical properties can be estimated by the modifications in the chemical structure during the accelerated photodegradation of PE. They found a relationship between the development of carbonyl group and the changes of elongation and strength at break. In contrast to this approach, Tincer et al. [1981] reported that no simple correlation exists between the build-up of carbonyl species and the change of mechanical properties such as stress or strain at break or elastic modulus under natural weathering of LDPE. Severini et al. [1986] investigated the environmental degradation of stabilised LDPE. They mentioned in their study that the decay of the mechanical properties could not be related to the variation in concentration of vinyl species and in

crystallinity. Qayyum et al. [1993] suggested that UV ageing could result in chain scission and breakage of tie molecules which in turn could cause disentanglements in the amorphous phase releasing molecular fragments for crystallisation. This would cause densification and ultimately changes to the material physical properties. Tidjani et al. [1993] wisely suggested that the prediction of weathering resistance of polymers can be based on both mechanical changes and modifications in chemical structure to minimise erroneous prediction.

2.5.4. Residual Stresses

The effect of residual stresses on the performance of pipes have been an area of concern [Bhatnager and Broutman, 1990]. PE pipe is manufactured by extrusion and is commonly quenched with water on the exterior surface in order to be collected onto a roller while the interior surface is left to cool slowly from heat loss through the wall. Since the thermal conductivity of PE is very low approximately 0.25 W/s m °C [Kline and Hansen, 1970] and if the wall thickness is about 0.017 metre, then the cooling rate for the interior surface is relatively slow. The exterior surface solidifies while the inner region is still in a molten state, when the interior finally cools sufficiently to crystallise it will shrink tending to exert a hoop-like compressive stress through the pipe's thickness [Choi and Broutman, 1983]. Different cooling rates on the inner and outer surfaces of the pipe wall create a gradient of morphology which result in residual stresses [Hodgkinson and Williams, 1983]. Investigations by Bratnagar et al. [1985] showed the presence of residual stresses in longitudinal and circumferential directions. Generally, compressive axial and circumferential components exist in the outer layers of the pipe wall. However, tensile components dominate towards the bore. They deduced these stresses by shaving thin films from different locations from PE pipes and observed the direction they curl. The presence of these

stresses is directly related to the microstructure within the pipe wall. Consequently, the resistance of a PE material towards crack propagation and, thus, its service lifetime will be affected by the state of these stresses and the morphology across the pipe wall [Chaoui et al., 1987]. However, no interpretation nor links were established in the literature on how these two major stress elements can change the pipe properties with ageing.

2.5.5. Hydrostatic Pressure Testing

Life prediction of PE pipe for gas distribution is generally based on the hydrostatic pressure test. A pipe is pressurised with water and the failure time is measured as a function of internal pressure. Because of the viscoelastic character of PE, the failure of this material is time-temperature dependent. Failures in PE pipes can be traced to either creep or slow crack growth [Popelar et al., 1991]. ASTM D 2837 [1988] describes a method for conducting hydrostatic pressure testing of pipes. The procedure estimates the 50 year hydrostatic strength by extrapolating stress rupture data gathered over a period of at least 10,000 hours. The standard permits estimates to be made for the long-term strength at a specific temperature provided that data have been established for temperatures above and below this temperature; i.e., while interpolation is permitted, extrapolation is not. With reference to Figure 2.5, the hydrostatic test shows a knee in the curve. Generally, the shallow sloped region of the curve is characterised by ductile type failure, and corresponds to high stress levels and short failure times. The dotted sloped region of the creep rupture curve corresponds to lower stress levels and longer failure times and where a brittle-type failure is predominant. The point where the slope changes, the knee, can be characterised as a type of ductile-brittle transition.

Extensive research has been reported on creep testing of PE pipes. Earlier work by Takayangi et al. [1967] on HDPE has shown that both rotational and transitional motion of chains are contained within a relaxation (the knee), and it is shown from Takayangi and co-workers work that this relaxation is due mainly to the crystalline portion of the polymer. The molecular changes occurring at the transition are thought, in Takayangi and co-workers results, to be relevant to the slow crack growth process. A theoretical treatment of this transition requires knowledge of its molecular origin.

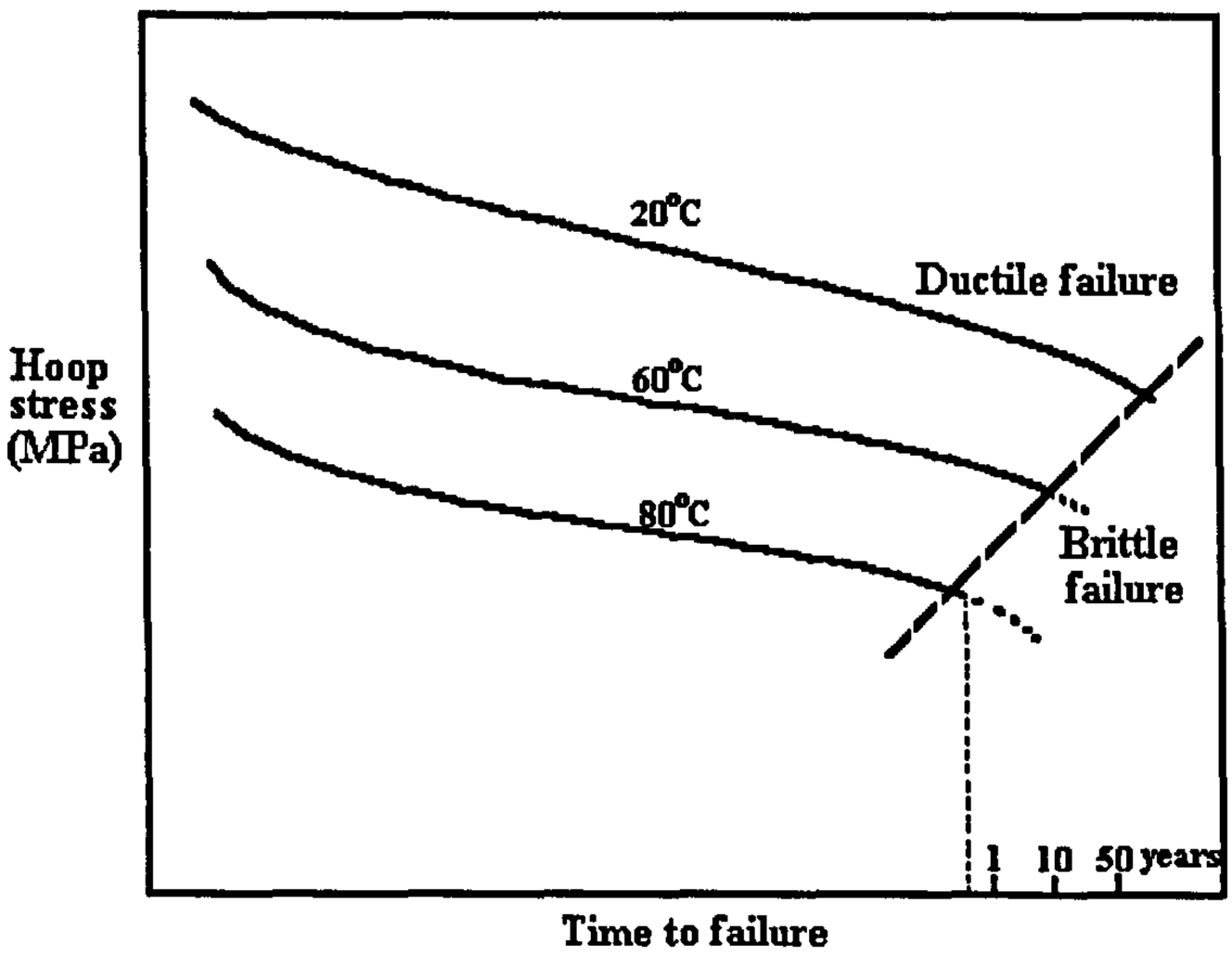

Figure 2.5. Schematic illustration of creep-failure time curves for Rigidex MDPE at 20, 60 and 80°C [Rigidex product data].

The earlier work on PE pipe used this transition to rank pipe material and predict long term behaviour. For instance, Gebler [1989] reported on the long-term behaviour and ageing of HDPE pipes. The author explained that the position of the flat section in the curve is said to be determined largely by the density and the corresponding yield stress of the polymer. He also found that selective copolymerisation shifted the whole curve upwards. He stated that the knee region in the creep curve could be shifted to shorter or longer times by changes in the molecular weight and with proper

processing and degree of stabilisation.

The application of linear elastic fracture mechanics to glassy polymers, such as poly(methyl methacrylate) and polystyrene, is now well established [Williams et al., 1987]. The linear elastic fracture toughness of PE was investigated by Williams et al. [1987] in particular the dependence on specimen thickness and width, crack length, mode of loading and temperature. They argued that there are limitation in applying the concept of linear elastic fracture mechanics to HDPE and recommend that the tests should be carried out at low temperatures. Another experimental investigation was carried out by Bragaw [1979] to study slow crack growth in notched MDPE specimens. He found that the crack speed was multivalued and discontinuous as a function of the stress intensity factor. In both studies they concluded that linear fracture mechanics is an invalid concept for the design of the non-linear PE material used in piping systems.

Popelar et al. [1991] developed a method from stress relaxation tests and demonstrated that short term tests could be achieved by the use of appropriate shift functions. Brown [1992] has also developed a short term quality control test called the "PENT" test, based on creep rupture test, to predict the performance of a gas pipe system. He declared that if the lifetime in the PENT test is at least 150 hours then the gas piping systems can be expected to have practically no slow crack growth failures before 100 years. The interesting observation in this work was the detection of a critical stress which produced the same type of brittle fracture as those observed on in-service failures.

Clearly, a considerable effort in terms of time, labour, etc. could be saved in developing and design parameters if the failure process could be accelerated. Furthermore, if the accelerated data in turn could be used to infer

the life time of pipes under typical operating conditions then it will provide a reliable means for the condition assessment programme of pipeline systems. Because of the nature of the hydrostatic pipe testing, it is difficult to observe the early stages of brittle fracture [Barker et al., 1983] within a short period of time. Adding to all of this the test standard states that "results obtained at one temperature can not, with any certainty, be used to estimate values for other temperatures".

2.5.6. Fatigue Testing

Natural gas distribution pipes are subjected to a variety of stresses during their lifetime. These stresses vary in intensity and frequency and may be caused by installation procedures, rock impingement, or simply by the internal gas pressure [Alferink and Wolters, 1991]. Most field failures of plastics pipe which have been reported in the public domain have been attributed to the propagation of brittle cracks through the material starting at rock impingement sites, gouges, scratches, inherent material flaws, etc. [Lustiger, 1983]. Resistance to brittle fracture, therefore, can be expected to be the determining factor in establishing the lifetime of installed plastic pipes [Mruk, 1985]. The extrapolation of failure data obtained under typical hydrostatic pressure testing (ASTM D 2837), generally provides conservative results [Kanninen et al., 1990; Kadota et al., 1991] and require long time (years) to generate a brittle fracture [Chan and Williams, 1981]. Therefore, accelerated tests are desirable to assist in making rapid decisions. This has motivated the development of accelerated tests that attempt to reproduce the observed slow crack growth failure morphology in a much shorter time than would occur in service. This may be achieved through the use of "fatigue" cyclic loading [Greig, 1988; Kurian et al., 1989; Lawrence and Sumner, 1989; Kasakevich et al., 1990; Kadota et al., 1993]. A round robin study [Brown, 1992] established a strong comparison

between fatigue testing and the constant load test. The latter can be expected to give a reasonable measure of resistance to failure in the field and hence provides a baseline for comparison of laboratory results and field experience. The former is of considerable practical interest since a fatigue test can be as much as two orders of magnitude faster than constant load tests.

Many variables can affect the fatigue crack propagation resistance of a polymer. For example, it was found that introducing a compressive component in the fatigue cycle accelerated fatigue failure [Strebel and Moet, 1991]. High level of stresses cause earlier and more ductile failures than do lower stresses [Barry and Delatycki, 1989]. Some polymers are sensitive to the type of loading waveform [Dear, 1991]. Increasing the frequency may decrease the testing time, but it also increases the hysteretic heating of the specimen [Huang and Brown, 1992]. Moreover, PE can fail under load in a brittle or ductile manner [Barry and Delatycki, 1989]. Obviously, different polymers will have different resistances to fatigue crack propagation, but the same polymer may also display different fatigue characteristics depending on the conditions under which it was processed [Strebel and Moet, 1992]. For example, if processing produces anisotropy within the polymer component, fatigue properties of the component will vary depending on molecular orientation [Barry and Delatycki, 1992; Lu et al., 1993]. The thickness of the specimen, which affects the stress state at the crack tip, is also an important factor affecting the fatigue crack propagation in a polymer [Egan and Delatycki, 1995]. In the experiment reported by Goolsby et al. [1983], the notch sensitivity of HDPE was evaluated using uniaxial tensile deformation and fractographic analysis. They found that tendencies toward notch sensitivity were evident in the failure modes as 'notch strengthening'. Lu and Brown [1990] termed this behaviour notch blunting.

The rate of slow crack growth by fatigue testing can be described by $a=A\Delta K^4$ [Barker, 1980], where (A) is a constant for a given resin and temperature, and (K) is the stress intensity. Chan et al. [1981] reported that the initiation rate for slow crack growth in PE pipe resin can be represented by, $\delta=A\Delta K^{4.7}$. They also showed that (A) and (δ) have the same dependency on (K). The exponent (4.7) was explained on a model that involved the spacing of defects in the resin and the spread of these defects. This explanation was never taken seriously because different PE resins contain different concentrations of branches, branch lengths, pigments and particle sizes, and yet it was claimed by both reports that most PEs agree with both equations.

In a simple approach in a recent publication by Brown and Lu [1995], showed that the resistance to slow crack growth can be measured by any one of three quantities:

(i) the rate of crack opening prior to fracture initiation;
(ii) the time for fracture initiation; and
(iii) the time for complete fracture.

The slow crack growth process in PE has been demonstrated by Bubeck et al. [1982] to be a two-stage process involving an incubation time and the actual crack growth. The incubation time increases with decreasing stress and appears to be the time necessary to form sufficient voiding/crazing ahead of a flaw (e.g. notch). The microstructure, as controlled by branching and the thermal history, can be expected to have a considerable influence on craze nucleation and growth during the slow crack growth process, as well as on other physical properties. This was supported by Lu et al. work [1993], where slow crack growth was found to be dependent on both the molecular structure, the morphology and the packing

of the molecules. Barry et al. [1992] also showed that the fracture behaviour of high density PE (HDPE) can be interpreted in terms of the morphology of the polymer. In their work, correlation of the morphological data and the fracture parameters demonstrated that the resistance to crack initiation was influenced by the frequency of side chains. In recent study by Egan et al. [1995], the fracture toughness and crack growth rate were found to be most strongly dependent on the molecular weight of the resin. Their results also showed that when variations in molecular weight were minimal, it was found that increasing the short branch content offers considerable scope for improving the fracture toughness.

Plane stress single edge notched (SEN) and plane strain arc-shape specimens shown in Figure 2.6 were found to facilitate fatigue crack propagation behaviour in MDPE pipe systems [Strebel and Moet, 1993].

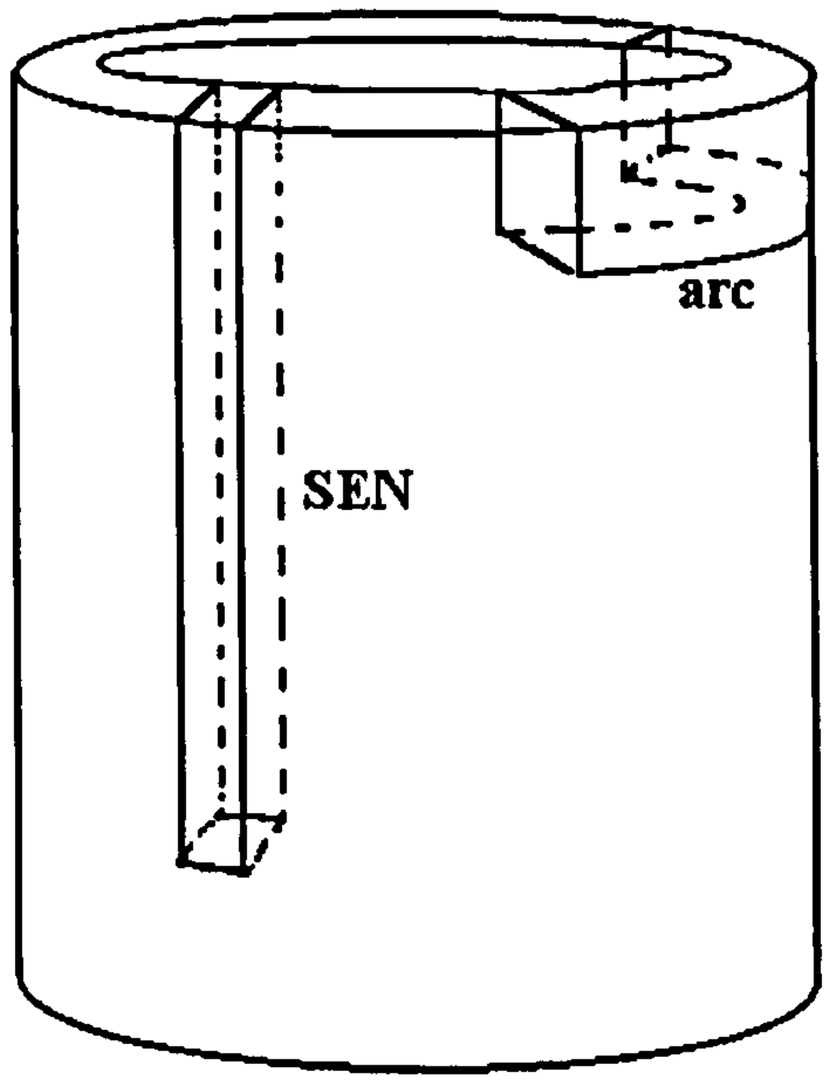

Figure 2.6. Respective origins of arc and SEN geometries.

A Crack Layer Theory was recently developed and explained by Strebel and Moet [1993] to accommodate fatigue crack propagation. The Crack Layer Theory considers the crack and its accompanying damage zone as a single entity,

which propagate through the material. This theory relates the crack propagation velocity (da/dN) to the energy release rate (J) and the irreversible work (W_i) by;

$$\frac{da}{dN} = \frac{bW_i}{gR - J} \qquad (2.2)$$

where;

R = resistance moment, is a measure of the amount of damage around the crack.

b = the dissipation coefficient, is the fraction of irreversible work (W_i) spent on fracture.

g = the specific enthalpy of damage, is the intrinsic resistance of the material to crack propagation.

a = crack length.

N = number of cycles.

The specific enthalpy of damage and the dissipation coefficient are determined from the fit of the experimentally determined da/dN, W_i, R, and J values. da/dN, is determined from the first derivative of the crack length vs. number of cycles. W_i, is the area of load-displacement hysteresis the shaded area in Figure 2.7.

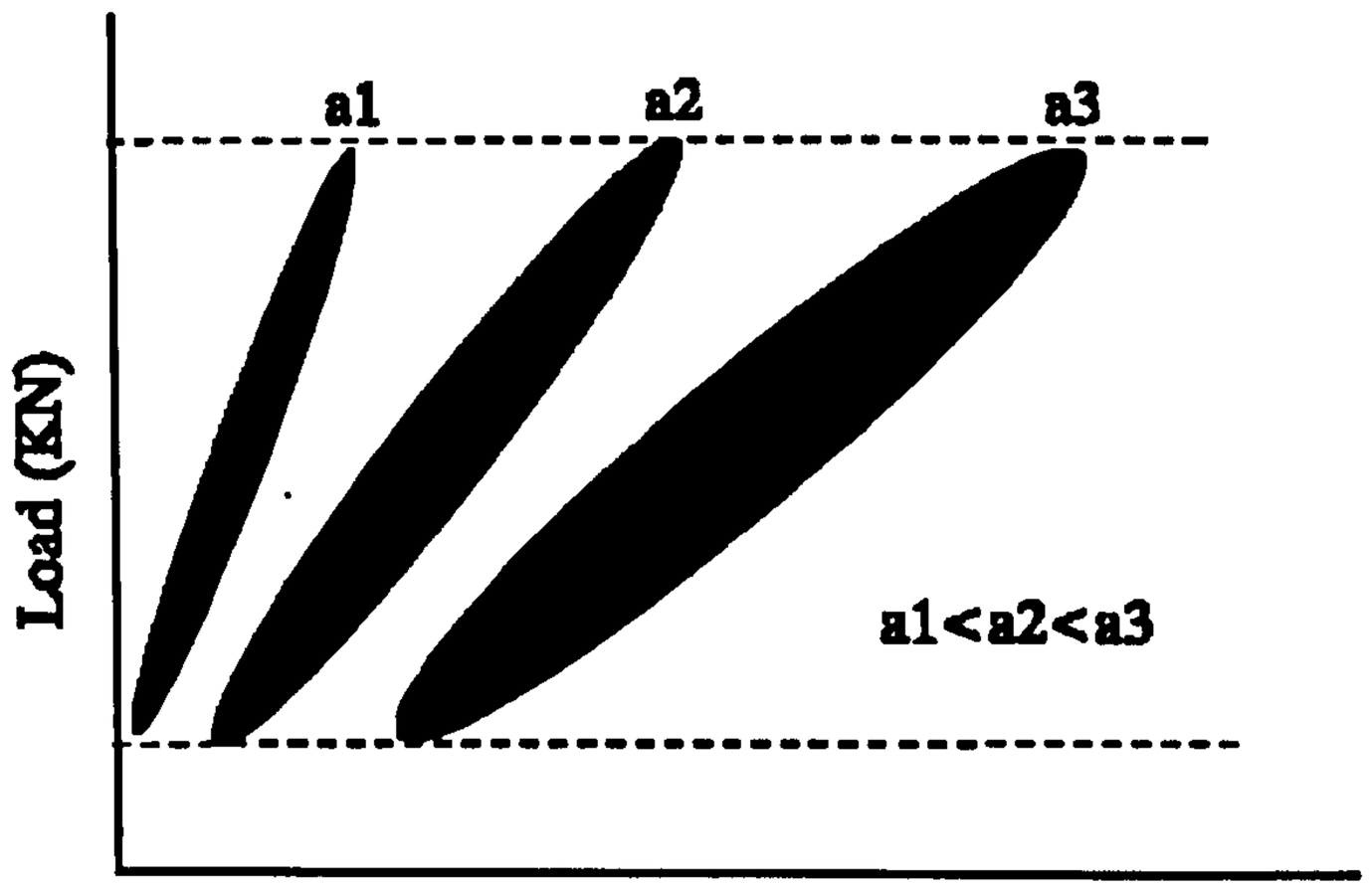

Figure 2.7. The irreversible work is proportional to the area of the hysteresis loop.

The energy release rate, J, normalised to the initial specimen thickness. B_o, is the change in potential energy, P, with the crack length.

$$J=\frac{-dP}{daB_o} \qquad (2.3)$$

In order to account for any crack advance that may occur during loading, the potential energy is taken to be the area above the unloading curve to the hysteresis loop (Figure 2.8).

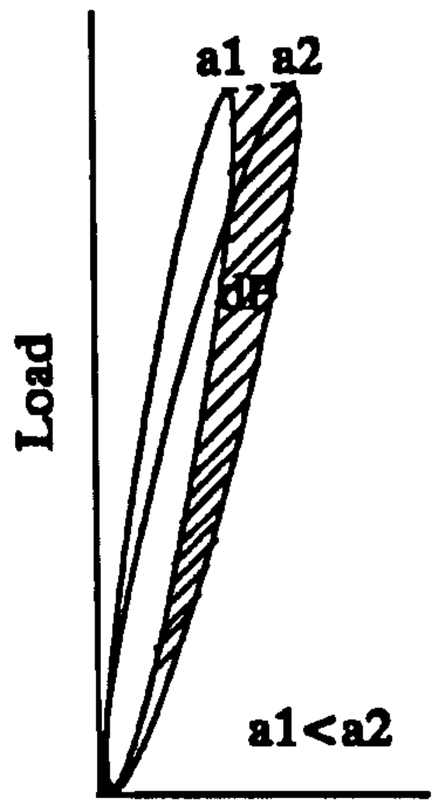

Figure 2.8. The difference between the areas above the unloading curves is proportional to the energy release rate.

Thus, the change in this area per change in crack length is equal to the energy release rate. This method is similar to that outlined by Begley and Landes [1987]. Strebel showed that elastic-plastic energy release rate solutions only account for small scale yielding near the crack tip and thus neglect other forms of damage, such as extensive crazing and/or specimen thinning. In the SEN system, this type of damage is present in each specimen and can act as energy sinks. As a result, an elastic-plastic solution neglects a considerable portion of the energy absorbing damage in the specimen, and therefore it predicted a larger energy release rate than that observed.

The remaining variable in equation one is the resistance moment. To determine the resistance moment, the damage ahead of the crack tip must be identified and measured. During crack propagation in plane stress specimens the crack tip is typically accompanied by a zone of uniformly yielded material. The damage due to crazes is calculated using;

$$R_{craze}=\frac{Vfd}{B_o a} \qquad (2.4)$$

where;

V = volume occupied by the craze

f = volume fraction of material within the craze

d = material density

B_o = initial specimen thickness

a = crack length

Since loaded plane-stress specimens exhibit large scale yielding, this type of deformation should also be considered when calculating (R).

$$R_{yield}=\frac{Vd}{aB_o} \qquad (2.5)$$

Since the craze zone is located within the yield zone, its volume contribution should be removed from the R_{yield}.

$$R_{yield\ craze}=R_{yield}-2R_{craze} \qquad (2.6)$$

These calculations yield two R values. Strebel and Moet [1993] noted that the crazing is a very localised, intense form of damage that forms membranes of yielded material and voids. Therefore, calculations of (R) values was based on density changes and relate to a scaling factor. Using this factor, the two resistance moments can give the total resistance moment: $R = R_{craze} + R_{yield\ craze}$.

The variables in equation (2.2) are established, and it may be written in the linear form:

$$\frac{J}{R}=g-\frac{bW_i}{RB_o da/dN} \qquad (2.7)$$

By plotting J/R against $W_i/RB_o da/dN)$, the constants g and b can be determined.

The energy release rate, irreversible work, and crack velocity can be calculated from the hysteresis loops and crack propagation data. However, the calculation of the resistance moment requires significant sectioning and microscopy of fractured and partially fractured specimens to quantify the size of the damage zone. Furthermore, there were several theoretical assumptions when the direct measurement of a quantity was unattainable. Specifically, correction factors were applied to the zone width and plastic zone length. In addition, to the assumption that the relative effect of each damage type is dependent on the material density change in each. Finally, the crack length measurement is very difficult to comprehend.

CHAPTER THREE

CHAPTER THREE

EXPERIMENTAL

3.1. Descriptions of Materials

3.1.1. PE Resins

Three types of PE resins were used in this study:

(i) Gas grade, medium density PE (MDPE) - Rigidex 00240 R919, PE-hexene, manufactured by BP (UK) using the Phillips process. This resin is referred to as Rigidex throughout this study.

(ii) Gas grade, high density PE (HDPE) - Solvay Eltex TU B125, PE-butene, manufactured by Solvay & Cie (Belgium) using a Ziegler-type manufacturing process. This resin is referred to as Eltex throughout this study.

(iii) Gas grade, medium density PE (MDPE) Aldyl-A 5046, PE-octene, manufactured by Du Pont (UK). This resin is referred to as Aldyl-A throughout this study.

The three PE resins constitute the main pipe materials currently used by British Gas plc.

The materials were supplied as freshly extruded pipes and pellets. Some relevant properties of these three resins are listed in Tables 3.1 to 3.3. In the case of Aldyl-A 5046 resin, it was difficult to obtain further information as this resin system is no longer in production.

Table 3.1. Selected properties for the Rigidex PE resin [Rigidex product data].

Average branch frequency	4 branch/1000C
Density (ASTM 1505)	940 kg/m^3
MFI load 2.16 (ASTM D 1238)	0.2 g/10min
Stress at yield 50mm/min (ASTM D 638)	18 MPa
Ultimate elongation (ISO R 527)	>600 %
Flexural modulus (ASTM D 790)	700 MPa
SCR F_{50} (ASTM D 1525)	>1000 h
VICAT (ISO 306 A)	116 °C
Thermal conductivity (BS 874)	0.25 W/m K
Coefficient of linear expansion (ASTM D 696)	1.5×10^{-4} K^{-1}

Table 3.2. Selected properties for the Eltex PE resin [Eltex product data].

Average Branch frequency	3 branch/1000C
Mn (GPC)	10×10^3
Mw (GPC)	250×10^3
Mz (GPC)	1500×10^3
Density (ASTM D 1505)	951 kg/m^3
MFI load 2.16 (ASTM D 1238)	<0.15 g/10min
Stress at yield 50, 100mm/min (DIN 53455)	25 MPa
Stress at break 50, 100mm/min (ISO R 527)	39, 37 MPa
Ultimate elongation 50, 100mm/min (ISO R 527)	>600 %
Young's modulus (ISO R 527)	1200 MPa
SCR F_{50} (ASTM 1693)	>1000 h
VICAT load 1kg (ASTM D 1525)	127 °C
Thermal conductivity 23°C (DIN 52612)	0.38 W/m K
Coefficient of linear expansion (ASTM D 696)	1.3×10^{-4} K^{-1}
Specific heat 23°C (Calorimetric)	1.9 kJ/kg K

Table 3.3. Available properties for the Aldyl-A PE resin [information supplied by British Gas].

Average branch frequency	5 branch/1000C
Mn (GPC)	27×10^3
Mw (GPC)	108,400
Mz (GPC)	4
Density (ASTM D 1505)	935 kg/m^3
MFI load 2.16 (ASTM D 1238)	<0.9 g/10min

3.1.2. PE Pipes

A 3 m length of 180 mm OD SDR11 Solvay Eltex TU B125 (coded 169 36 92) pipe was supplied by British Gas. A freshly extruded pipe batch of 48 m of 180 mm OD SDR11 (coded 300A2005 94) and 125 mm OD SDR11 (coded 306B3003 94) Rigidex 00240 R919 were purchased from Waven plc (UK). These pipes were supplied in 6 m lengths. On arrival at Brunel University, all the pipes were cut into 3 m sections and stored in a dark environment to protect them from ultra violet degradation. A batch of 125 mm OD SDR11 Aldyl-A 5046 (coded 1511B25) pipes from a previous project at Brunel University was also used. In this study, all the 125 mm OD SDR11 pipe size is referred to as 125-pipe and all the 180 mm OD SDR11 pipe size is referred to as 180-pipe.

3.1.3. PE Pellets

Two 25 kg bags each of pellets and powder of the Rigidex 00240 resin were provided by BP (UK). Another two 25 kg bags each of pellets and powder of the Eltex TU B125 resin were obtained from Solvay (Belgium). It was not possible to secure Aldyl-A resin in the form of pellets or powder as the resin is not currently produced.

3.1.4. Compression Moulded Plaques

A custom-made mould was used to produce the compression plaques with dimensions of 200 mm x 200 mm x 12 mm as shown in Figure 3.1.

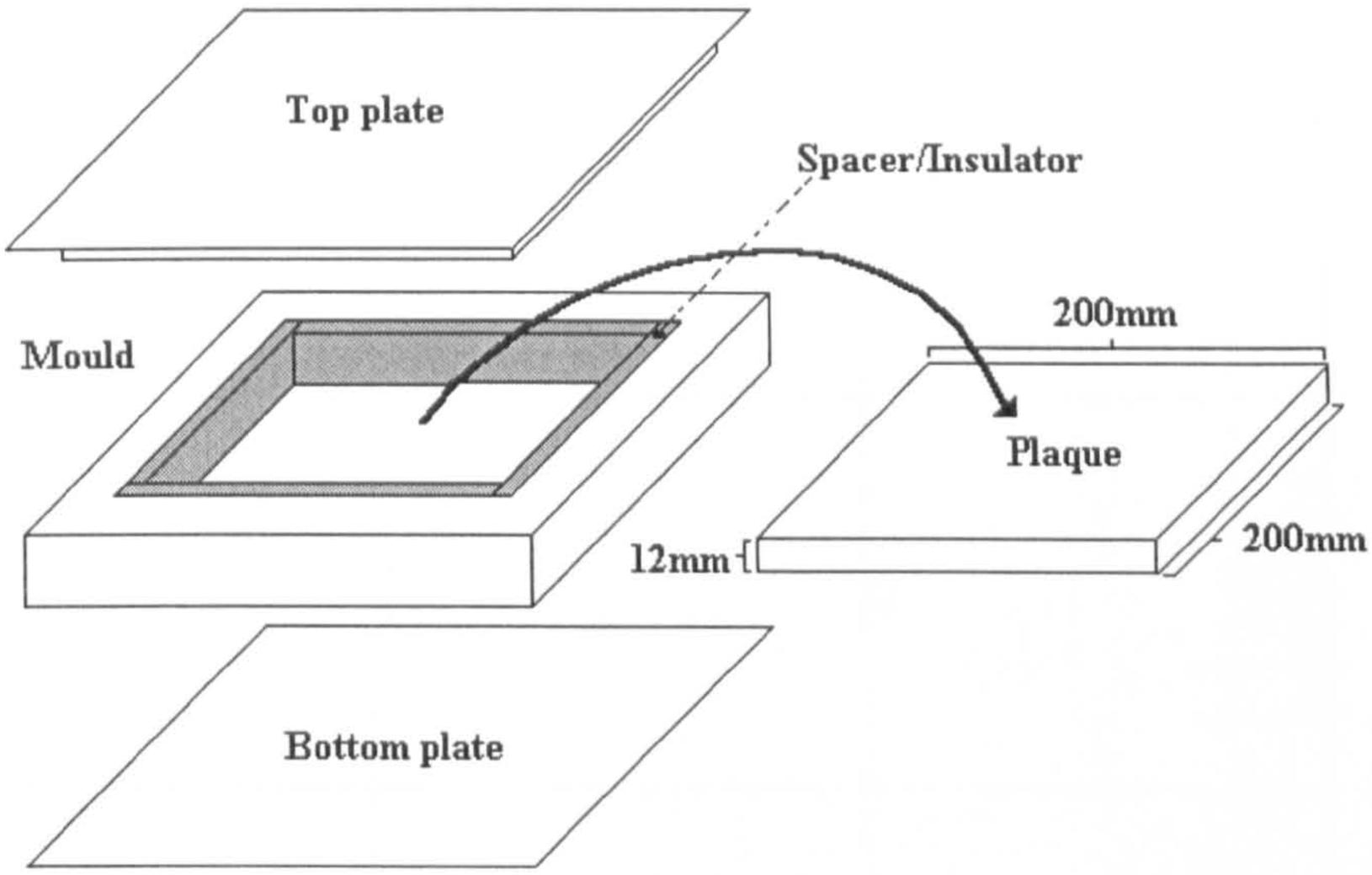

Figure 3.1. Schematic illustration of the mould used for the production of the PE compression moulded plaques.

Approximately 580 g of pellets were placed into the mould cavity. The mould assembly was transferred to a pre-heated press at 150°C and held for 30 minutes under a pressure of 1.25 MPa. The heat source was then switched off while maintaining the pressure. The mould was left to cool down to 80°C at a cooling rate of 1 °C/min before the pressure was released and the mould was removed from the press. The crystallinity content of the moulded plaques was determined by enthalpy measurements using the DSC. Plaques were also produced to study the effect of crystallinity on fatigue fracture behaviour of single edge notched specimens. These plaques were moulded at 140, 145, 150, 155, 160, 165 and 170 °C. Seven plaques each were made using the Rigidex and Eltex resins.

3.1.5. Additives

The details of known additive systems used in Rigidex and Eltex resins are presented in Tables 3.4 and 3.5. At the time of writing the Aldyl-A additive system was not available. Samples of the additives used in the Rigidex and Eltex resin systems were obtained from Ciba Geigy plc. (UK). Santonox R was obtained from Flexsys plc (UK).

Table 3.4. Summary of the known additives in Rigidex resin (private communication - BP Polymer Additive Section).

Additive	Structure	Chemical name	Melting point (°C)	Concentration % (w/w)
Antioxidant 1	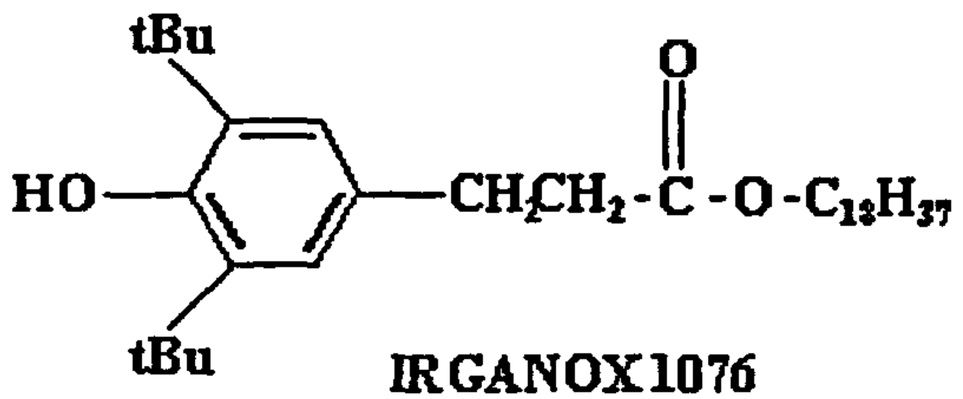 IRGANOX1076	Octadecyl 3-(3,5-di-tertbutyl-4-hydroxphenyl) propionate	55	0.05
Antioxidant 2	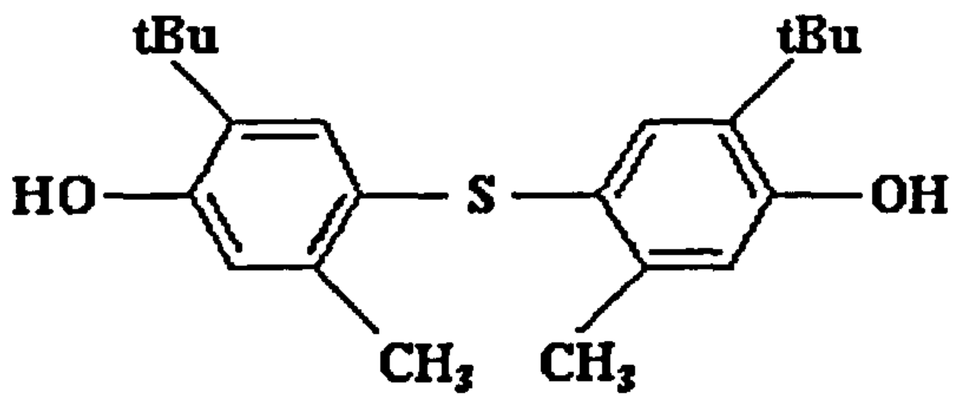 SANTANOX R	4,4'-Thiobis(2-tert-butyl-5-methyl phenol)	161	0.1
UV stabiliser	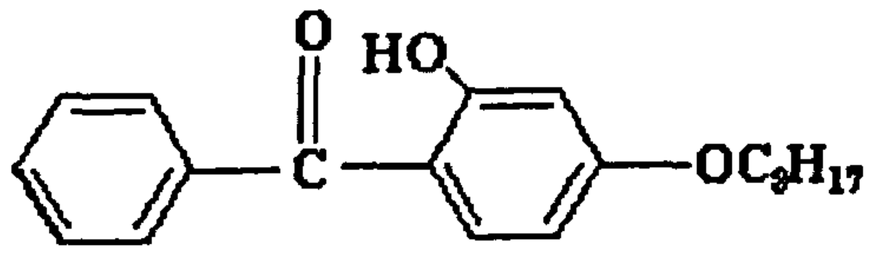 CYASORB UV531	2,Hydroxy-4-n-octyloxybenzophenone	50	0.25
Pigment		Cadmium Sulphide	not applicable	1

Table 3.5. Summary of the known additives in Eltex resin (private communication - British Gas plc).

Additive	Structure	Chemical name	Melting point (°C)	Concentration (%) w/w
Antioxidant 1	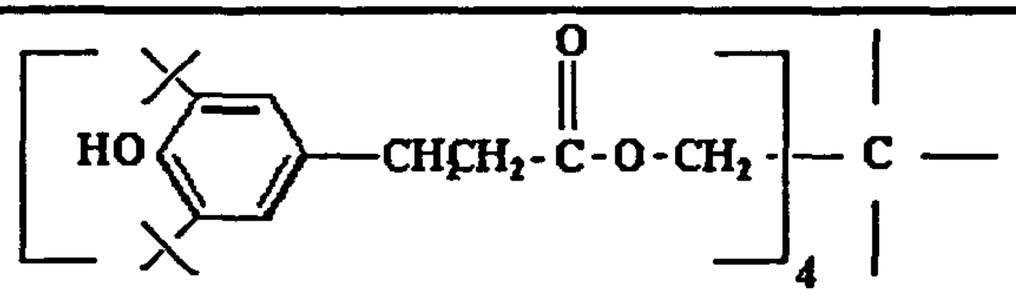 IRGANOX1010	Pentaerythritoltetrakis(3-(3,5-di-tert-butyl-4-hydroxyphenyl)propionate)	110-125	0.12
Antioxidant 2	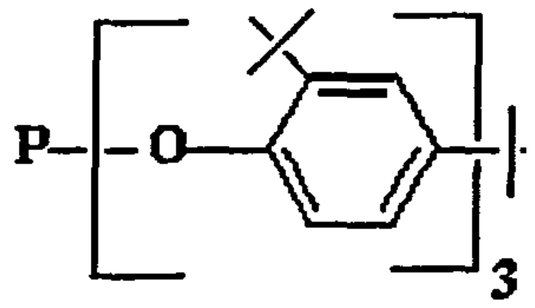 IRGAFOS168	Phenol,2,4-bis(1,1-dimethylethyl)-, phosphite	186	0.12
UV stabiliser	TINUVIN 770 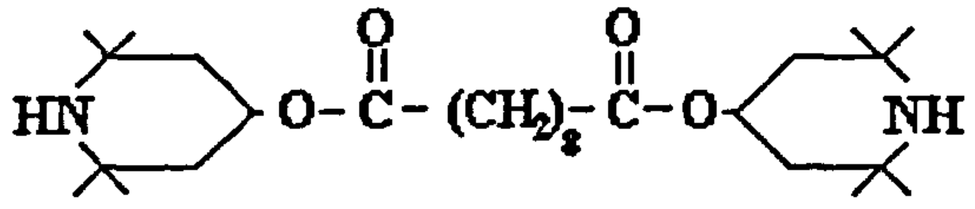	Bis(2,2,6,6-tetramethyl-4-piperidyl)sebacate	85	0.12
Antiacid		Calcium stearate	unknown	0.12
Pigment 1 and pigment 2		un-specified	not applicable	0.5

3.2. Production and Conditioning of Test Specimens

The test specimens used in this study were prepared from pipes and compression moulded plaques. A schematic illustration of the various samples generated are shown in Figure 3.2.

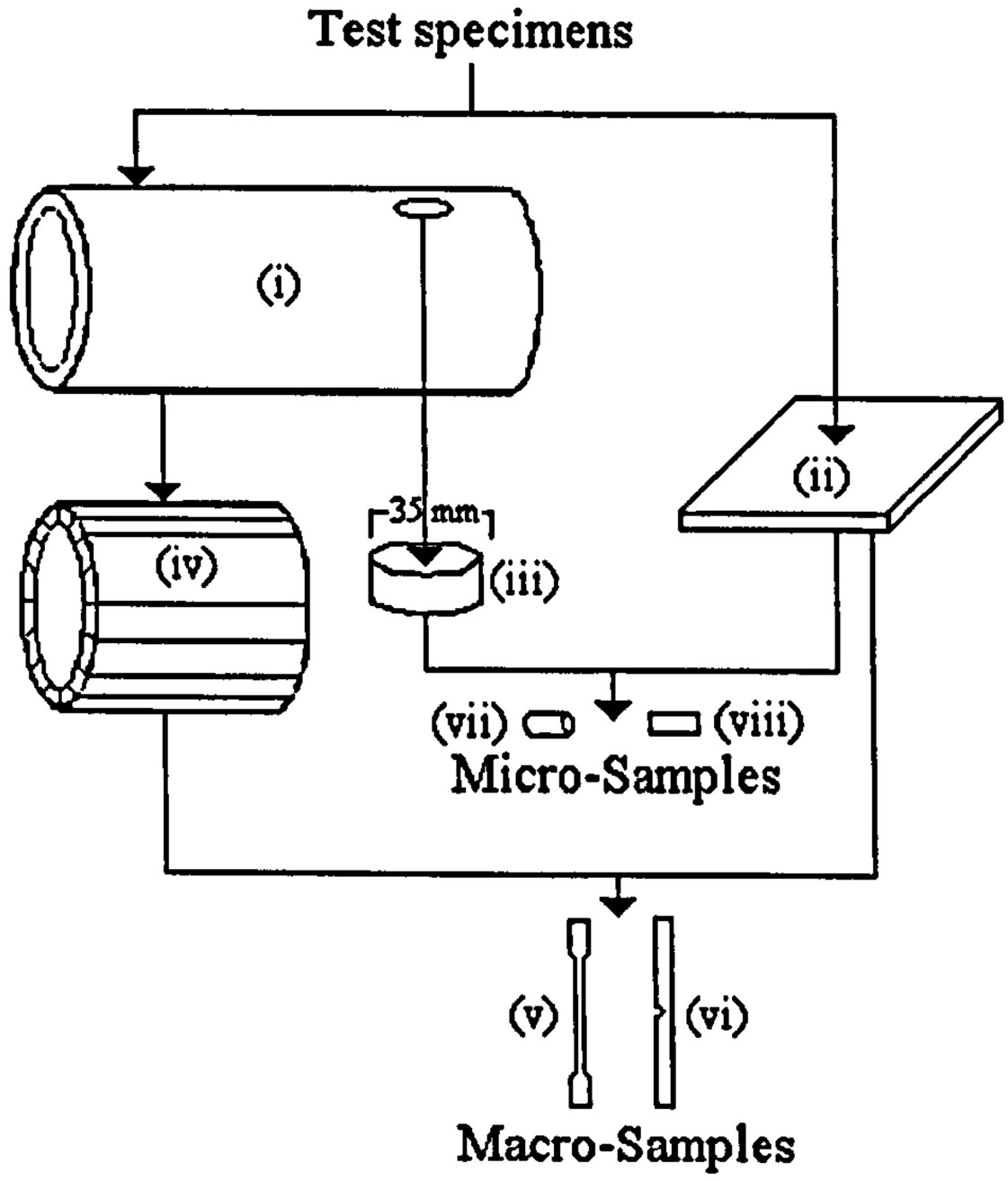

Figure 3.2. Schematic illustration of the macro- and micro-samples obtained from (i) a pipe, (ii) a plaque and (iii) a disk sample obtained using a cutter. Items 1v-viii are described in the text.

In this study, macro-samples were cut from 180-pipes and 125-pipes. Two samples were produced from longitudinal strips which were cut from around the circumference of the pipe as shown in Figure 3.2(iv). Figure 3.2(v) represents a 'profile' specimen used for tensile testing and Figure 3.2(vi) represents a single-edge-notched (SEN) specimen which was used for fatigue testing. Disk samples, as shown in Figure 3.2(iii), were cut directly from plaques and pipes using tapping-tee cutters (a tapping-tee is a component used in PE pipe systems to make a service connection). Two types of micro-samples were produced from the disk samples. The first type of micro-samples were prepared by using a belt-hole puncher which gave cylindrical samples as shown in Figure

3.2(vii). These samples were used for OIT, HPLC and TGA analysis. The second type of micro-samples were microtomed thin films as shown in Figure 3.2(viii). These samples were produced using a Reichert-Jung microtome model 2035. The microtomed samples were used for FTIR spectroscopy and micro-tensile testing.

3.2.1. Macro-Samples Preparation

The term macro-samples is used to describe test specimens which were used for static and dynamic mechanical testing. A custom-made pipe cutting machine was used to cut and profile the macro-samples from pipes. The design diagram of the pipe cutting machine is shown in Appendix 1. Photographs of this machine along with its key components are presented in Figures 3.3 to 3.7. The machine utilised a twin cutter arrangement as shown in Figure 3.3(i) and a specially designed clamping fixture (Figure 3.3 (ii)) to hold a 200 mm pipe section (Figure 3.3(iii)) firmly in position while cutting to produce the strips. Strips of thickness 14 mm and 20 mm were produced by changing the spacer between the two cutters.

Tensile Specimens

The custom-pipe cutting machine was used with a different clamping fixture, see Figure 3.4, and a profiled flying cutter, see Figure 3.6, to produce "dog-bone" tensile samples from the 20 mm thick strips. The tensile test specimens were designed to comply with ISO 6259-3, see Figure 3.8. The sample thickness was approximetly 12 mm for the 125-pipes and plaques and 17 mm for the 180-pipes.

Single-Edge-Notched (SEN) Specimens

The 14 mm thick strips were notched just prior to fatigue testing. Three types of notching methods were considered. (i) The custom-made machine mentioned previously was equipped with a notching wheel as shown in Figure 3.7 was used to produce a Vee-notch. (ii) The second method

involved the use of a disposable blade, model HISTORESIN Reichert-Jung 70-2218-550. The notching procedure was carried out by securing the test specimen and the blade in a vice. The blade was then pushed into the strip using the vice. A spacer was used to control a notch depth 3 mm. (iii) The third method involved the use of a SABRE G32002 model disposable razor which was held by a clamp fixture. A weight of 30 kg was placed on top of the razor holding the clamp. The imposed weight forced the razor into the PE sample at an average speed of 0.5 mm/min.

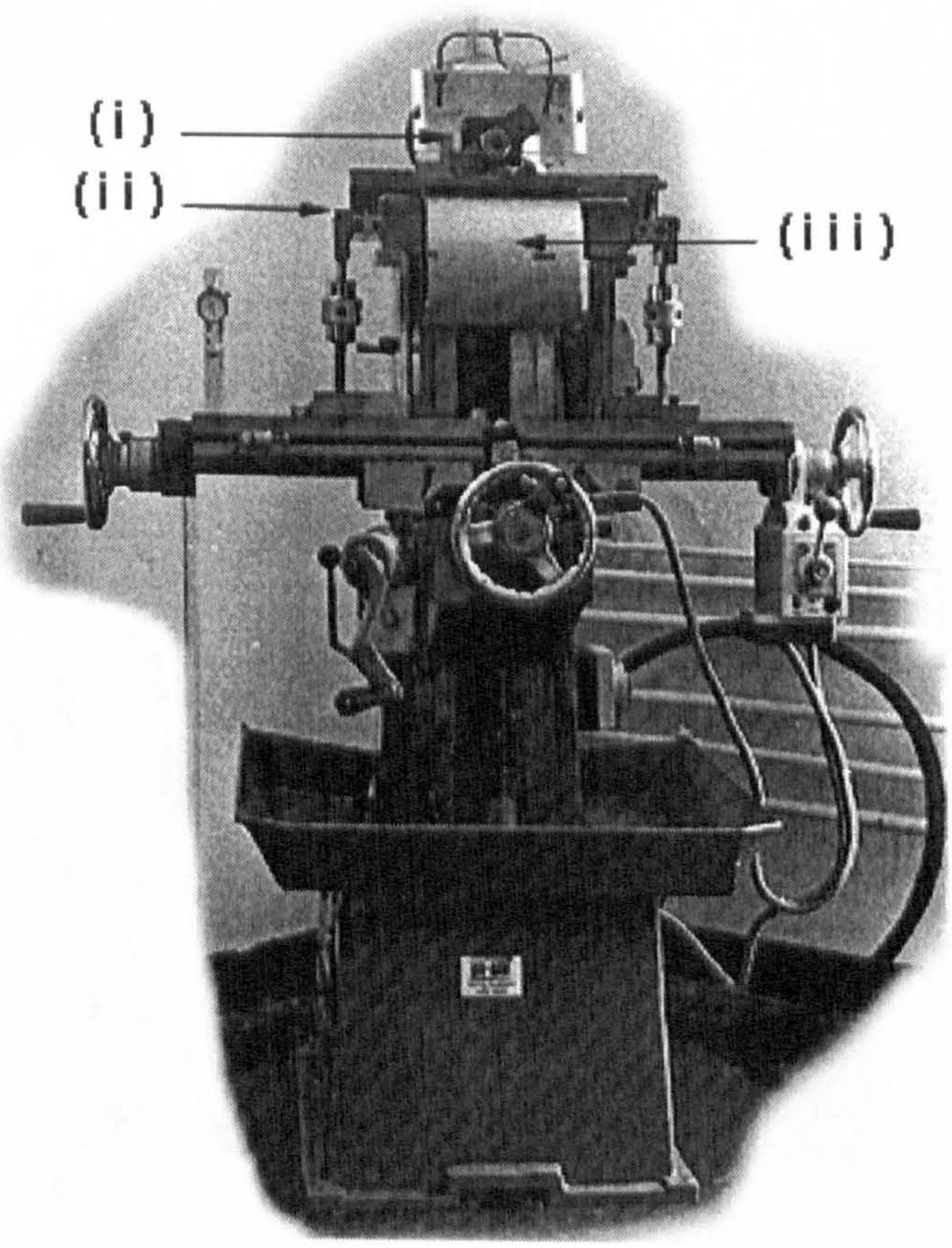

Figure 3.3. Photograph of the custom-made pipe cutting machine. Key component are (i) the twin cutter, (ii) the clamping arrangements fixture and (iii) a pipe sample.

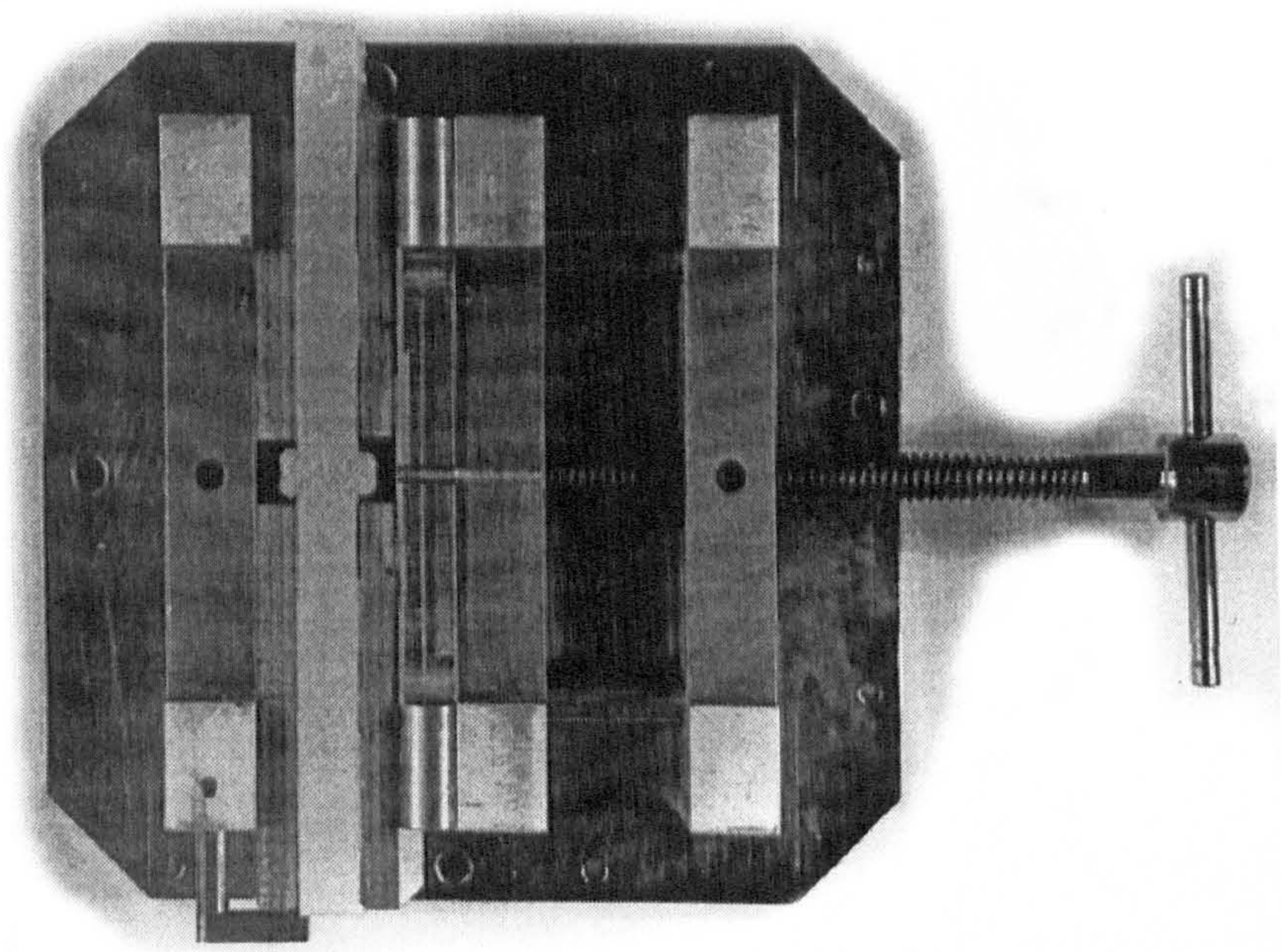

Figure 3.4. The gripping device for profiling and notching the strips.

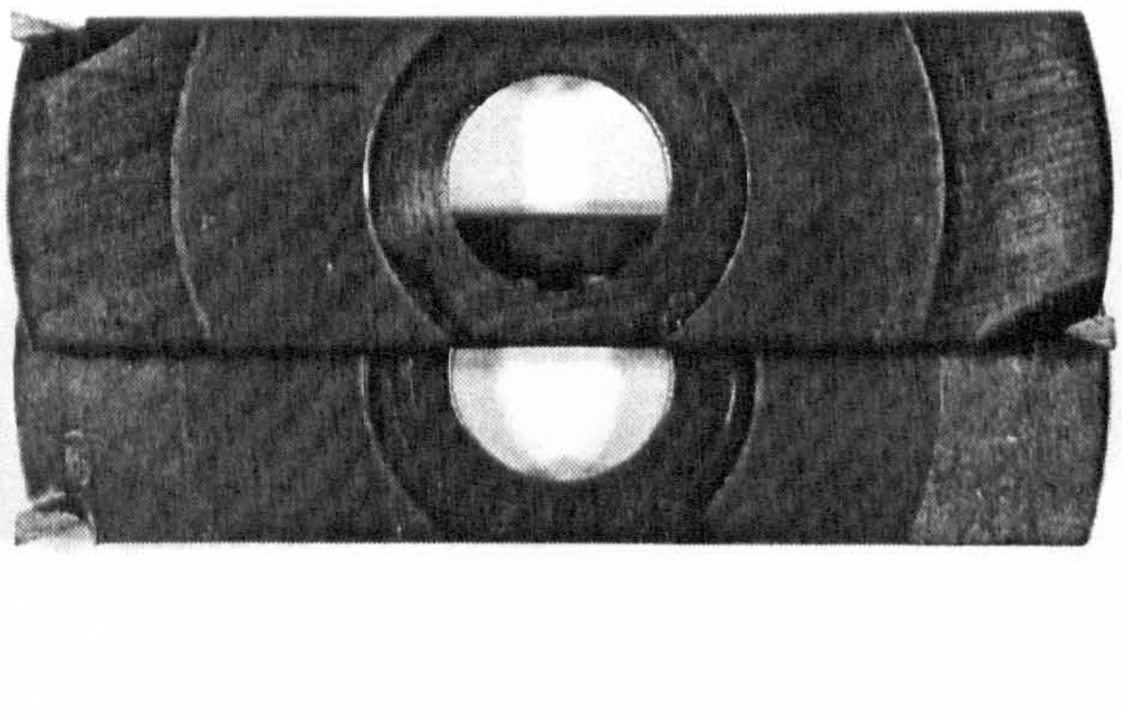

Figure 3.5. Photograph of the twin cutters.

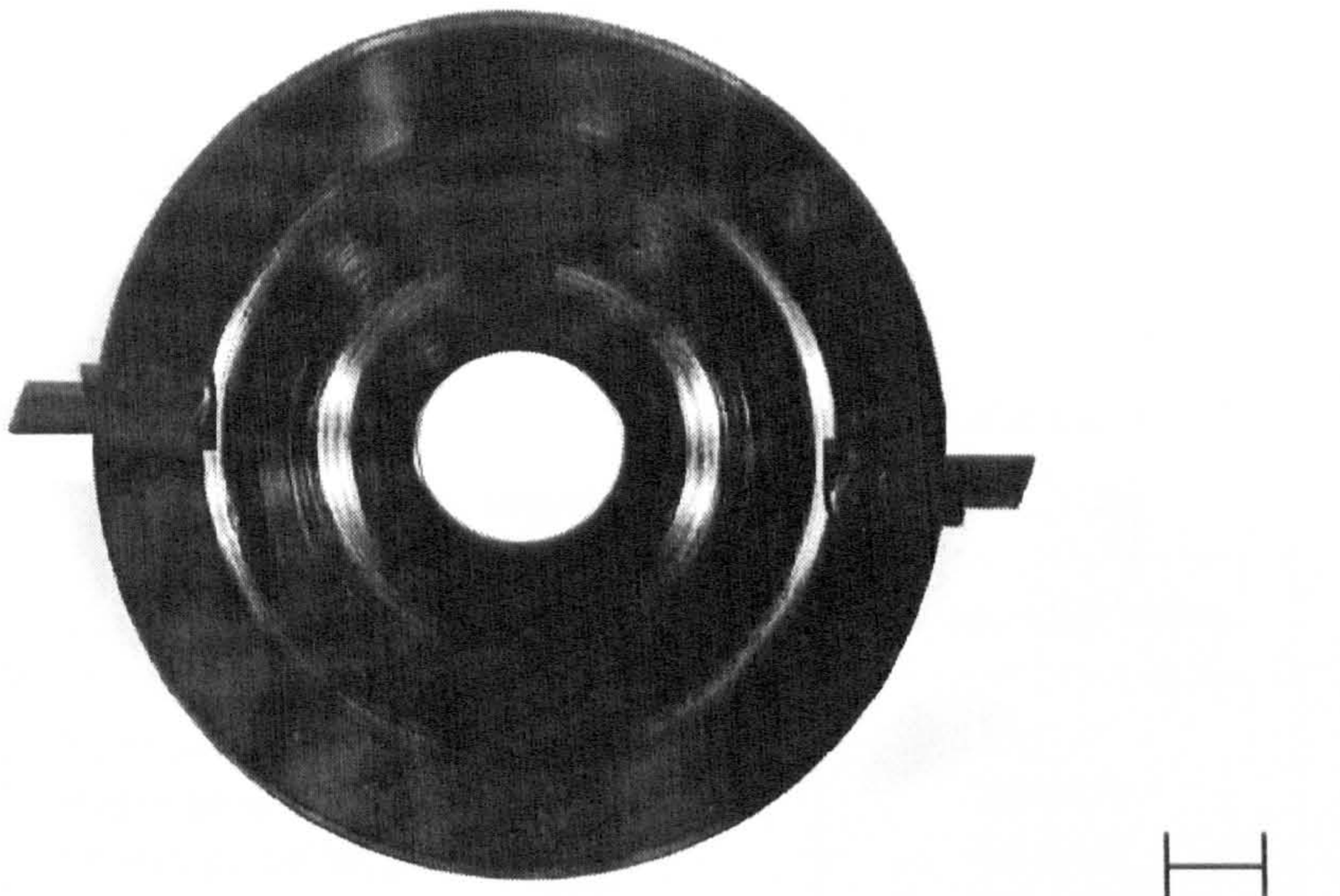

Figure 3.6. Photograph of the fly-cutters wheel for profiling the strips in order to produce dog-bone tensile test specimens.

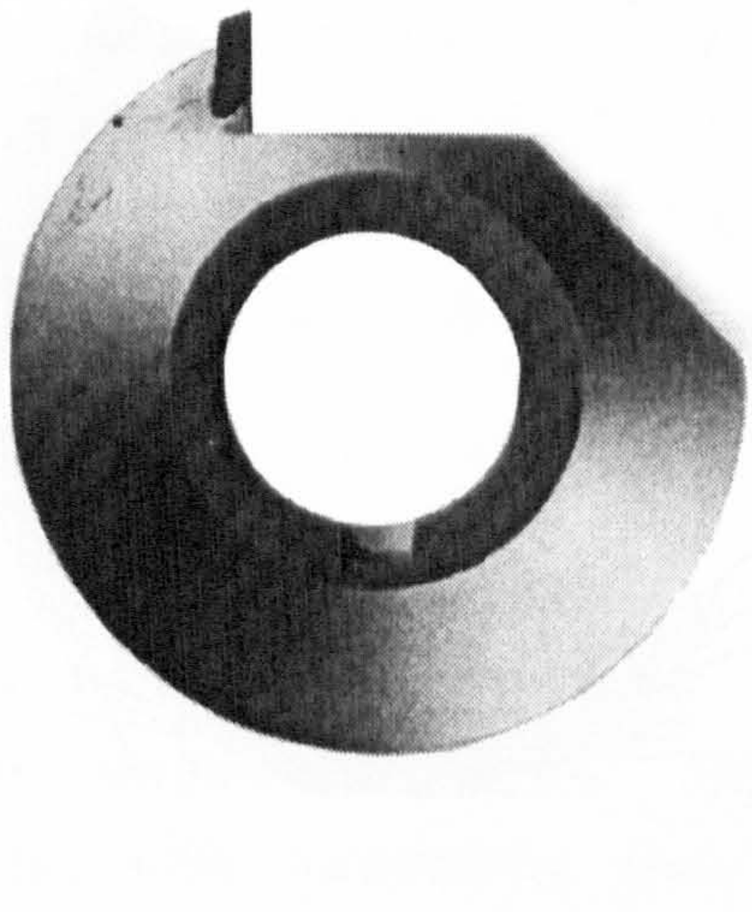

Figure 3.7. Photograph of the notching wheel.

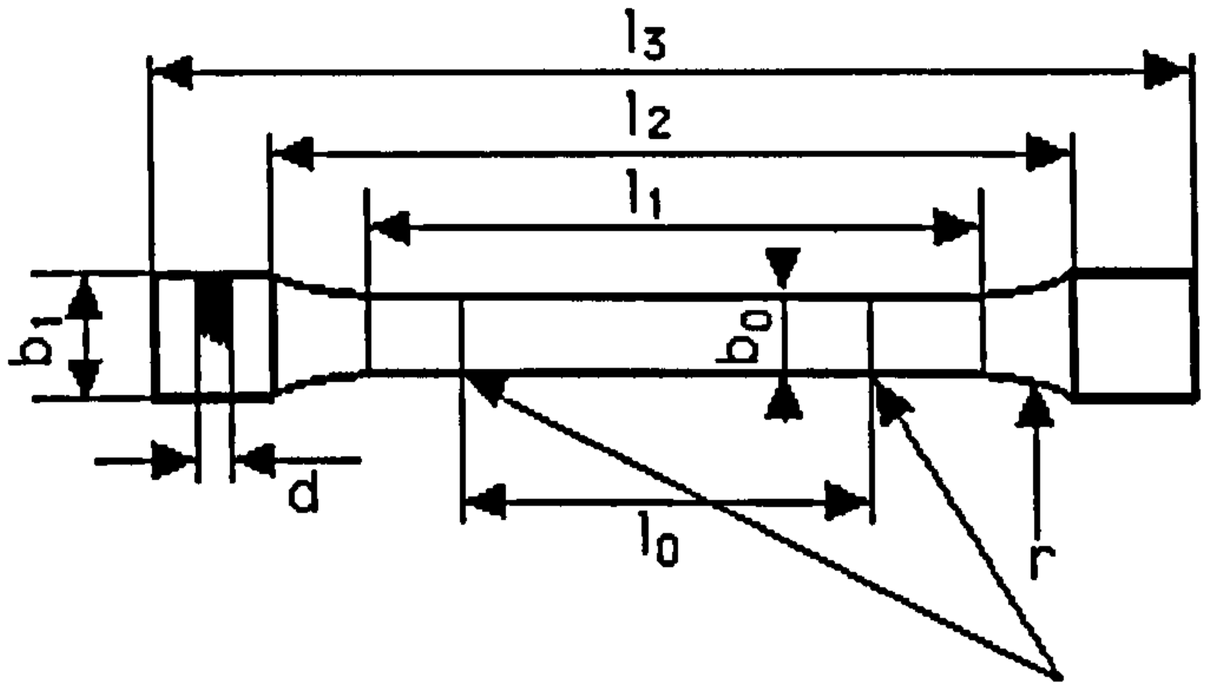

Gauge marks

Table of dimensions

Symbol	Description	Dimensions (mm)
l_3	Minimum total length	150
b_1	Width of ends	20 ± 0.5
l_1	Length of calibrated part	60 ± 0.5
b_0	Width of calibrated part	10 ± 0.5
r	Minimum radius	60
l_0	Gauge length	50 ± 0.5
l_2	Intitial distance between the jaws	115 ± 0.5
d	Thickness	5 < d > 12

Figure 3.8. Tensile specimens in accordance with ISO 6259-3.

3.2.2. Micro-Sample Preparation

The term micro-sample has been used in this work to describe a procedure whereby very small samples and films were obtained from pipes and compression moulded plaques. These samples were used to characterise the pipe material via a number of mechanical, chemical and spectroscopic techniques.

Tapping Tee

In order to obtain small sections of a PE pipe material without having to excavate long lengths of pipe, a conventional tapping tee assembly was used to produce a disk 35 mm in diameter. The tapping tee was welded to a pipe via an electrofusion joint and a cutter was then introduced to bore-out a disk of material from the pipe as shown in Figure 3.2(iii).

Belt hole puncher

A standard belt-hole puncher (BHP) with 5 mm inside diameter was used to obtain cylindrical specimens for thermal analysis experiments. The BHP was attached to an adapter which in turn fitted into an air pressurised stamp-press. A photograph of the BHP tool is shown in Figure 3.9.

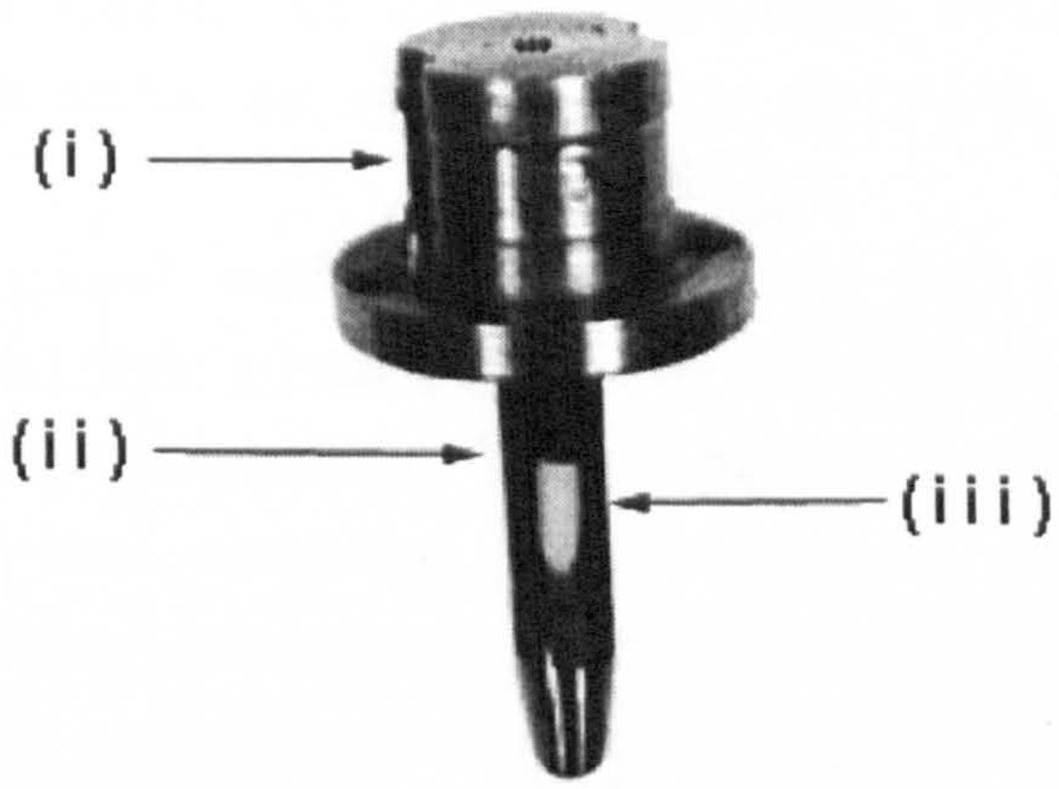

Figure 3.9. Photograph of the BHP tool: (i) the adapter, (ii) the 5mm BHP and (iii) the cylindrical sample produced.

Microtomy

A Reichert-Jung model 2035 microtome was used to obtain thin films for micro-tensile testing and FTIR spectroscopy. Both the inner and outer pipe surfaces were retained for the micro-tensile specimens. The microtome was fitted with a variable speed motor to provide a controllable speed for microtomy and to obtain reproducible film thickness. The quality of the cutting-edge was identified as a primary prerequisite for obtaining good quality microtome films. A blade polisher was used to maintain a high quality cutting-edge on the microtome blades.

3.2.3. Ageing Environments

In order to gain an understanding of the ageing behaviour

and chemical and physical characteristics of PE gas pipeline systems, ageing regimes were designed for both the pipes and the compression moulded plaques. The following ageing regimes were tested:

(i) air circulating oven at 80°C;
(ii) water bath at 23°C;
(iii) water bath at 80°C;
(iv) vacuum-oven (1 bar) at 80°C;
(v) air (in the dark) at 23°C (baseline reference); and
(vi) pipes from site as supplied by British Gas plc.

More than 65 pipe sections, 300 mm in length, and 20 compression moulded plaques were subjected to the above mentioned ageing regimes. The Rigidex samples were aged for one year. The samples were removed from the ageing environments every three months for analysis and testing. In the case of pipe samples made from the Eltex and Aldyl-A resins, they were removed after one year of ageing.

3.3. Analytical Techniques

3.3.1. Fourier Transform Infrared (FTIR)

Identification of PE resins and quantification of specified functional groups formed as a function of ageing were performed using a Nicolet FTIR 710 model spectrometer. Spectra were obtained between 4000 to 400 cm^{-1} using a resolution of 4 cm^{-1}. An average of 50 spectra were recorded in the absorbance mode. The test specimens for FTIR experiments consisted of 70 μm thick microtomed films.

The identification method of gas grade PE resins using FTIR spectroscopy is explained in Appendix 2.

3.3.2. Oxidation Induction Time (OIT)

A Perkin-Elmer DSC-7 was used for conducting the OIT experiments. The tests were carried out in accordance

with British Gas specifications PL2-Part:1. The flow rate for both the nitrogen and the oxygen was set at 50 ml/min. The BHP was used to obtain specimens of uniform diameter (cylindrical) from pipes and plaques. Three samples were cut from the cylindrical specimen representing the surface, middle and bore of a pipe or the middle and the two surfaces of a plaque. A sample weight of 12 ± 2 mg was used for all the OIT samples. Six samples were used to obtain an average for each test.

The OIT experiment involved heating the sample in an open DSC pan from 30°C to 200°C at a heating rate of 10 °C/min under a nitrogen environment. The sample was held at 200°C for 5 min before switching to oxygen. The DSC-7 was equipped with a programmable gas switcher unit. The OIT samples were located in the centre of the DSC pan and care was taken to ensure that there was no contact between the sample and the pan cover. The gas inlet and outlet tubes associated with both oxygen and nitrogen were checked and cleaned regularly. The OIT value was measured from the time of switching the gases (from nitrogen to oxygen) up to the onset of oxidation. The onset of oxidation was defined [PL2-Part:1, 1994] as the steepest part of the exotherm. This was achieved by drawing tangents to the steepest part of the exotherm and the onset was defined by the intercept of the two tangents as shown in Figure 3.10.

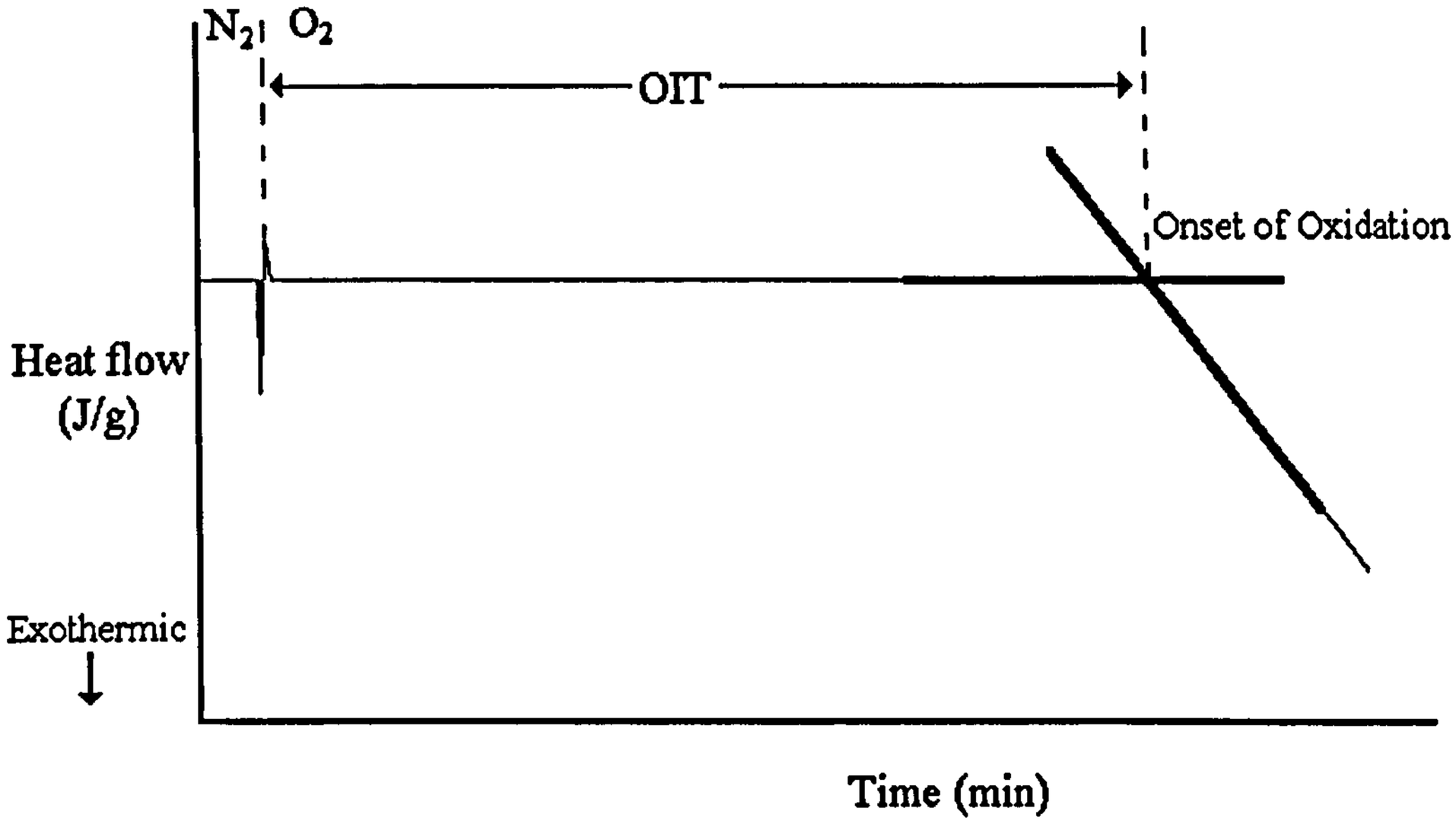

Figure 3.10. A schematic illustration of an ideal OIT trace.

3.3.3. Thermogravimetric Analysis (TGA)

TGA analysis was carried out using a Perkin-Elmer TGA-2 model. The TGA was calibrated using Calcium Oxalate before each set of experiments. The temperature within the furnace was checked with Alumel and Nickel magnetic transition temperatures at 163°C and 354°C, respectively. A sample mass of 25 ± 1 mg was used and the sample was heated from 30°C to 200°C at the rate of 10 °C/min in a nitrogen environment. The sample was held at 200°C for ten hours and the weight loss was monitored over this period.

3.3.4. High Performance Liquid Chromatography (HPLC)

A Perkin-Elmer HPLC 410 model was used to quantify the additive concentrations in the Rigidex pipe resin. The UV detector was set at 290 nm for Santonox R and Chimassorb 81 and 215 nm for Irganox 1076. The mobile phase was methanol (HPLC grade) and the flow rate set at 1 ml/min. A clean 25 µl syringe was used each time to inject a sample into the column (Spherisorb ODS2 250 mm x 4.6 mm).

Standard solutions of Santonox R, Chimassorb 81 and Irganox 1076 were prepared in the following

concentrations 0.1, 0.3, 0.6, 0.8 and 1 mg/ 100 methanol ml. These solutions were used for calibration purposes. A typical chromatogram of the additives investigated is shown in Figure 3.11. The concentration for each additive was calculated from its relevant peak area.

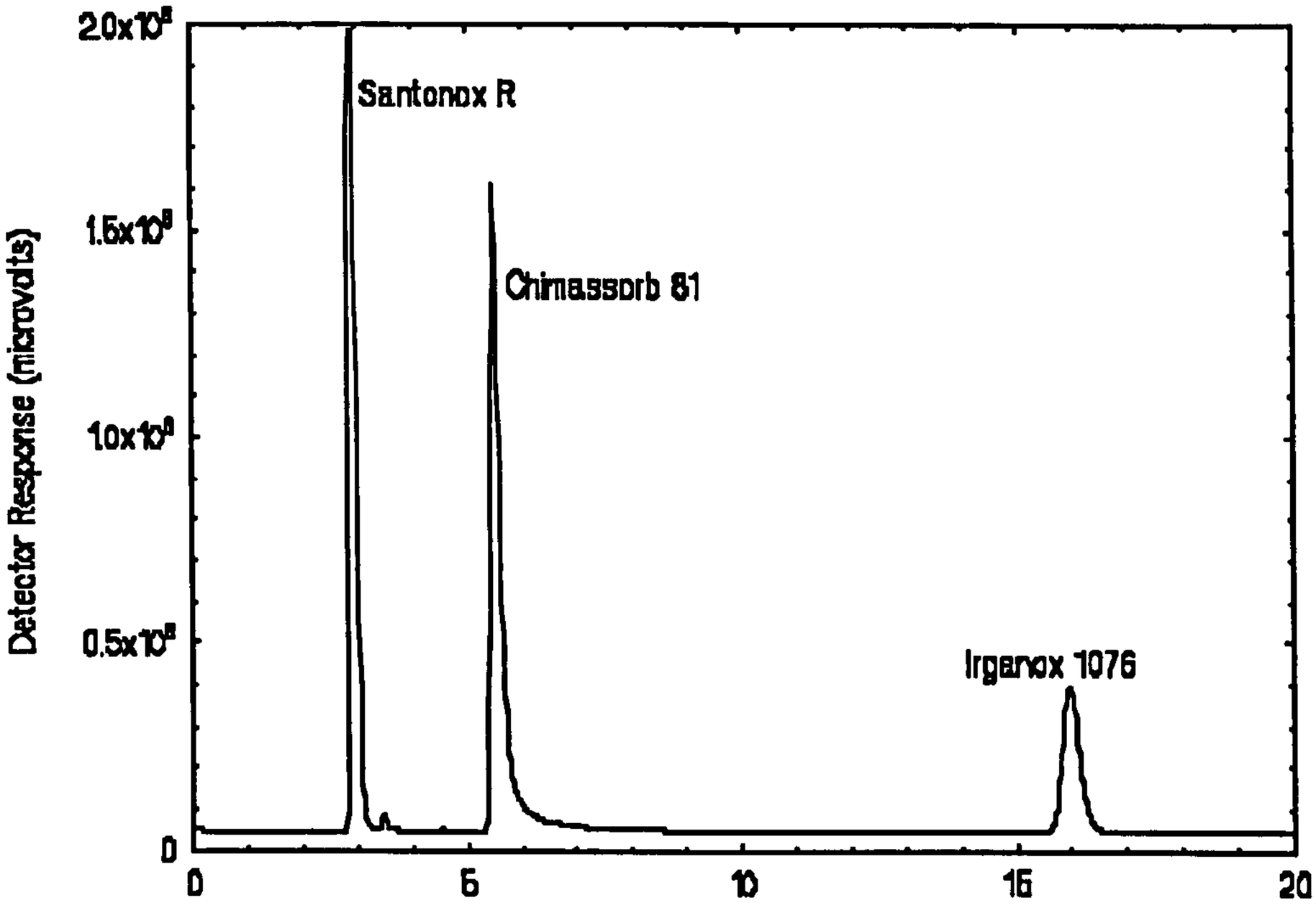

Figure 3.11. Chromatogram of Santonox R, Chimassorb 81 and Irganox 1076 additives.

Two procedures were evaluated for extracting the additives from the Rigidex polymer namely, the standard Soxhlet method and a 'microwave' method. A summary of the two methods is shown in Figure 3.12.

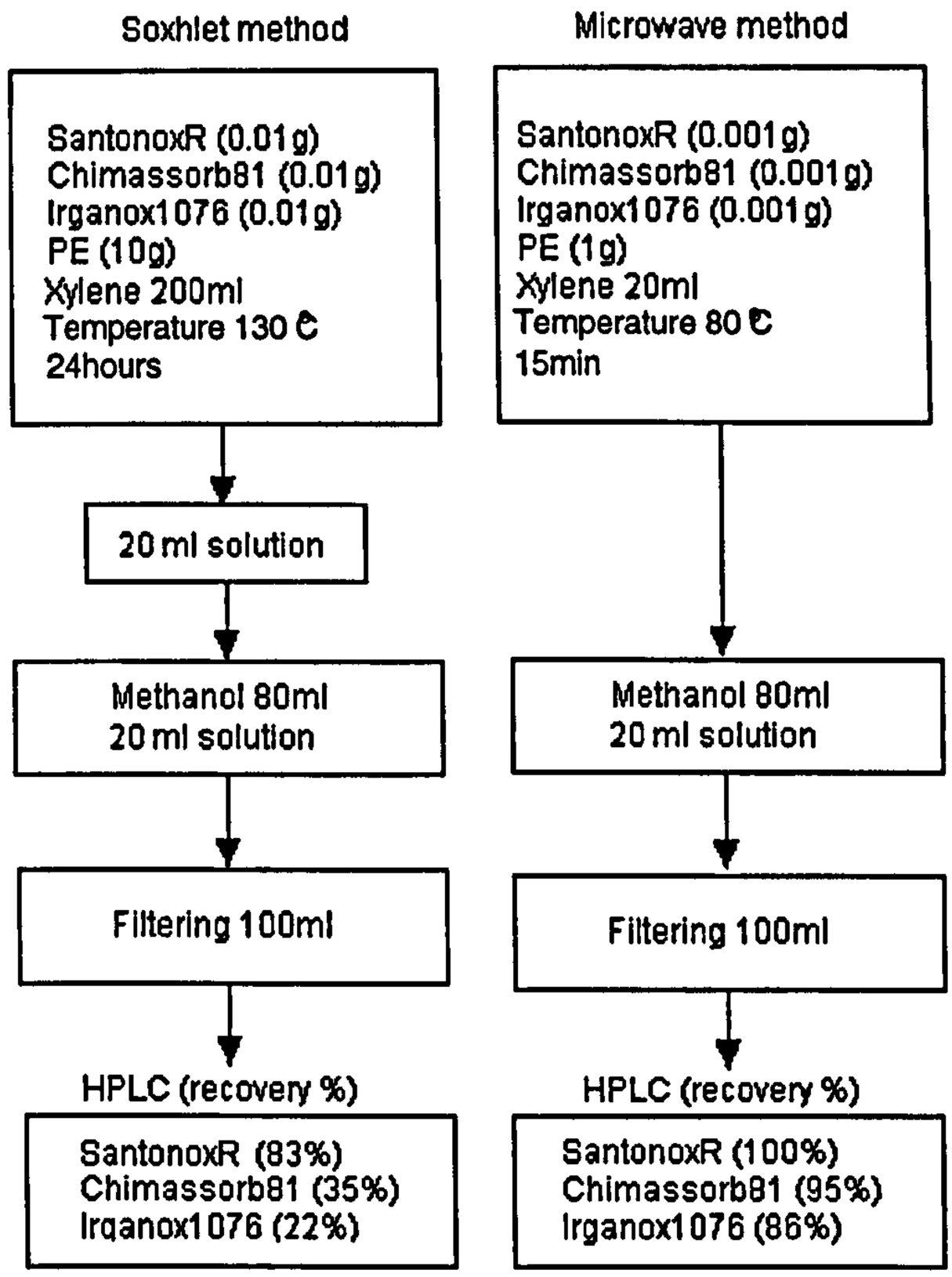

Figure 3.12. A flow diagram summarising the Soxhlet and microwave extraction procedures.

Soxhlet extraction method

A schematic illustration of the Soxhlet apparatus used to extract the additives form the PE samples is shown in Figure 3.13. 200 ml of xylene along with 10 g of the PE sample were placed inside a thimble. The mixture was refluxed for 24 hours at 130°C. A 20 ml sample was removed and transferred to a beaker containing 80 ml of methanol to extract the PE. The beaker was then transferred to a refrigerator for one hour. The precipitated polymer was filtered using a standard filtering apparatus. A sample of the filtered solution was taken for HPLC analysis.

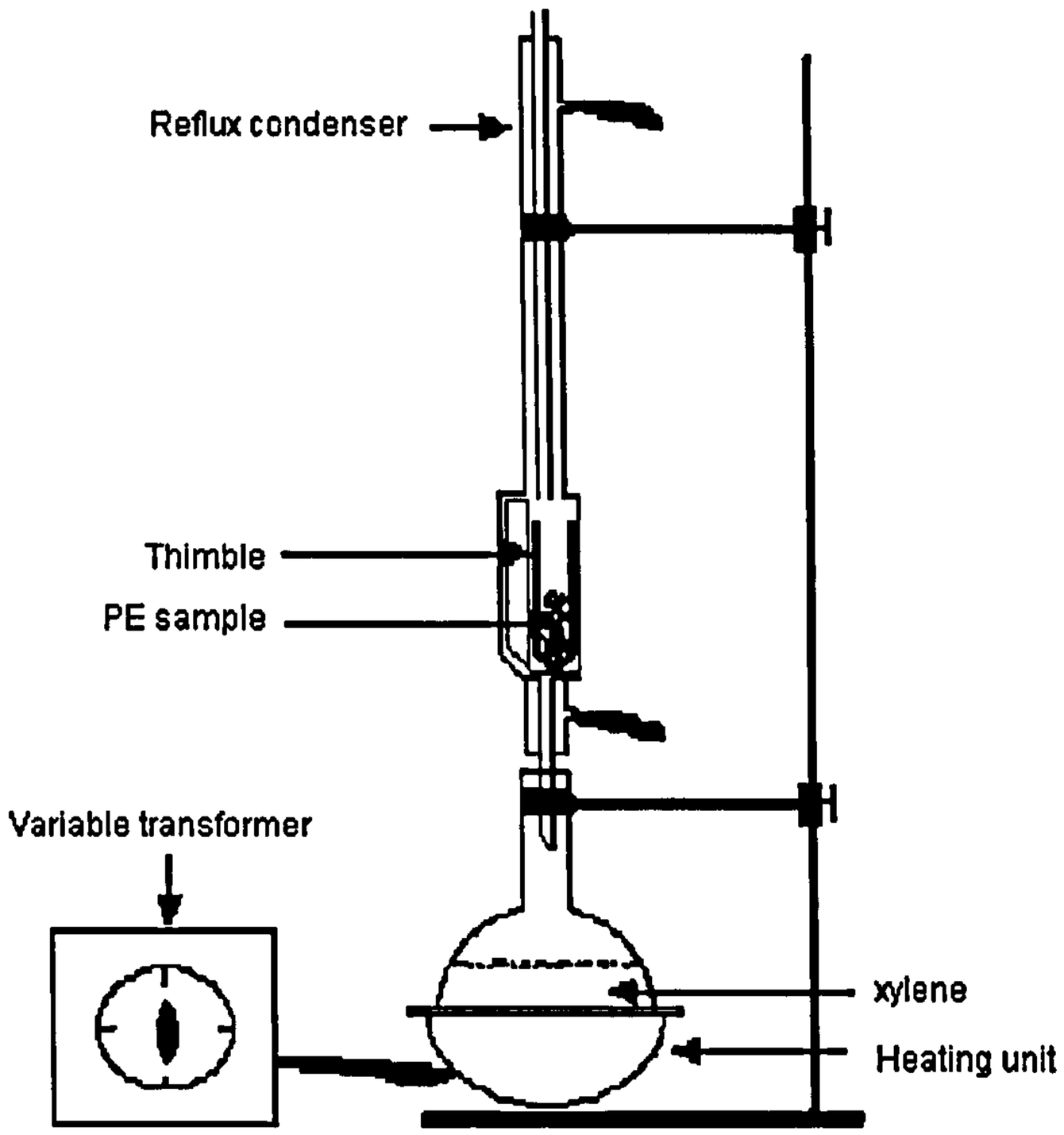

Figure 3.13. Schematic illustration of the Soxhlet extraction set-up.

Microwave extraction method

An extraction procedure which involved the use of a microwave oven was developed during the course of this project. 20 ml of xylene was placed in a glass vial along with 1 g of microtomed PE film. A glass stopper was used to seal the vial. The vial and its contents were placed in a microwave oven (650 W) and heated under full power for 15 min. The content of the vial was transferred to a beaker with 80 ml methanol and then cooled in a refrigerator for one hour. The precipitated polymer was filtered using a standard filtering apparatus. A sample of the filtered solution was taken for HPLC analysis.

3.3.5. Enthalpy of Fusion

A Perkin-Elmer DSC-7 instrument was used to measure the enthalpy of fusion of the PE samples. The enthalpy of fusion was measured by integrating the area under the heat flow vs temperature trace. The data was normalised

by dividing the area by the sample mass. The integration was performed by specifying a temperature range between 50°C to 160°C as shown in Figure 3.14. The integration of the area was carried out by the DSC-7 software. A minimum of six samples per polymer sample type were used.

The crystallinity was calculated by assuming that a sample of 100% crystalline would yield an enthalpy of fusion of 293 J/g [Mathot and Pijpers, 1983]. A sample mass of 12 ± 2 g was used throughout the study. The PE sample was heated from 30°C to 200°C at heating rate of 10 °C/min under nitrogen. The nitrogen flow rate was set at 50 ml/min. Prior to conducting the DSC experiments, the instrument was calibrated using pure Indium (melting temperature 156.6°C).

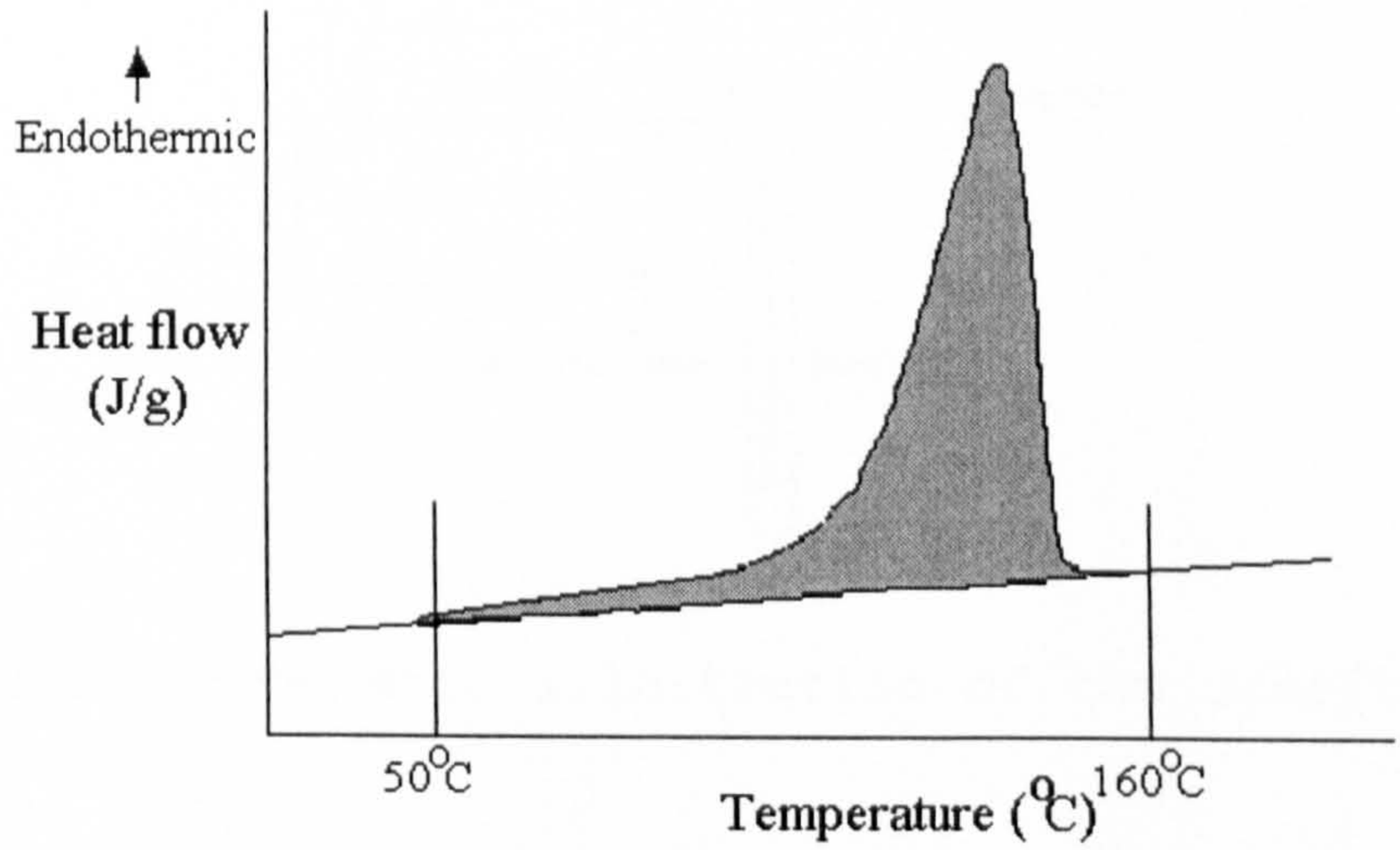

Figure 3.14. A typical DSC trace for a PE sample.

3.3.6. Density Measurements

The density column contains a mixture of two liquids whose density varies along a linear scale from top to bottom of a density column. The two liquids used in this experiment were isopropanol (0.785 g/ml) and diethylene glycol (1.11 g/ml). With reference to Figure 3.15, flask A contained 61.9% isopropanol and 38.1% diethylene glycol. Flask B contained 40.2% isopropanol and 59.8%

diethylene glycol. This gave a density range of 0.07 g/ml from the top to the bottom of the column i.e., the minimum density at the top was 0.91 g/ml and the maximum density at the bottom was 0.98 g/ml. The density column was left for 24 hours to equilibrate. The column was calibrated using reference floats of known density. The temperature of the coloumn was maintained at 23 °C. A mesh basket, suspended from a motor at the top of the column, was used to introduce the specimens into the density column. The samples were left to equilibrate for a period of 24 hours after which their relative position were noted. The density of each specimen was determined from their relative position and the calibration curve.

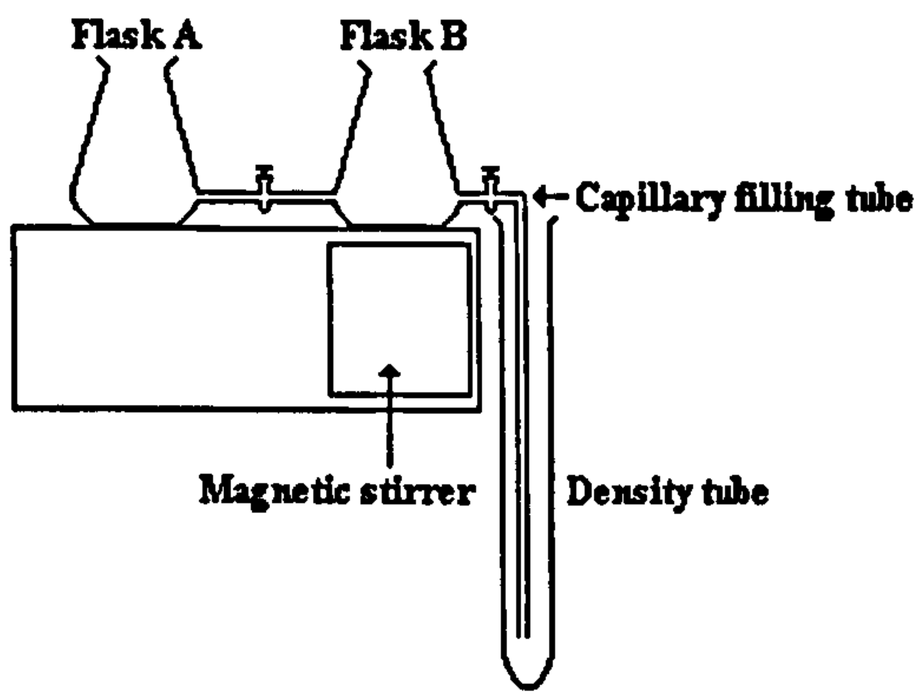

Figure 3.15. Schematic illustration of the density column setup.

3.3.7. Gel Content

The gel content of the PE samples were determined in compliance with the ASTM D 2765-90. The insoluble fraction in a PE sample was extracted using the Soxhlet apparatus described previously in section 3.3.4. Xylene was used as the solvent.

3.4. Mechanical Testing

3.4.1. Macro-Tensile Testing

The tensile tests were carried out in compliance with ISO 6259-3 using a computer controlled mechanical testing

machine (Instron 4206). The cross-head speed used was 1 mm/min and the modulus recorded as the secant modulus at 2% strain. All the tensile tests were conducted at 23°C temperature and in a humidity controlled laboratory. The dimensions of the tensile specimens used were described in section 3.2.1. A minimum of six samples per sample type were used.

3.4.2. Micro-Tensile Testing

The tensile tests on the thin films were carried out on an Instron 1026 tensile testing machine which was connected to a PC for data acquisition and manipulation. The machine was equipped with pneumatic grips and the grip-to-grip separation was 10 mm with an overall specimen length of 30 mm. A cross-head speed of 1 mm/min was used. The secant modulus at 2% strain was recorded. The average dimensions of the micro-tensile specimens were 70 μm thick x 35 mm total long x 17 or 12 mm width depending on the wall thickness of the pipe wall. All the tensile tests were conducted at 23°C temperature and in a humidity controlled laboratory. A minimum of six samples per polymer type were used.

3.4.3. Fatigue Testing

Single-edge-notched (SEN) specimens were used for the fatigue experiments. The fatigue tests were carried out on an Instron 8032 servo-hydraulic machine using a sinusoidal wave with a constant loading rate of 1.5 kNs^{-1}. A stress ratio of 0.1 was used along with a peak stress of 8 MPa. The peak stress chosen was approximately 33% of the yield stress for the Eltex resin and 44% of the yield stress for the Rigidex resin. An environmental chamber was used to maintain the sample temperature at 30°C. An extensometer was mounted on the SEN specimens to monitor the crack opening displacement. A schematic illustration of the fatigue set-up is shown in Figure 3.16. The accuracy of the extensometer was ±5 μm. The fatigue machine was connected to a PC for data acquisition. The

stress and crack opening were monitored per cycle employing a software which was written in this study.

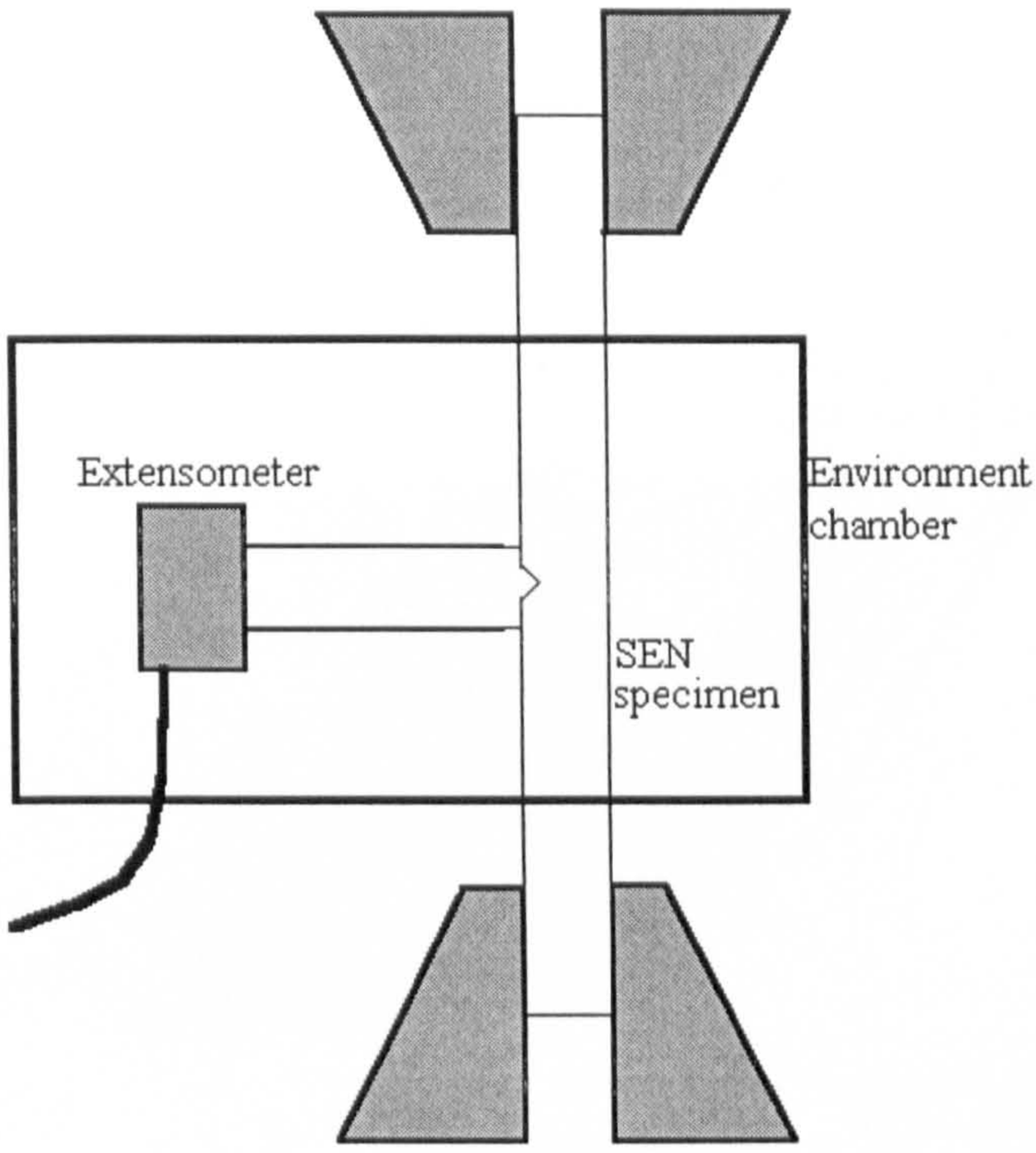

Figure 3.16. Illustration of the fatigue experiment set-up.

To prevent the sample from slipping in the jaws, the grips on the Instron fatigue machine were modified as shown in Figure 3.17.

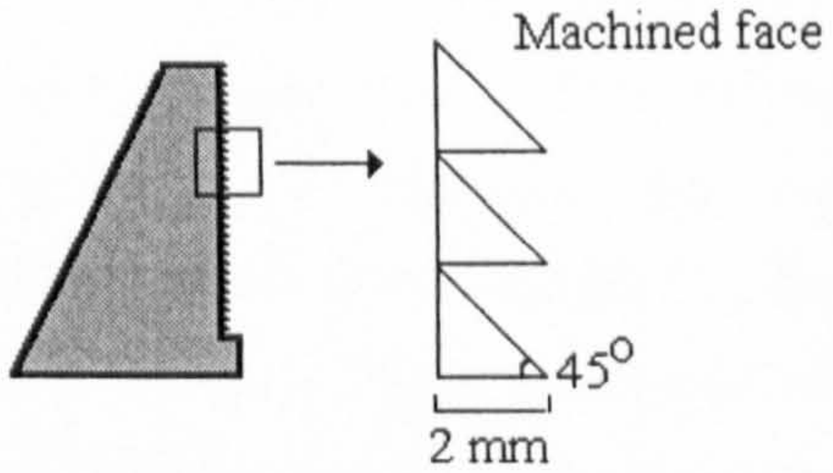

Figure 3.17. Schematic illustration of the grip-face modification.

Fracture toughness (J_{1c})

The method presented in the second chapter (Literature Review) by Strebel and Moet [1992] for determining the value of the J-integral at crack initiation was used in this study. A computer and data acquisition card were connected to the fatigue machine. The written software was used to log the data during the fatigue test as shown in Figure 3.18.

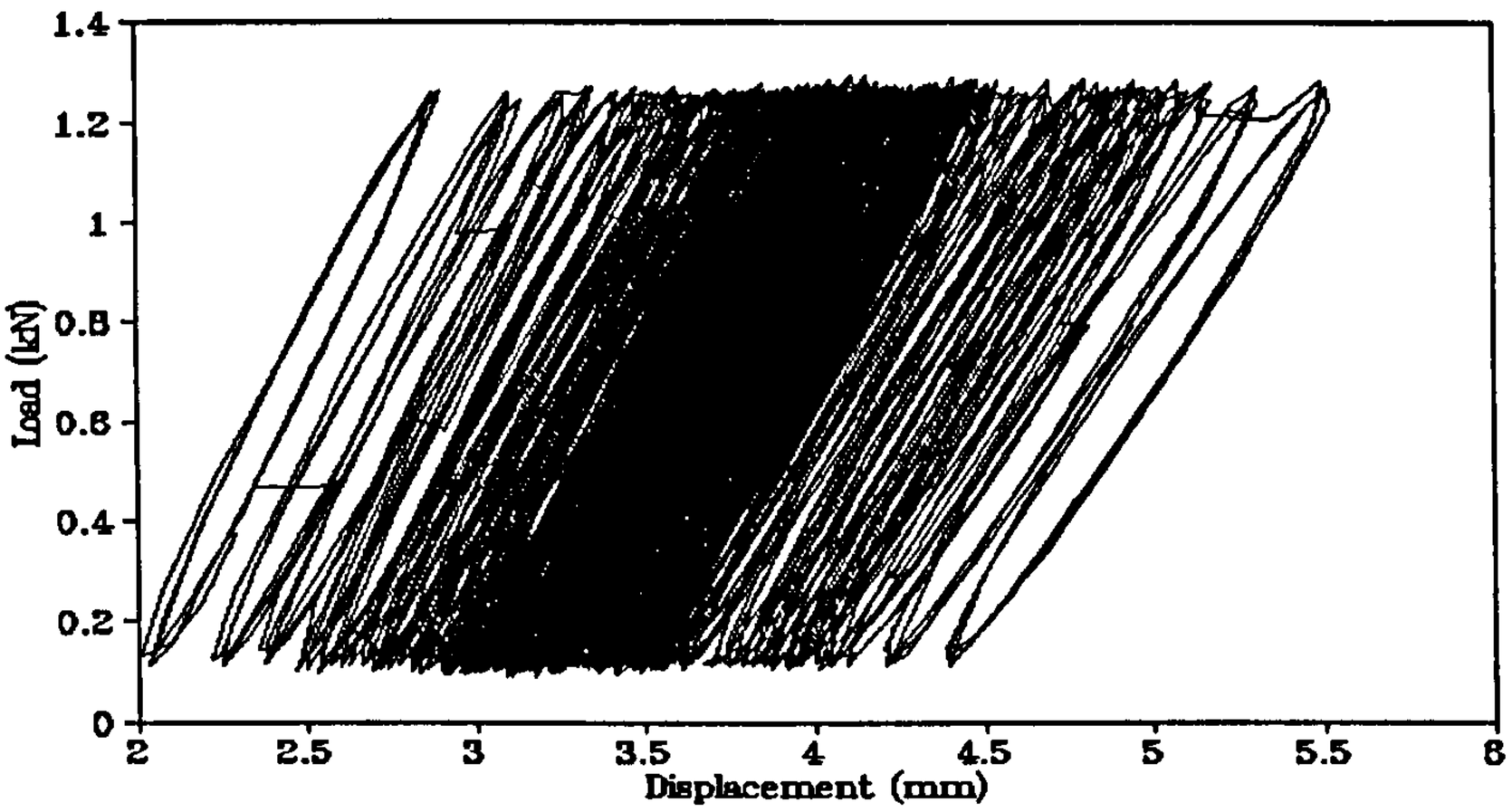

Figure 3.18. Hysteresis recorded during a fatigue test using a SEN specimen. The test specimen was obtained from a compression moulded Rigidex plaque.

3.4.4. Residual Stresses

A split-ring overlap method developed by Broutman and Bhatnager [1985] was used to measure the residual stresses in pipes. A ring approximately 10 mm wide was cut from a pipe. A single cut through the wall in the axial direction was introduced. The free ends relative to the other, were pushed to create an overlap. The extent of overlapping indicated the magnitude of the residual stresses. An approximation for the residual stress on the inner wall was obtained using the following relationship:

$$s_{inner} = 0.2277\ E\ (d/D_o)\ g(SDR) \qquad (3.1)$$

where,

s_{inner} = residual stress at the inner wall,

E = Young's modulus (500 MPa for Rigidex),

D_o = initial outside diameter,

g(SDR) = constant (0.0673 for 125-pipe), and

d = overlap (after 5 min).

3.5. Microscopy

3.5.1. Scanning Electron Microscopy (SEM)

A Cambridge S250 streoscan was used to study fracture surfaces produced from the fatigue testing. The SEM specimens were prepared by cutting the fractured specimen 10 mm away from the primary fracture zone. The sample was mounted on a specimen holder and a thin layer of gold was sputtered onto the specimens.

3.5.2. Polarised Light Optical Microscopy

A Leitz Aristomet polarised light microscope was used to study the microstructure and the nature of damage development in the SEN specimens. Microtomed films, 30 μm thickness, were used in this study.

CHAPTER FOUR

CHAPTER FOUR

OXIDATIVE STABILITY OF PE PIPE RESINS

4.1. Introduction

This chapter discusses the oxidative stability of the Rigidex, Aldyl A and Eltex pipe resin systems investigated in this study as a function of the specified ageing conditions. Other issues considered were as follows: (i) the scatter in the OIT test and an investigation to reduce the observed scatter; (ii) the selection of an appropriate OIT test condition which could be applied to the three different PE resin systems; (iii) explanations for the observed trends in OIT results; (iv) the development of a test method involving HPLC analysis to measure the concentrations of the additives; and (v) a comparative study on the relative sensitivity of the OIT test, HPLC analysis and FTIR spectroscopy to detect the ageing process.

4.2. Factors Affecting The OIT value

In the early stages of this study, it was noticed that there was a spread in the OIT results of up to ±9 minutes. A brief programme of work was undertaken to investigate the influence of the possible reasons for the observed scatter. This included investigating sample mass, gas flow rate and the procedure for determining the onset of oxidation in the OIT test. The samples used in this work were taken from one compression moulded plaque made from Rigidex resin. This was done to reduce the material variability.

4.2.1. Sample Mass

Figure 4.1 shows the influence of sample mass on the OIT value for the Rigidex resin. A maximum sample mass of 14 mg was used. Above this mass, the sample came in contact with the DSC sample holder cover and the net result of this was significant scatter in the OIT value.

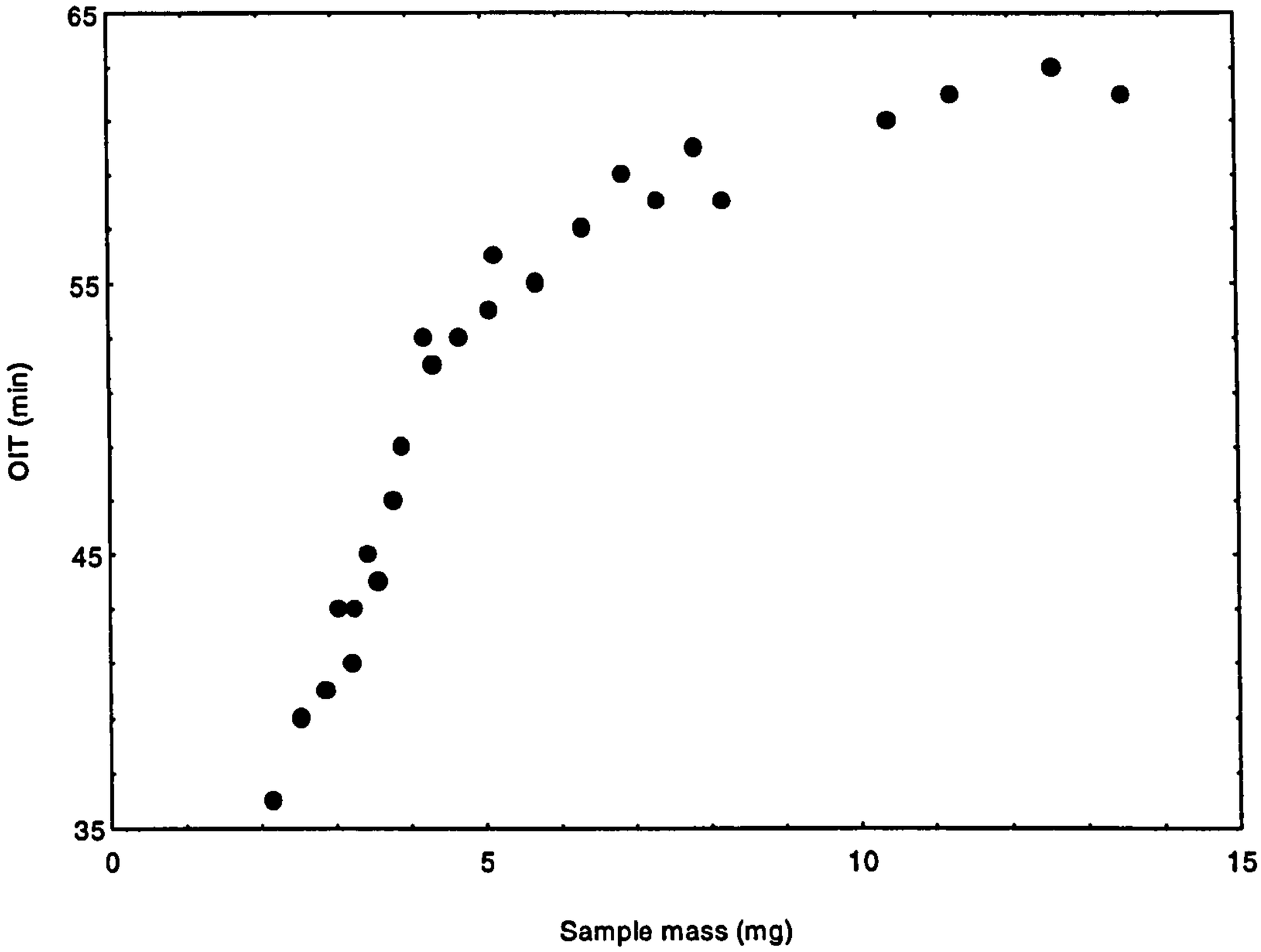

Figure 4.1. OIT as a function of sample mass.

With reference to Figure 4.1, an increase in the OIT value was observed up to about 5-6 mg. The increase was less profound above this sample mass range. The observed trend may be due to one or more of the following reasons. (i) Surface area of the OIT sample. As the surface area increases, the induction time decreases. (ii) Instrumental thermal lag. As the sample mass increases the thermal lag will also increase causing a delay in the OIT value. Evidence for the latter was supported by inspecting the effect of sample mass on the melting points as shown in Figure 4.2.

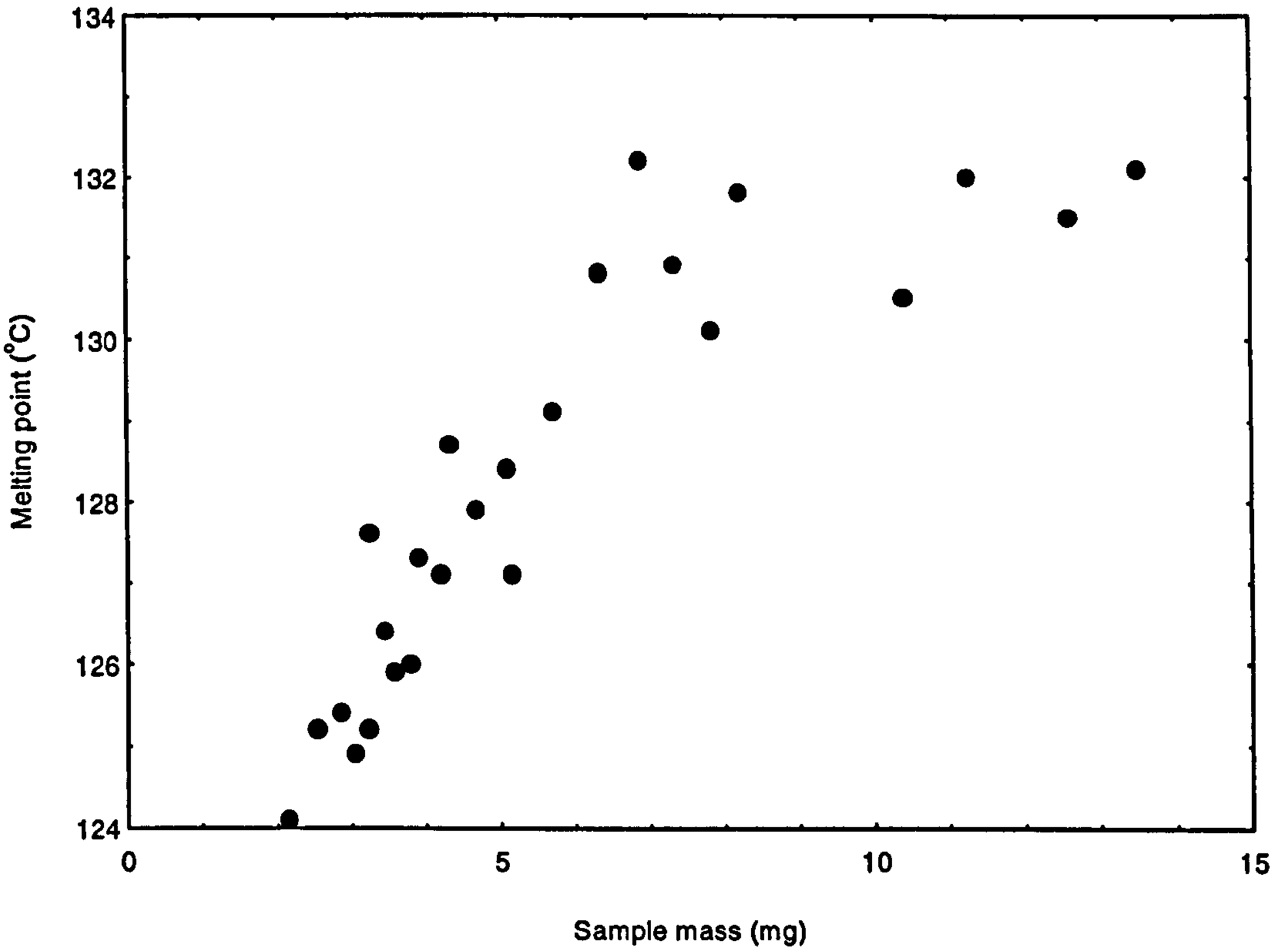

Figure 4.2. Melting point as a function of sample mass. The samples used were from the same compression moulded plaque made from the Rigidex resin.

Karlsson et al. [1990] reported on the variation in the OIT value with sample mass. They used an oxidation induction temperature test rather than an oxidation induction time test. However, their results showed an increase in the oxidation induction temperature as the sample mass was reduced. This is contrary to what would be expected. Since, they did not offer any explanations for their observation, a brief study was undertaken to establish the relationship between the oxidation induction temperature and sample mass. The oxidation induction temperature test was carried out by heating the sample from 40°C at a heating rate of 10 °C/minutes in an oxygen environment. The appearance of an exotherm was defined as the oxidation induction temperature. A plot of

the oxidation induction temperature versus the sample mass is shown in Figure 4.3.

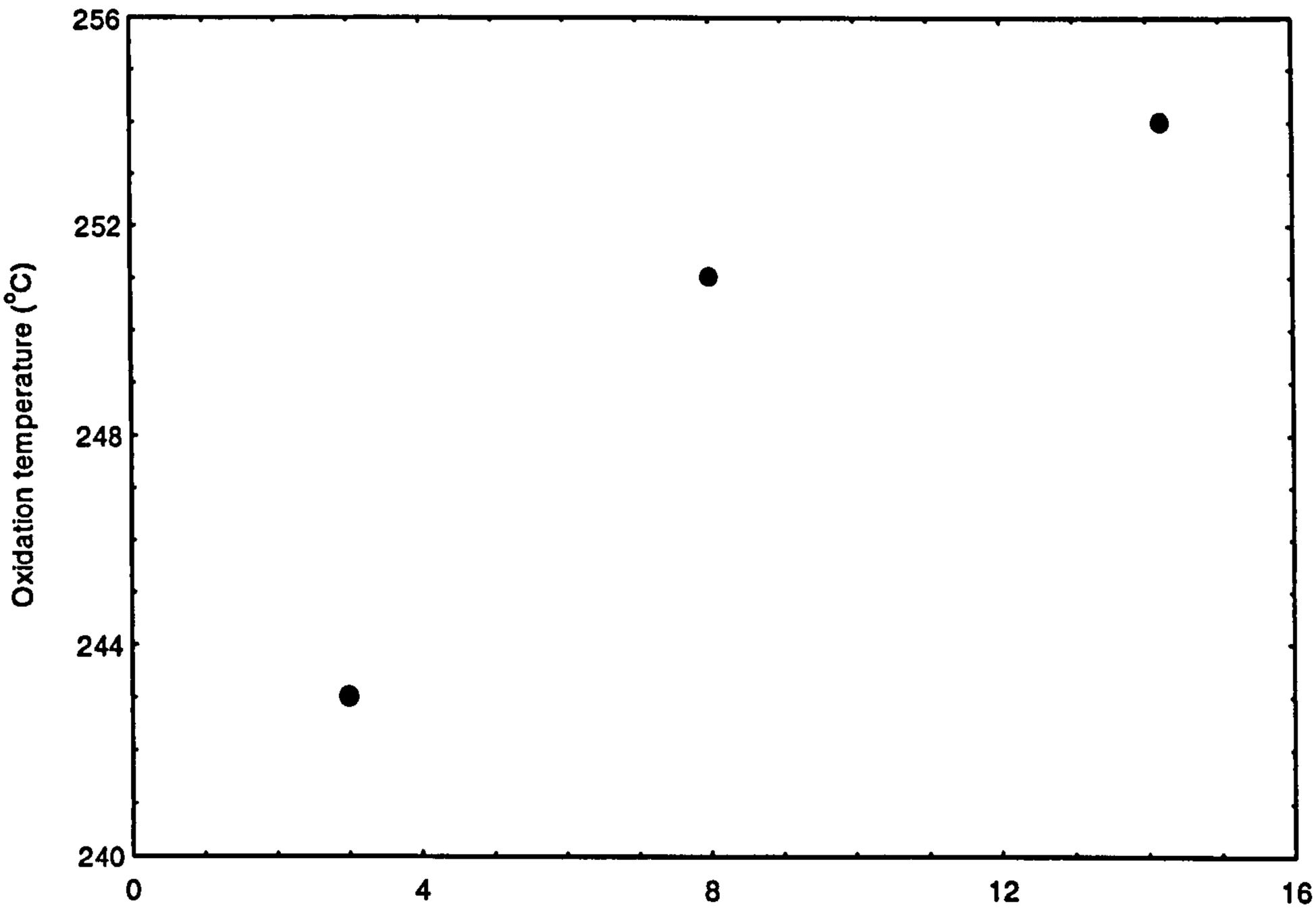

Figure 4.3. Oxidation induction temperature as a function of sample mass. The samples used were from the same compression moulded plaque made from the Rigidex resin.

With reference to Figure 4.3, an apparent increase in the oxidation induction temperature with sample mass was observed. This trend is obviously contrary to that reported by Karlsson et al. [1990].

4.2.2. Gas Flow Rate

In this investigation, the gas flow rate was varied from 10 to 50 x 10^{-6} m^3/minute and the sample mass was maintained at approximately, 12 ± 1 mg. Figure 4.4 shows the relationship between the OIT value as a function of the gas flow rate for the Rigidex resin.

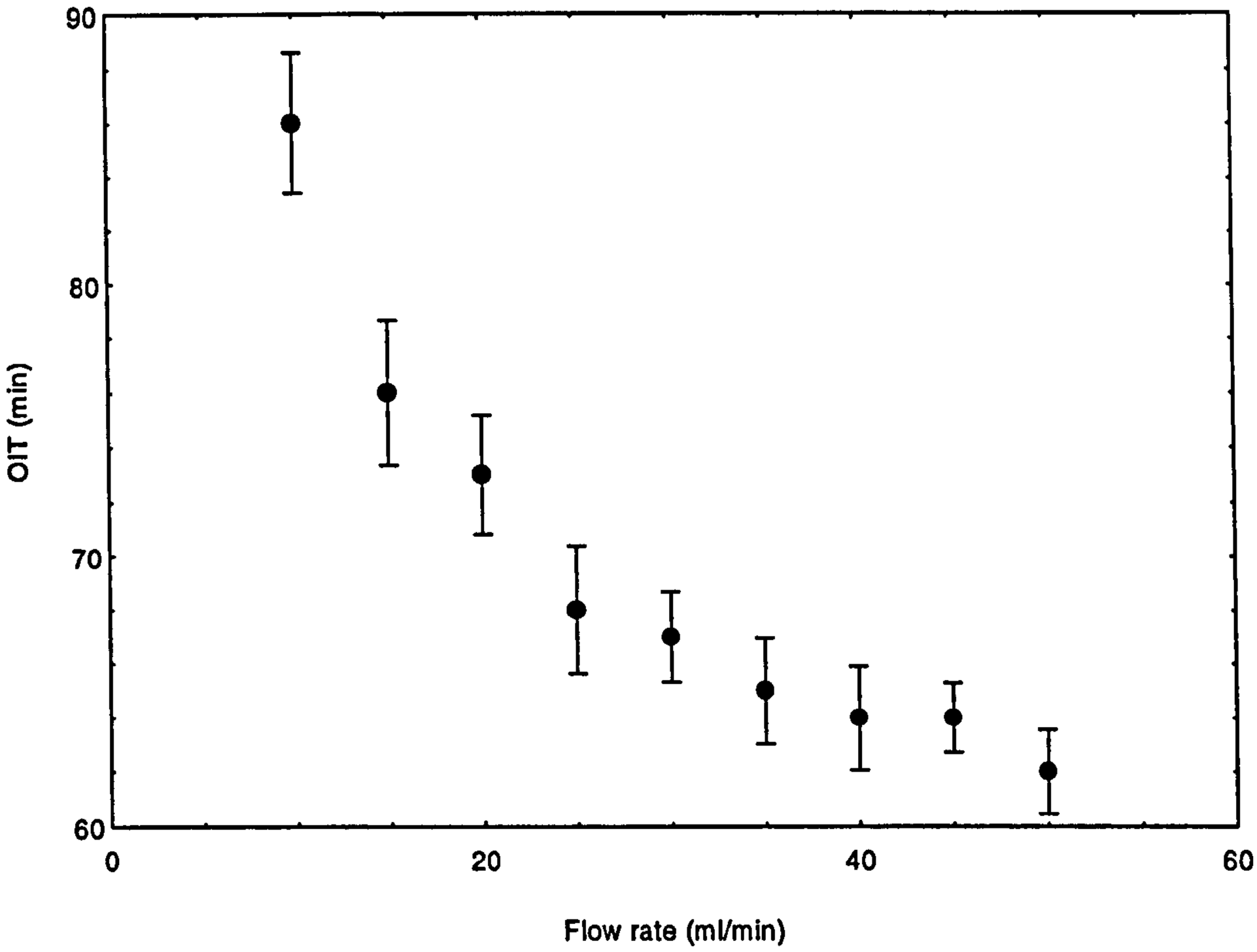

Figure 4.4. OIT as a function of oxygen flow rate. The samples used were from the same compression moulded plaque made from the Rigidex resin.

It is clear from Figure 4.4 that the OIT value decreased as the gas flow rate was increased. It is proposed that the observed reduction in the OIT value may be attributed to an increase in loss of antioxidants from the OIT sample as the gas flow rate was increased. This result is in a good agreement with work reported by Karlsson et al. [1990].

4.2.3. Determination Of The OIT Value

Another possible reason for the observed scatter in the OIT results is in the method used to determine the onset of oxidation. Figure 4.5(i) illustrates an ideal OIT trace and Figure 4.5(ii) illustrates a typical OIT trace which is representative of those obtained in this study.

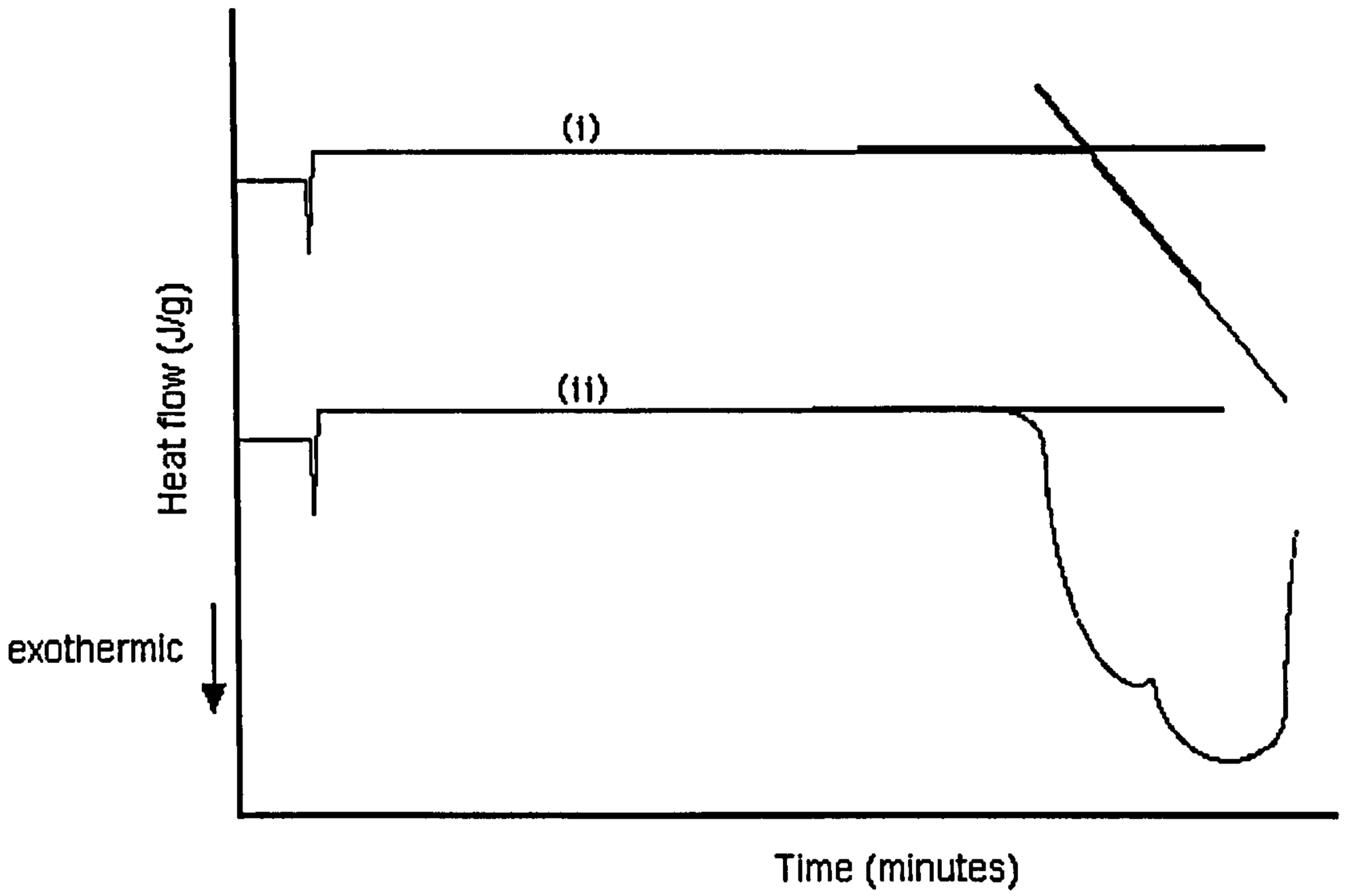

Figure 4.5. (i) An ideal and (ii) an example of a typical OIT traces obtained in this study. The non-linearity made it difficult to specify the location of the tangent to the exothermic peak.

Figure 4.5(ii) illustrates the difficulty in defining a tangent to the exothermic peak due to its non-linearity. This non-linearity in the exothermic peaks was found to give a error of approximately ±9, ±4 and ±3 minutes in the OIT for the Eltex, Rigidex and Aldyl A resins, respectively.

4.3. Arrhenius Relationship

An investigation was undertaken to select an appropriate OIT test temperature for the three polymer systems. This study was necessary as the additive packages in the three polymers were different. Hence, it was important to select an appropriate temperature for the OIT test which would be suitable for the three polymers. In addition to this, if a linear Arrhenius relationship was obtained,

then it could be assumed that the degradation mechanism(s) were similar over the specified temperature range. Therefore, OIT tests were conducted over a temperature range of 180-230°C. From the Arrhenius equation:

$$\ln (OIT) = A + E_a/RT \qquad (4.1)$$

A = intercept
R = gas constant
E_a = activation energy
E_a/R = slope

A linear relationships was obtained from plotting ln (OIT) versus 1/T for the three polymers investigated in this study, see Figures 4.6 to 4.8.

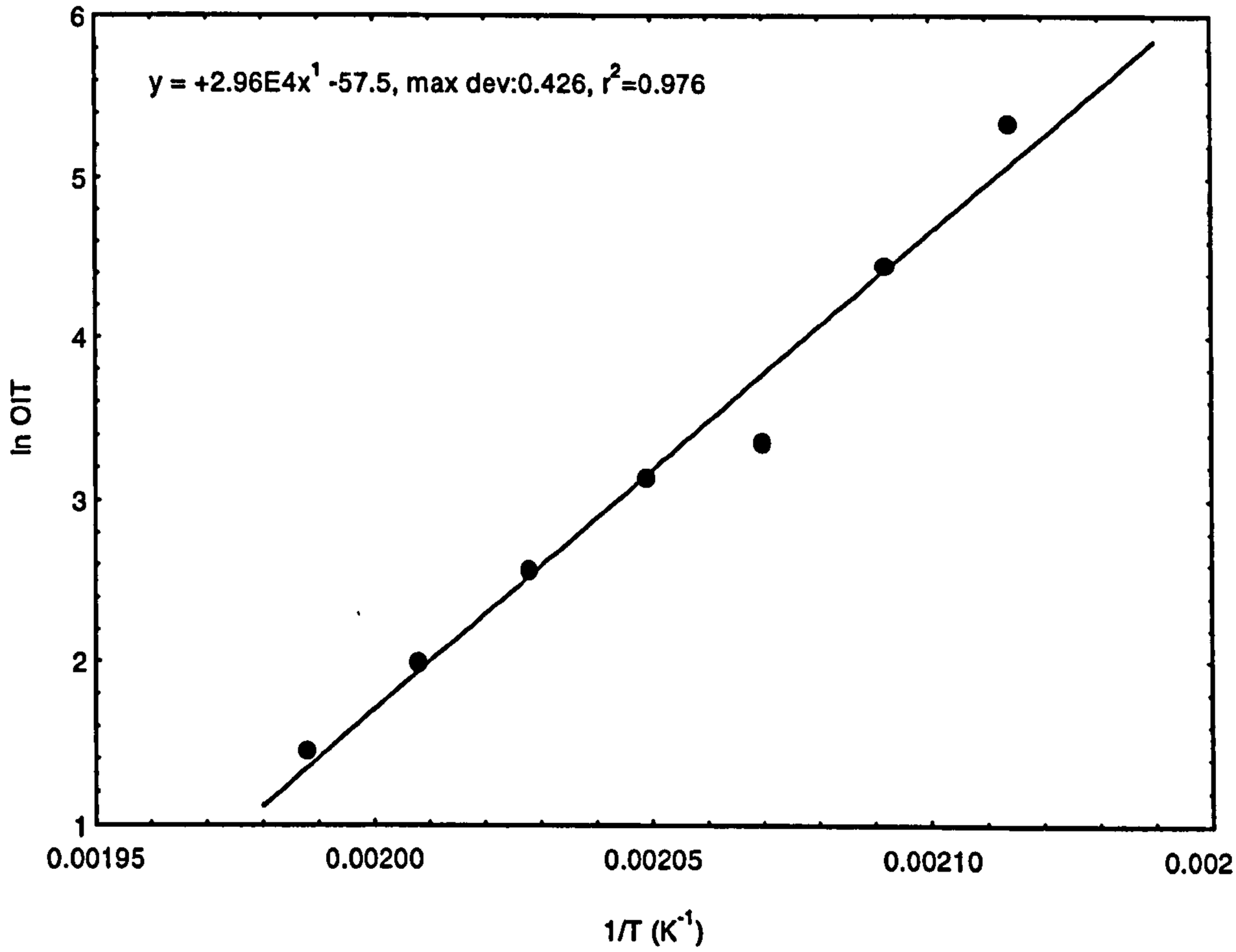

Figure 4.6. Arrhenius plot for the Eltex resin. Virgin Eltex pellets were used for theses experiments.

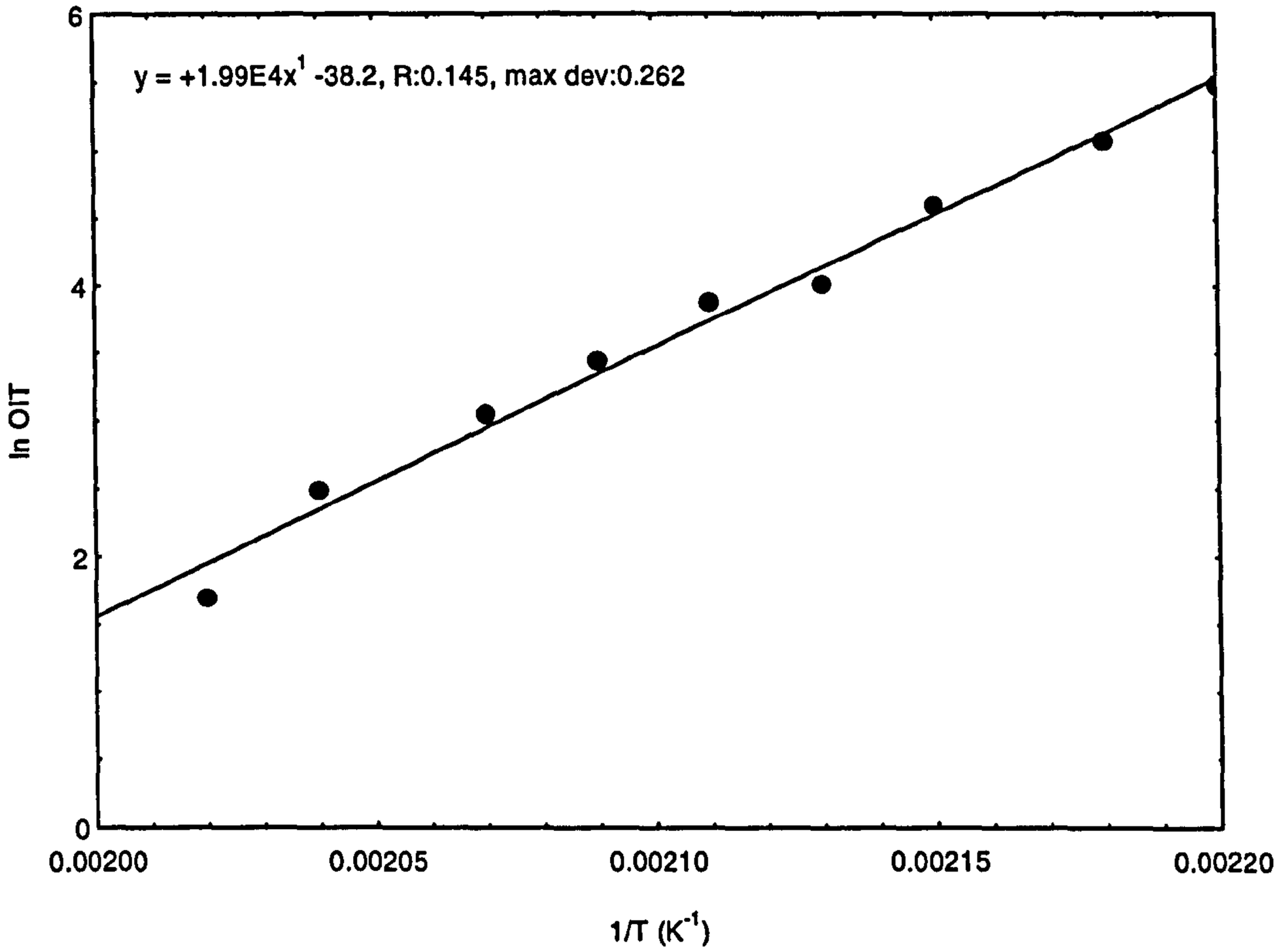

Figure 4.7. Arrhenius plot for the Rigidex resin. Virgin Rigidex pellets were used for theses experiments.

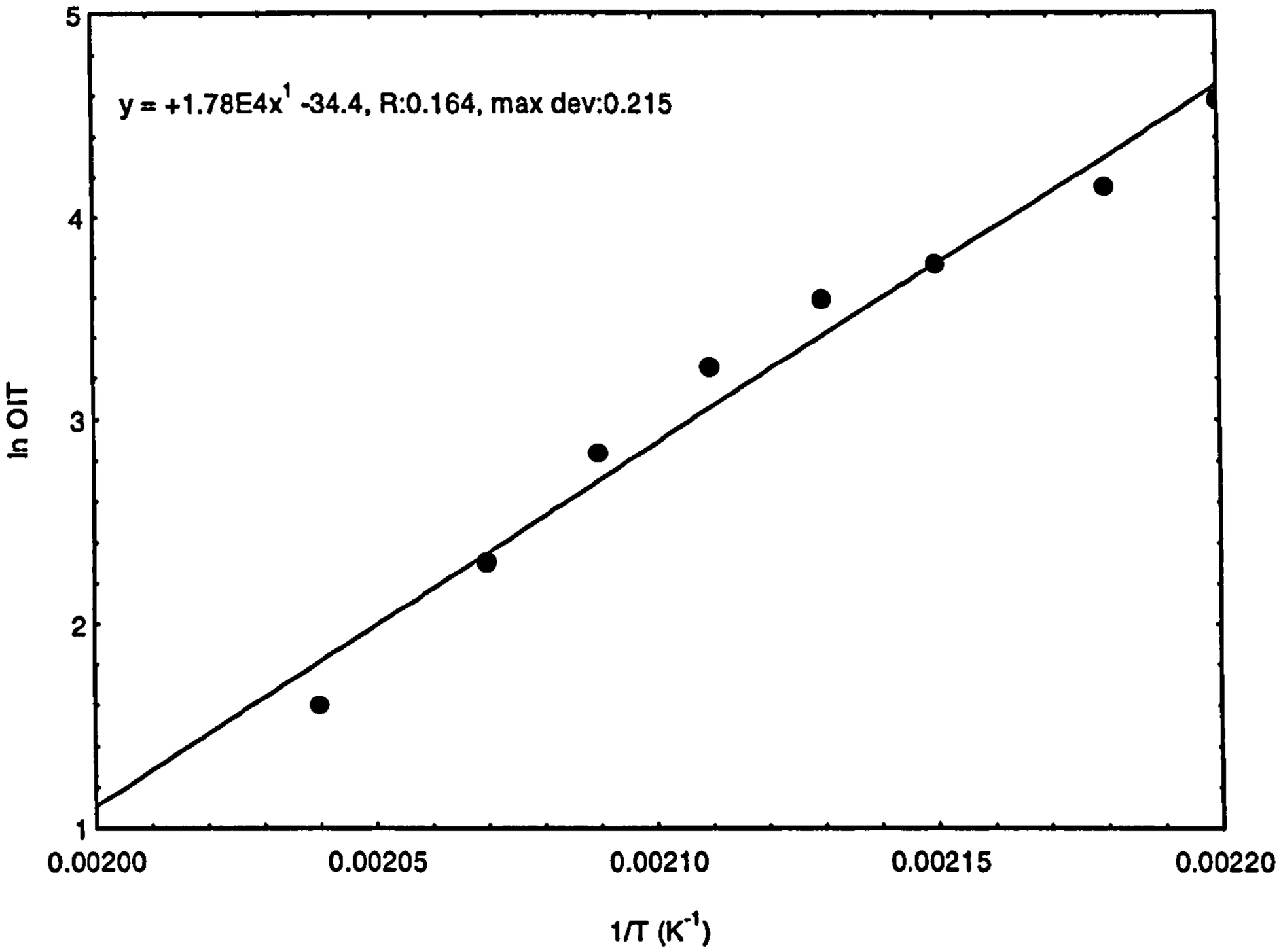

Figure 4.8. Arrhenius plot for the Aldyl A resin. The OIT samples used were obtained from the surface of a virgin Aldyl A pipe.

The activation energies of oxidation (E_a), temperature range used and the range of OIT values obtained for the three resins are summarised in Table 4.1.

Table 4.1. A summary of the activation energies for oxidation for the three polymer systems along with the temperature range and corresponding OIT range at the minimum and maximum temperature ranges.

PE resin	E_a ($kJmol^{-1}$)	Temperature range (°C)	OIT range (min)
Eltex	246	200 - 230	207 - 4
Rigidex	165	180 - 220	239 - 5
Aldyl A	148	180 - 210	97 - 5

The OIT test temperature of 200°C was found to be suitable for the three polymer systems. Below 200°C, the induction time for the Eltex resin extended to more than five hours thus making the test impractical.

4.4. Interpretation Of OIT Traces

Most of the OIT traces obtained for the virgin and aged Rigidex and Eltex polymer systems resembled that shown in Figure 4.5(ii). The convoluted double exothermic peaks were often observed in the OIT traces. Unlike Rigidex and Eltex polymer resins, the Aldyl A resin showed only one major exothermic peak. However, the Aldyl A pipes which was aged in water for one year at 23°C displayed an additional small but detectable exothermic peak prior to the major exothermic peak as illustrated in Figure 4.9. According to the Gas Standard PL2/1, the onset of the first exothermic peak defines the OIT value.

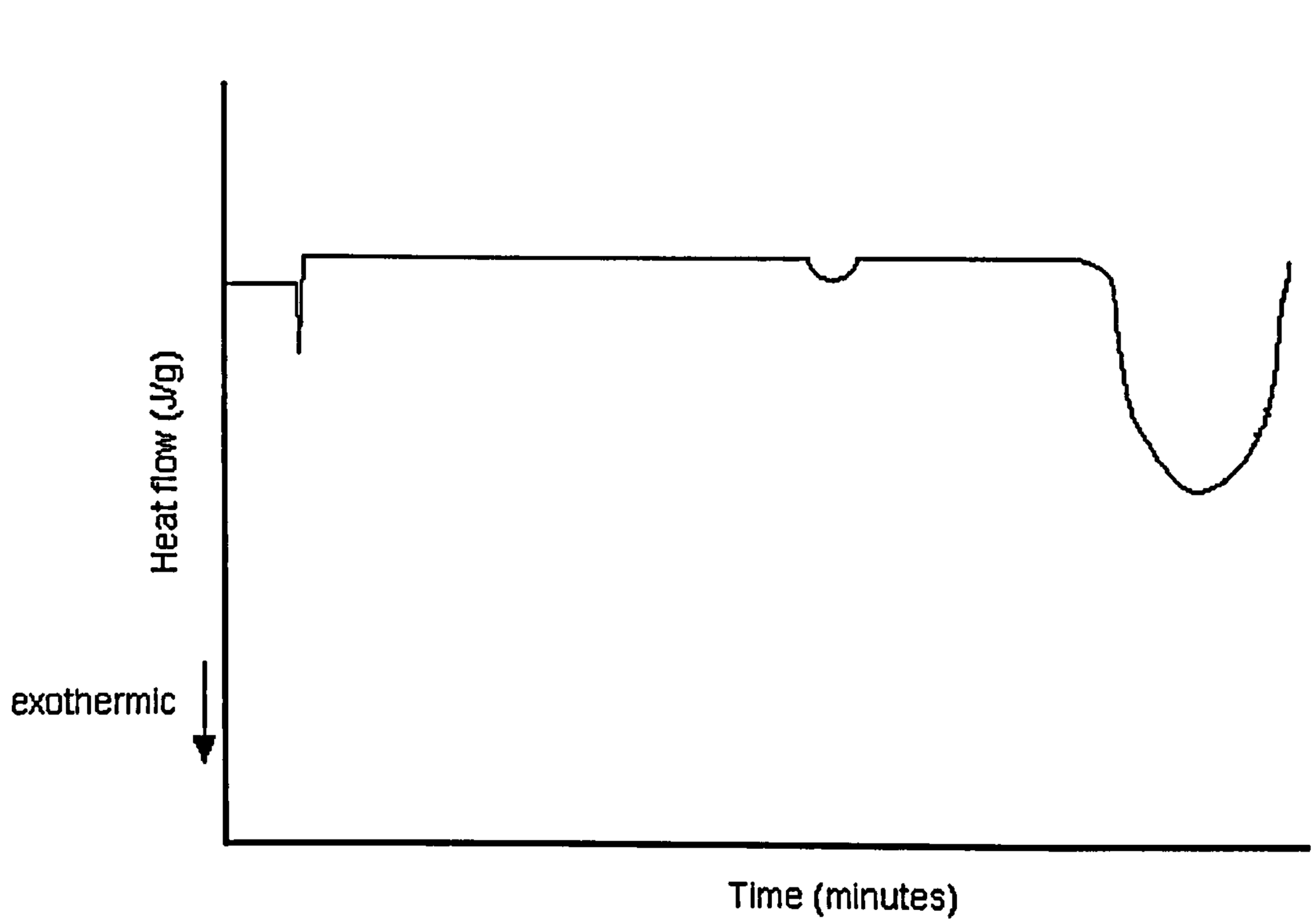

Figure 4.9. A typical OIT trace for the Aldyl A pipe aged in water for one year at 23°C.

A brief investigation was undertaken to try and explain the observed OIT trace shown in Figure 4.9. Samples were prepared from the surface of a virgin Aldyl A pipe and from the surface of the Aldyl A pipe which was aged in water for one year at 23°C. TGA, gel-content and FTIR analysis were used to assist in interpreting the OIT traces.

TGA:

The TGA experiments were carried out in oxygen at 200°C. This was similar to the test conditions used in the OIT experiments. For the virgin sample, there was about a 1% reduction in sample weight up to 25 minutes. This is believed to be due to vaporisation of additives and/or loss of moisture. After 25 minutes, the weight loss increased rapidly and the sample started to decompose as shown in Figure 4.10. This weight loss was attributed to thermo-oxidative decomposition of the sample.

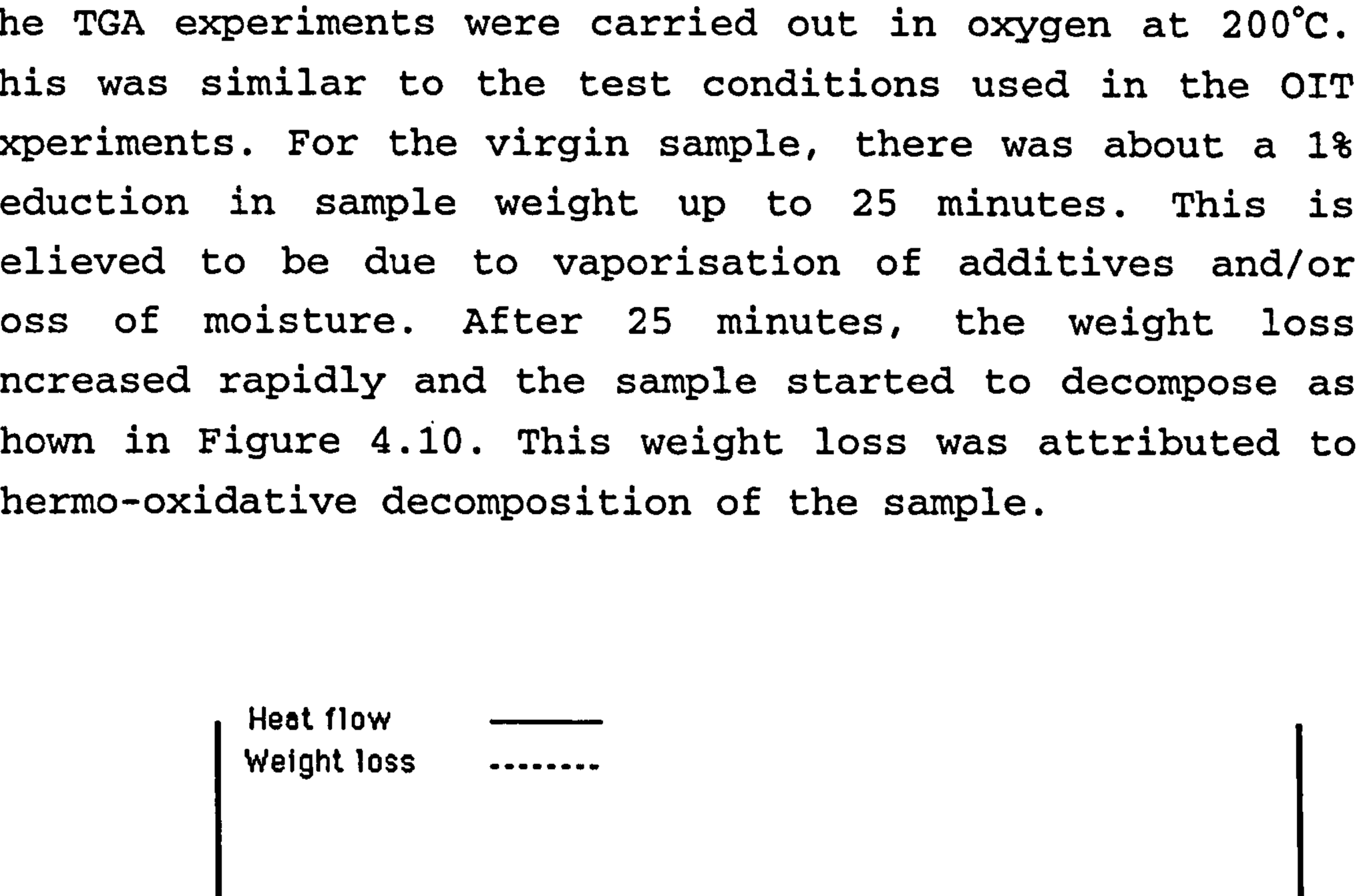

Figure 4.10. Superimposed TGA and OIT traces for the virgin Aldyl A polymer resin.

With reference to Figure 4.10, the TGA trace, the mass-loss after 25 minutes is seen to correspond to the onset of the exotherm in the DSC trace.

Gel-content and FTIR:

In the first series of experiments, the OIT tests were terminated at 23 minutes (just prior to the exothermic reaction shown in Figure 4.10) and the corresponding specimens were used for gel-content and FTIR analysis. According to the gel-content results, no cross-linking was found before 23 minutes for the virgin Aldyl A sample. Evidence for thermal oxidation was not detected via FTIR spectroscopy.

In the second series of experiments, the OIT tests were terminated after 25 minutes and the gel-content was measured. The presence of a gel content suggested that cross-linking had take place above and beyond approximately 25 minutes. An increase in the carbonyl index was also detected using FTIR spectroscopy indicating that thermo-oxidation had taken place.

In the third series of experiments, an Aldyl A pipe which was aged in water for one year at 23°C was used. The OIT tests were terminated after the first exothermic peak was detected at about 30 minutes, see Figure 4.11.

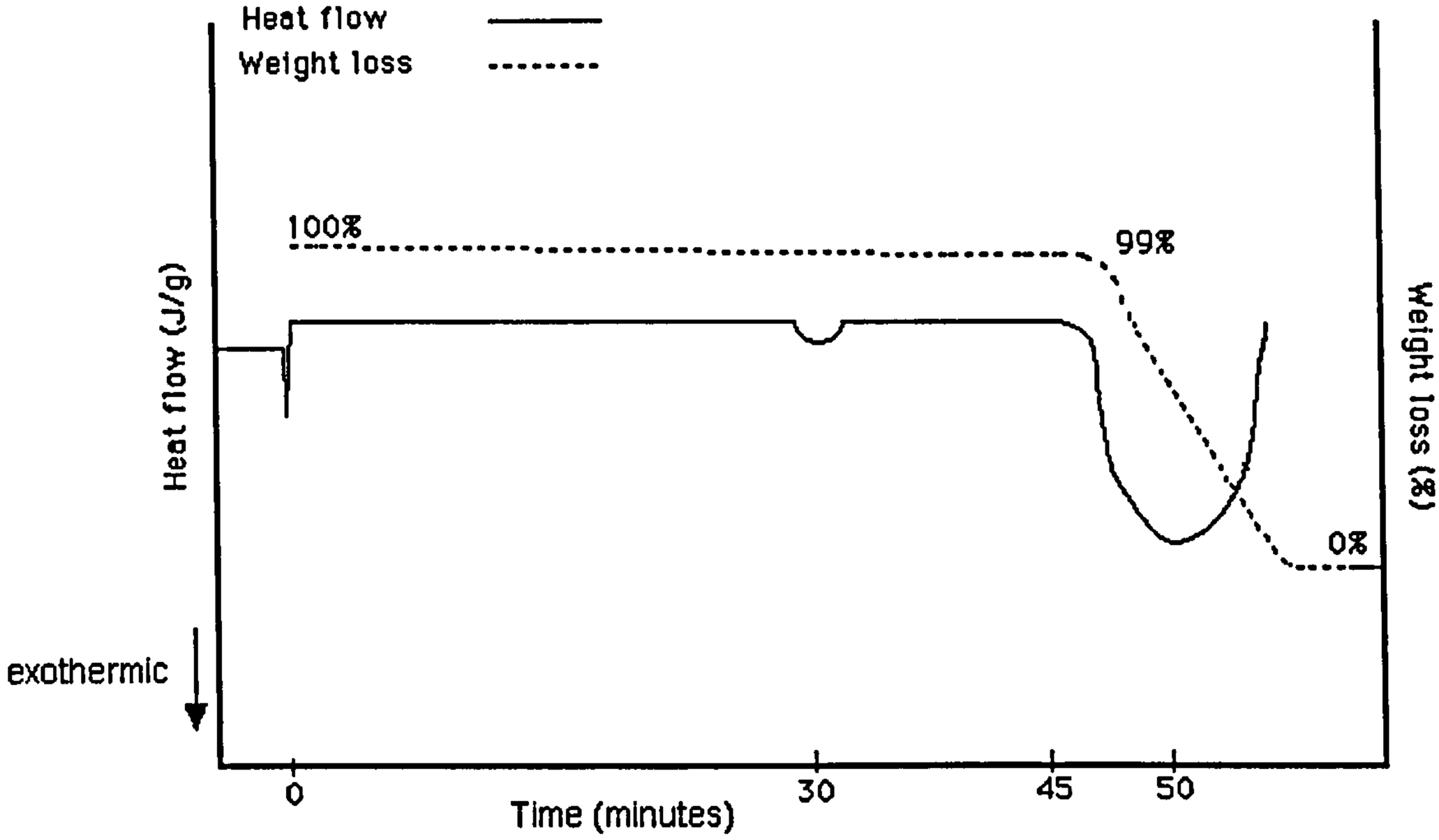

Figure 4.11. TGA and OIT traces for the Aldyl A polymer which was previously aged in water for one year at 23°C.

The gel-content results showed that approximately 12% of the sample had cross-linked. These specimens did not indicate the presence of oxidation when analysed using FTIR spectroscopy. Therefore, it is proposed that the first exothermic peak in Figure 4.11 may be attributed to the presence of a cross-linked fraction in the polymer. No gel fractions were obtained in the specimens where the OIT was terminated before 30 minutes.

In the final series of experiments, the OIT test was again terminated after the occurrence of the small first peak as shown in Figure 4.11. The OIT tests were then repeated using the same samples. In this case, only a major exothermic peak was detected. Since no information was available on the additive system used for the Aldyl A resin, it was difficult to give a definitive reason for

the observed first peak. However, the evidence suggests that the first peak may be due to the polymer containing a cross-linked fraction.

4.5. FTIR Spectroscopy And HPLC Analysis

The feasibility of using FTIR spectroscopy and HPLC analysis were evaluated to detect the oxidative stability of PE pipes as a function of the specified ageing conditions.

4.5.1. FTIR Spectroscopy

A summary of the relevant infrared absorption peaks for polyethylene pipe material was compiled and is listed in Appendix 3. Relevant functional groups of interest in this study were oxidised products or by-products produced during ageing. These included carbonyl, hydroperoxides and several vinyl groups [Konar and Ghosh, 1988].

Figure 4.12 shows the absorbance of the methylene peak at 2018cm^{-1} (reference peak for normalised purposes) for each film plotted against its corresponding thickness. Since linear relationships were obtained for the three polymer resins used in this study, the peak at 2018cm^{-1} was considered suitable to be used as the internal standard for the three resins. This peak was assigned to the rocking mode of trans-methylene sequence and was said to be due to both crystalline and amorphous regions in PE [Wedgewood and Seferis, 1983]. Film samples from the same resin with identical thickness gave a spread of ± 0.02 in the absorbance for the peak at 2018cm^{-1}.

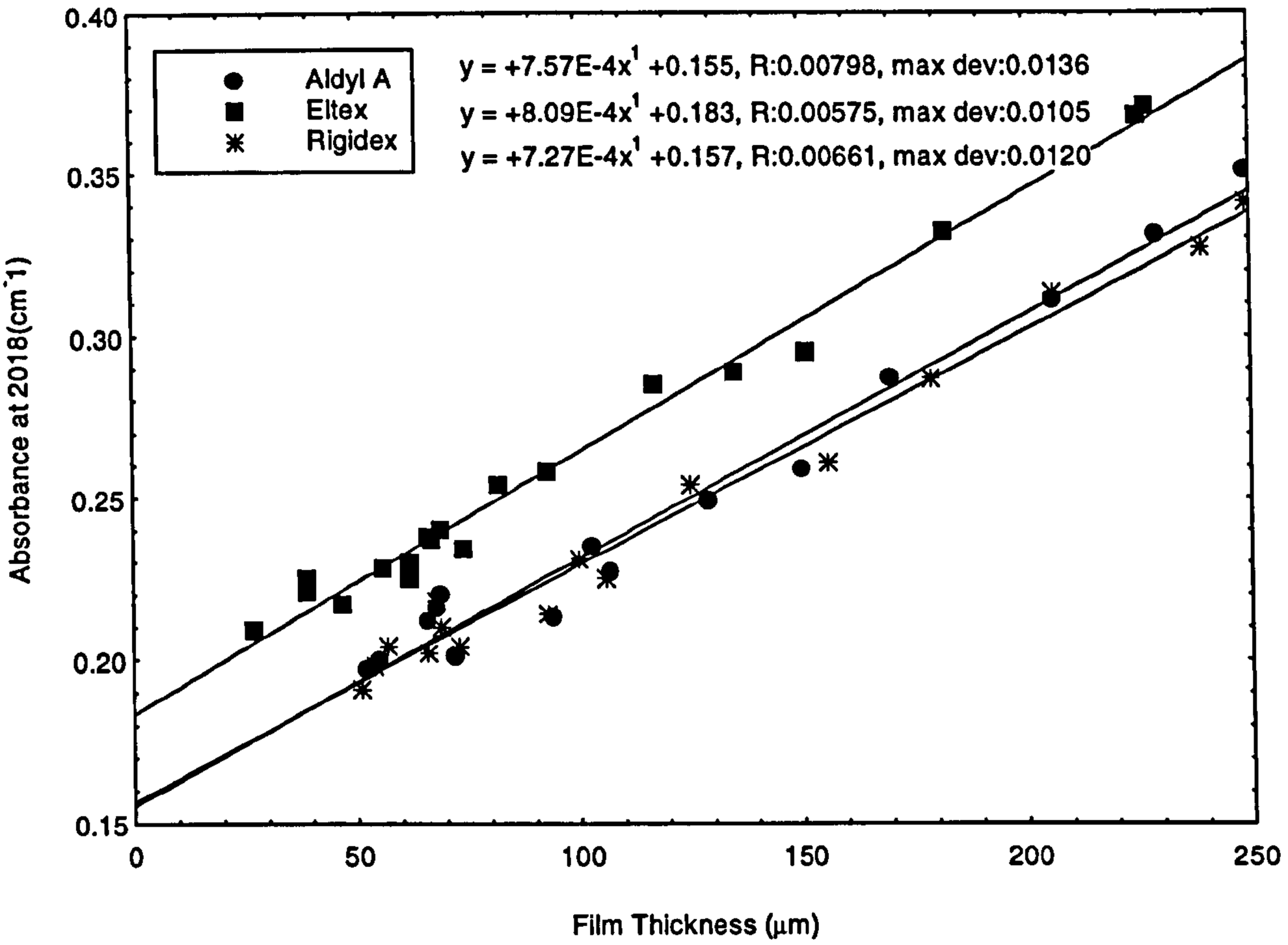

Figure 4.12. Absorbance at 2018cm^{-1} as a function of film thickness for the Aldyl A, Eltex and Rigidex polymer resins.

All the infrared data were normalised to the intensity of the internal standard at peak 2018cm^{-1}.

Figures 4.13 to 4.15 show the normalised absorbance of hydroperoxide, vinyl and carbonyl groups plotted as a function of ageing time.

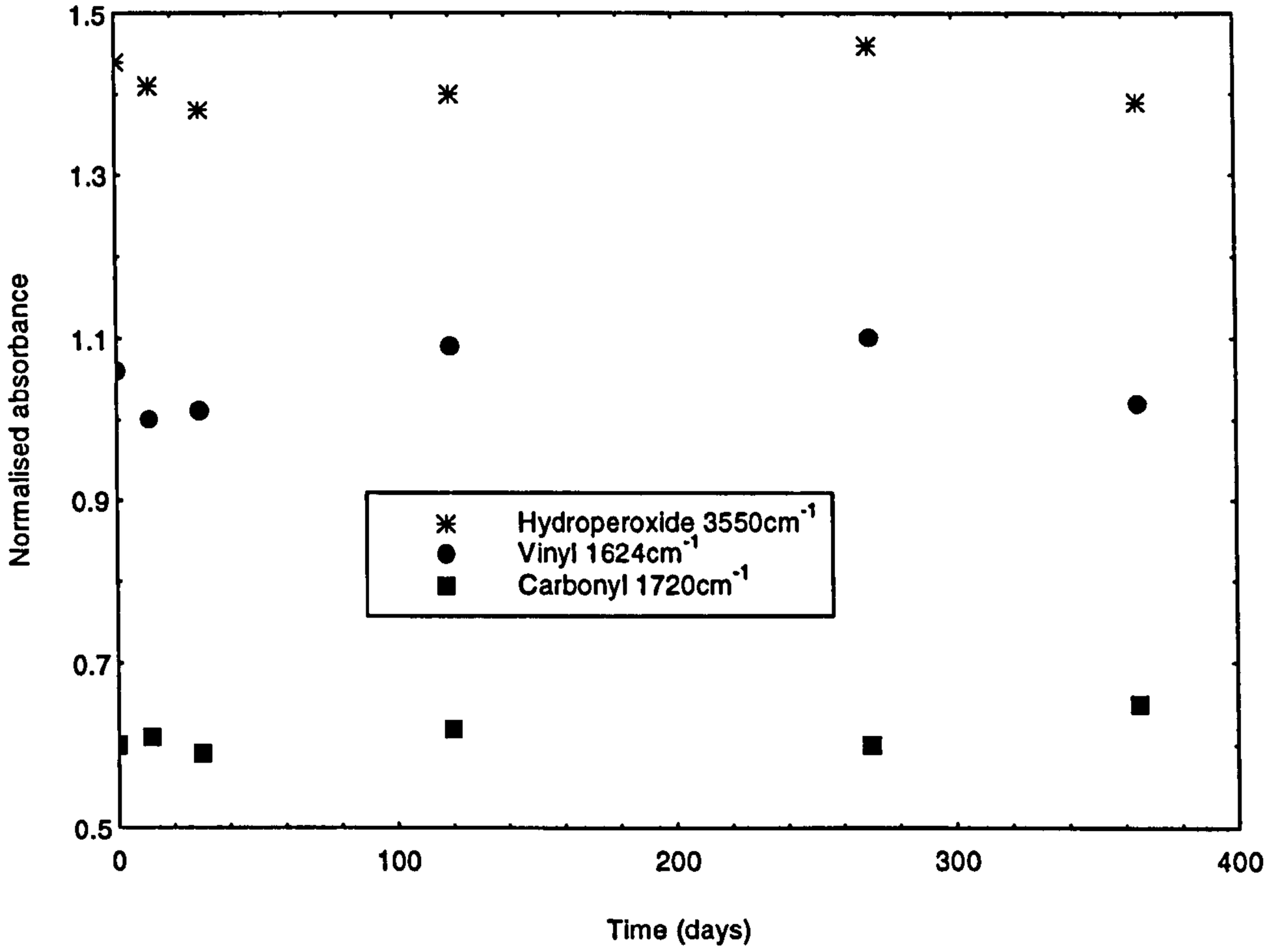

Figure 4.13. Normalised absorbance for the hydroperoxide (3550cm^{-1}), ketone (1720cm^{-1}) and terminal vinyl (1624cm^{-1}) groups for Aldyl A film aged in an air circulating oven at 80°C as a function of time.

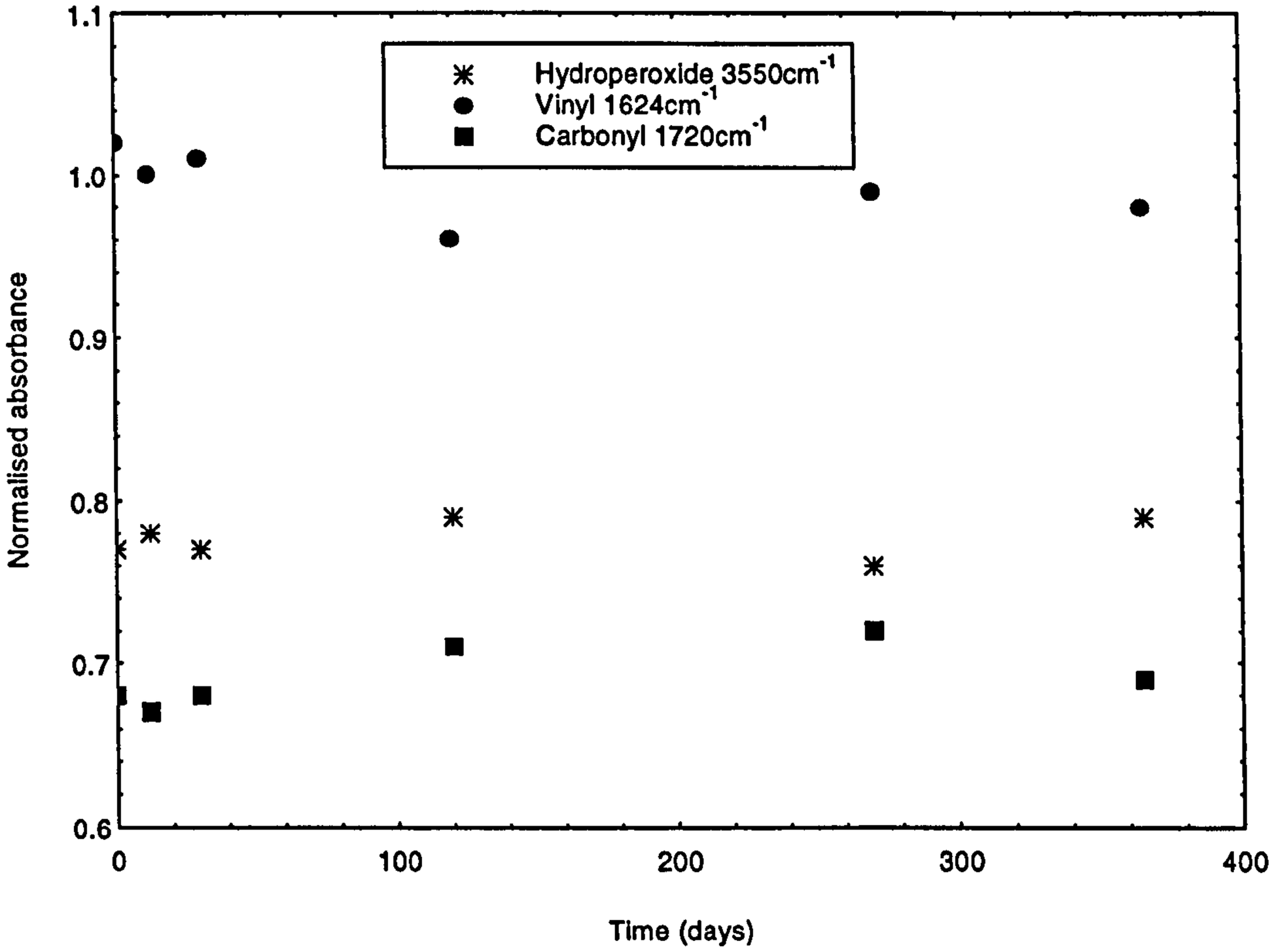

Figure 4.14. Normalised absorbance for the hydroperoxide ($3550cm^{-1}$), ketone ($1720cm^{-1}$) and terminal vinyl ($1624cm^{-1}$) infrared groups for Rigidex film aged in an air circulating oven at 80°C as a function of time.

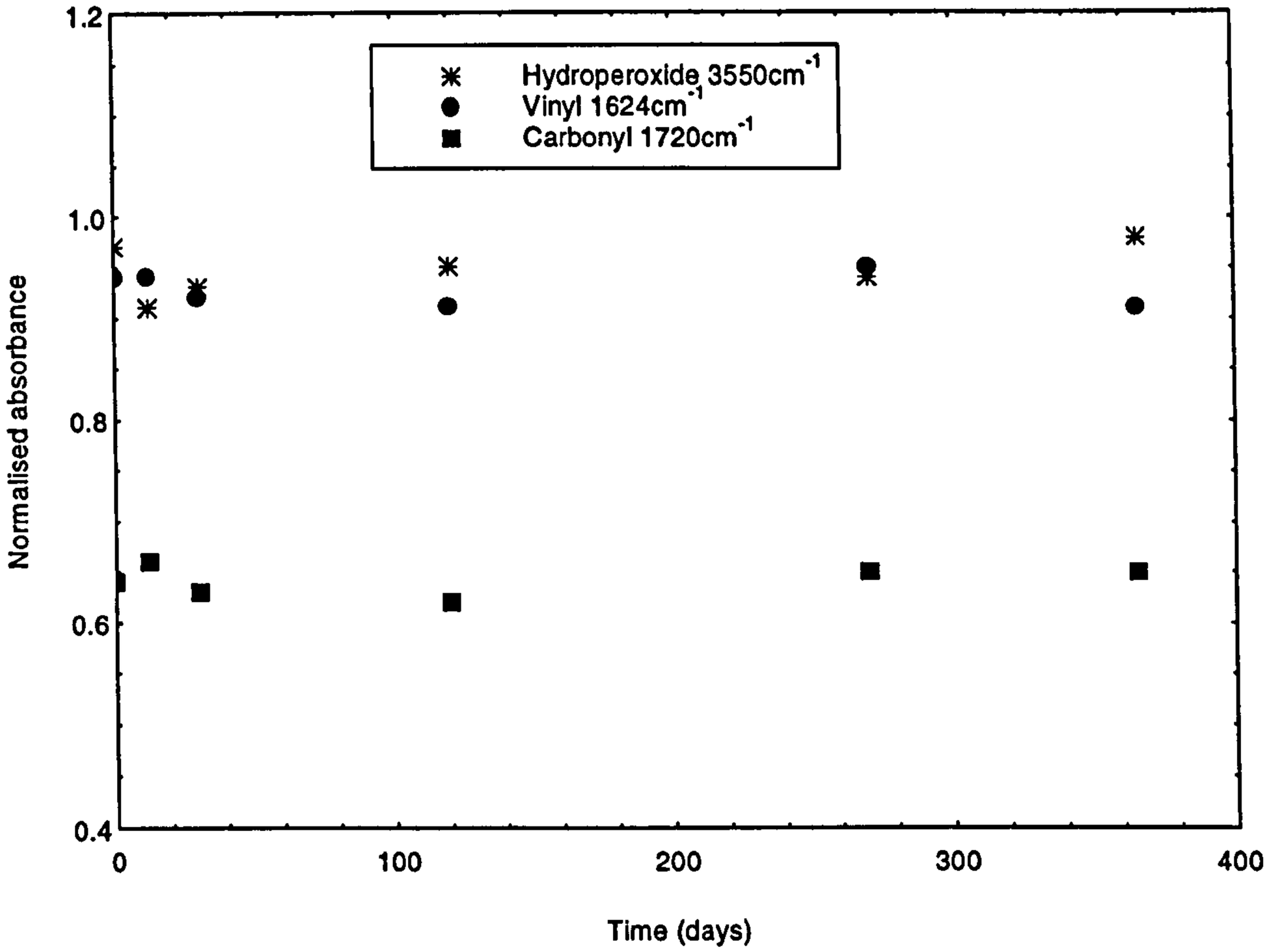

Figure 4.15. Normalised absorbance for the hydroperoxide ($3550cm^{-1}$), ketone ($1720cm^{-1}$) and terminal vinyl ($1624cm^{-1}$) infrared groups for Eltex film aged in an air circulating oven at 80°C as a function of time.

Figures 4.13 to 4.15 clearly show that the only detectable change as a function of ageing period was the sensitivity of the FTIR instrument which is known [Korolyov and Marugin, 1996] to be affected by humidity and temperature. Similar results were obtained for the three polymer resins in the different ageing conditions.

4.5.2. Additive Concentrations

HPLC analysis was used to obtain information on the known additives and their concentrations in the Rigidex resin. Two additives extraction methods were evaluated, namely, the conventional Soxhlet method and a microwave method. The latter was developed during the course of this project. The microwave method was favoured primarily

because of the high recovery of the additives. A summary of the additives recovered via the two methods is given in Table 4.2. Rigidex pellets were used in this investigation.

Table 4.2. The percentages of additives recovered for the Rigidex resin using the Soxhlet and the microwave methods.

Additive	Soxhlet method percentage recovered (%)	Microwave method percentage recovered (%)
Irganox 1076	22	86
Chimassorb 81	35	95
Santonox R	83	100

Possible reasons for the low recovery of the additives using the Soxhlet method may be attributed to the low melting points of the additives and their relative volatility. The microwave method on the other hand involves the use of a closed system and this is the reason for high recovery of the additives.

It should be mentioned that when using the HPLC analysis, two peaks were detected for Santonox R at 2.9 minutes and 3.5 minutes, as shown in Figure 4.16. This fact was recognised when Santonox R was isolated from the rest of the additives. Fresh Santonox R showed only one peak at 2.9 minutes. However, when exposed to the thermal treatment using the microwave method, the occurrence of the 3.5 minutes peak was much more pronounced. The actual reason for this is not known but some amount of the additive may have partially degraded or undergone chemical change. Therefore, both areas under the two peaks were taken into consideration when calculating the concentration of Santonox R concentration.

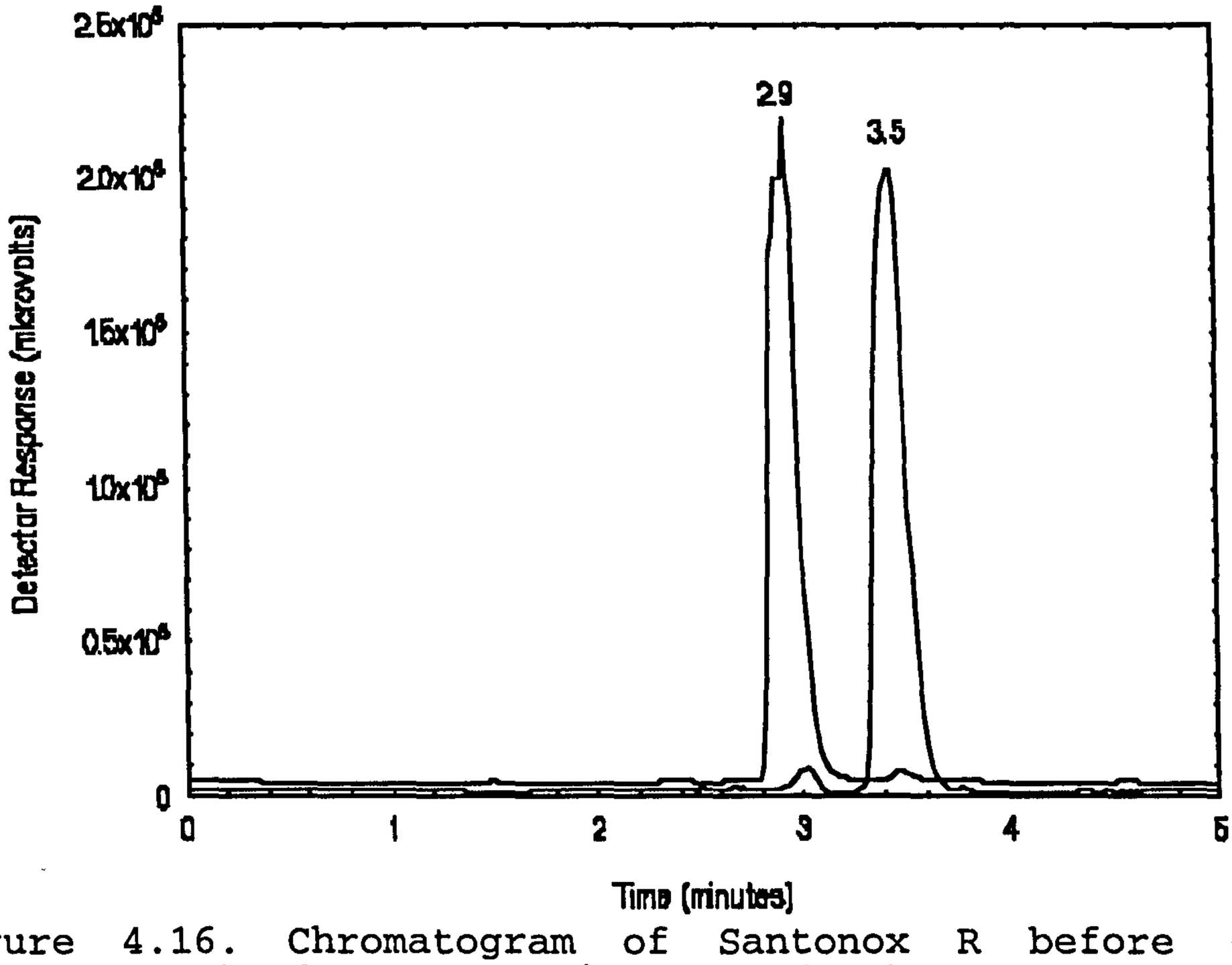

Figure 4.16. Chromatogram of Santonox R before (2.9 minutes) and after (3.5 minutes) the heat treatment in xylene.

After establishing the extraction method and the calibration procedures, the additives were extracted from the aged and unaged Rigidex 180-pipe samples. The concentrations of Santonox R, Irganox 1076 and Chimassorb 81 were determined and are summarised in Table 4.3.

Table 4.3. Santonox R (SR), Irganox 1076 (IR1076) and Chimassorb 81 (CH81) additives concentrations. % = (additive weight/PE sample weight)x100 for aged and virgin Rigidex 180-pipe and plaque samples for one year.

Sample	Conc.% Surface	Conc.% Middle	Conc.% Bore
Virgin pipe	SR = 0.12 CH81 = 0.08 IR1076 = 0.04	SR = 0.13 CH81 = 0.1 IR1076 = 0.06	SR = 0.12 CH81 = 0.07 IR1076 = 0.04
Pipe aged in water at 23°C	SR = 0.1 CH81 = 0.06 IR1076 = 0.04	SR = 0.12 CH81 = 0.1 IR1076 = 0.06	SR = 0.11 CH81 = 0.06 IR1076 = 0.04
Pipe aged in an air circulating oven at 80°C	SR = 0.12 CH81 = 0.12 IR1076 = 0.06	SR = 0.12 CH81 = 0.02 IR1076 = 0.03	SR = 0.12 CH81 = 0.13 IR1076 = 0.06
Pipe aged in water at 80°C	SR = 0.1 CH81 = 0.1 IR1076 = 0	SR = 0.12 CH81 = 0.01 IR1076 = 0.02	SR = 0.11 CH81 = 0.11 IR1076 = 0
Pipe aged in a vacuum-oven at 80°C	SR = 0.11 CH81 = 0.03 IR1076 = 0.03	SR = 0.13 CH81 = 0.01 IR1076 = 0.04	SR = 0.12 CH81 = 0.04 IR1076 = 0.03
Virgin plaque	SR = 0.12 CH81 = 0.07 IR1076 = 0.05	SR = 0.13 CH81 = 0.08 IR1076 = 0.04	SR = 0.12 CH81 = 0.06 IR1076 = 0.05

From Table 4.3 the following conclusions can be made:

(i) In the water ageing regimes, the results suggested that some of the additives had leached out. To confirm this, samples of water from the water baths for the Rigidex pipes which had been carried out at 23°C and 80°C were taken for HPLC analysis. The three additives were found present in the water in different proportions and in both ageing regimes.

(ii) In the case of an air circulating oven ageing, diffusion is thought to play a significant role during the thermal ageing process. The results indicated that Chimassorb 81 and Irganox 1076 migrated from the middle of the pipe towards the outer surfaces. This process can

be referred to as "blooming" to compensate reductions in the additives near the surfaces.

(iii) Both Chimassorb 81 and Irganox 1067 concentrations were reduced during vacuum-oven ageing. These reductions occurred throughout the pipe wall. It is reasonable to suggest that the volatility of the additives was a primary reason for the observed reduction in their concentrations.

With reference to Table 4.3, the results from 80°C ageing experiments indicate that this regime should not be considered as an accelerated test. This is because this temperature (80°C) is well above the melting point of some of the additives used in PE pipe resins. However, the design criteria for these PE pipes are based on 80°C hydrostatic tests and, hence, the selection of 80°C as the temperature for the laboratory-based ageing studies.

4.6. OIT Data

The OIT test was used in this study to investigate the effect of ageing on the thermo-oxidative stability of the three PE resins. The pipe samples made from the three PE resins were subjected to different ageing environments for a period of one year. A summary of the OIT data obtained is presented in Tables 4.4 to 4.6. Each result in the three tables represent an average of six test samples.

Table 4.4. OIT data for pipe samples made from the Aldyl-A resin aged in the specified environments for one year.

Sample/Position	Surface (minutes)	Middle (minutes)	Bore (minutes)
Virgin 125-pipe	26 (3.2)	45 (6.2)	33 (5.4)
125-pipe aged in water at 23°C	33 (2.2) 51 (3.4)	31 (1.2) 50 (4.5)	36 (6.7) 54 (2.2)
125-pipe aged in an air circulating oven at 80°C	22 (4.3)	23 (1)	22 (2.1)
125-pipe aged in water at 80°C	60 (8.6)	43 (2.9)	55 (3.3)
125-pipe aged in a vacuum-oven at 80°C	57 (4.5)	33 (3.9)	57 (5.2)
125-pipe from site laid in 1978 excavated 1995, age=17 years	22 (2.2)	26 (4.4)	30 (4)
125-pipe from site laid in 1971 excavated 1995, age=24 years (resin 5044)	22 (6.6)	23 (3.5)	25 (7.5)
8"pipe from site laid in 1978 excavated 1995, age=17 years	22 (6.9)	24 (3.1)	25 (5.1)
125-pipe (tan) from site laid in 1971 excavated 1995, age=24 years (resin 5044)	14 (2.6) 33 (1.9)	16 (4.5) 55 (6.1)	17 (1.9) 48 (2.8)

Standard deviation in parenthesis.

Table 4.5. OIT data for pipe and plaque samples made from the Rigidex resin aged in the specified environments for one year.

Sample/Position	Surface (minutes)	Middle (minutes)	Bore (minutes)
Virgin 125-pipe	58 (2.2)	65 (3.1)	60 (3.3)
125-pipe aged in water at 23°C	40 (3.3)	63 (5.1)	41 (6.6)
125-pipe aged in an air circulating oven at 80°C	70 (7.3)	49 (2.3)	74 (5.8)
125-pipe aged in water at 80°C	11 (3.7)	42 (1.1)	18 (2.7)
125-pipe aged in a vacuum-oven at 80°C	53 (5.4)	58 (2.9)	58 (3.3)
125-pipe site sample laid in 1981 excavated 1995, age=15 years	61 (3.3)	63 (2.1)	63 (6)
Virgin 180-pipe	60 (1.4)	63 (5.4)	60 (6.4)
180-pipe aged in water at 23°C	50 (2.5)	65 (5.5)	53 (5.1)
180-pipe aged in an air circulating oven at 80°C	75 (9.5)	52 (6.3)	79 (7.5)
180-pipe aged in water at 80°C	14 (3.9)	40 (2.2)	17 (4.1)
180-pipe aged in a vacuum-oven at 80°C	51 (5.1)	55 (7)	56 (3.2)
Virgin Rigidex plaque	65 (1.2)	64 (0.6)	65 (0.9)
Plaque aged in water at 23°C	44 (8.7)	60 (5.7)	43 (2.2)
Plaque aged in an air circulating oven at 80°C	71 (5.6)	54 (3.7)	73 (4.5)
Plaque aged in water at 80°C	12 (5.5)	41 (4.4)	11 (1.1)
Plaque aged in a vacuum-oven at 80°C	57 (4)	58 (2.2)	56 (1.2)

Standard deviation in parenthesis.

Table 4.6. OIT data for pipe samples made from the Eltex resin aged in the specified environments for one year.

Sample/Position	Surface (minutes)	Middle (minutes)	Bore (minutes)
Virgin 180-pipe	140 (3.6)	156 (4.4)	154 (4.5)
180-pipe aged in water at 23°C	118 (8.2)	160 (6.1)	147 (7.4)
180-pipe aged in an air circulating oven at 80°C	25 (3.6)	116 (6.4)	40 (4.4)
180-pipe aged in water at 80°C	13 (6.6)	28 (6.4)	17 (1.1)
180-pipe aged in a vacuum-oven at 80°C	83 (1.1)	157 (2.5)	158 (7.2)

Standard deviation in parenthesis.

With reference to Tables 4.4 to 4.6, to clarify the various complicated behaviour observed for the three resins such as the recording of two OIT values, each of the ageing conditions is discussed separately.

4.6.1. Ageing in Water at 23°C

With reference to the Aldyl A OIT data summarised in Table 4.4, the presence of the first (small) peak in the OIT trace was attributed to cross-linking in the polymer as described in section 4.4. This cross-linking may have increased the polymer's resistance to thermo-oxidation and increased the major peak to an average of 52 minutes.

With reference to the Rigidex OIT data summarised in Table 4.5, no significant changes were observed for the mid sections of the pipes and plaque samples. This implied that the mid sections were not affected after one year of ageing in water at 23°C. Conversely, the outer surfaces (surface and bore of the pipes) of the same samples showed a marked reduction in the OIT. With reference to the HPLC data in Table 4.3, it appeared that this reduction was caused by the leaching of about 0.02% of Santonox R.

With reference to the Eltex OIT data summarised in Table 4.6, this showed no significant change for the mid section of the pipe. 16% and 5% reductions were recorded in the OIT for the pipe surface and bore, respectively. It could be argued that some of the additives were leached to the water from the pipe surfaces thus causing the OIT to drop. It is also possible that these additives may have leached more readily from the surface of the pipe surface compared with the bore thereby giving a lower OIT for the surface. This may be due to the lower density of the pipe surface. HPLC analysis is needed to elucidate further the trend in the OIT data for this polymer.

4.6.2. Ageing in an Air Circulating Oven at 80°C

With reference to the Aldyl A OIT data summarised in Table 4.4, the OIT values showed 15%, 49% and 34% reductions for the pipe surface, mid and bore, respectively when compared to the virgin pipe. There are two possible reasons for the observed reductions in the OIT values: (i) evaporation of additives and (ii) migration from the mid section of the pipe to the inner and outer pipe surfaces. It appears that the mechanisms were working concurrently.

With reference to the Rigidex OIT data summarised in Table 4.5, this showed an average increase in the OIT of 16% and 23% for the pipe surface and bore, respectively, but the mid section of the samples showed an average reduction of about 20%. A similar trend was observed for the plaques aged under identical conditions. The Rigidex 180-pipe samples which were aged in an air circulating oven for one year were monitored every three months. Figure 4.17 illustrates profiles of the OIT values for the pipe surface, mid and bore sections obtained from these experiments.

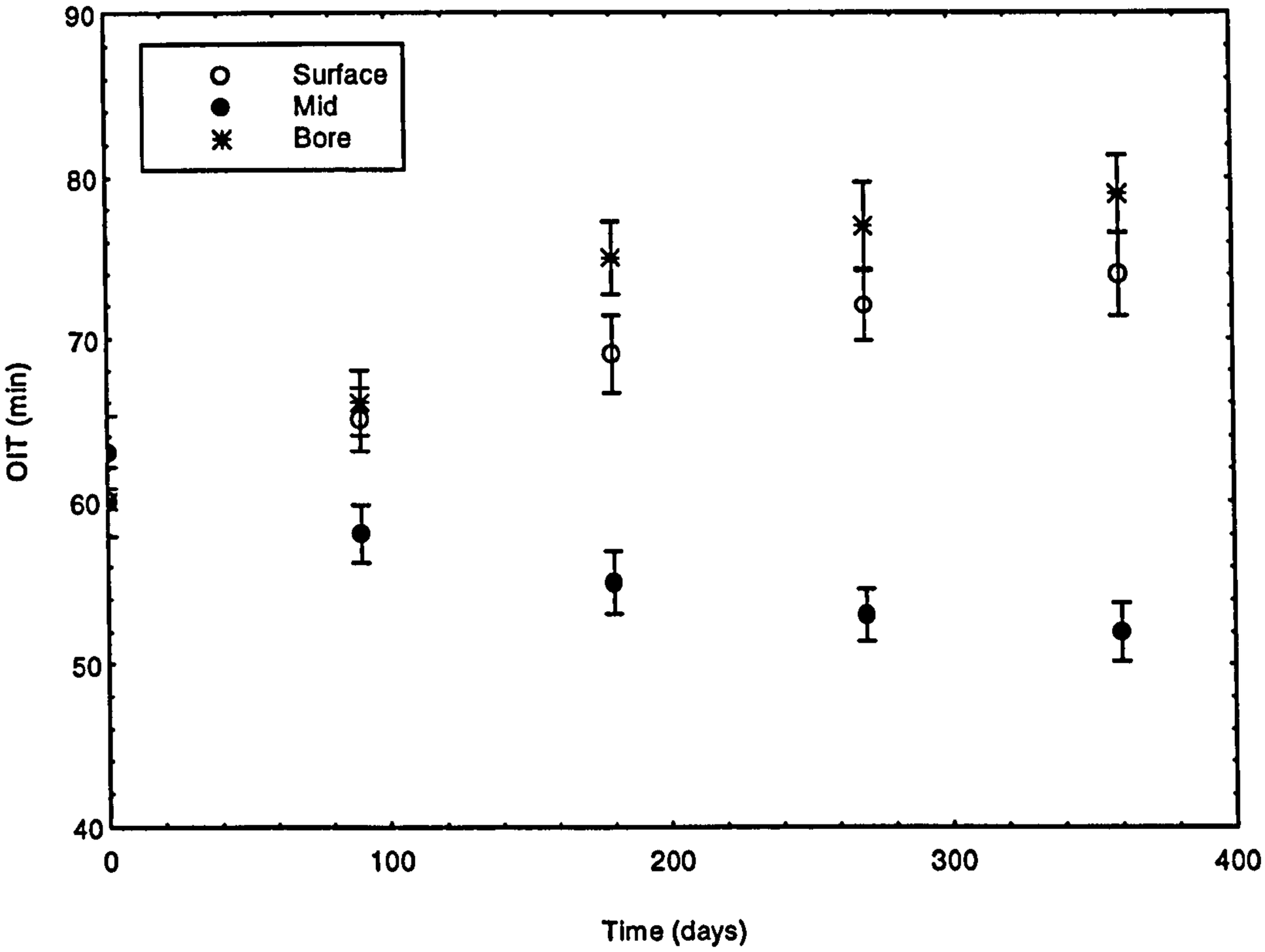

Figure 4.17. OIT results for the surface, mid and bore of Rigidex 180-pipes as a function of ageing time. The ageing was carried out in an air circulating oven for one year at 80°C.

Figure 4.17 shows that the OIT values for the pipe surface and bore increased rapidly at the start. This increase was less marked for the rest of the ageing period. The HPLC results presented in Table 4.3, suggested that some of the additives had migrated from the mid section to the surface and bore. However, this decrease in the OIT for the mid-section did not match the increase registered for the pipe surface and bore. An investigation was undertaken to measure the OIT values across the pipe wall. Cylindrical samples were obtained from a virgin pipe and the air circulating oven aged 180-pipe samples using the belt hole puncher. Nine specimens

were cut from each cylinder. The results from this study are presented in Figure 4.18.

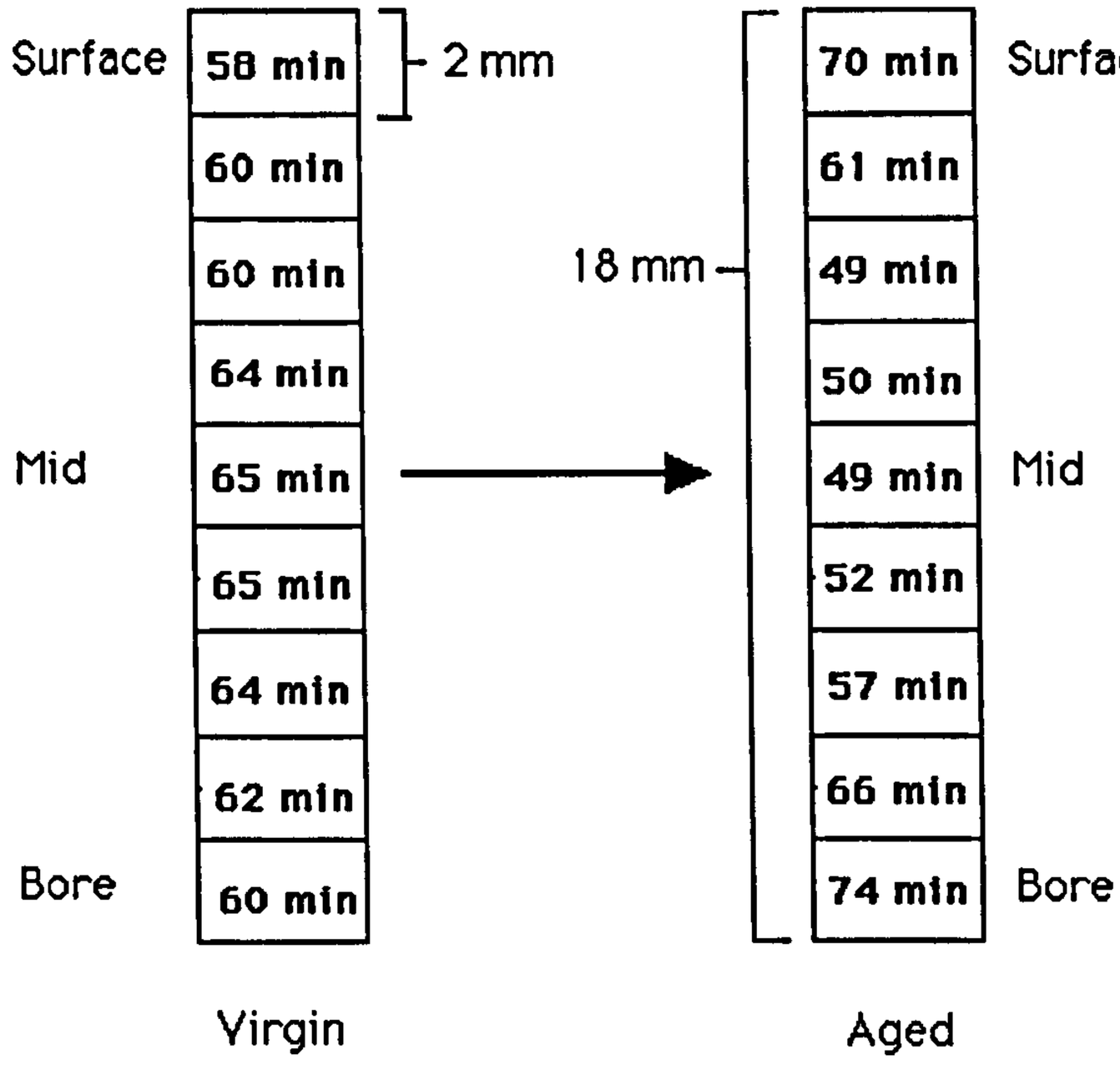

Figure 4.18. Average OIT profiles across the pipe wall for a virgin and an aged Rigidex 180-pipes. The ageing was carried out in an air circulating oven for one year at 80°C.

The OIT profiles in Figure 4.18 indicated clearly an uneven distribution of additives throughout the pipe wall after one year of ageing. These results also confirm that the surface and bore of the pipe were more resistant to thermo-oxidation when compared to the mid section. This behaviour and the results from the HPLC technique suggested the possibility of the antioxidants migrating from the mid regions to the inner and outer surfaces of the pipe.

With reference to the Eltex OIT data summarised in Table 4.6, reductions in the OIT of approximately 82%, 25% and 74% were recorded for the surface, mid and bore sections of the pipe, respectively.

4.6.3. Ageing in Water at 80°C

With reference to the Aldyl A OIT data summarised in Table 4.4, the OIT data show a significant increase over the virgin sample by 130% and 66% for the surface and bore, respectively. This was an unexpected result as there was no change in OIT for the mid section. It is difficult to propose any reasons for this observation because information on the additives used in this polymer was not available. In addition to this, further work has to be carried out using HPLC analysis to rectify the observed trend in the OIT values. The suggestion that the additives may undergo hydrolysis at high temperatures and that this in turn may boost the additives' performance [Tochacek and Sedlar, 1993] should be further investigated.

With reference to the OIT data for Rigidex summarised in Table 4.5, average reductions of 75%, 33% and 75% were recorded for the surface, mid and bore, respectively when compared to the virgin pipe sample. With reference to the HPLC results in Table 4.3, Chimassorb 81 and Irganox 1076 were not present in the aged sample and there was a small reduction in Santonox R concentration. It is possible that there were two complementary processes working simultaneously which resulted in the large reductions in the OIT values: (i) migration of the additives from the mid section towards the sample surfaces and (ii) leaching of the additives to the water. HPLC analysis of water samples taken from the water baths confirmed the presence of the three additives used in the Rigidex polymer.

With reference to the Eltex OIT data summarised in Table 4.6, this showed reductions corresponding to 91%, 82% and 89% for the surface, mid and bore sections of the pipe, respectively. It is proposed that the migration and leaching of the additives could be responsible for the observed reductions in the OIT values. HPLC analysis is necessary to elucidate further these trends.

4.6.4. Ageing in a Vacuum at 80°C

With reference to the Aldyl A OIT data summarised in Table 4.4, increases of 119% and 72% were recorded for the pipe surface and bore respectively when compared to the virgin pipe. The mid section showed a reduction of 27%. Although the additive system in the Aldyl A resin was unknown, it is apparent from the OIT results that the migration of additives from the mid to the surfaces is a possible mechanism.

With reference to the OIT data for the Rigidex polymer summarised in Table 4.5, this showed modest reductions in the OIT for the three sections of the pipe wall. With reference to the HPLC analysis in Table 4.3, it appeared that one of the additives, namely, Chimassorb 81 was lost from the pipe sample during the vacuum-oven ageing experiments. Chimassorb 81 is known to be as a UV stabiliser and, therefore, may not have had a significant effect on the OIT value. The concentration of Irganox 1076 was also found to decrease by a small amount. Therefore, it is possible that this small reduction in Irganox 1076 decreased the OIT values.

With reference to the Eltex OIT data summarised in Table 4.6, a 40% reduction was recorded for the pipe surface with no changes for the mid and bore regions. It is possible too that the density variations within the pipe wall could have played a significant role in the observed results.

4.6.5. Samples Aged In-Service

With reference to the OIT data for the Aldyl A summarised from site in Table 4.4, the "tan-pipe" and the 125-pipe which was reported to have been laid in 1971 were made from the 5044 resin and the rest were made from the 5046 resin. It is difficult to draw a profile of how the antioxidants may have behaved during the years of natural ageing because the history of each pipe is totally

different. Furthermore, it also depends on the resin manufacturing process, storage time, the manner it was handled before installation and its environment during natural ageing, pH level and temperature cycle. Moreover, and more importantly, the nature of the additive packages in the Aldyl resins were unknown.

Continuing with the Aldyl A OIT results presented in Table 4.4, reductions in the OIT values were recorded for all the pipes made from the 5046 resin. The reduction was more pronounced in the mid region of the pipes. It could be argued that the additives had diffused from the mid section to the pipes surfaces during the natural ageing and some amounts were lost to the surrounding environment. It is also possible that some amount had reacted to protect the polymer from oxidation during natural ageing. The surprising result was the two exothermic peaks observed in the OIT trace for the tan pipe. This result was reproduced in the laboratory with aged samples in water at 23°C (section 3.6.1.) but, in this case the first peak was at a lower OIT value than the pipe aged in water. It was not clear as to how this would affect the pipe performance in service in the future.

With reference to the OIT data for Rigidex summarised in Table 4.5, according to the OIT test it appeared that the performance of the antioxidant system in Rigidex pipe did not undergo any detectable change in the 15 years of natural ageing. However, as this sample was the only supplied Rigidex pipe sample from site, it is inappropriate to generalise.

It was not possible to secure any Eltex pipe sample from site as this resin is a relatively new resin in the gas industry.

CHAPTER FIVE

CHAPTER FIVE

PHYSICAL CHARACTERISATION OF PE PIPE RESINS

5.1. Introduction

This chapter is devoted to physical characterisation of the Rigidex, Aldyl A and Eltex pipe resin systems before and after subjecting them to the specified ageing conditions. Issues studied were as follows. (i) An investigation into the relationship between the density of the sample and the degree of crystallinity. (ii) The effect of ageing on crystallinity and density. (iii) Interpretation of the DSC (heat flow) traces for the virgin and aged samples. (iv) A discussion on the phenomenon known as "physical ageing".

5.2. Correlation Between Density and Crystallinity

A brief study was undertaken to establish the relationship between the density and the degree of crystallinity for the three PE resins. The degree of crystallinity and density measurements were obtained via DSC and density column respectively. The samples were taken from the surface, mid and bore of the three unaged pipe samples and a compression moulded Rigidex plaque. The belt hole puncher as described in section 3.4.2 was used to obtain test specimens. In Figure 5.1, a linear relationship was observed between the sample density (via the density column) and its degree of crsytallinity (via DSC).

The average densities across the pipe wall were 954, 946 and 944 kg/m^3 for the Eltex, Rigidex and Aldyl A pipe resins respectively. The average degrees of crystallinity across the pipe wall were 63%, 52% and 51% for Eltex, Rigidex and Aldyl A pipe resins respectively.

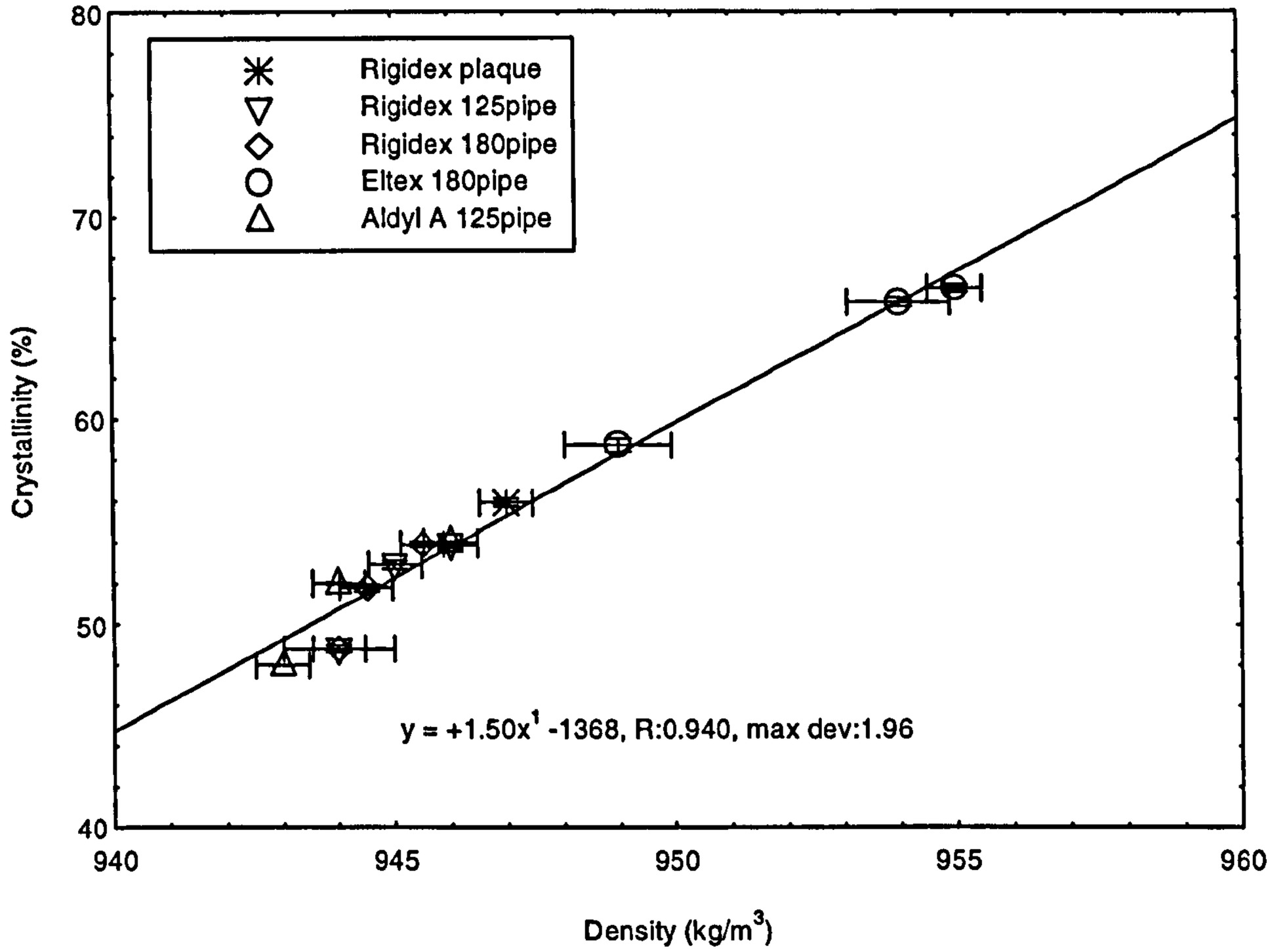

Figure 5.1. Correlation between the degree of crystallinity and density for the three pipe samples and a Rigidex plaque. The samples were taken from the surface, mid and bore of the pipe samples.

With reference to Figure 5.1, irrespective of the pipe resin the bore section always gave the highest density. This was followed by the mid and surface regions. This observed variation in the density profile has been attributed to the extrusion process where the outer surface of the pipes are quenched with water. The bore region is usually left to cool to ambient temperature. This differential cooling rate across the pipe wall thickness results in a corresponding crystallinity gradient.

The data presented in Figure 5.1 showed a good linear relationship. However, for densities lower than 944 kg/m^3,

the results showed a small deviation from the observed linear behaviour. A similar observation was also reported by Mandelkern et al. [1986]. They varied the cooling regime for PE samples and obtained a range of sample densities. They found that quenched samples deviated from the general trend. They offered the following explanation: The total volume of a fully amorphous PE molecule represents the volume occupied by the random PE chains and the free volume. The volume of the polymer chains can occupy only one volume but the free volume may vary depending on the cooling rate and thus, the sample density may vary according to the total volume.

In terms of accuracy and practicality, the degree of crystallinity measurements via DSC offered a rapid method to investigate the effect of ageing on the density of PE pipe samples. The scatter in the density data via the density column was slightly higher than the DSC experiments. Furthermore, the density column had a maximum lifespan of one week due to the evaporation of isopropanol. The isopropanol was one of the constituent liquids used to maintain a specified density range in the column.

5.2.1. Densification of Pipe Materials

At the time of preparing the density column only one aged pipe sample was available for testing namely, Eltex pipe. This pipe sample was aged in an air circulating oven for one year at 80°C. The densities of the aged pipe and freshly extruded Eltex pipe are presented in Table 5.1.

Table 5.1. The densities of the surface, mid and bore sections of virgin Eltex 180-pipe and Eltex 180-pipe which was aged in an air circulating oven for one year at 80°C.

Sample/Position	Surface density (kg/m^3)	Mid density (kg/m^3)	Bore density (kg/m^3)
Virgin 180-pipe	949 (0.4)	953 (0.5)	955 (0.1)
180-pipe aged in an air circulating oven for one year at 80°C	954 (0.2)	955 (0.4)	956 (0.1)

Standard deviation in parenthesis.

With reference to Table 5.1, the densities of the aged pipe increased by 0.42%, 0.2% and 0.1% for the pipe surface, mid and bore, respectively. As discussed in chapter 4, oxidation or chemical changes in PE samples were not detected during the ageing experiments at 80°C. Therefore, it is appropriate to suggest that the increase in densification of pipe material appeared to be as a result of changes in the pipe morphology due to thermal ageing.

5.2.2. Thermal Ageing

A study was undertaken to investigate the effect of thermal ageing on the degree of crystallinity of PE pipe resin. Figure 5.2 represents the degree of crystallinity as a function of time for the Rigidex pipes which were aged in an air circulating oven for one year at 80°C. each datum point represents an average of 3 individual specimens.

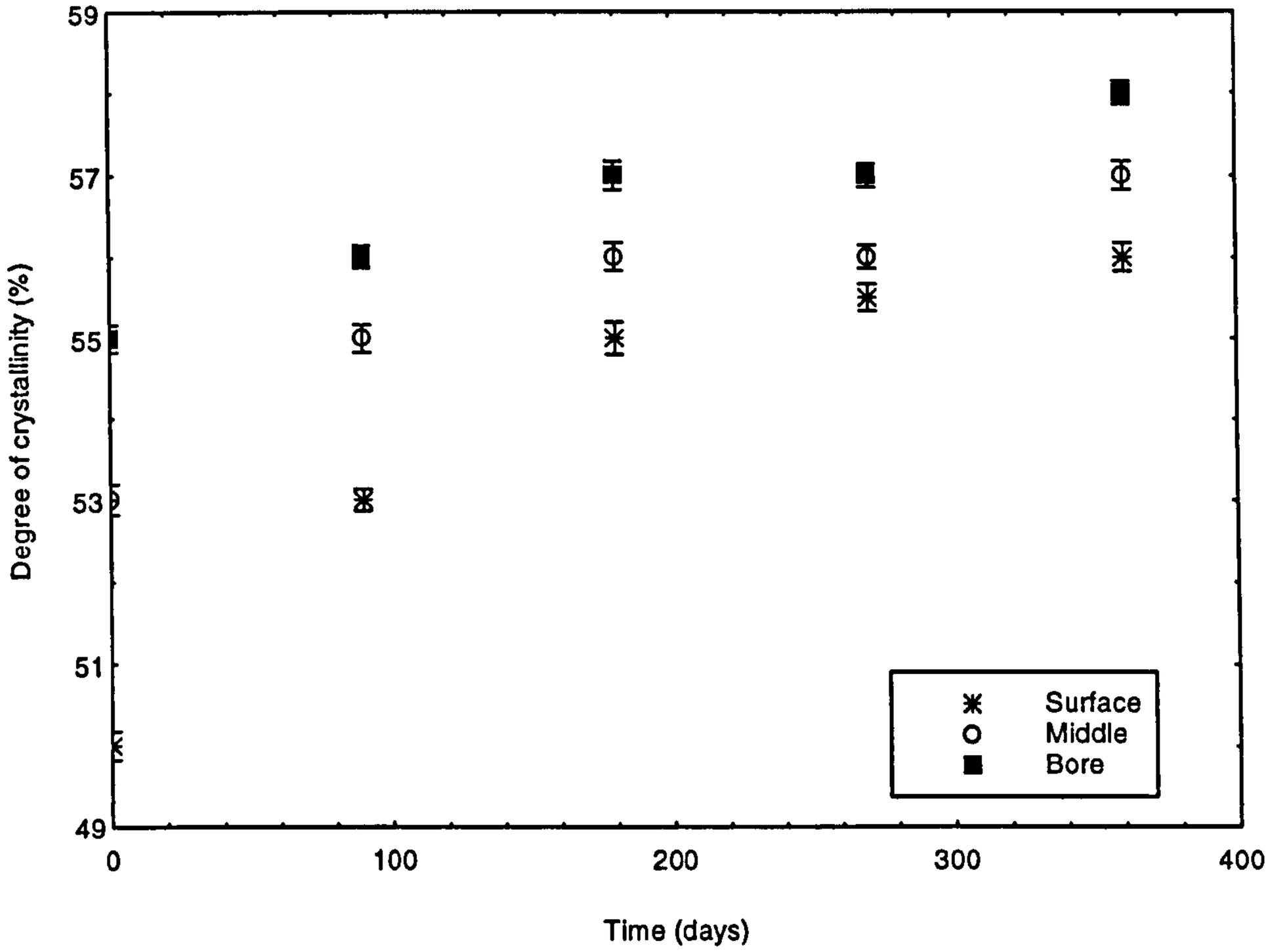

Figure 5.2. Crystallinity (via DSC) as a function of ageing for the surface, mid and bore sections of a Rigidex 180-pipe. Ageing was carried out at 80°C in an air circulating oven for a period of one year.

At the beginning of the thermal ageing experiments, the overall rate of crystallinity increased rapidly as shown in Figure 5.2. The surface region showed the highest rate of increase in crystallinity when compared to the mid and bore regions. This agreed closely with the density measurements reported earlier. The crystallinity across the pipe wall increased at a slower rate after 200 days. Results reported in the literature [Blacker et al., 1995] showed that prolonged annealing of PE samples at relatively high temperatures, had little effect on the physical structure of the spherulites. Possible reasons for the increase in crystallinity with annealing can be

obtained by examining the DSC traces of the thermally aged and unaged samples.

5.2.3. Examination of DSC Traces

Figure 5.3 illustrates typical DSC traces for (a) an unaged and (b) a PE sample which was aged in an air circulating oven for one year at 80°C.

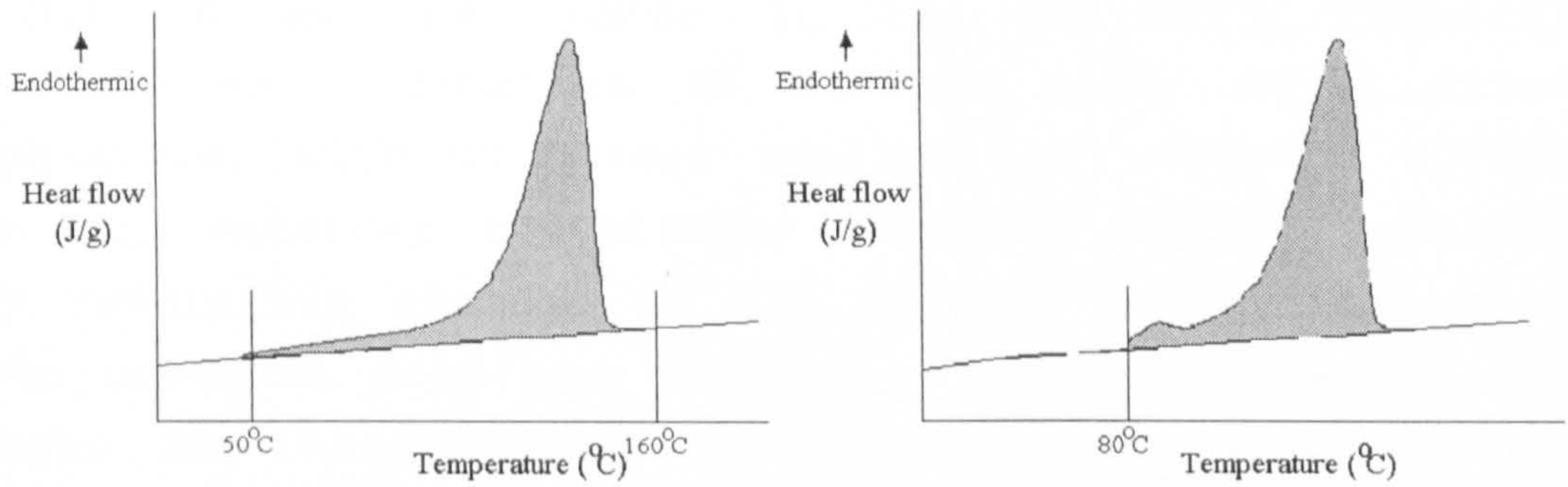

(a) (b)

Figure 5.3. A typical DSC traces for (a) an unaged PE sample and (b) thermally aged PE sample for one year at 80°C.

The PE samples exhibited a distribution of melting points starting as low as 50°C as shown Figure 5.3(a). It is appropriate here to suggest that a portion of the PE samples aged at 80°C was in a molten state and that the sample at this temperature could be described as a melt-crystallised system. This description is very important in relation to the physical ageing phenomenon which is explained below.

In the early stages of the thermal ageing experiments, the DSC traces showed a small but noticeable melting endothermic peak below 80°C. This was the case for all the three pipe resins samples which were aged at 80°C. This peak was observed to shift towards 80°C as a function of ageing time. After six months of thermal ageing, the peak stabilised at approximately 92°C. The major melting peaks

observed for the PE samples did not appear to shift to higher values during the entire ageing duration at 80°C.

5.3. Physical Ageing

The term "physical ageing" comprises a broad class of behaviours. For example, a constant load applied to a polymer sample for a period of time (creep), is considered physical ageing as is even where the load fluctuates (fatigue). To narrow the definition of this term to what is meant by physical ageing in this study it is defined as the change in the polymer's physical structure as a function of storage time, at a fixed temperature, with no stress applied and under no effect from any external conditions. Physical ageing involves only reversible changes to the polymer properties which is in contrast from the concept of chemical ageing. Any changes in the physical structure of PE material are expected to affect the bulk properties of the polymer such as mechanical properties, dielectric response, specific volume, enthalpy, so on.

Physical ageing is a very well known phenomenon in amorphous polymers. Struik [1978] identified that many amorphous solids are not in thermodynamic equilibrium at temperatures below their glass transition. Later he also published a series of papers [Struik, 1987(a);(b); 1989(a);(b)] which acknowledged and showed that semicrystalline polymers also exhibit a similar behaviour. In this study only semicrystalline PE pipe material is discussed.

The physical ageing definition mentioned above needs to specify the ageing temperature i.e., below or above its glass transition temperature (Tg). In the case of PE material, there are three significant ranges of temperature at which a PE material can be aged as shown in Figure 5.4.

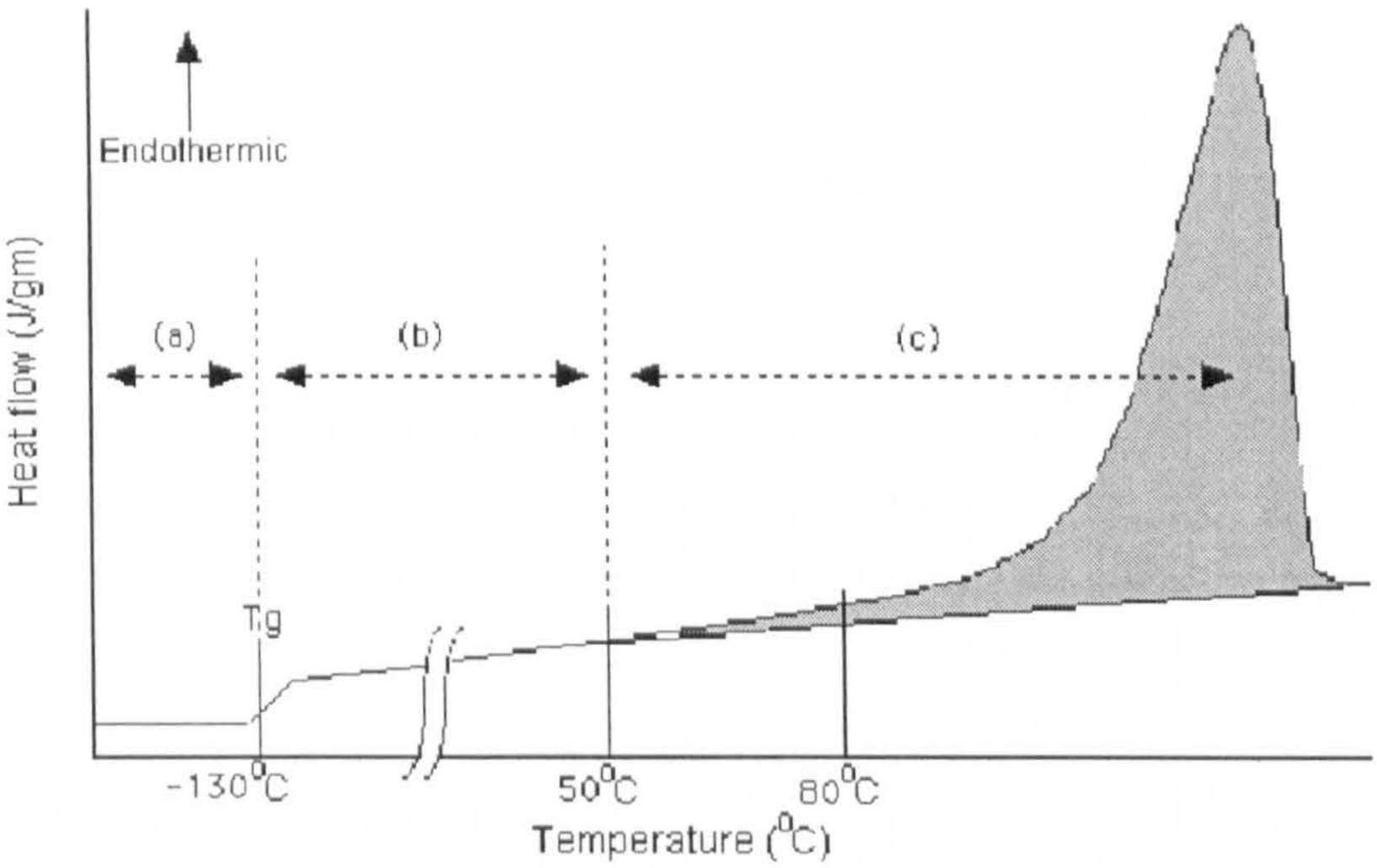

Figure 5.4. A typical DSC scan of a PE sample. The three temperatures ranges are (a) below Tg, (b) above Tg and up to a temperature where no melting can occur, approximately 50°C, and (c) from this temperature up to the melting point of PE material.

5.3.1. Physical Ageing Below Tg

The basic thermodynamic state of an aged polymer below its Tg i.e., an aged glassy polymer, was recognised long time ago by Struik [1978]. He described it in terms of the non-equilibrium thermodynamic state of glassy materials. For example, its known that on cooling from the equilibrium melt state, a transformation to a glass occurs at a Tg for a polymer. When the molecular rearrangements needed for the material to accommodate to the changing temperature slows down to such an extent that they require a time scale longer than that available by the imposed cooling rate, then the glassy polymer will have excess thermodynamic quantities (volume, enthalpy, entropy) and there will be a driving force to reduce these towards an equilibrium state. Therefore, at a constant temperature below Tg, the phenomenon of physical ageing can be manifested as a reduction in the polymer volume because of a slow release with time in molecular

motion to reach an equilibrium state. This reduction in volume will continue until an equilibrium is established at the ageing temperature. This basic thermodynamic description of the state of the glassy polymer has been universally accepted for many years. For example, in the earliest thermodynamic treatments by Davies et al. [1953].

5.3.2. Physical Ageing Above Tg

When considering ageing above the Tg of PE material, there are two possibilities, regions (b) and (c) as shown in Figure 5.4.

Region (c) in Figure 5.4

This a case when the ageing temperature is high enough to melt a portion of the crystallised polymer as in region (c). A good example of this is the thermal ageing at 80°C used in this study. This accelerated test temperature was selected according to the BG and ISO hydrostatic test standards. At this temperature a melt-crystallised system was created and with ageing a recrystallisation process toke place and increased the crystallinity content as the results indicated. The reorganisation process of the lamellae structure above 80°C possibly can be described by two approaches. The first is similar to the process occurring during primary crystallisation and the other is a secondary crystallisation process. With respect to primary crystallisation, the polymer chains fold to form crystals with a thickness which is just greater than the minimum stable thermodynamic value as described by Barham et al [Barham and Keller, 1989]. The crystals formed have high free energy (due to the fold surface) and are far from an equilibrium structure. Therefore, with ageing they tend to grow thicker (to reduce their free energy) at 80°C. They initially grow in very thin lamellae which thicken with time in a single step to twice, three times or four times the original thickness as illustrated in Figure 5.5. When the crystal thickness reaches a certain

value (critical thickness at 80°C) and the free energy available is insufficient to reshape the thickness of the crystal, it will freeze.

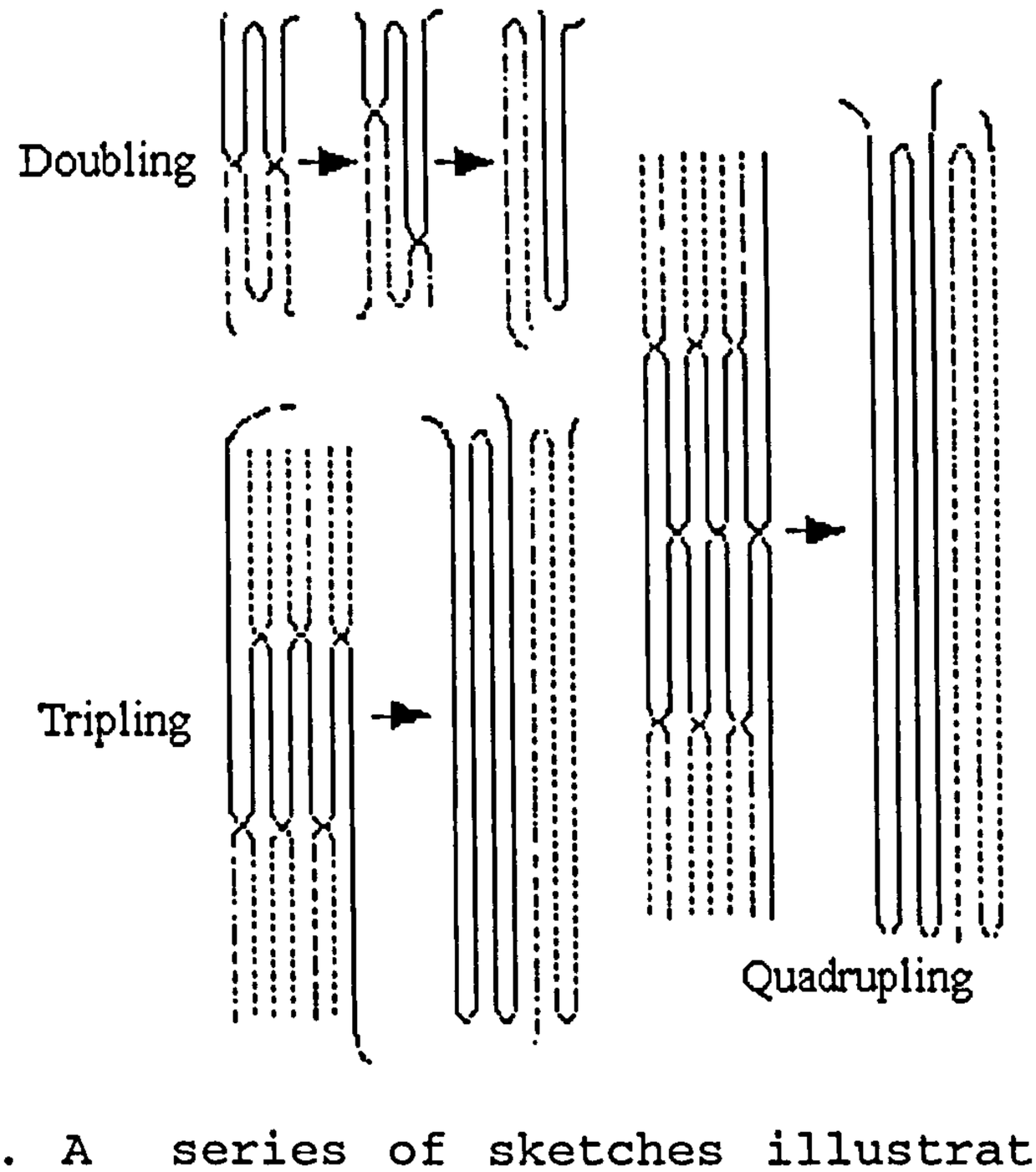

Figure 5.5. A series of sketches illustrating a simple model for refolding to produce lamellae of doubled, tripled and quadrupled thickness for annealed PE sample [Barham and Keller, 1989].

With respect to the secondary crystallisation process, this considers the polymer chains in the interface region between the crystalline and the amorphous phases as depicted in Figure 5.6. La is the thickness of the interface region before ageing (virgin sample). When aged at 80°C the thickness is reduced to Lb due to partial melting. This will enable the material in the interface region to rearrange. Hence in the current situation Lc will increase and become greater than the original thickness La after a period of ageing at 80°C.

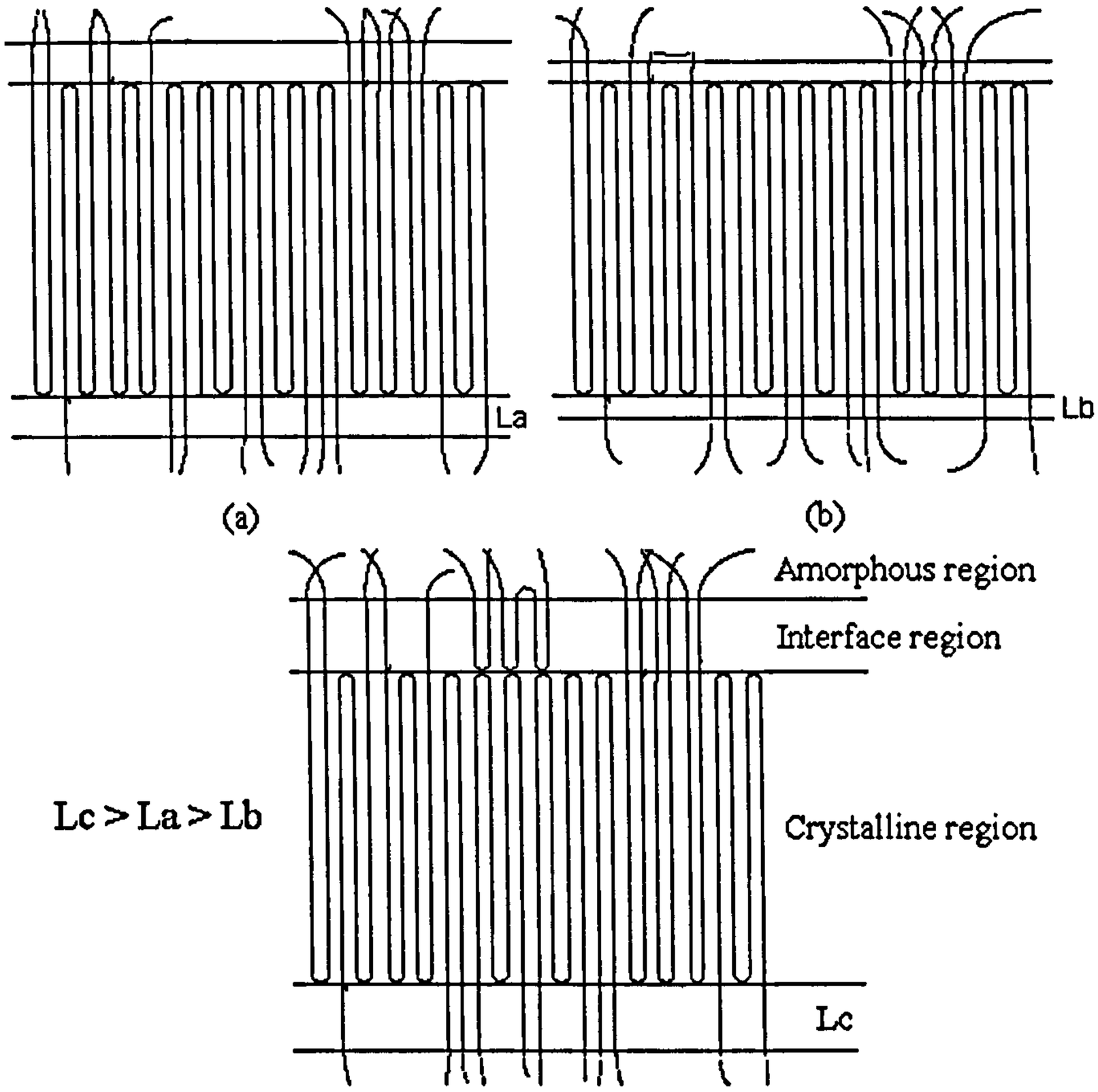

Figure 5.6. Schematic illustration of the two phase model with different crystalline interfacial thickness. (a) virgin resin, (b) initial stages of ageing at 80°C and (c) after ageing for a period of one year at 80°C.

In both the primary and the secondary crystallisation approaches, if the polymer sample is removed from the ageing environment at 80°C after a period of time, the newly formed crystals do not undergo any changes. Therefore, with time more and more crystals will be formed above the 80°C barrier until it becomes very difficult for the remaining amorphous (disorganised) polymer chains to reorganise and fold. For example, in this study up to 200 days of ageing at 80°C the crystallinity increased rapidly. But after ageing for a period of one year a half year the degree of

crystallinity increased very little as shown in Table 5.2.

Table 5.2. Degree of crystallinity for a virgin plaque, one year and one and a half year aged plaques. All the plaques were made from Rigidex resin and the ageing was carried out in an air circulating oven at 80°C.

Sample	Crystallinity (%)
Virgin Rigidex plaque	55 (0.3)
Rigidex plaque aged in an air circulating oven for 1 year at 80°C	59 (0.2)
Rigidex plaque aged in an air circulating oven for 1.5 year at 80°C	60 (0.2)

Standard deviation in parenthesis.

Primary and secondary crystallisation exhibit different kinetic and physical structural signatures and they also differ in many other respects. Primary crystallisation occurs from the melt, secondary crystals generally grow in a confined space. However, it is difficult to isolate which of the two process, if not both, had occurred in the thermal ageing environments used in this study. A further detailed study involving X-ray small angle is required to resolve this issue.

Region (b) in Figure 5.4

In this case the ageing temperature is above Tg but, low enough not to melt any existing crystals as indicated in Figure 5.4 region (b). The interesting aspect of this approach is if the physical ageing process occurs at temperatures above the Tg then the amorphous phase should be in an equilibrium state. Yet, as reported by Struik [1978], the ageing of semicrystalline polymers was found to be similar to the ageing of amorphous polymers. This observation led Struik to explain these results in terms of an "extended Tg" in semicrystalline polymers. To expand this concept, ageing in semicrystalline polymers occurs, as in amorphous polymers, as a consequence of structural changes in the amorphous phase. He described

the amorphous phase as containing bulk amorphous regions, which are at a distance from the crystalline phase, and the constrained amorphous regions are said to be located near the crystalline lamellae as illustrated in Figure 5.6(a). He argued that the constrained material will have a higher Tg than the unconstrained material. This will lead to a range of Tgs extending above the normal Tg of the bulk amorphous region. Therefore, physical ageing might be expected at temperatures above the conventional Tg as structural rearrangements and reduction in free volume occur in the constrained amorphous regions [Struik, 1987(a);(b); 1989(a);(b)]. This will lead to an increase in the crystallinity of the material.

Beyond the physical ageing definition of a constant temperature, there is still the possibility that a polymer could be subjected to a fluctuating temperature in-service for example, from -20 to 35°C. The mechanical test results of Cooper et al. [1972] showed that when a linear PE cooled slowly from point to point starting at room temperature and held for one hour at each temperature before measurement, exhibits structural changes.

With reference to the above discussion and in particular the extensive work by Struik on a variety polymeric materials which indicated that changes in enthalpy (crystallinity), free volume and free volume distribution is the most acceptable explanation to the phenomenon of physical ageing in polymers. In order to gain a greater understanding about this phenomenon in semicrystalline PE, it is important that each of the above changes be isolated and studied individually as a function of time and temperature.

In conclusion, it appears that the physical ageing phenomenon plays a significant role in the restructuring of PE pipe materials. The important question which should

be addressed is what detrimental effects this phenomenon would inflict on the pipe performance as a function of its expected service-life.

5.4. Degree of Crystallinity Data

The extent of crystallinity was used in this study to investigate the effect of ageing on the physical structure of the three PE resins. The pipe samples made from the three PE resins were subjected to the specified ageing environments for a period of one year. A summary of the crystallinity contents obtained is presented in Table 5.3 to 5.5. Each result in the three tables represent an average of six test samples.

Table 5.3. Degree of crystallinity (%) data for pipe samples made from the Aldyl-A resin aged in the specified environments for one year.

Sample/Position	Surface	Middle	Bore
Virgin 125-pipe	47 (0.1)	53 (0.1)	54 (0.1)
125-pipe aged in water at 23°C	47 (0.1)	52 (0.1)	54 (0.1)
125-pipe aged in an air circulating oven at 80°C	53 (0.1)	56 (0.2)	57 (0.1)
125-pipe aged in water at 80°C	53 (0.4)	55 (0.4)	57 (0.1)
125-pipe aged in a vacuum-oven at 80°C	54 (0.3)	54 (0.2)	57 (0.2)
125-pipe from site laid in 1978 excavated 1995, age=17 years	49 (0.1)	56 (0.2)	57 (0.3)
125-pipe from site laid in 1971 excavated 1995, age=24 years (resin 5044)	49 (0.3)	56 (0.3)	57 (0.1)
8"pipe from site laid in 1978 excavated 1995, age=17 years	48 (0.1)	56 (0.4)	57 (0.3)
125-pipe (tan) from site laid in 1971 excavated 1995, age=24 years (resin 5044)	52 (0.1)	56 (0.1)	57 (0.1)

Standard deviation in parenthesis.

Table 5.4. Degree of crystallinity (%) data for pipe and plaque samples made from the Rigidex resin aged in the specified environments for one year.

Sample/Position	Surface	Middle	Bore
Virgin 125-pipe	49 (0.4)	52 (0.4)	54 (0.4)
125-pipe aged in water at 23°C	50 (0.4)	54 (0.3)	55 (0.1)
125-pipe aged in an air circulating oven at 80°C	55 (0.2)	58 (0.5)	59 (0.1)
125-pipe aged in water at 80°C	56 (0.1)	57 (0.1)	59 (0.1)
125-pipe aged in a vacuum-oven at 80°C	56 (0.1)	57 (0.3)	58 (0.1)
125-pipe site sample laid in 1981 excavated 1995, age=15 years	51 (0.3)	54 (0.4)	55 (0.2)
Virgin 180-pipe	50 (0.4)	53 (0.5)	55 (0.4)
180-pipe aged in water at 23°C	51 (0.2)	54 (0.4)	55 (0.1)
180-pipe aged in an air circulating oven at 80°C	56 (0.1)	57 (0.4)	58 (0.3)
180-pipe aged in water at 80°C	56 (0.2)	58 (0.1)	59 (0.1)
180-pipe aged in a vacuum-oven at 80°C	56 (0.1)	57 (0.1)	58 (0.1)
Virgin Rigidex plaque	55 (0.3)	57 (0.5)	55 (0.2)
Plaque aged in water at 23°C	57 (0.4)	56 (0.1)	55 (0.1)
Plaque aged in an air circulating oven at 80°C	58 (0.1)	59 (0.1)	59 (0.1)
Plaque aged in water at 80°C	59 (0.4)	59 (0.3)	59 (0.1)
Plaque aged in a vacuum-oven at 80°C	59 (0.3)	59 (0.5)	59 (0.1)

Standard deviation in parenthesis.

Table 5.5. Degree of crystallinity (%) data for pipe samples made from the Eltex resin aged in the specified environments for one year.

Sample/Position	Surface	Middle	Bore
Virgin 180-pipe	59 (0.7)	65 (0.6)	66 (0.3)
180-pipe aged in water at 23°C	58 (0.3)	66 (0.5)	67 (0.1)
180-pipe aged in an air circulating oven at 80°C	66 (0.2)	68 (0.5)	68 (0.4)
180-pipe aged in water at 80°C	65 (0.4)	70 (0.1)	70 (0.1)
180-pipe aged in a vacuum-oven at 80°C	66 (0.6)	67 (0.5)	70 (0.1)

Standard deviation in parenthesis.

To clarify the various behaviour observed in Tables 5.3 to 5.5 for the three polymer resins, each of the ageing conditions is discussed in a separate section.

5.4.1. Ageing in Water at 23°C

This environment for one year had no effect on the degree of crystallinity for the three pipe samples.

5.4.2. Ageing in an Air Circulating Oven at 80°C

In this environment overall crystallinity was found to increase for all the three pipe resin samples and this was attributed to thermal ageing. The increase in the crystallinity across the pipe wall sections was very similar. The Aldyl A and Rigidex crystallinity results summarised in Tables 5.3 and 5.4 respectively showed an average increase of 7% throughout the pipes wall. The Eltex crystallinity data summarised in Table 5.5 showed an average increase of 6% in the degree of crystallinity throughout the pipe wall.

5.4.3. Ageing in Water at 80°C

The 80°C temperature in this environment for one year increased the crystallinity for all the three pipe resin samples. The increase in crystallinity was similar to that of the air circulating oven ageing condition at 80°C which was attributed to thermal ageing.

5.4.4. Ageing in a Vacuum at 80°C

Again thermal ageing resulted in an increase of 7% in the degree of crystallinity for the three pipe resin samples in this environment.

5.4.5. Samples Aged In-Service

With reference to Table 5.3, the pipes made from the Aldyl A 5044 resin were described as first generation gas pipes. The pipes used in this study and the two pipes obtained from site were made from the Aldyl A 5046 resin and were described as second generation pipes. The 5044

resin is a butene based polyethylene and the 5046 resin is an octene based polyethylene. Therefore, the crystallinity of a virgin pipe made from the 5044 resin would be expected to be higher than a virgin pipe made from the 5046 resin. This is because the introduction of longer side chains will reduce the order in the system [Edward, 1986]. In the absence of crystallinity data of virgin pipe samples made from 5044 resin it is difficult to determine whether the crystallinity increased or not during their lifetime. But for the samples made from the 5046 resin the average increase in their crystallinity was 4%. This was not expected as the degree of crystallinity increased without thermal treatment. If the in-service aged pipe samples made from resin 5046 were manufactured in an identical method to that of the virgin pipe samples then it appears that they behaved in a different manner compared to the laboratory aged pipes. This behaviour was attributed to the physical ageing phenomenon described earlier in the temperature range above Tg and below 50°C.

The crystallinity of the Rigidex pipe results shown in Table 5.4 was also found to increase by 1%.

It was not possible to secure any Eltex pipe sample from site as this resin is relatively new in the gas industry.

CHAPTER

SIX

CHAPTER SIX

STATIC MECHANICAL PROPERTIES OF PE PIPE RESINS

6.1. Introduction

This chapter deals with the macro- and micro-tensile testing of the three pipe resin systems before and after ageing. The effect of ageing on stress-strain traces and residual stresses were also discussed. Two types of micro-tensile specimens were evaluated in this study namely, dumb-bell and rectangular. The standard macro-tensile samples were cut directly from aged and unaged pipes. The sensitivity of the macro-samples to the rate of testing was investigated and accordingly a cross-head speed was selected for all the subsequent tensile test experiments. Issues relating to data acquisition are also discussed.

6.2. Evaluation of Micro-Tensile Samples

Two types of micro-tensile film samples were evaluated in this study. The first type was a dumb-bell film produced using a BS 903 standard 35 mm dumb-bell die and the second type was a rectangular film where the outer and inner pipe surfaces were retained. Figure 6.1 shows typical tensile traces for the two types of micro-tensile specimens used.

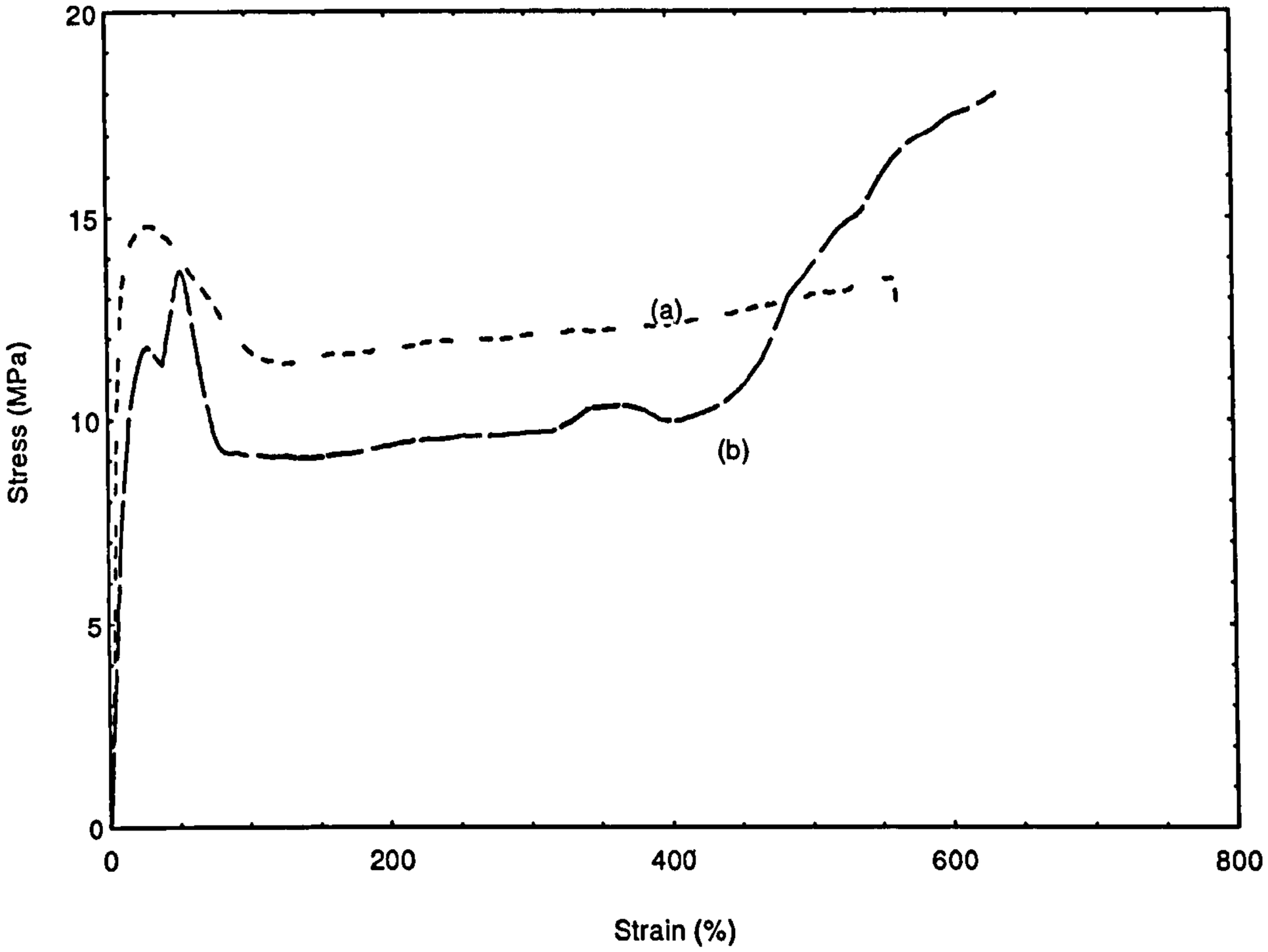

Figure 6.1. Typical stress-strain traces for (a) the rectangular test specimen geometry and (b) the dumb-bell micro-tensile samples. The samples were prepared from Rigidex 125-pipe.

In Figure 6.1 the data showed that the initial stress was proportional to the strain and Hooke's law was obeyed for both sample types. For the rectangular film (a) the curve reached a maximum and this is conventionally known as the yield point. In the case of the dumb-bell film (b) more than one peak was observed along the stress-strain trace. The measurements of a yield point in polymers is accepted as being the point where the stress-strain trace shows a local maximum [Brooks et al., 1992]. The occurrence of more than one peak was attributed to the appearance of more than one neck being formed along the gauge length as illustrated in Figure 6.2. The formation of the neck was due to a reduction in the film thickness in certain areas which created local stresses. The thickness variations were produced during the preparation of the dumb-bell

samples using the microtome. The cutting area of the dumb-bell sample facing the microtome's blade is dissimilar. Therefore, during slicing a thin dumb-bell film the stress exerted by the microtome blade on the sample face was not constant which caused the film thickness to vary. This was confirmed by measuring the thickness along the dumb-bell film samples using micrometer.

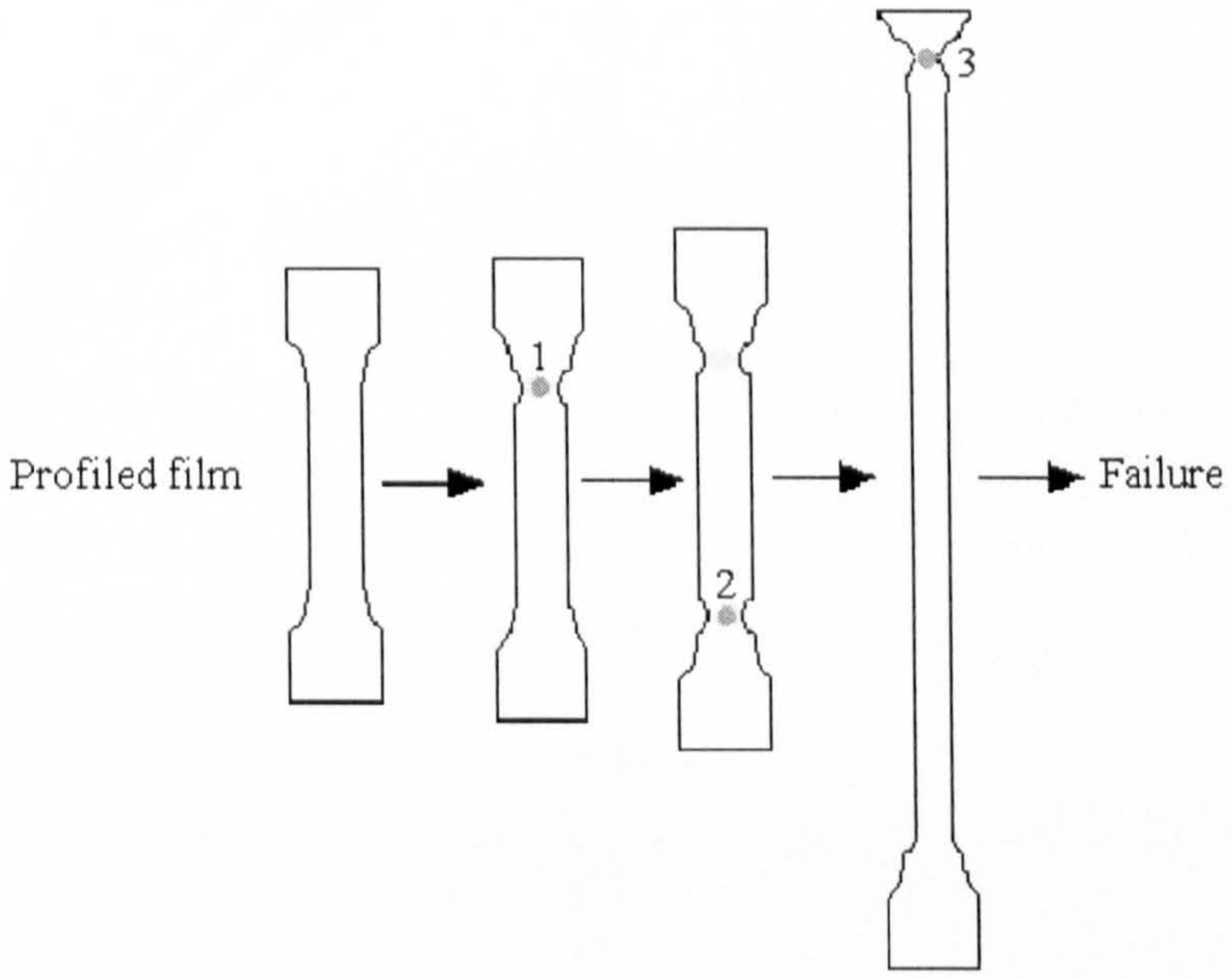

Figure 6.2. Successive stretching of a dumb-bell film sample in the uniaxial direction with formation of more than one neck (1, 2 and 3) along the gauge length.

Because the yield point was difficult to define for the dumb-bell film samples the rectangular geometry was preferred for the micro-tensile specimens in this study.

6.3. Cross-Head Speed

A brief study was undertaken to investigate the influence of the strain rate on the mechanical properties of macro-tensile samples. SEN specimens prepared from Rigidex compression moulded plaques were used for this investigation. The cross-head speed was varied from 0.1

to 10^3 mm/min and the stress-strain curves were recorded as shown in Figure 6.3.

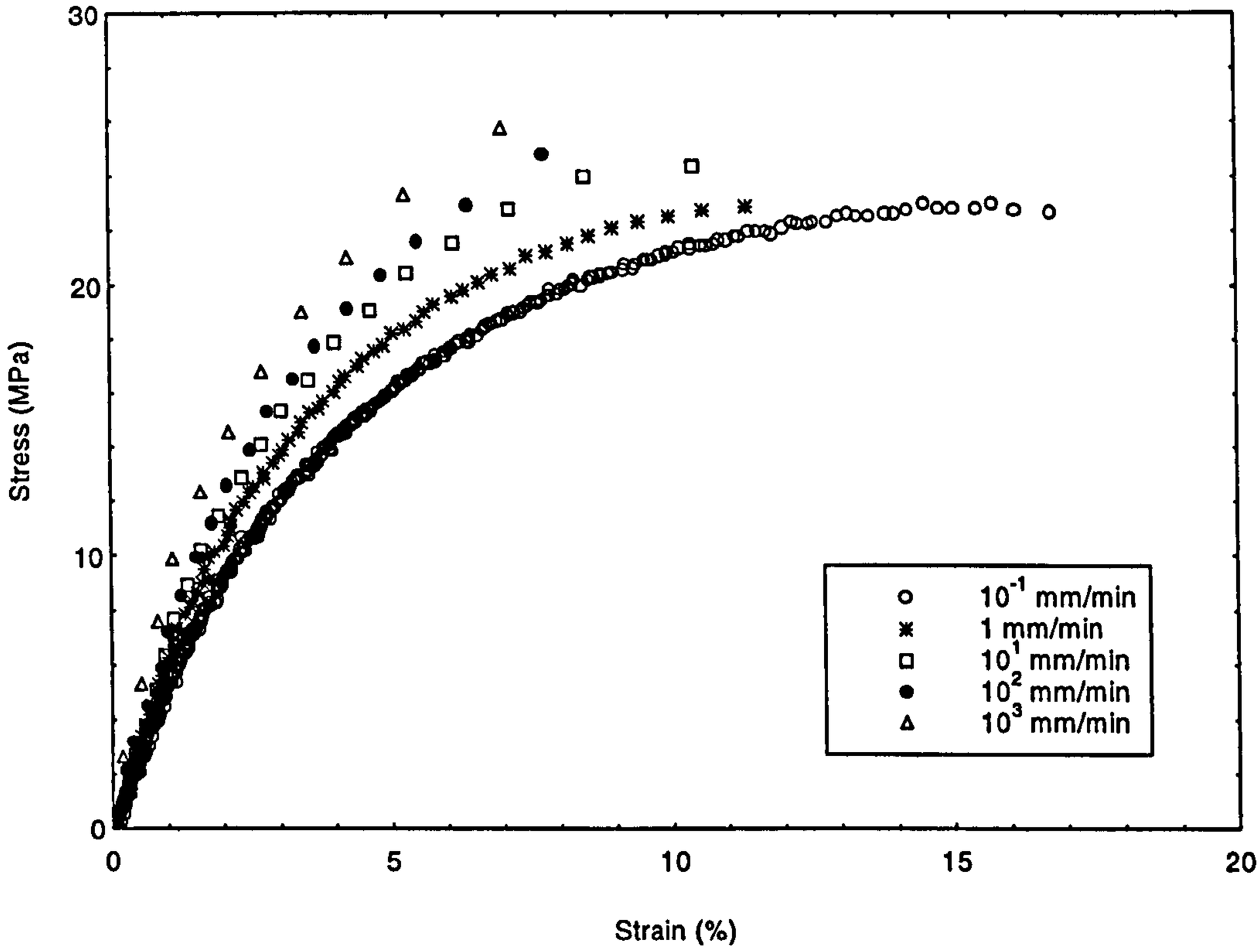

Figure 6.3. Stress vs. strain curves for the rectangular specimens at the specified cross-head speed.

It is clear from Figure 6.3 that PE is rate sensitive. The exact shape of the stress-strain curve for the SEN specimens was dependent on the rate of testing. From the stress-strain traces the tensile mechanical properties were obtained and are presented in Table 6.1. Each data value represent an average of 3 individual specimens.

Table 6.1. Mechanical properties obtained using SEN specimens at different cross-head speed.

Sample number	Cross-Head speed (mm/min)	Young's Modulus (MPa)	Stress at break (MPa)	Strain at break (%)
1	0.1	540	22.7	16.7
2	1	590	22.9	11.3
3	2	702	24.4	10.4
4	5	735	24.8	7.7
5	10	1030	25.6	7

With reference to Table 6.1, as the speed of testing was increased both the modulus and the stress at break increased but, the strain at break decreased. This was attributed to the viscoelastic characteristics of PE polymers. At high strain rates the ductility of the polymer decreased and the SEN specimens behaved in a brittle manner. Conversely, at low rates the polymer behaved in a more ductile manner. There is a similar interdependence of the properties upon test temperature. In general, it is found that the effect of increasing the speed of testing upon mechanical properties is the same as reducing the testing temperature. The cross-head speed was also found to affect the mechanical properties obtained via the micro-tensile testing. The cross-head speed was fixed throughout this study at 1 mm/min for both the macro- and micro-tensile testing.

6.4. Sampling Frequency

Two different software packages were used for the macro- and micro-tensile tests. The ability of the two software packages to process the data at different sampling frequencies was examined. The range of sampling frequencies accepted by the macro- and micro-tensile softwares were from 1-20 and 1-100 points/s respectively. The sampling frequency was varied in both cases and the modulus was calculated and presented in Table 6.2. The cross-head speed for both tests was 1 mm/min.

Table 6.2. Summary of the modulus results obtained from the macro- and micro-tensile tests along with the corresponding sampling frequency used. The samples used were macro standard tensile test specimen and rectangular films prepared from Rigidex plaques.

Macro-Tensile test		Micro-Tensile test	
Sampling frequency (point/s)	Young's Modulus (MPa)	Sampling frequency (point/s)	Modulus (MPa)
1	560 (51)	1	190 (26)
10	703 (34)	50	325 (22)
20	950 (67)	100	552 (32)

from Table 6.2 it clear that the sampling frequency at which the data was obtained had a considerable influence on the results for both the macro- and micro-test. Two issues were addressed:

(i) In both tests, the secant modulus at 2% strain increased as the sampling frequency was raised. This was attributed to the number of data points recorded by the softwares from zero up to 2% strain. At high sampling rates the initial stages of the stress-strain curves were represented by a large number of data points. This prompted both softwares to capture more information at the very initial stages of testing.

(ii) When the same sampling frequency was used for both the micro- and macro-tensile tests, the modulus results were dissimilar. This was associated with noise in the load-signal for the micro-tensile test and the correction which was made to rectify this problem. The problem was solved by filtering the load-signal but this created a delay in the data acquisition. By raising the sampling frequency from 1 to 100 point/s the delay was eliminated. Hence the modulus values quoted at 100 point/s for the micro-test and 1 point/s for the macro-test. The results are similar to the published information on Rigidex resin [BP Rigidex data product sheets].

6.5. Macro- And Micro-Tensile Data

A summary of the mechanical properties for the macro- and micro-tensile test results for the aged and unaged pipe resins is presented in Tables 6.3 to 6.8.

All the virgin and laboratory aged macro-tensile specimens showed a strain at break above 500% except the Aldyl-A (5044) resin samples from site.

The strain at break results for the micro-tensile specimens showed a large spread. This was attributed to

excessive specimen slippage during testing from the grips at high strains. The scratches induced by the microtome blade when preparing the film specimens also contributed to the scatter observed by dominating the failure modes.

Table 6.3. Macro-Tensile data for pipe samples made from the Aldyl-A resin aged in the specified environments for one year.

Sample	Young's Modulus (MPa)	Stress at yield (MPa)
Virgin 125-pipe	409 (73)	13.4 (0.1)
125-pipe aged in water at 23°C	422 (24)	13.8 (0.2)
125-pipe aged in an air circulating oven at 80°C	557 (85)	14.3 (1.4)
125-pipe aged in water at 80°C	576 (97)	14.5 (1.3)
125-pipe aged in a vacuum-oven at 80°C	579 (37)	14.6 (0.7)
125-pipe from site laid in 1978 excavated 1995, age=17 years	536 (34)	14 (0.1)
125-pipe from site laid in 1971 excavated 1995, age=24 years (resin 5044)	559 (19)	14.2 (1.5)
8"pipe from site laid in 1978 excavated 1995, age=17 years	533 (21)	14 (2.6)
125-pipe (tan) from site laid in 1971 excavated 1995, age=24 years (resin 5044)	571 (56)	14.8 (2.1)

Standard deviation in parenthesis.

Table 6.4. Macro-Tensile data for pipe and plaque samples made from the Rigidex resin aged in the specified environments for one year.

Sample	Young's Modulus (MPa)	Stress at yield (MPa)
Virgin 125-pipe	542 (65)	14.1 (0.3)
125-pipe aged in water at 23°C	547 (77)	14.1 (0.5)
125-pipe aged in an air circulating oven at 80°C	655 (52)	14.8 (1.6)
125-pipe aged in water at 80°C	658 (25)	15 (0.9)
125-pipe aged in a vacuum-oven at 80°C	660 (45)	15.2 (0.5)
125-pipe site sample laid in 1981 excavated 1995, age=15 years	547 (90)	14.2 (1.2)
Virgin 180-pipe	554 (42)	14.3 (0.2)
180-pipe aged in water at 23°C	560 (54)	14.5 (1)
180-pipe aged in an air circulating oven at 80°C	661 (92)	15 (1.2)
180-pipe aged in water at 80°C	662 (36)	15.2 (0.9)
180-pipe aged in a vacuum-oven at 80°C	662 (56)	15.3 (0.7)
Virgin Rigidex plaque	560 (51)	14.5 (0.2)
Plaque aged in water at 23°C	562 (97)	14.5 (0.9)
Plaque aged in an air circulating oven at 80°C	676 (24)	15.2 (1.5)
Plaque aged in water at 80°C	675 (46)	15.4 (1.4)
Plaque aged in a vacuum-oven at 80°C	677 (49)	15.4 (0.4)

Standard deviation in parenthesis.

Table 6.5. Macro-Tensile data for pipe samples made from the Eltex resin aged in the specified environments for one year.

Sample/Position	Young's Modulus (MPa)	Stress at yield (MPa)
Virgin 180-pipe	1010 (26)	18.3 (0.1)
180-pipe aged in water at 23°C	1023 (43)	18.6 (2.1)
180-pipe aged in an air circulating oven at 80°C	1147 (115)	19.2 (0.2)
180-pipe aged in water at 80°C	1153 (89)	19 (1.2)
180-pipe aged in a vacuum-oven at 80°C	1152 (46)	18.8 (0.2)

Standard deviation in parenthesis.

Table 6.6. Micro-Tensile data for pipe samples made from the Aldyl-A resin aged in the specified environments for one year.

Sample	Young's Modulus (MPa)	Stress at yield (MPa)	Strain at break (%)
Virgin 125-pipe	385 (44)	14.2 (1)	443 (122)
125-pipe aged in water at 23°C	396 (34)	14.5 (1.2)	507 (153)
125-pipe aged in an air circulating oven at 80°C	537 (25)	14.9 (0.9)	402 (173)
125-pipe aged in water at 80°C	557 (45)	14.9 (0.5)	415 (168)
125-pipe aged in a vacuum-oven at 80°C	551 (12)	14.9 (0.7)	389 (127)
125-pipe from site laid in 1978 excavated 1995, age=17 years	508 (36)	14.8 (1.3)	549 (131)
125-pipe from site laid in 1971 excavated 1995, age=24 years (resin 5044)	536 (32)	14.8 (1)	360 (128)
8"pipe from site laid in 1978 excavated 1995, age=17 years	515 (28)	14.7 (1.5)	448 (106)
125-pipe (tan) from site laid in 1971 excavated 1995, age=24 years (resin 5044)	540 (16)	14.8 (2.1)	392 (112)

Standard deviation in parenthesis.

Table 6.7. Micro-Tensile data for pipe and plaque samples made from the Rigidex resin aged in the specified environments for one year.

Sample	Young's Modulus (MPa)	Stress at yield (MPa)	Strain at break (%)
Virgin 125-pipe	512 (15)	15 (0.2)	674 (138)
125-pipe aged in water at 23°C	539 (36)	15 (1)	562 (172)
125-pipe aged in an air circulating oven at 80°C	622 (45)	17.8 (0.6)	476 (159)
125-pipe aged in water at 80°C	634 (43)	17.9 (1.2)	472 (144)
125-pipe aged in a vacuum-oven at 80°C	629 (17)	17.8 (0.9)	390 (135)
125-pipe site sample laid in 1981 excavated 1995, age=15 years	533 (39)	15.2 (0.2)	588 (174)
Virgin 180-pipe	534 (29)	15.4 (0.3)	866 (186)
180-pipe aged in water at 23°C	546 (42)	15.7 (0.8)	923 (179)
180-pipe aged in an air circulating oven at 80°C	649 (25)	18.1 (0.2)	705 (129)
180-pipe aged in water at 80°C	630 (32)	18.3 (1.7)	756 (117)
180-pipe aged in a vacuum-oven at 80°C	641 (11)	18.4 (0.8)	772 (151)
Virgin Rigidex plaque	595 (14)	17.1 (0.2)	535 (191)
Plaque aged in water at 23°C	607 (24)	17.2 (0.7)	555 (157)
Plaque aged in an air circulating oven at 80°C	677 (43)	19.2 (0.5)	435 (137)
Plaque aged in water at 80°C	681 (13)	19.4 (1.1)	408 (144)
Plaque aged in a vacuum-oven at 80°C	699 (31)	19.5 (0.6)	375 (187)

Standard deviation in parenthesis.

Table 6.8. Micro-Tensile data for pipe samples made from the Eltex resin aged in the specified environments for one year.

Sample/Position	Young's Modulus (MPa)	Stress at yield (MPa)	Strain at break (%)
Virgin 180-pipe	986 (19)	23.1 (0.1)	486 (146)
180-pipe aged in water at 23°C	984 (22)	23.3 (0.9)	476 (107)
180-pipe aged in an air circulating oven at 80°C	1123 (18)	24.4 (0.2)	409 (140)
180-pipe aged in water at 80°C	1129 (28)	24.6 (1.3)	397 (147)
180-pipe aged in a vacuum-oven at 80°C	1131 (36)	24.5 (0.2)	383 (99)

Standard deviation in parenthesis.

With reference to Tables 6.3 to 6.8, on one hand, the data indicated that the modulus for the macro-tensile test were slightly higher than that obtained for the micro-tensile test. This was attributed to the correction made to the load-signal discussed previously. On the other hand, the yield stresses for the micro-tensile tests were higher than that observed for the macro-tensile tests. This may be related to the geometry of the test specimen: the macro-tensile specimen geometry provided plane strain conditions and the micro-tensile film specimen provided plane stress conditions.

In general, the trend of the macro-tensile results presented in Tables 6.3 to 6.5 closely echoed that of the micro-tensile results in Tables 6.6 to 6.8. This correlation was important as the primary purpose of the micro-tensile test was to negate the need for long sections of pipes to be excavated and to facilitate the condition assessment programme. As discussed previously, micro-samples can be obtained using a tapping tee as described in section 3.2.2. Furthermore, the disk samples can be obtained without disrupting the flow of gas in PE pipelines.

Only the micro-tensile data summarised in Tables 6.6 to 6.9 are discussed and to clarify the various behaviour observed for the three polymer resins, each of the ageing conditions is reflected on in a separate section.

6.5.1. Ageing in Water at 23°C

With reference to the Aldyl A data presented in Table 6.6, after one year of ageing in water at 23°C an increase of 3% in the modulus value was recorded and the increase in the yield stress was approximately 2%. These results fall within the error spread in the test data of 10% and 7% for the modulus and yield stress values, respectively.

With reference to the Rigidex data presented in Table 6.7, the modulus and yield stress values were also within the experimental error. Therefore, it is appropriate to conclude that there were no significant changes in the tensile properties for the samples which were aged in water for one year at 23°C.

This was also the case for the Eltex data presented in Table 6.8.

In general, ageing the three PE resins in water for one year at 23°C had no effect on the tensile mechanical properties.

6.5.2. Ageing in an Air Circulating Oven at 80°C

With reference to the Aldyl A data presented in Table 6.6, there was a significant increase of 39% in the modulus value and approximately 5% in the yield stress after one year of ageing in an air circulating oven at 80°C. As the tensile properties are related to the extent of crystallinity in the polymer [Darras and Seguela, 1993], the observed increases in the modulus and yield stress are attributed to the increase in the crystallinity across the pipe wall as reported in chapter five section 5.3.

With reference to the Rigidex data summarised in Table 6.7, the modulus and yield stress increased by an average of 19% and 15%, respectively. This was also attributed to the increase in the crystallinity as a consequence of the thermal ageing treatment. The crystallinity for Rigidex samples increased by an average of 7% after one year of thermal ageing.

For the Eltex sample presented in Table 6.8, the data indicated that the modulus and yield stress increased by 14% and 6%, respectively. The change in the degree of crystallinity for Eltex pipe sample was 6%.

Although, the average increases in the crystallinity across the thickness of the three pipe resin samples aged in an air circulating oven for one year at 80°C was approximately the same, the deterioration in the tensile properties was not. This behaviour was expected because the three resins have a different short branch frequency, molecular weight and molecular weight distribution. Hence their individual responses to a specific thermal ageing regime will have a different outcome on the general mechanical properties.

6.5.3. Ageing in Water at 80°C

With reference to the Aldyl A results presented in Table 6.6, there was an increase of 45% and 5% in the modulus and yield stress values, respectively, after one year of ageing in this environment. The increase in crystallinity was 7% and the tensile results were similar to the results obtained when the samples where aged in the air circulating oven for one year at 80°C.

In the case of the Rigidex results summarised in Table 6.7, the modulus and yield stress increased by an average of 24% and 19%, respectively. These results are slightly higher than those obtained for the samples which were aged in an air circulating oven. The results in chapter

five also showed that the crystallinity for the thermally aged in water samples was fractionally higher than the crystallinity for the oven aged samples. During the 80°C ageing programme it was necessary to move these specimens from one water bath to another because the site where the pipe were being aged was being relocated. It is not known if this had an influence on the ageing process.

With reference to the Eltex data presented in Table 6.8, ageing in water for one year at 80°C also caused an increase in the modulus and yield stress. The observed increase was similar to the increase observed for the air circulating oven ageing experiments.

6.5.4. Ageing in a Vacuum at 80°C

With reference to the Aldyl A data presented in Table 6.6, the modulus and yield stress increased by 43% and 5%, respectively. This behaviour was similar to that observed in the water and oven aged samples for one year at 80°C.

In the case of the Rigidex results summarised in Table 6.7, the modulus and yield stress values increased by an average of 23% and 18%, respectively. These results were similar to those obtained from ageing the Rigidex samples at 80°C in water and an oven at 80°C.

For the Eltex data presented in Table 6.8, the increase in the modulus was 15% and 6% for the yield stress. This behaviour was also in line with all the thermally aged Eltex samples.

Overall, the modulus and the yield stress increased for all the thermally aged samples. This increase was attributed to the increase in crystallinity due to thermal ageing because there was no evidence of oxidative degradation in these samples.

6.5.5. Samples Aged In-Service

With reference to the data for the Aldyl A samples from site presented in Table 6.6, the increase in the yield stress was 4% for all the samples. But, the increase in the modulus varied as follows:

(i) increase in the modulus for the 125-pipe age=17 years was 32%;
(ii) 40% was for the 125-pipe age=24 years (resin 5044);
(iii) 34% was for the 8"pipe age=17 years; and
(iv) 40% was for the 125-pipe (tan) age=24 years (resin 5044).

The crystallinity of a virgin pipe made from the 5044 resin would be expected to be higher than a virgin pipe made from the 5046 resin as discussed in chapter 5 section 5.3.5. Therefore, the increase in the modulus and yield stress recorded for the pipe samples made from the 5044 resin could be considered as expected. But the increase observed in the tensile properties for the other two pipe samples made from the same resin as the pipes used in this study was surprising. These samples were not expected to record over a 30% and 4% increase in the modulus and the yield stress, respectively.

It was not possible to secure any Eltex pipe sample from site as this resin is a relatively new resin in the gas industry.

6.6. The Effect of Ageing on Static Mechanical Properties

6.6.1. Residual Stresses Measurements

The objective of this investigation was to find the effect of laboratory ageing on the residual stresses in PE pipes. The residual stress in the pipe wall are usually developed during the manufacture of PE pipes during the cooling and solidification process. As a consequence of the cooling regime imposed, tensile stresses develop on the inner surface of the pipe and compressive stresses on the outer surface [Williams and

Hodgkinson, 1981]. The ring method was used to estimate the residual stresses for Rigidex 125-pipes. A summary of the residual stress results is presented in Table 6.9.

Table 6.9. Residual stress data for virgin and aged Rigidex 125-pipes.

Sample	Residual Stress (MPa)
Virgin Rigidex	1.71 (0.05)
125-pipe aged in water for one year at 23°C	1.7 (0.04)
125-pipe aged in an air circulating oven for one year at 80°C	1.18 (0.01)
125-pipe aged in water for one year at 80°C	1.21 (0.02)
125-pipe aged in a vacuum-oven for one year at 80°C	1.19 (0.02)

Standard deviation in parenthesis.

With reference to Table 6.9, no significant change in the residual stresses were observed for the pipe aged in water for one year at 23°C. The residual stresses for the pipes annealed at 80°C decreased significantly. This behaviour was related to the crystallinity across the pipes wall. An important factor to note is the relative increase within the pipe wall as shown in Figure 6.4.

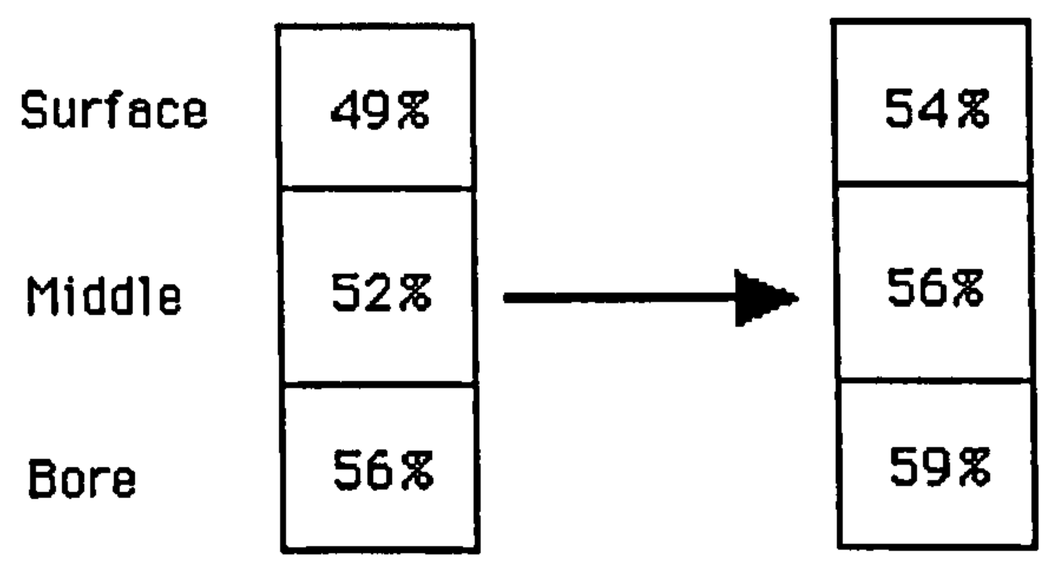

Figure 6.4. The degree of crystallinity for virgin and annealed 125-pipe for the pipe surface, middle and bore. The annealed pipe was aged in an air circulating oven for one year at 80°C.

With reference to Figure 6.4, after one year of thermal ageing the increase in crystallinity was the highest for the pipe surface section followed by the middle and the bore. It could be argued that the spread in the crystallinity across the pipe wall grew narrower as a result of annealing which slightly relieved the residual stresses on the inner surface of the pipe. It was reported [Broutman and Bhatnager, 1985] that in some cases annealing eliminated the residual stresses on the inner pipe wall.

6.6.2. Stress-Strain Traces

Figure 6.5 depicts two stress-strain traces and each represent an average of six individual micro-tensile tests conducted for the aged and unaged Rigidex plaques. The ageing was carried out in an air circulating oven for one year at 80°C.

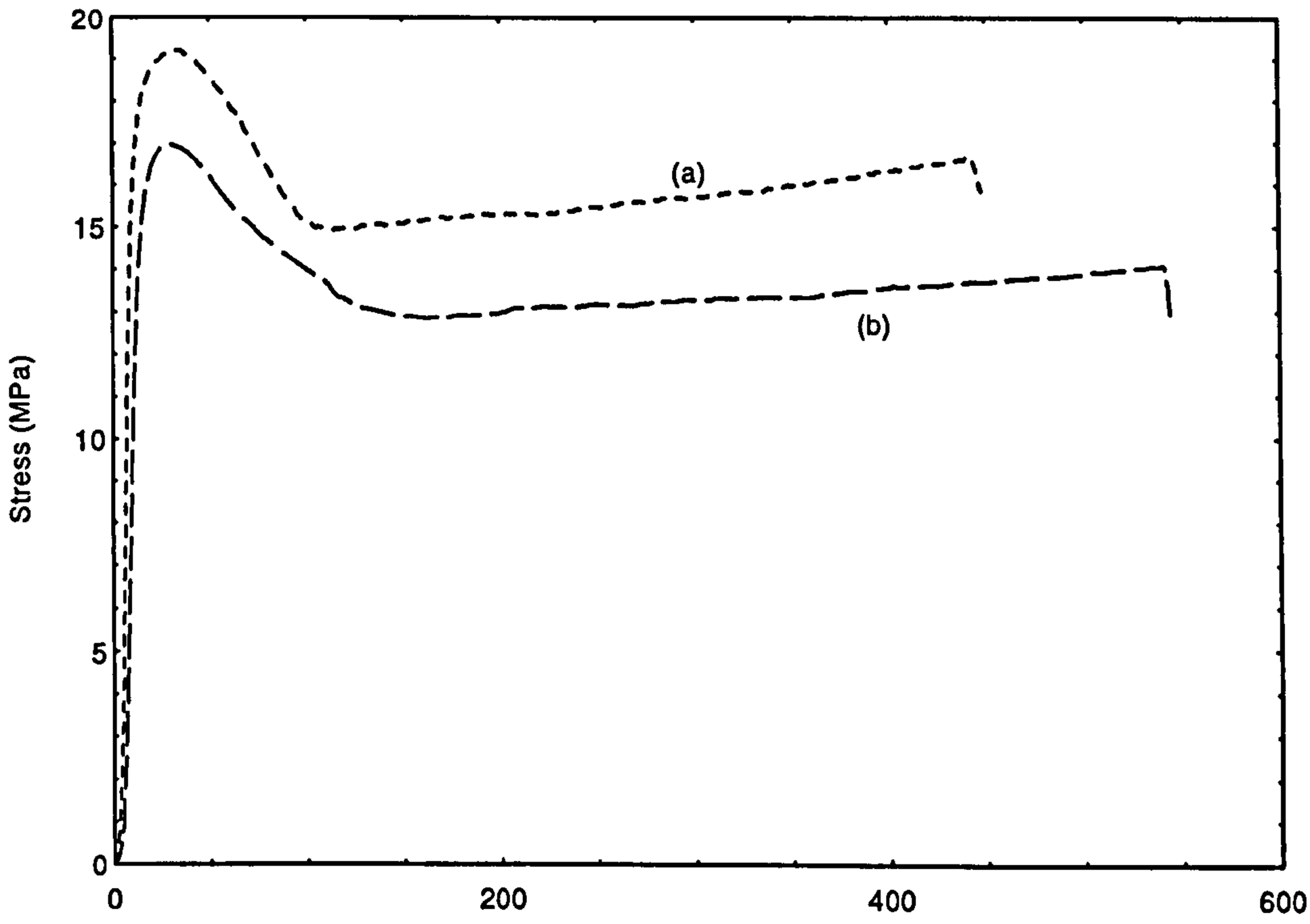

Figure 6.5. Micro-tensile stress-strain traces for samples prepared from (a) Rigidex plaque aged in an air circulating oven for one year at 80°C and (b) unaged Rigidex plaque.

With reference to Figure 6.5, the modulus increased by 20% and the stress at yield by 15%, but, the strain at break showed a reduction of approximately 20%. As pointed out in chapter 5, annealing the polymer at 80°C increased the crystallinity. This caused the polymer sample to behave in a more brittle-like manner. The relation between thermal ageing and the mechanical properties is supported by an early report published in the literature by Clements et al. [1979] which established a direct correlation between the mechanical properties of a PE sample and its crystallinity and more importantly the correlation was retained for annealed samples.

6.6.3. Tensile Mechanical Properties

The macro- and micro-tensile tests carried out on pipe resin specimens indicated that the laboratory ageing experiments had a profound effect on the tensile properties. As there was no chemical ageing detected in these samples the effect was attributed to physical ageing. Physical ageing in the form of increased crystallinity of pipe samples was believed to be the main reason for the changes in the tensile properties. The tensile properties (modulus, stress at yield and elongation at break) data for the micro-tensile specimens are presented in Figures 6.6 to 6.11 taken form Tables 6.6 to 6.8 along with the respective average (surface, middle and bore) crystallinity for each sample as shown in Figures 6.6 to 6.11.

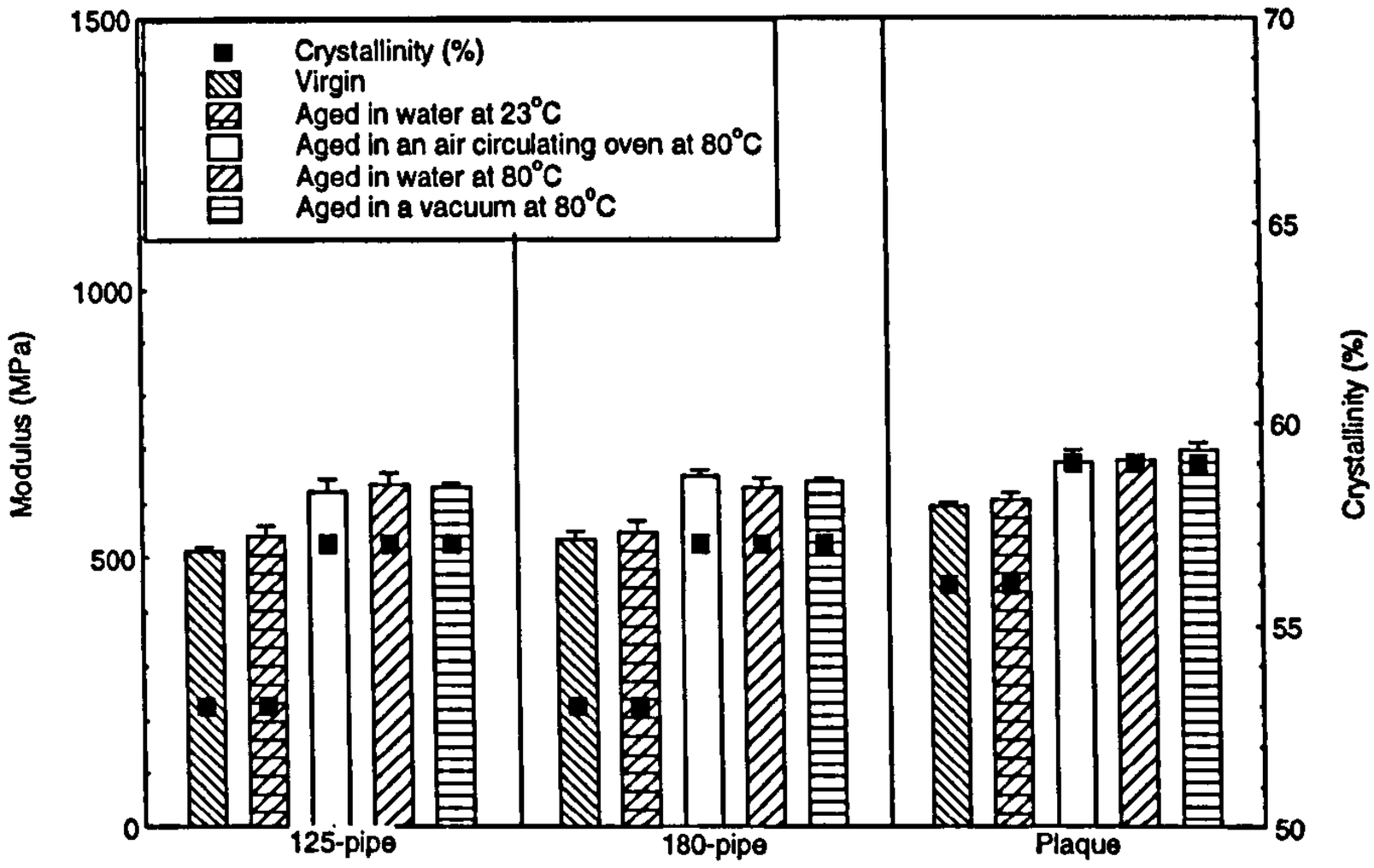

Figure 6.6. The Young's modulus results for the Rigidex micro-tensile specimens along with their respective crystallinity. The ageing experiments were for one year.

With reference to Figure 6.6, the virgin plaque sample showed the highest modulus value when compared with the two virgin pipe samples. This was attributed to the crystallinity of the plague sample which was higher than the rest of the Rigidex samples. It is also clear form Figure 6.6 that there was an increase in the modulus values for all the thermally aged Rigidex specimens as their crystallinity increased with ageing. This result is supported the work carried out by Crist [1989]. He showed that thermal ageing of PE samples also increased the initial modulus. He explained by means of small angle x-ray scattering that the increase in the polymer crystal thickness is the dominant factor in increasing the modulus. He extended the work to achieve the same result by blending a variety of PE grades to obtain different crystal thickness. He attributed the increase in the modulus not only to the increase in the lamella thickness upon annealing, but also to the increase in the elastic modulus of the amorphous region. The latter was ascribed to the constrains imposed by the expanding crystals on the amorphous region.

The modulus of the three PE pipe resin samples used in this study was plotted with their crystallinity as shown in Figure 6.7.

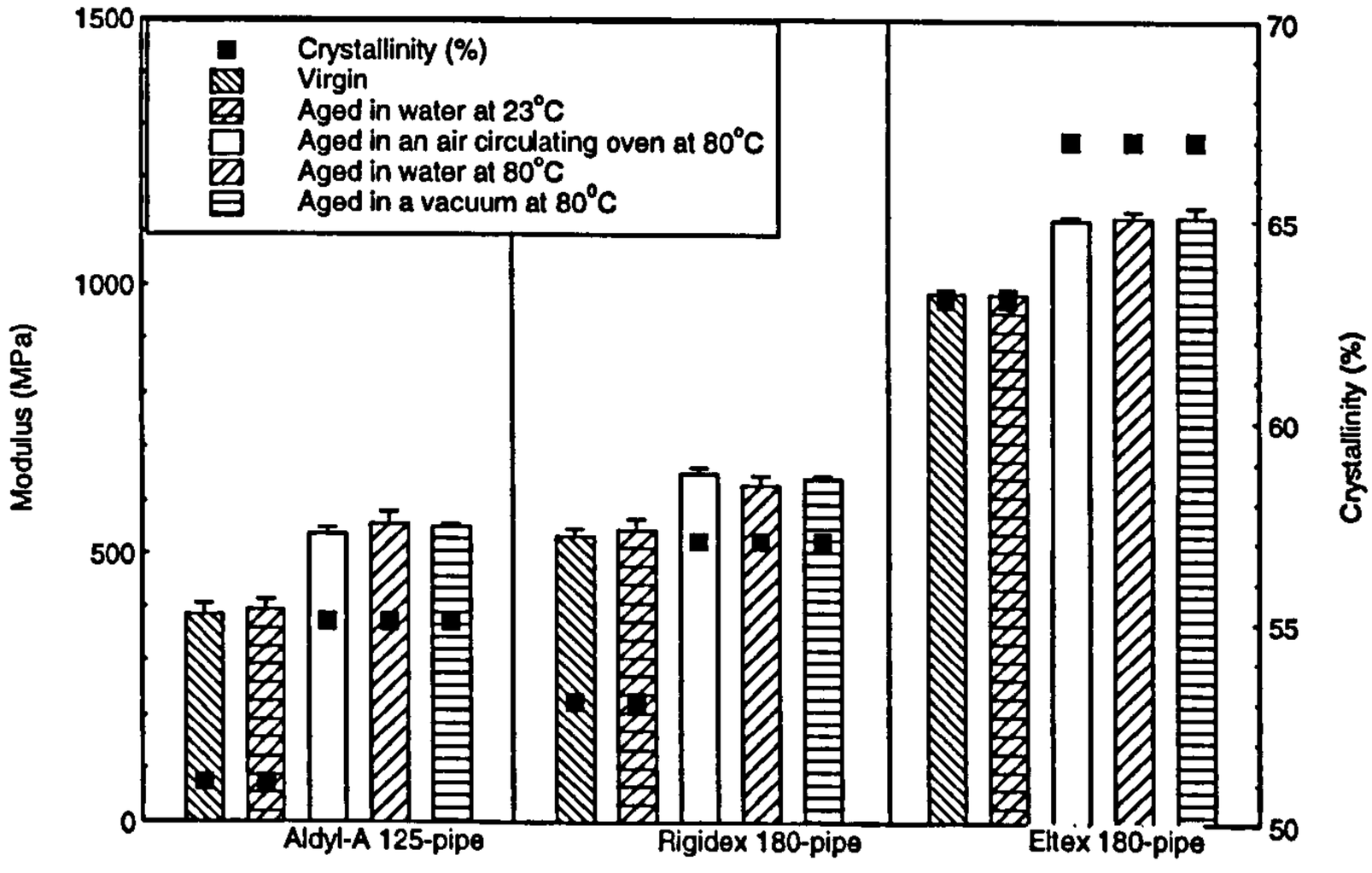

Figure 6.7. The modulus results for the Aldyl-A, Rigidex and Eltex micro-tensile pipe specimens along with their respective crystallinity. The ageing experiments were for one year.

With reference to Crist's [1989] work and the results in Figure 6.7, the modulus of each virgin PE pipe resin sample indicated that there was a direct link with its crystallinity and upon thermal ageing this trend was maintained. This result was expected as each PE resin has a different thermal history, molecular weight, molecular weight distribution and branch length and frequency. Each of these factor considerably controls the crystallinity of PE samples. For example, the Eltex resin has the highest molecular weight, the lowest branch frequency and branch length when compared with the Rigidex and the Aldyl-A resins. Therefore, it was expected to find the Eltex resin with the highest crystallinity followed by the Rigidex and then by the Aldyl-A. The modulus of the Rigidex resin is higher than the Aldyl-a resin also for the same reasons. It could be said here that the crystallinity order for the three PE resins originated the same modulus order.

Ogita et al. [1991] also demonstrated how the modulus value of ultrahigh-molecular-weight polyethylenes was influenced by the changes in the crystallinity of the materials. They specifically related these changes to the dependence of the crystallinity on the molecular weight of the PE resin. They showed that the resin with the higher molecular weight gave the higher modulus value which again supports the results of this study.

In the case of the yield stress results, it was found that there were no significant differences when compared with the modulus results as presented in Figures 6.8 and 6.9.

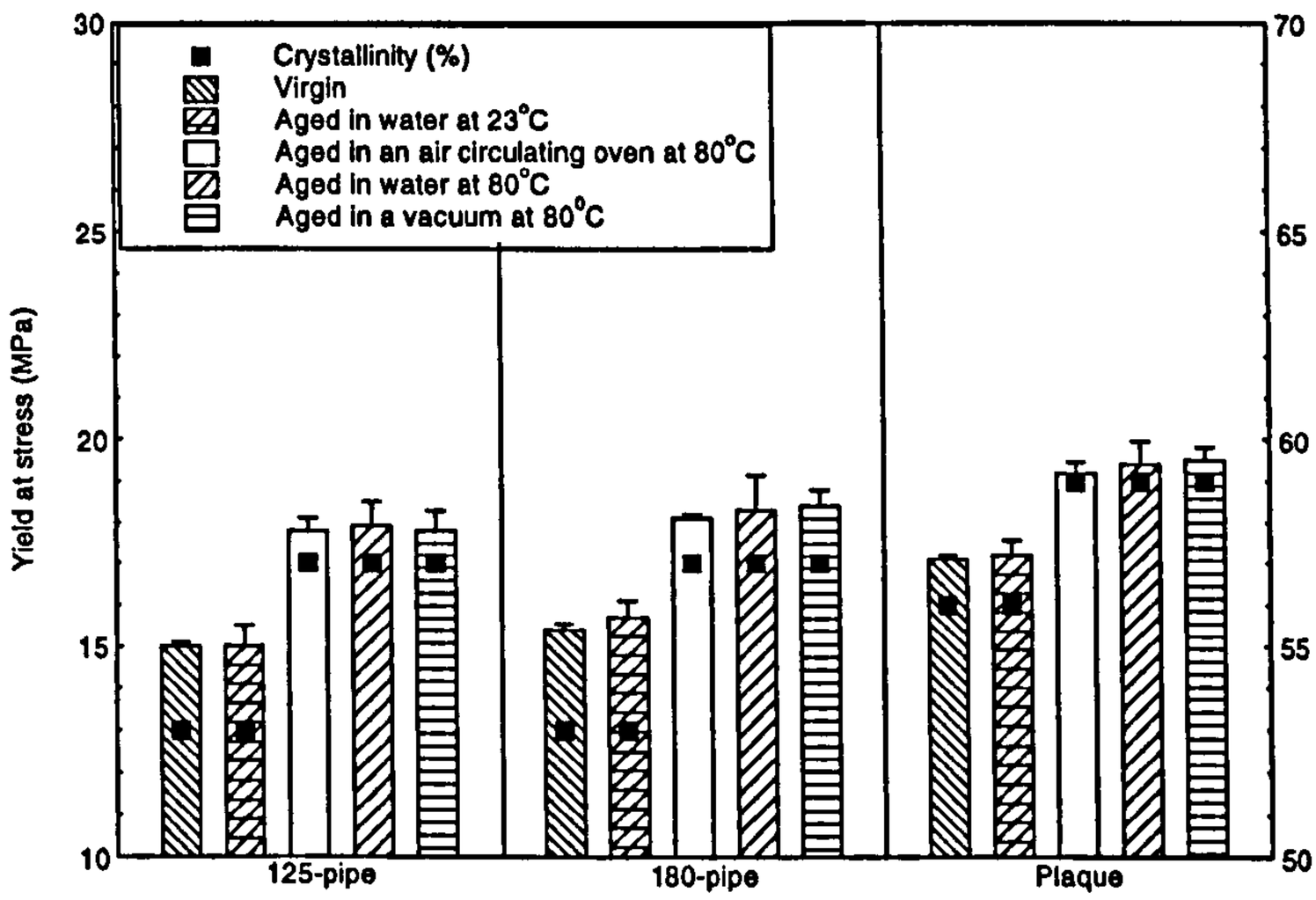

Figure 6.8. The stress at yield results for the Rigidex micro-tensile specimens along with their respective crystallinity. The ageing experiments were for one year.

In Figure 6.8, the plaque specimens were seen to exhibit the higher yield stress than the 125-pipe and 180-pipe samples. This was again attributed to the higher crystallinity of the plaque samples when compared with the rest.

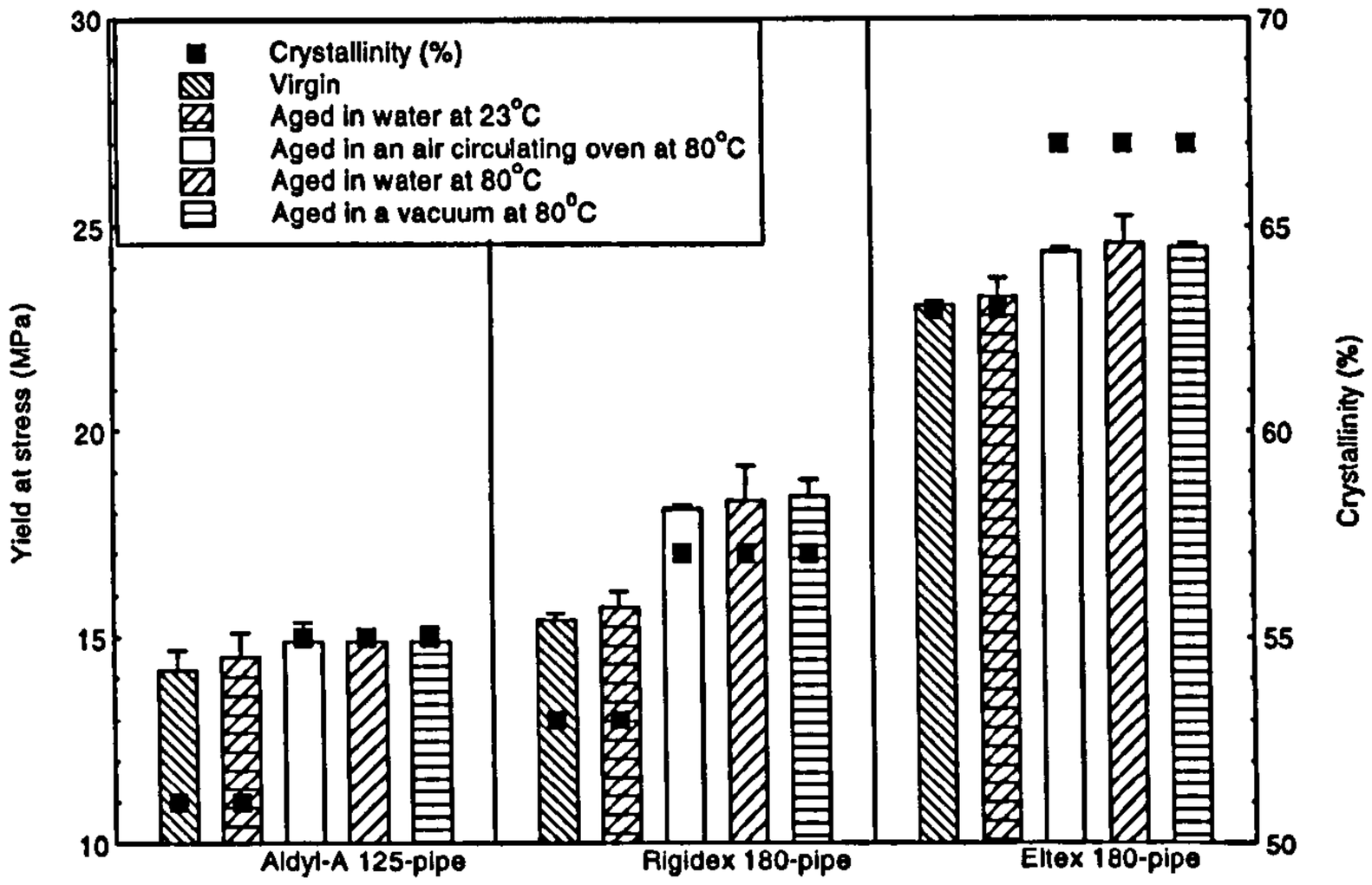

Figure 6.9. The stress at yield results for the Aldyl-A, Rigidex and Eltex micro-tensile pipe specimens along with their respective crystallinity. The ageing experiments were for one year.

With reference to Figure 6.9, the Eltex specimens with the highest crystallinity when compared with the Aldy-A and the Rigidex samples showed the highest yield stress. This was followed by the Rigidex samples and then by the Aldyl-A samples which had the lowest crystallinity. Upon thermal ageing all the three PE pipe resin samples showed an increase in the yield stress.

Graham et al. [1997] recently studied nominal stress-strain curves of a series of random ethylene-hexene copolymers having narrow composition and said to be most probable molecular weight distributions. A series of such molecular weight copolymers with a constant concentration of branches were crystallised under a variety of conditions. In each molecular weight series the level of crystallinity was approximately constant. Particular attention was focused on the yield region and the nature of the yielding process. It was found that the yield stress was not solely dependent on the crystallinity level. Moreover, the shape of the curve in the yield

region was very dependent on the molecular weight and the crystallisation mode. These changes in yielding correlated quite well with the overall crystallite structure which was characterised by thin section transmission electron microscopy. They also found that the orthorhombic unit cell of polyethylene was maintained in all the samples despite the changes that occurred in the overall crystallite structure.

To further clarify the interconnection between the crystallinity and the molecular weight and their effect on tensile properties the following discussion is presented. The argument that the sample crystallinity has a profound effect on the tensile mechanical properties was well demonstrated by Darras and Seguela [1993] publication. In their work they studied the modulus and the tensile yield of four ethylene/1-butene copolymers covering the crystallinity range of 33% to 74% in relation to their lamella thickness. The samples were prepared from melt-crystallisation and from solution-crystallisation at various concentrations in decalin in order to span a wide range of lamellae thickness. In the case of melt-crystallised samples they showed that the modulus and the yield stress depended on the direct correlation between the lamellae thickness and the crystallinity of the sample. But, for the samples prepared via solution-crystallisation, they found that the tensile properties depended only on the lamellae thickness rather than on crystallinity. The molecular weight also was shown by Mandelkern et al. [1991] to have a profound influence on the modulus and the yield stress of crystalline polymers. They analysed the tensile properties of molecular weight fractions of linear polyethylene covering the range from 10^4 to 10^6. They found that the molecular weight was a physical structural parameter that influenced key tensile properties such as the initial modulus and the yield stress. This structural parameter was also found to determine the transition

between brittle and ductile deformations which in turn can be related to the elongation at break of the PE resin.

The strain at break for the Rigidex pipe resin samples was plotted along with their respective crystallinity in Figure 6.10.

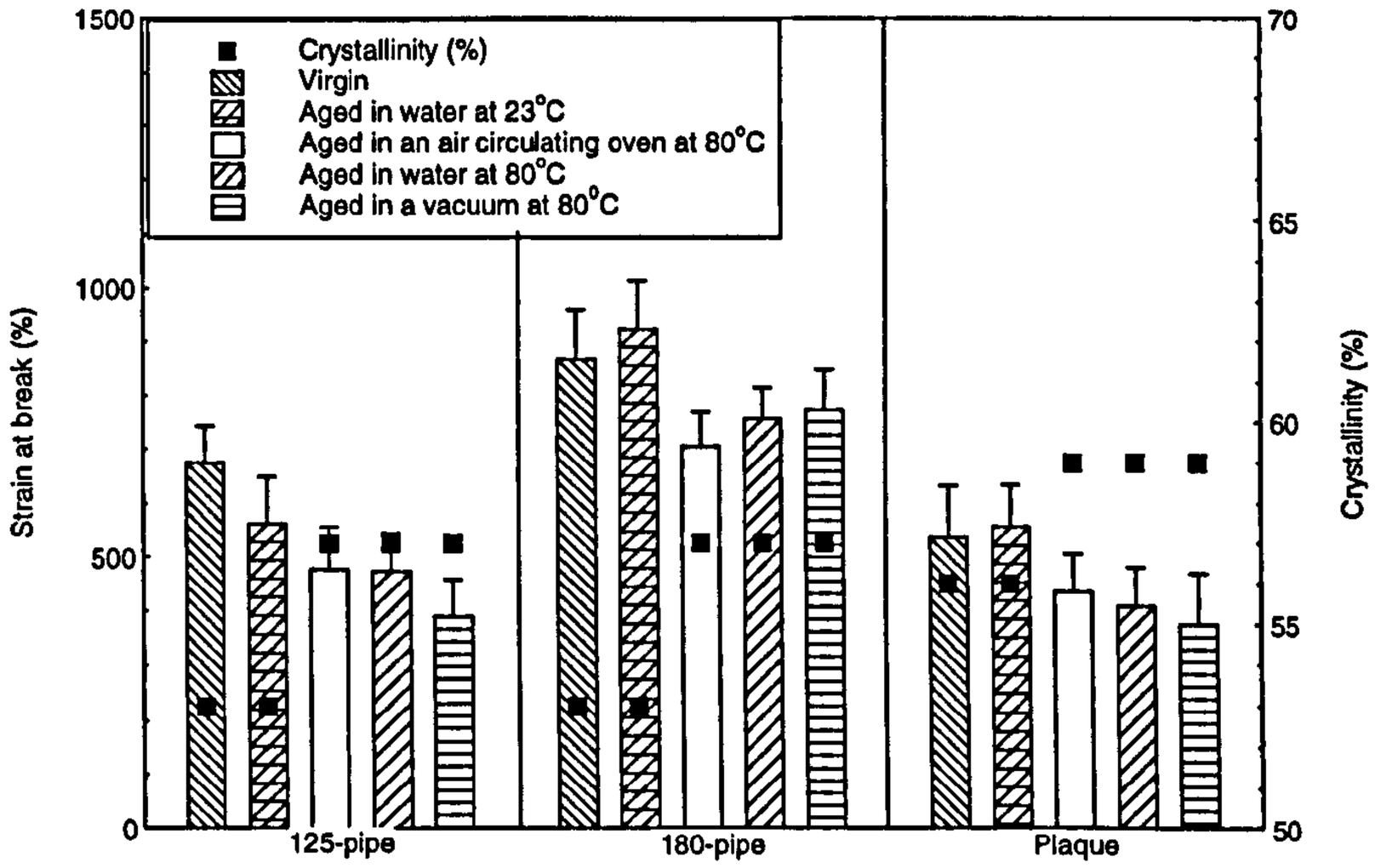

Figure 6.10. The micro-tensile strain at break results for the Rigidex specimens along with their respective crystallinity. The ageing experiments were for one year.

Although the average crystallinity was the same in Figure 6.10 for the unaged 125-pipe and 180-pipe the strain at break was not. This was attributed to the difference between the width of the two specimens used. The width of the 125-pipe and 180-pipe specimens were approximately 12 mm and 17 mm, respectively. It was found that during the test at high strains some of the material was slipping out from the grips area. This means the wider the micro-tensile film sample the higher the value of the strain at break will be. Because it was difficult to remedy this action effectively, the strain at break results for micro-specimens with the same width were compared together. For example, the width of both the 125-pipe and the plaque specimens was 12 mm. Each showed different

elongation at break values. This was attributed to the higher crystallinity of the plaque samples. The trend was maintained upon thermal ageing due to an increase in the crystallinity for these samples. The effect of crystallinity on the elongation at break is discussed below on the basis of the understanding that the structural variables of PE resins which include molecular weight distribution, branch length and branch density are directly linked to the crystallinity and the mechanical properties of semi-crystalline polymers [Lustiger 1996].

The micro-tensile strain at break results for the Aldyl-A and Rigidex 125-pipes were plotted along with their respective average crystallinity in Figure 6.11.

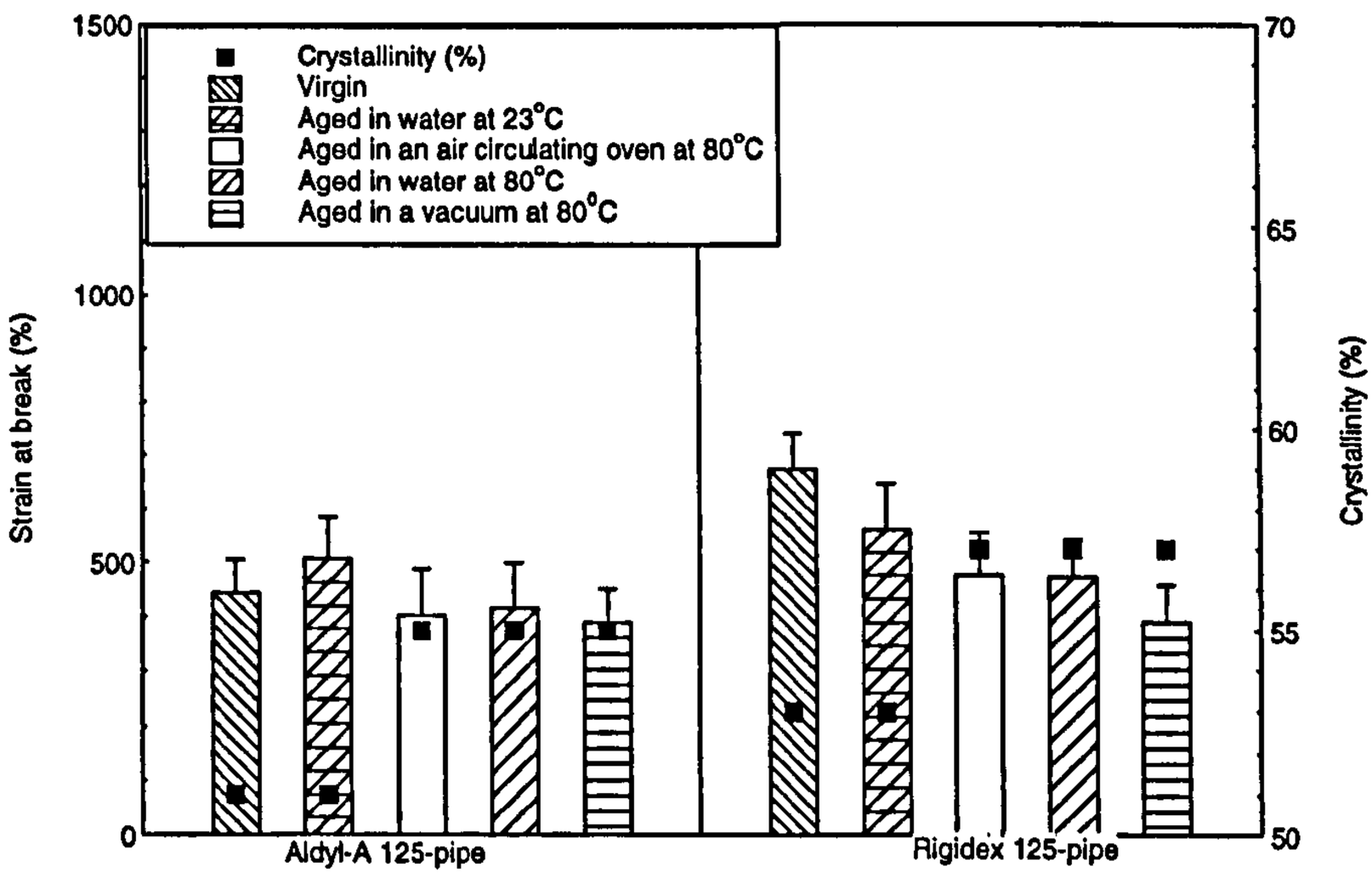

Figure 6.11. The micro-tensile strain at break results for the Aldyl-A and Rigidex 125-pipe specimens along with their respective crystallinity. The ageing experiments were for one year.

With reference to Figure 6.11, the two PE resin systems differ entirely with respect to their molecular weight, molecular weight distribution, branch density and branch length. Ultimately, these structural variables have profound effect on the physical states of the resultant PE resin in its solid form which was the subject of

Kennedy et al.'s [1994] investigation. They used a variety of linear PE resins with different structural variables to control the crystallinity. They found that the ultimate properties not only depended on the crystalline region but also on the molecular weight, emphasising the importance of the non-crystalline regions. The molecular weight of the three PE resins used in this can be related to their MFI values [Bezprozvannykh et al., 1986]. The Rigidex resin with $MFI_{2.16}$=0.2 g/10min has a higher molecular weight than Aldyl-A resin with $MFI_{2.16}$=0.9 g/10min. Therefore, according to Kennedy et al.'s [1994] work the Rigidex resin should have a higher elongation at break property than the Aldyl-A which is in a good agreement with results in Figure 6.11. Upon thermal ageing the crystallinity increased of these PE samples which resulted in a decrease in the elongation at break. This clearly indicates the role of the crystalline phase on the strain at break value. The result seen in Figure 6.11 could be interpreted as a combination of the effect of the PE resin variables on the physical structure which in turn effect the elongation at break property. This result is further demonstrated when the strain at break for the Rigidex and the Eltex pipe resins was plotted with their respective average crystallinity in Figure 6.12.

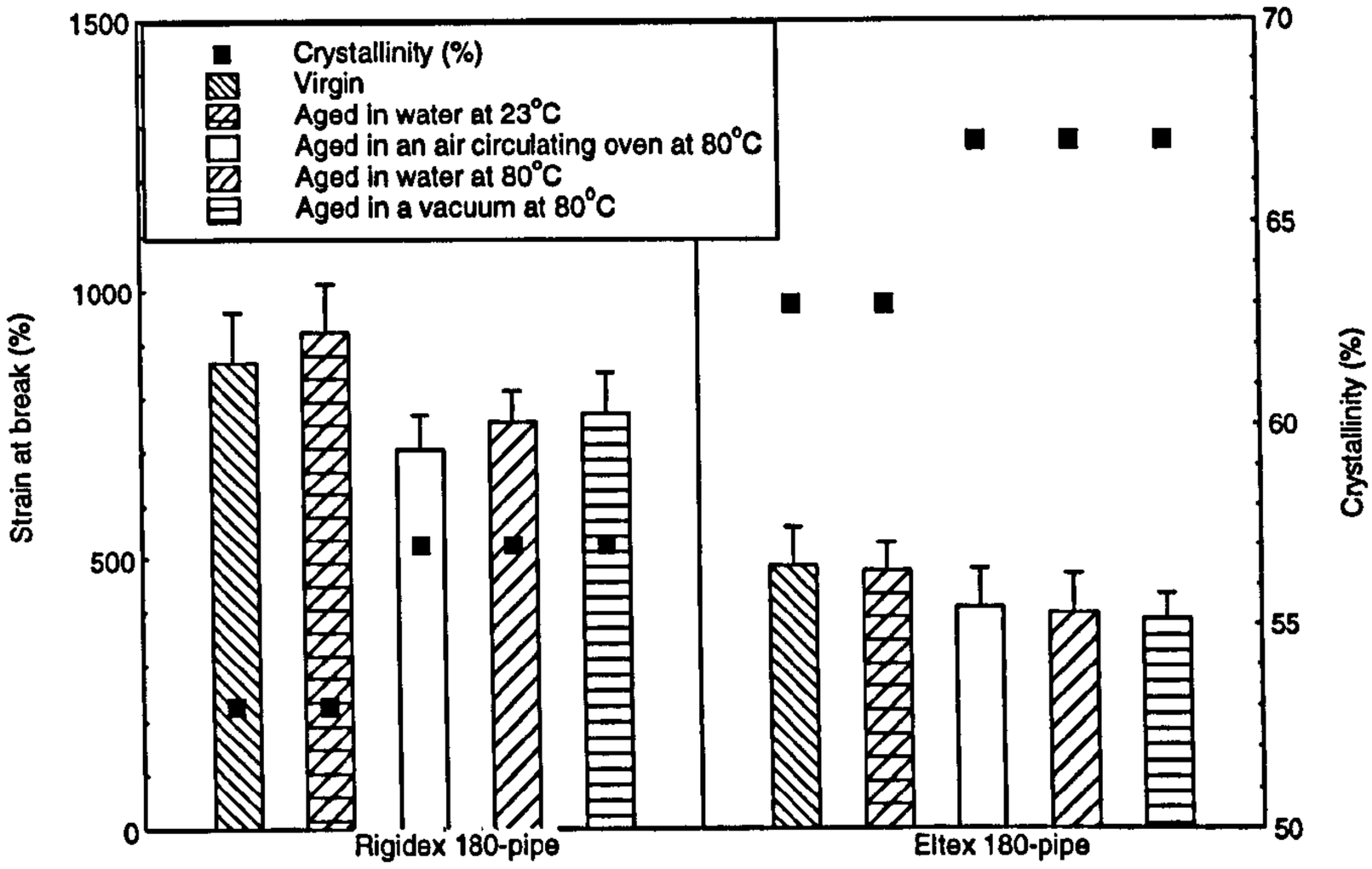

Figure 6.12. The micro-tensile strain at break results for the Rigidex and Eltex 180-pipe specimens along with their respective crystallinity. The ageing experiments were for one year.

Using the $MFI_{2.16}$ of the Eltex resin which is 0.1 g/10min and the $MFI_{2.16}$ of the Rigidex resin which is 0.2 g/10min, it is possible to suggest that the former has a higher molecular weight. Therefore, the elongation at break for the Eltex resin is expected to be higher than that of the Rigidex resin which is clearly not true in Figure 6.12. The unaged Eltex resin sample showed a strain at break lower than the Rigidex resin sample. It is generally accepted that increasing the crystallinity of the polymer, in this case the Eltex resin, will reduce the strain at break [Kurtzet al., 1997]. However, it is more complicated than this as described recently by Butler and Donald [1997]. They investigated thin spherulitic films of polyethylene (PE) by casting them from xylene solution. The films were deformed on copper grids and their deformation microstructure was studied using optical and transmission electron microscopy. A range of molecular weights, branch amounts and types, and thermal histories was used to study the influence of sample microstructure on the deformation behaviour. They found

that the spherulite boundaries were the weakest regions of spherulitic structures in all types of PE. They were able to increase the strain at break of the films by increasing the tie-molecule density and the disentanglement resistance. Three methods for increasing the toughness were suggested and they were: (i) decreasing the crystallisation time in order to increase the tie-molecule density, (ii) increasing the molecular weight in order to increase the tie-molecule density, and (iii) incorporating short-chain branches on the main chains in order to increase the tie-molecule density and increase the disentanglement resistance. Incorporation of short-chain branches was shown to be the most effective way of strengthening spherulitic structures, with the toughest films being those made of branched PE that had been crystallised rapidly. The branch length and spherulite size were found to be unimportant.

CHAPTER

SEVEN

CHAPTER SEVEN

DYNAMIC MECHANICAL PROPERTIES OF PE PIPE RESINS

7.1. Introduction

This chapter is dedicated to the design and use of a fatigue test method to assess the performance of the three aged and unaged pipe resins used in this study. The fatigue sensitivity of single-edge-notched (SEN) specimens was investigated with respect to (a) notching method, (b) loading rate, (c) stress level, (d) test temperature and (e) the specified ageing conditions. This test method was developed to produce specimen failures within a few days. The fatigue fracture toughness of aged and unaged Rigidex resin samples was calculated from the load/displacement hysteresis data. Fracture surfaces of the SEN specimens were examined using SEM in order to study the fracture modes. Microtomed films prepared from pre-fatigued SEN specimens were also inspected using polarised light microscopy to give an insight into the mode of crack propagation. Finally, the fatigue test was used to rank the three aged and unaged pipe resin samples with respect to resistance to crack propagation in the form of cycles to failure.

7.2. Fatigue Test

Traditional pipe fracture resistance tests include constant load methods. For example, the design criteria for PE pipes is based on the ISO 9080 hydrostatic test method. This test consumes large amounts of pipe, is costly and requires months or years to generate a brittle fracture. This failure mode is of interest because it is the most common failure mode observed for pipes in-service [Derringer, 1989; Parmer and Bowman, 1989; Showaib et al., 1995; Marshall et al., 1995]. The purpose of the current programme was to assess the sensitivity of the PE pipe resin samples towards crack propagation under dynamic loading. The fatigue test is regarded as an

accelerated test method because under fluctuating loads, polymers will fail at stress levels much lower than they can withstand under monotonic loading conditions [Kadota et al., 1993].

Prior to defining the methodology for the fatigue test, several investigations were carried out to establish the following: (i) appropriate notching method, (ii) loading rate, (iii) maximum stress level and (iv) test temperature.

7.2.1. Notching Method

In the initial stages of this fatigue study, it was recognised that the time-to-failure of a SEN specimen was sensitive to the method of notching. Careful consideration was given to the following: (i) the shape of the notch tip; (ii) notching speed; and (iii) notch location with respect to the pipe wall.

Notch Geometry:

Reynolds and Lawrence [1993] reported that the fatigue lifetime of the same SEN samples can extend many times because of notch blunting. Three types of notches were considered in this study and the details were given in section 3.2.1. The notches were produced via: (a) the custom-made pipe cutting and notching wheel; (b) a disposable microtome blade; and (c) a disposable razor blade. Typical examples of nothes obtained using these methods are shown in Figure 7.1a, 1b and 1c.

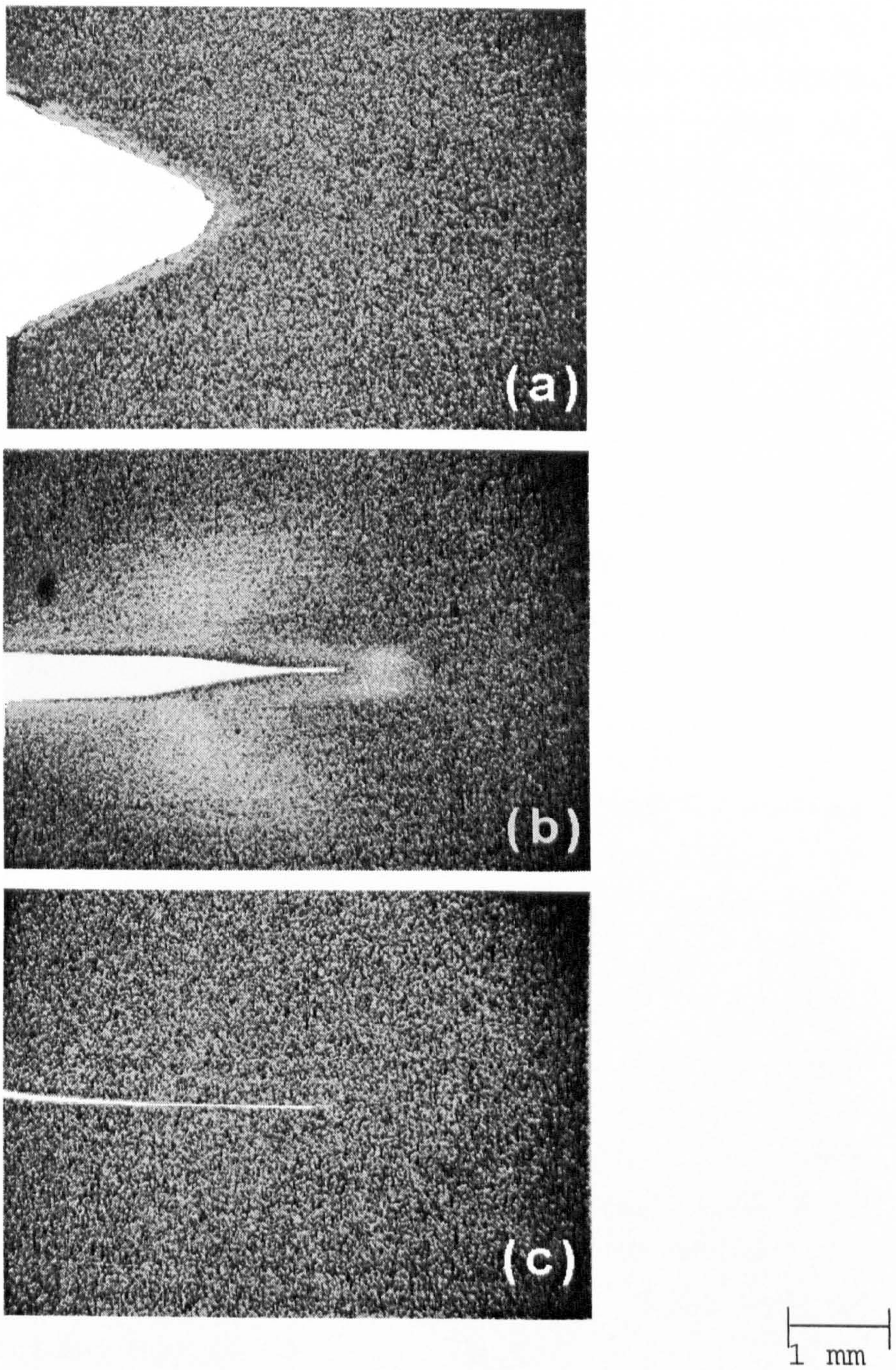

Figure 7.1. Micrographs of notches obtained from the use of (a) notching wheel; (b) disposable microtome blade and (c) disposable razor blade.

With reference to Figure 7.1 (a) and (b), stress-whitening is clearly visible. This was observed even at a slow rate of notching (0.5 mm/min). In order to avoid microscopic deformation of the microstructure caused by the blade, a very thin razor blade was used. This was seen to produce minimum stress-whitening as shown in Figure 7.1(c). However, because the razor blade was very thin it tended to curve while notching. This type of notch was used throughout the fatigue experiments. The speed at which the razor blade was pressed into the sample was also investigated.

It should be mentioned that in the early stages of this study it was noticed that any attempt to manually sharpen an existing notch resulted in significant scatter in the results. This was because the manual sharpening could not be carried out in a reproducible manner and furthermore this resulted in a variation in notch depth, irregular notch front, etc.

Notching speed:

A simple experiment was carried out to investigate the effect of notching speed on the fatigue sensitivity of SEN specimens. A standard tensile machine Instron 1024 model was used to hold (upper grip) a strip cut from a Rigidex plaque and the razor blade with a clamp was positioned in the lower grip. The two grips were brought very close together before notching at 0.1, 0.5, 1, 5 to 10 mm/min. Three SEN specimens were tested for each cross-head speed. The fatigue test conditions used were as specified in section 3.4.4. Figure 7.2 shows the effect of notching speed on the fatigue lifetime of compression moulded Rigidex SEN specimens.

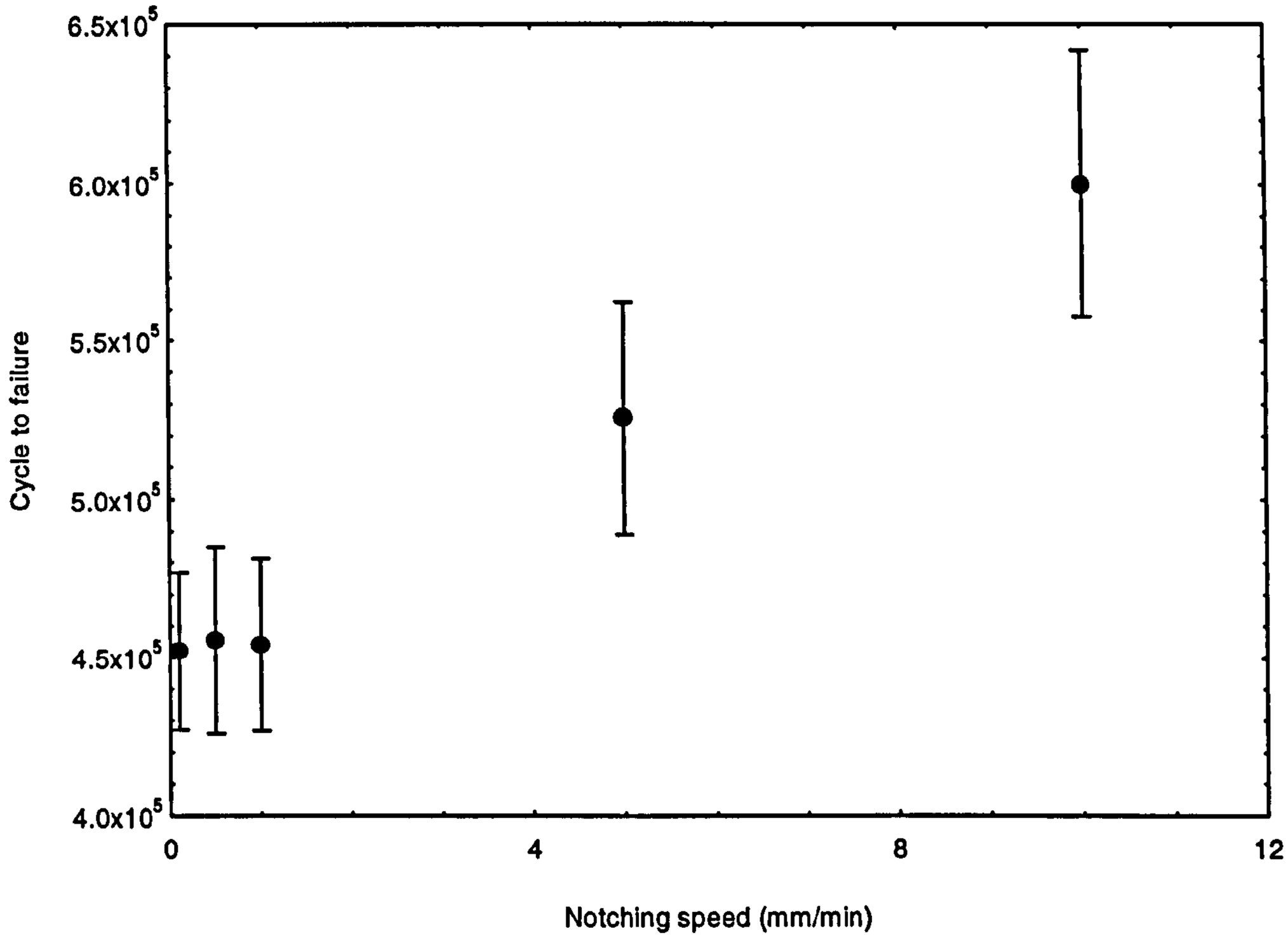

Figure 7.2. The effect of notching speed on the fatigue lifetime of the SEN specimens. The SEN samples used were prepared from Rigidex plaques. The notch depth was 3 mm for all the samples tested.

It is clear from Figure 7.2 that the total time to failure was related to the speed of notching. Pascaud et al. [1997] reported that the high speed of notching increased the radius at the notch tip. They explained that this led to an incubation period to the actual crack initiation and subsequently increased the total time to failure. Other researchers [Strebel and Moet, 1991; Swei et al., 1991; Lu and Brown, 1990; Yeh and Lin, 1993] termed this behaviour notch blunting which is produced at the notch tip. Below cross-head speeds of 1 mm/min, the fatigue lifetime of the SEN specimens was consistent at approximately $4.5x10^5$ cycle. This investigation and the reports mentioned in the literature prompted the use of

0.5 mm/min as a notching speed throughout the fatigue experiments.

Notch Location:

A brief study was undertaken to understand the effect of the location of the notch in relation to the outer surface, mid section and bore surface of the pipe as shown in Figure 7.3.

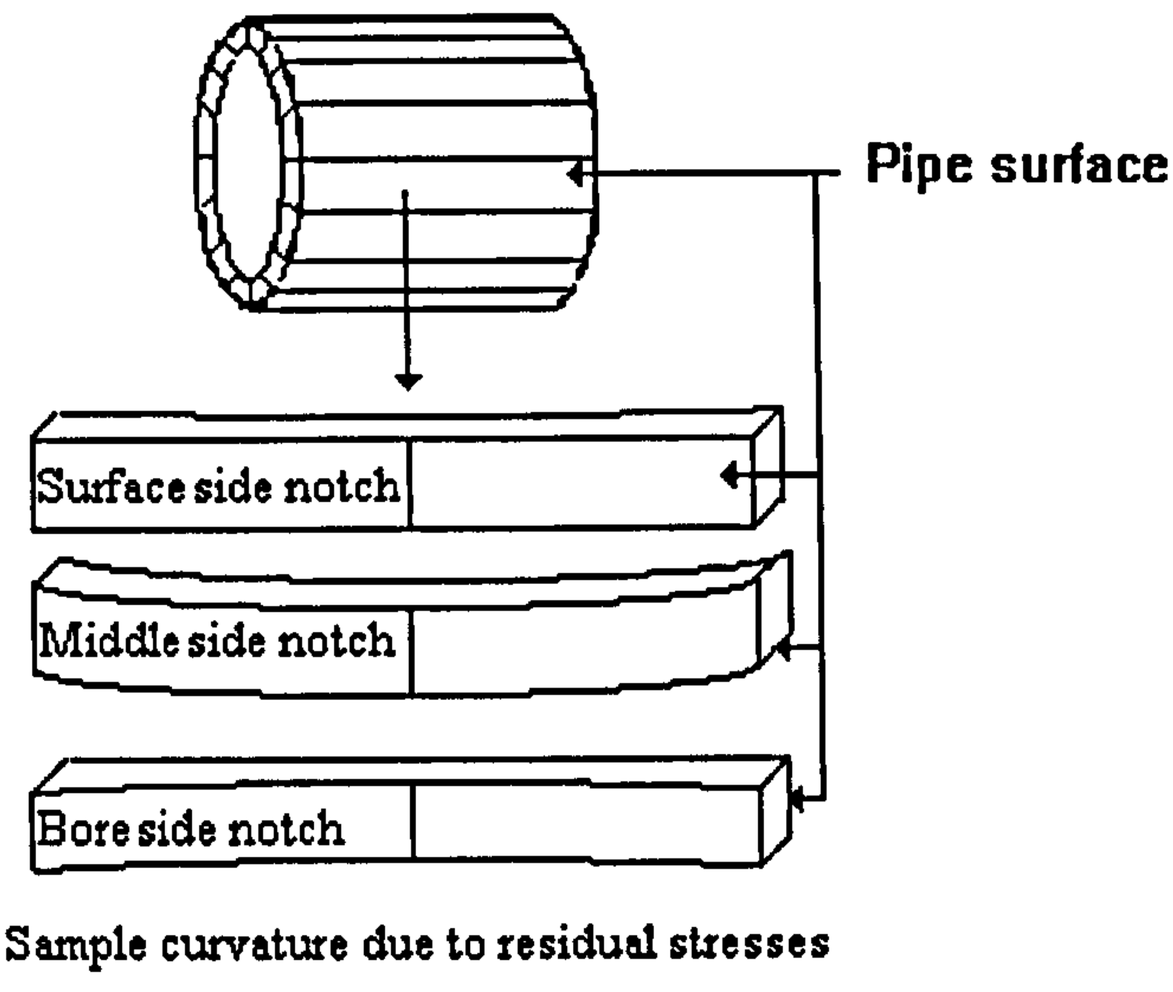

Figure 7.3. Schematic illustration of SEN specimens with the three notch locations with respect to the pipe wall. The SEN specimens were cut from Rigidex 180-pipe

Due to the crystallinity gradient across the pipe wall, the SEN specimens prepared from the 180-pipe were not straight strips after cutting as shown in Figure 7.3. According to Williams et al. [1981] this variation in crystallinity created residual stresses in the pipe wall and this was said to partially relax upon cutting the strips. Figure 7.4 shows the crack opening displacement traces of the three SEN specimens as a function of fatigue cycles.

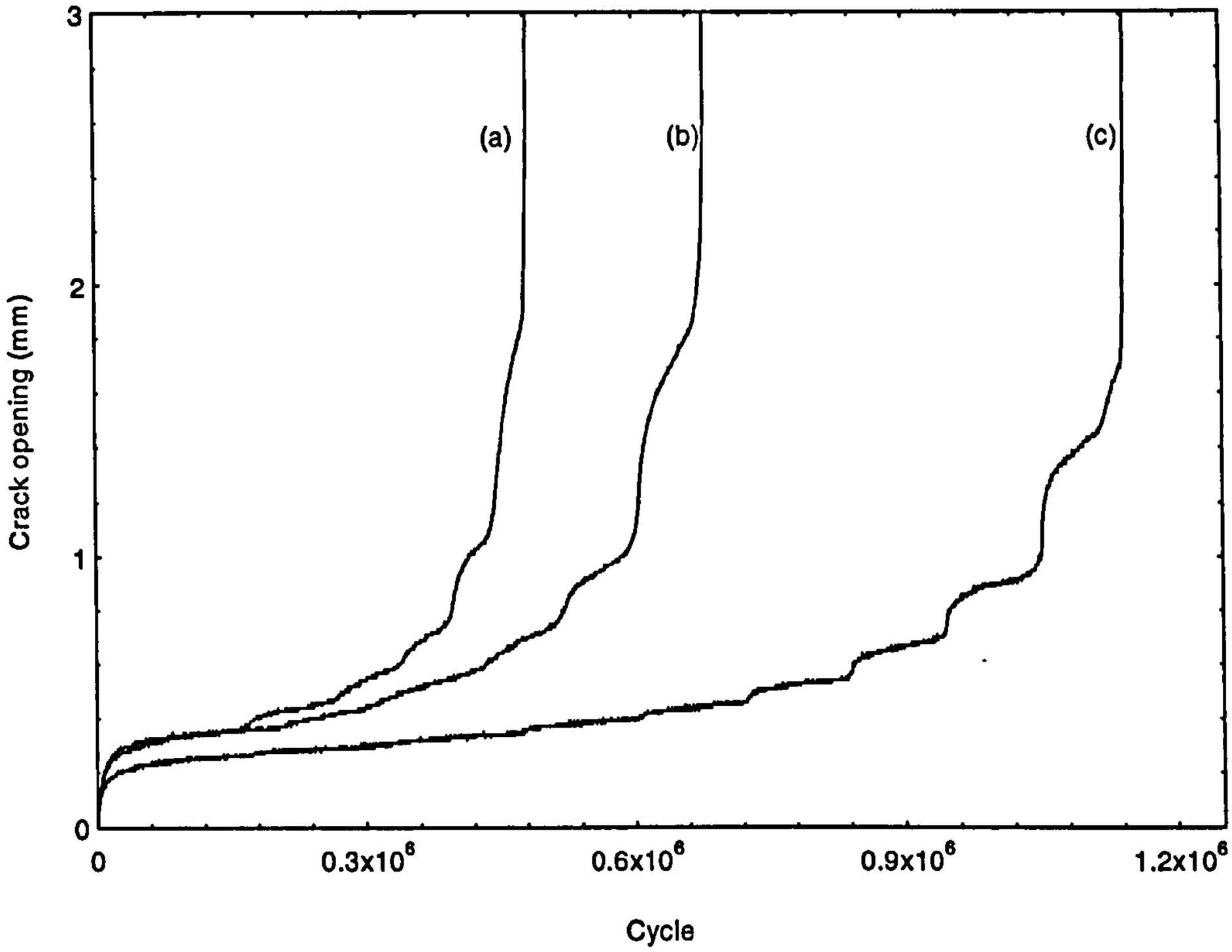

Figure 7.4. Crack opening displacement traces as a function of fatigue cycle for (a) bore, (b) side and (c) surface notched SEN specimens. Each trace represent an average of three SEN specimens.

It is clear from Figure 7.4 that the location of the notch influenced the rate of crack opening. Chaoui et al. [1987] also reported similar results for medium density PE (MDPE). They suggested that the morphology ahead of the notch influenced the rate of fatigue crack propagation. As a variation exists in the crystallinity across the pipe, and by changing the location of the notch, the level of crystallinity ahead of the notch tip was different for each case. The crystallinity at the pipe surface was found to be the lowest and as the crack propagation behaviour is governed by the plasticity at the crack tip, the SEN specimen with the surface notch had the longest fatigue lifetime as shown in Figure 7.4.

Lu et al. [1994] suggested that there was an anisotropy in the degree of molecular orientation caused by the extrusion process. They concluded that this discrepancy in the pipe wall affected the fatigue lifetime of samples taken from the surface or the bore of the pipe. In order to relate the fatigue life to crystallinity, SEN specimens were prepared from three Rigidex and Eltex plaques each with different degrees of crystallinity. The effect of crystallinity on the fatigue lifetime is shown in Figure 7.5.

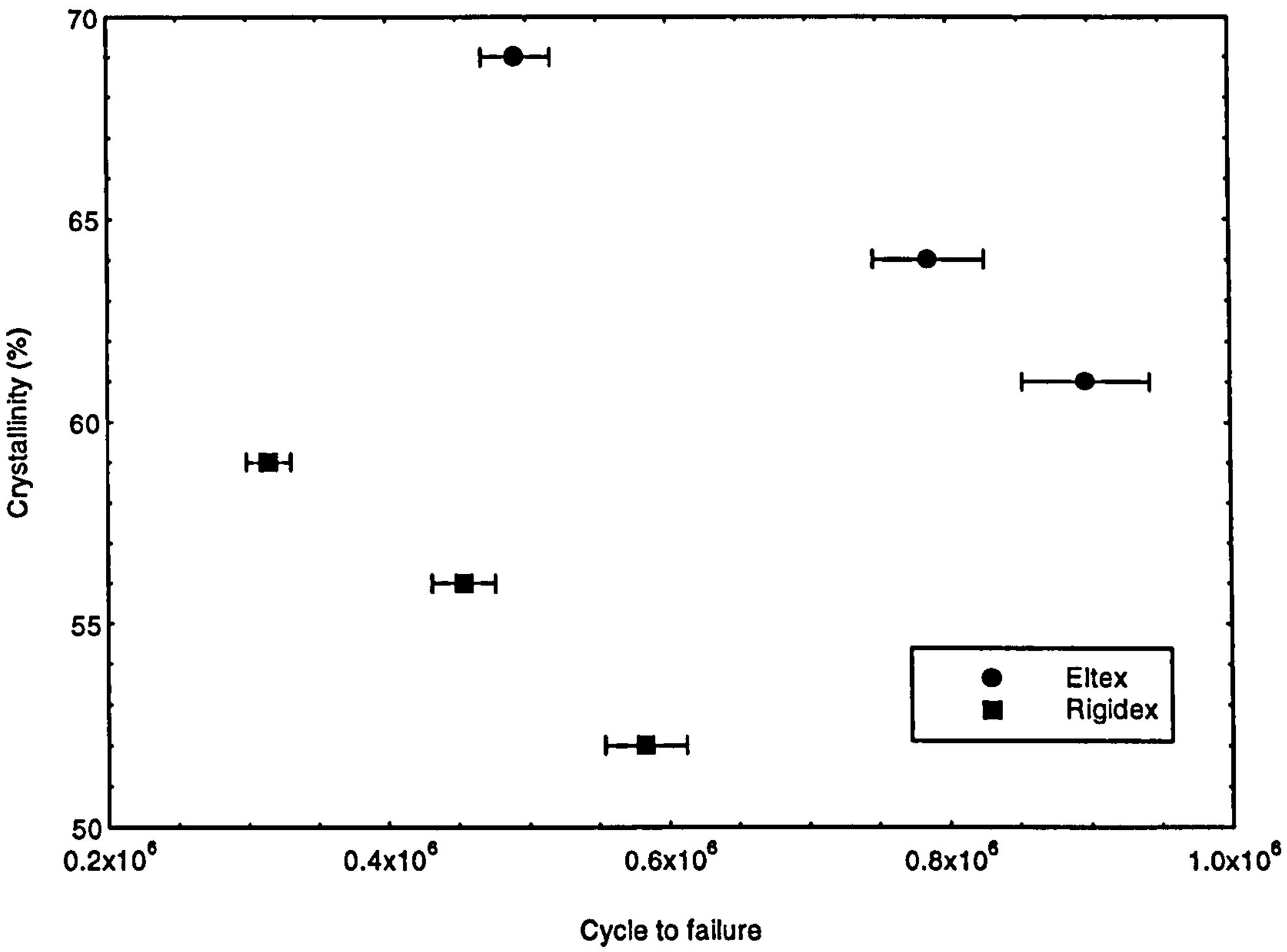

Figure 7.5. Crystallinity as a function of cycle to failure for SEN specimens prepared from Eltex and Rigidex plaques.

It was immediately apparent from Figure 7.5 that as the degree of crystallinity for both materials increased, the fatigue life was reduced. Elkoun et al. [1997] observed a similar behaviour and suggested that PEs with high crystallinity are more prone to fracture. They reached this conclusion by varying the thermal history of a PE

resin and therefore varying the crystal thickness and relating it to failure times. They found that the samples with thicker lamellae i.e., high crystallinity, failed quicker.

With reference to Figure 7.5, it is interesting to note that the Eltex resin showed a higher resistance to crack growth when compared to the Rigidex resin even when the crystallinity for both resins were approximately the same at 60%. This observation implies that when the crystallinity of two different PE resins is identical their fatigue lifetime may not be the same. Researchers in this field [Kim et al., 1977; Nunes et al., 1982; Yeh et al., 1994; Zhou et al., 1996] found that the fatigue lifetime of PE resin samples with similar crystallinity contents were dependent on the molecular weight and molecular weight distribution of the polymer.

7.2.2. Loading Rate

An investigation was carried out to study the effect of loading rate on the temperature of the SEN specimens and their corresponding fatigue lifes. Compression moulded SEN specimens prepared from Rigidex plaques were used in this study. Figure 7.6 shows temperature traces for the SEN specimens under the specified loading rates. Each trace represents an average of three individual experiments. The temperatures were obtained via three thermocouples embedded in the vicinity of the crack. The temperature of the environmental chamber which contained the SEN specimens was maintained at 30°C.

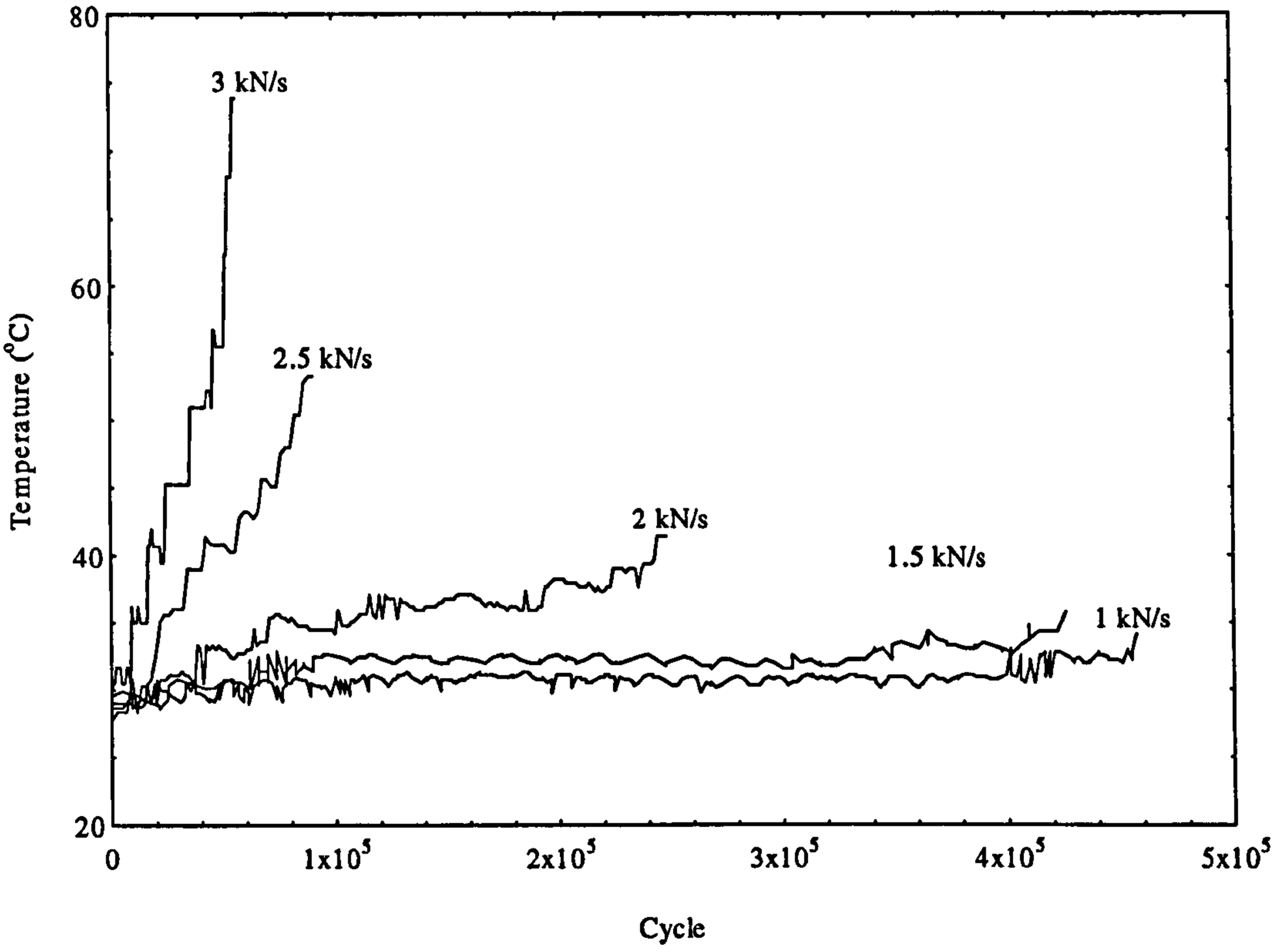

Figure 7.6. Temperature traces of the SEN specimens as a function of fatigue cycle at the specified loading rates.

With reference to Figure 7.6, at 1 and 1.5 kN/s loading rates the heat generated in the specimens was easily dissipated to the surrounding environment and the sample reached thermal equilibrium during fatigue testing. However, at higher loading rates, the temperature of the test specimens was found to increase due to insufficient heat dissipation from the specimen to the surroundings. Lu et al. [1995] reported that any increase in a semi-crystalline sample temperature will result in a decrease in the stress at yield. It should be mentioned that the heat was not measured exactly at the crack tip (process zone) and hence it is possible to speculate that the material in this zone could have reached higher temperatures than that measured. In order to reduce the testing time and to avoid excessive heating of the sample, 1.5 kN/s was selected as an appropriate loading

rate for the fatigue test. All subsequent samples were tested at this rate.

7.2.3. S-N Curves

After selecting the appropriate notching method and the loading rate, an investigation was carried out to determine the operating parameters, namely, the stress level and the test temperature. S-N curves of SEN specimens prepared from Rigidex plaques are presented in Figure 7.7. Each datum represents an average of three samples.

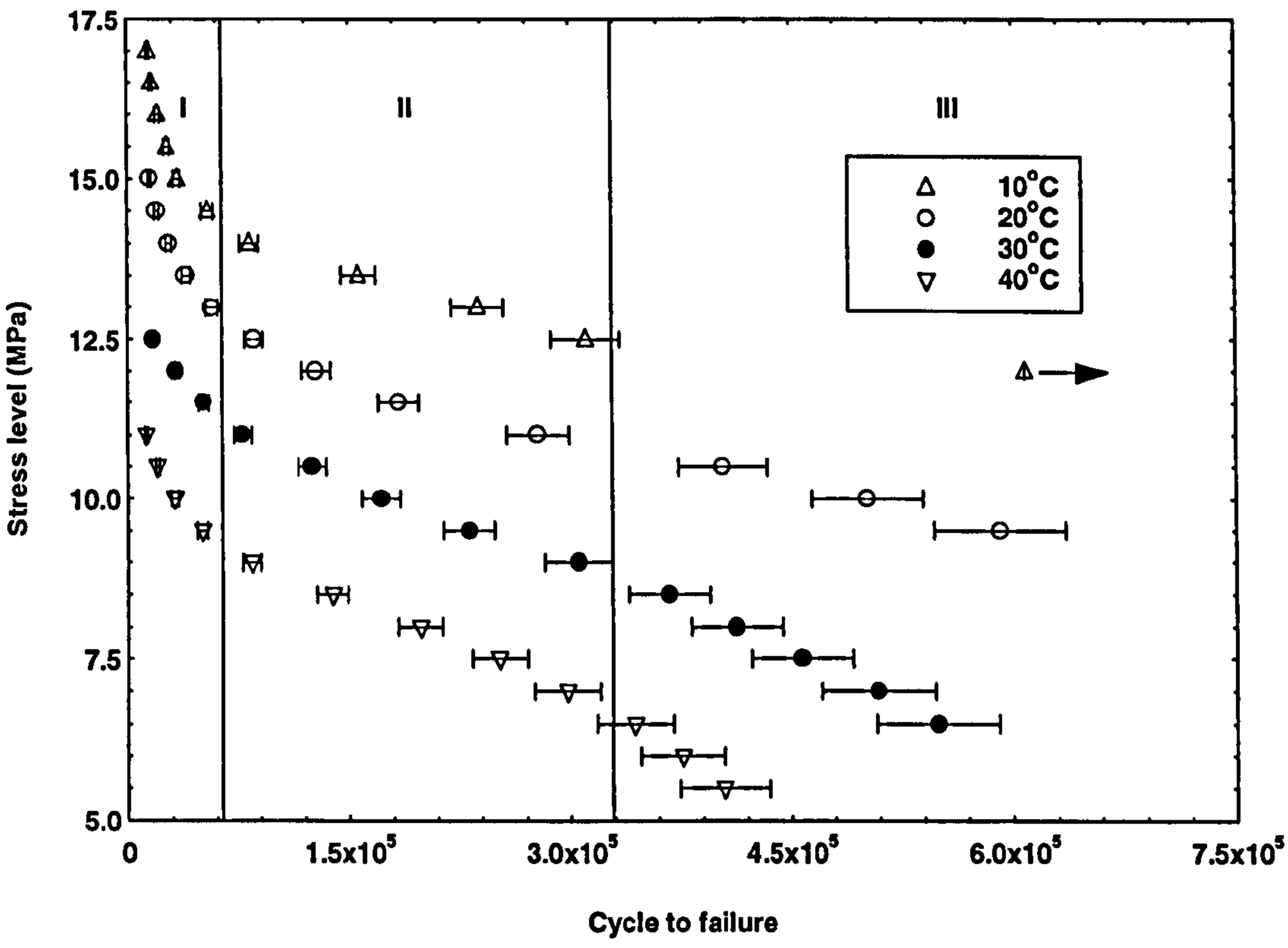

Figure 7.7. S-N curves at different temperatures for the Rigidex plaque SEN specimens. The separation lines indicats whether a specimen failed in (I) a rapid ductile mode, (II) a ductile mode or (III) a ductile-brittle manner. The arrow indicates a run out sample.

With reference to Figure 7.7, the SEN specimens tested at 10°C only failed in a ductile manner within the time-scale of the fatigue test. The failure of SEN specimens in zone

(I) was described as excessive yielding of material due to the high applied stresses. A change in failure mode from ductile (II) to ductile-brittle transition (III) was seen more easily for specimens tested at low stress levels and high test temperatures. Typical surfaces of failed SEN specimens taken from the three zones are shown in Figure 7.8.

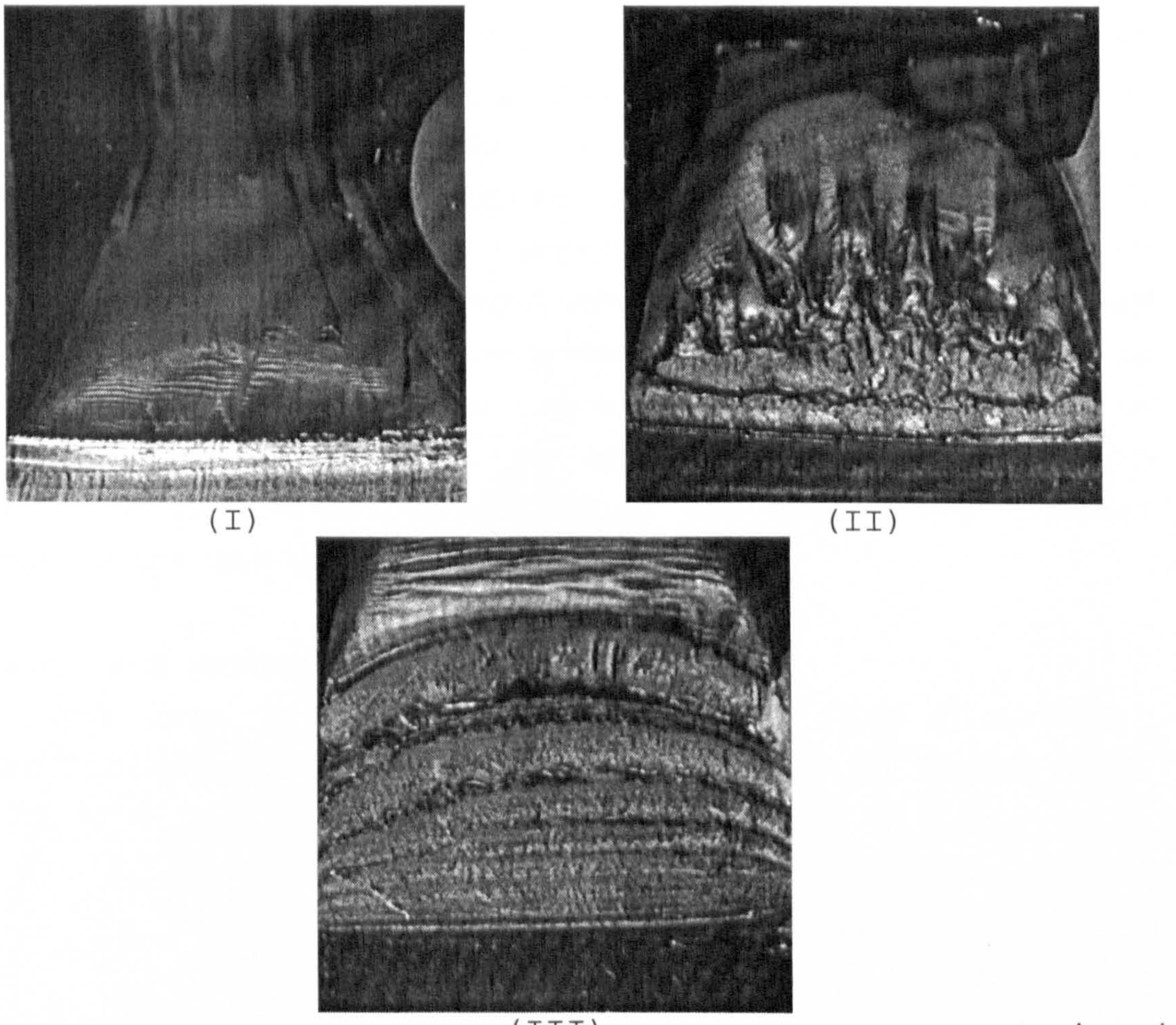

Figure 7.8. Macrographs of typical surfaces for Rigidex plaque SEN specimens failed in the three zones indicated in Figure 7.7. (I) Excessive yielding, (II) ductile and (III) ductile-brittle failure.

S-N curves for PE pipes via the hydrostatic pressure test [ASTM D 2837, 1988] also provide three distinct failure modes. Generally, a shallow slope is characterised by a ductile-type failure, and this in turn corresponds to

high stress levels and short failure times. A steeper line of the creep rupture curve corresponds to lower stress levels and longer failure times and where a brittle-type failure is predominant. A point where the slope changes, the knee, is characterised as a type of ductile-brittle transition.

To ensure a ductile-brittle failure, a stress level of 8 MPa was chosen and the environmental chamber temperature was maintained at 30°C. The reason behind the choice of 30°C was because part of the SEN test specimen was outside the environmental chamber, as illustrated in section 3.4.3. The laboratory temperature fluctuated between 18°C to 29°C. If the chamber temperature was set at 20°C or less, then the strain amplitude experienced by the SEN specimen outside the environmental chamber could be higher than that near the crack which was located inside the chamber. Therefore, to ensure a uniform strain amplitude in the neighbourhood of the notch, the chamber temperature was set at 30°C.

7.2.4. S-N Mathematical Models

The S-N data in region (II) and (III) from Figure 7.8 were fitted with linear equations as shown in Figure 7.9.

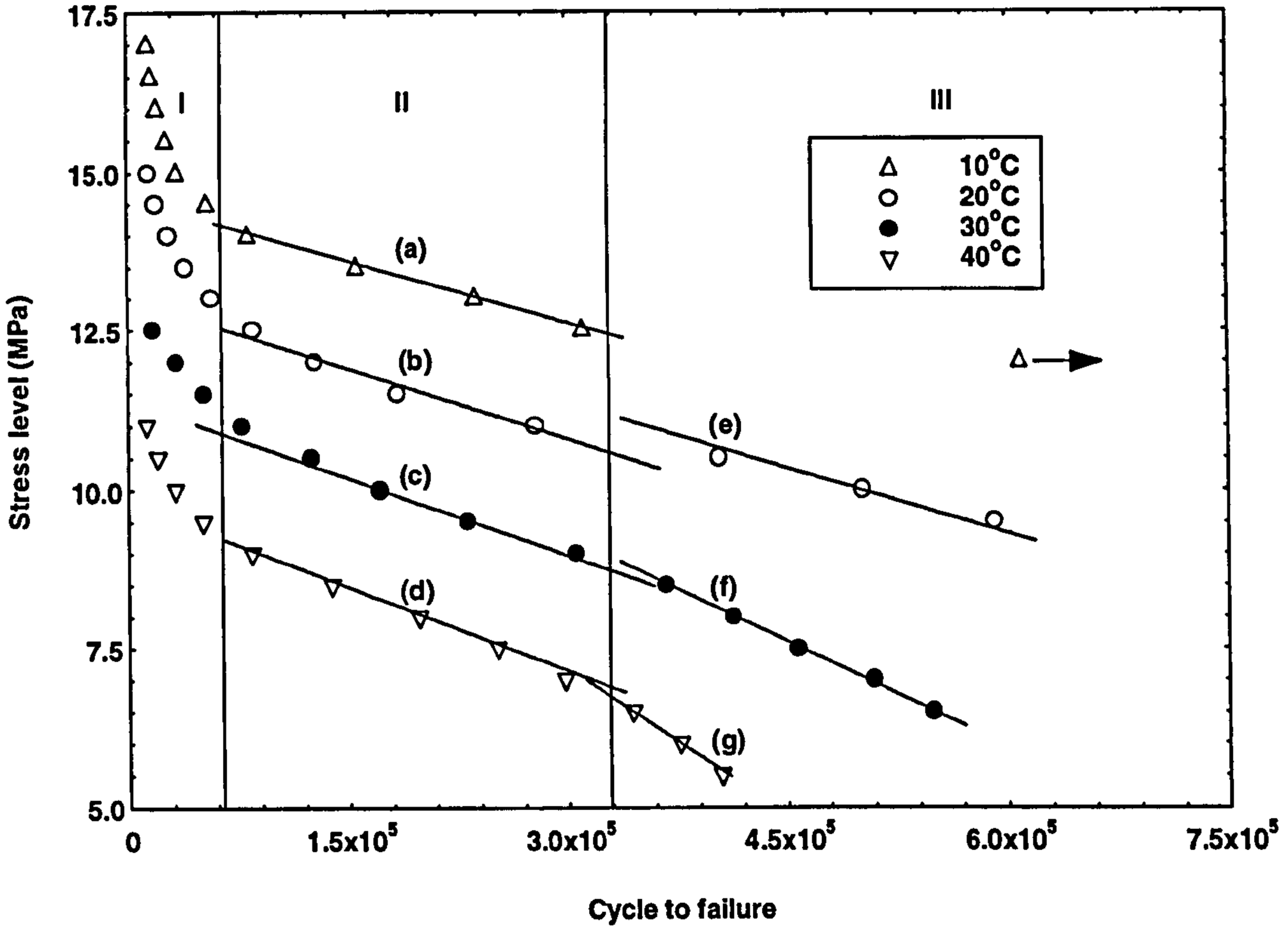

Figure 7.9. The data from Figure 7.8 was fitted with linear equations in the ductile failure (II) and ductile-brittle failure (III) regions.

With reference to figure 7.9, it is possible to represent the linear equations in zone (II) and (III) by mathematical models. The fitted linear equations in zone (II) are:

(a) $S = -6.6\text{x}10^{-6}\ Cy + 14.6$, R=0.06, max dev=0.06;
(b) $S = -7.35\text{x}10^{-6}\ Cy + 13$, R=0.12, max dev=0.15;
(c) $S = -8.1\text{x}10^{-6}\ Cy + 11.4$, R=0.26, max dev=0.51; and
(d) $S = -8.85\text{x}10^{-6}\ Cy + 9.8$, R=0.1, max dev=0.16.

The mathematical model which represent these linear equations is:

$$S = -(0.075T+5.85)\text{x}10^{-6}\ Cy + (16.2 - 0.16T) \qquad (7.1)$$

The fitted linear equations in zone (III) are:

(e) $S = -0.68x10^{-5}$ Cy + 13.4, R=0.14, max dev=0.15;
(f) $S = -1.11x10^{-5}$ Cy + 12.6, R=0.31, max dev=0.05; and
(g) $S = -1.54x10^{-5}$ Cy + 11.8, R=0.51, max dev=0.07.

The mathematical model which represent these linear equations is:

$$S = -(0.043T-0.18)x10^{-5}\ Cy + (15-0.08T) \qquad (7.2)$$

Stress = S
Temperature °C = T
Cycle = Cy

With reference to the mathematical formulas (7.1) and (7.2), it is possible to predict the fatigue lifetime of a Rigidex plaque specimen for given stress at given temperature using these models. The S-N model demonstrated that it is also possible to obtain master curves (the relationship between the peak stress and cycle to failure) for specified temperature with known ductile and ductile-brittle transition failure points.

7.2.5. Fractography

Fracture surfaces of failed fatigue SEN specimens were examined using SEM to characterise the fatigue failure modes. Figure 7.10 shows a macrograph of the fracture surface of a fatigue failed SEN specimen which was prepared from a Rigidex plaque. The fracture surface showed a type of repetitive discontinuous ductile-brittle mechanism which became more ductile at longer crack lengths. Striations, which are evidence of discontinuous crack growth, can be observed clearly on the fracture surface. The light areas represent apparent brittle fatigue failures and the dark bands represent ductile crack arrest.

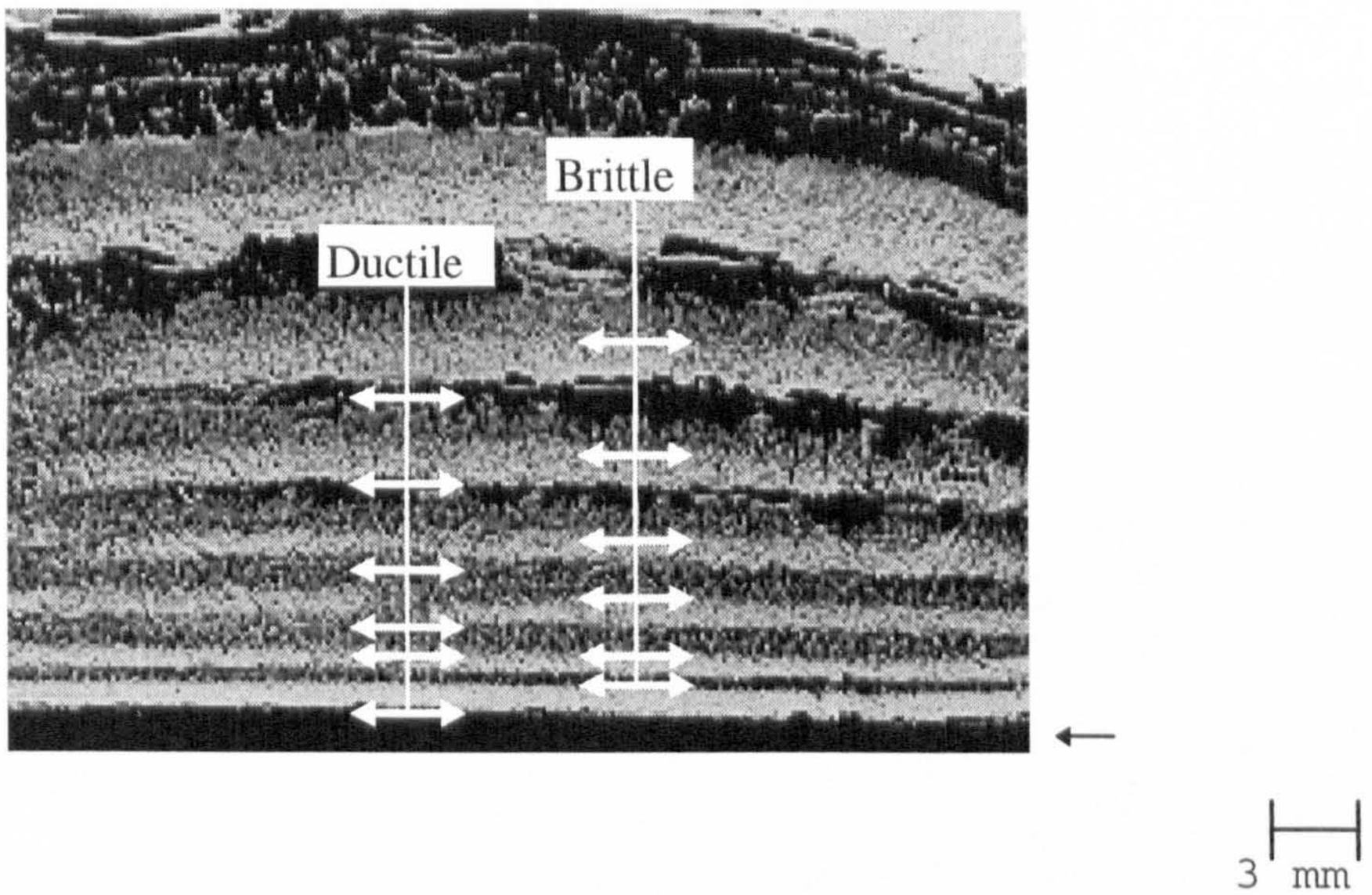

Figure 7.10. SEM macrograph showing the fracture surface of a fatigued failed SEN Rigidex specimen.

The boundary of the bands, which differentiate the ductile crack arrest line were curved. This is due to an increased plane stress contribution towards the edges of the SEN specimen [Strebel and Moet, 1991]. The discontinuous crack growth bands start from the notch tip as indicated by the black arrow in Figure 7.10. The first band represents the notch region, followed by other bands

which are indicative of brittle crack advance. The brittle crack eventually undergoes transition to ductile arrest which is associated with excessive material drawing as shown in Figure 7.11.

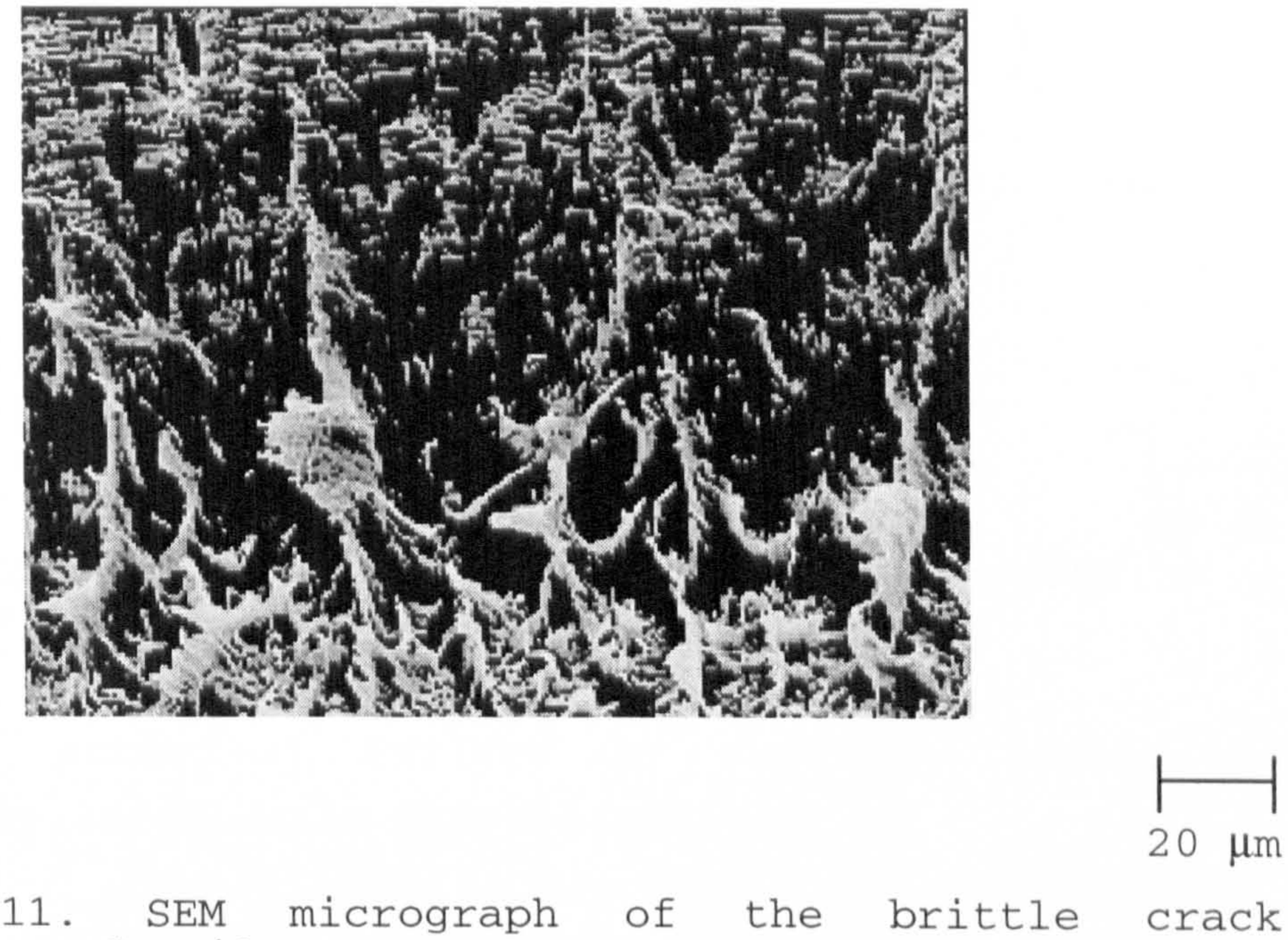

Figure 7.11. SEM micrograph of the brittle crack transition to ductile arrest.

Across the propagating direction, the ductile and brittle bands become progressively larger. The ductile band as the next arrest line is approached becomes smoother as shown in Figure 7.12.

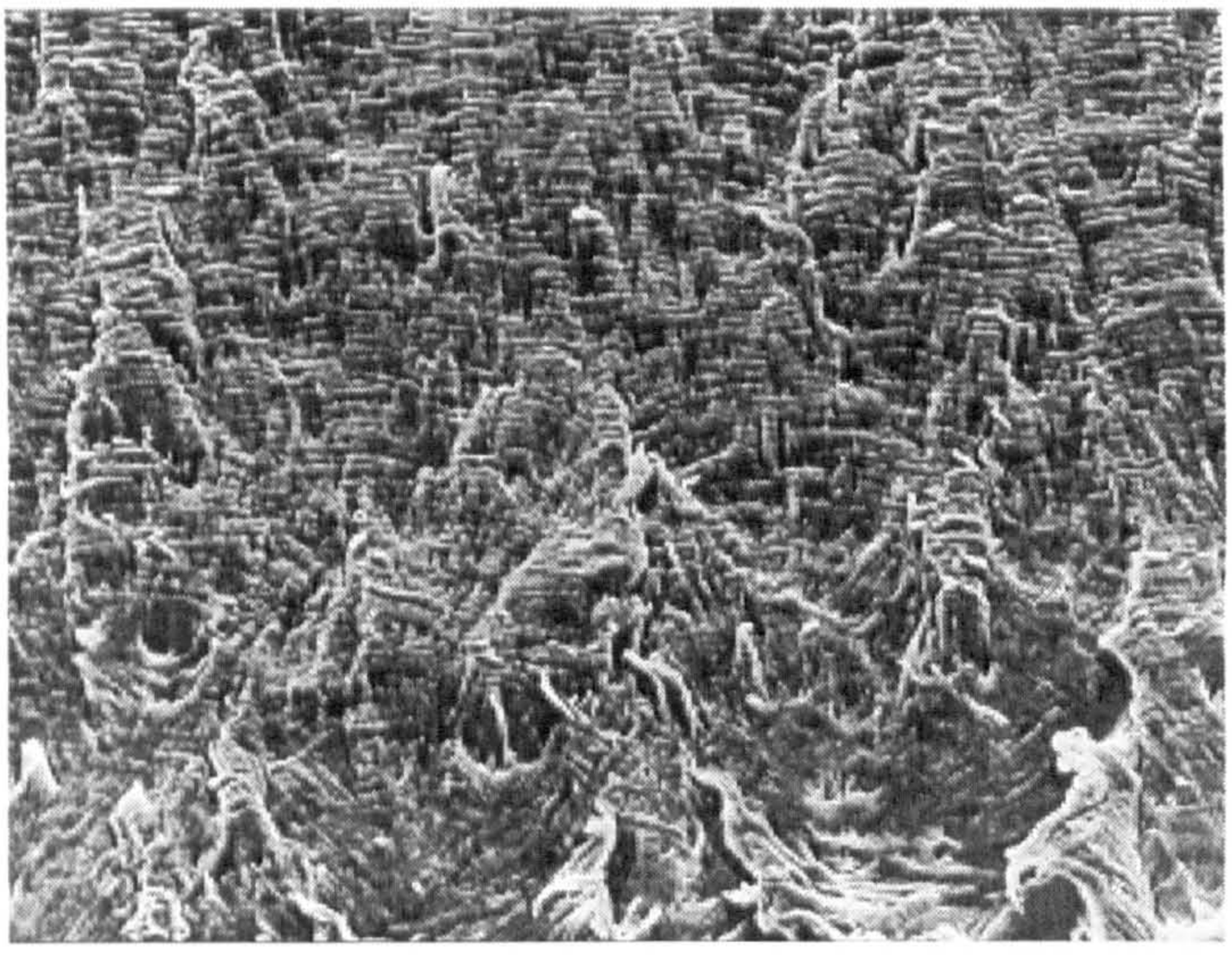

Figure 7.12. SEM micrograph of the ductile arrest at a later stage of crack growth.

The final stage of failure by ductile tearing is dominated by large scale plastic pull-out.

Higher magnification of a brittle band revealed a great deal of deformation and micro-scale crushed yielded material as shown in Figure 7.13.

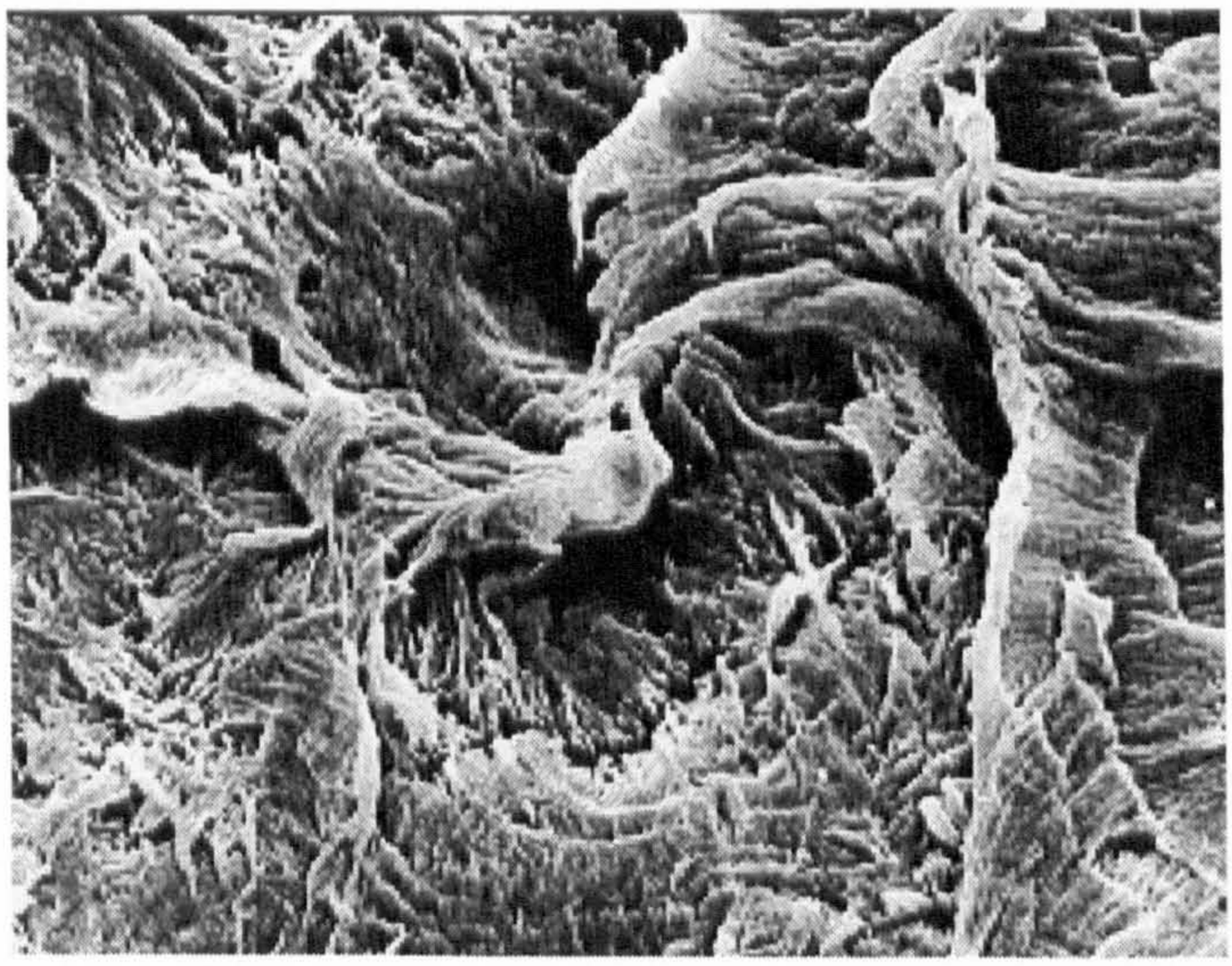

Figure 7.13. SEM micrograph of brittle band at higher magnification showing microfeatures.

Time-dependent behaviour such as fatigue lifetime of polymers is attributed to their viscoelastic character which in turn reflects the microstructure of chain molecules [Lu et al., 1995]. The type of viscoelastic response of the polymer seen in Figure 7.13 greatly influenced the time spent in various stages during fatigue crack propagation. The Rigidex resin was designed to have an average of 4 branches every 1000 carbon atoms with high molecular weight to ensure low crystallinity content and thus provide a high viscoelastic response.

When comparing the fracture surface of SEN specimens made from HDPE Eltex pipe resin with MDPE Rigidex resin it was found that the former had less ductile deformed bands, as seen in Figure 7.14. Yet, it was shown earlier that at similar crystallinity content the fatigue lifetime of the Eltex resin is about twice that of the Rigidex resin. Barry et al. [1992] working on fatigue behaviour of HDPE suggested that the deformability of the material is governed by the degree of order and thickness of the crystalline regions, the number of tie molecules between crystalline regions and physical entanglements within the non-crystalline regions. The HDPE Eltex resin was said to have been designed to have these properties to resist crack growth [Solvay Eltex product sheets]. This very high molecular weight bimodal resin with about three branches every 1000 carbon atoms has a greater probability of forming tie molecules than the Rigidex resin [Lu et al., 1995] and therefore would be expected to be more resistant to crack propagation.

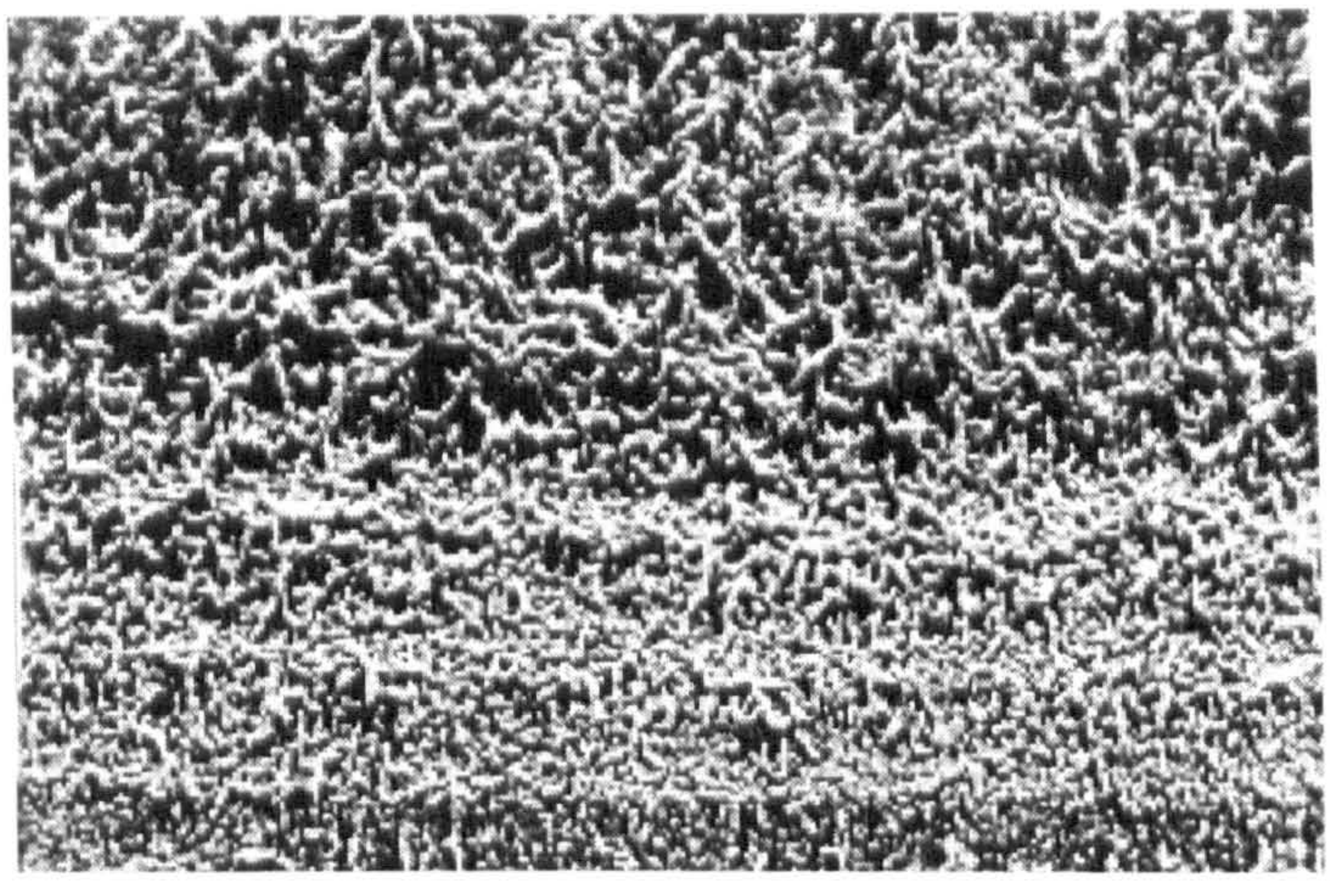

Figure 7.14. SEM micrograph of a fatigue fractured SEN specimen surface made from HDPE Eltex pipe resin.

At higher magnification of the brittle failure, evidence for the low level of micro-ductility is as seen in Figure 7.15.

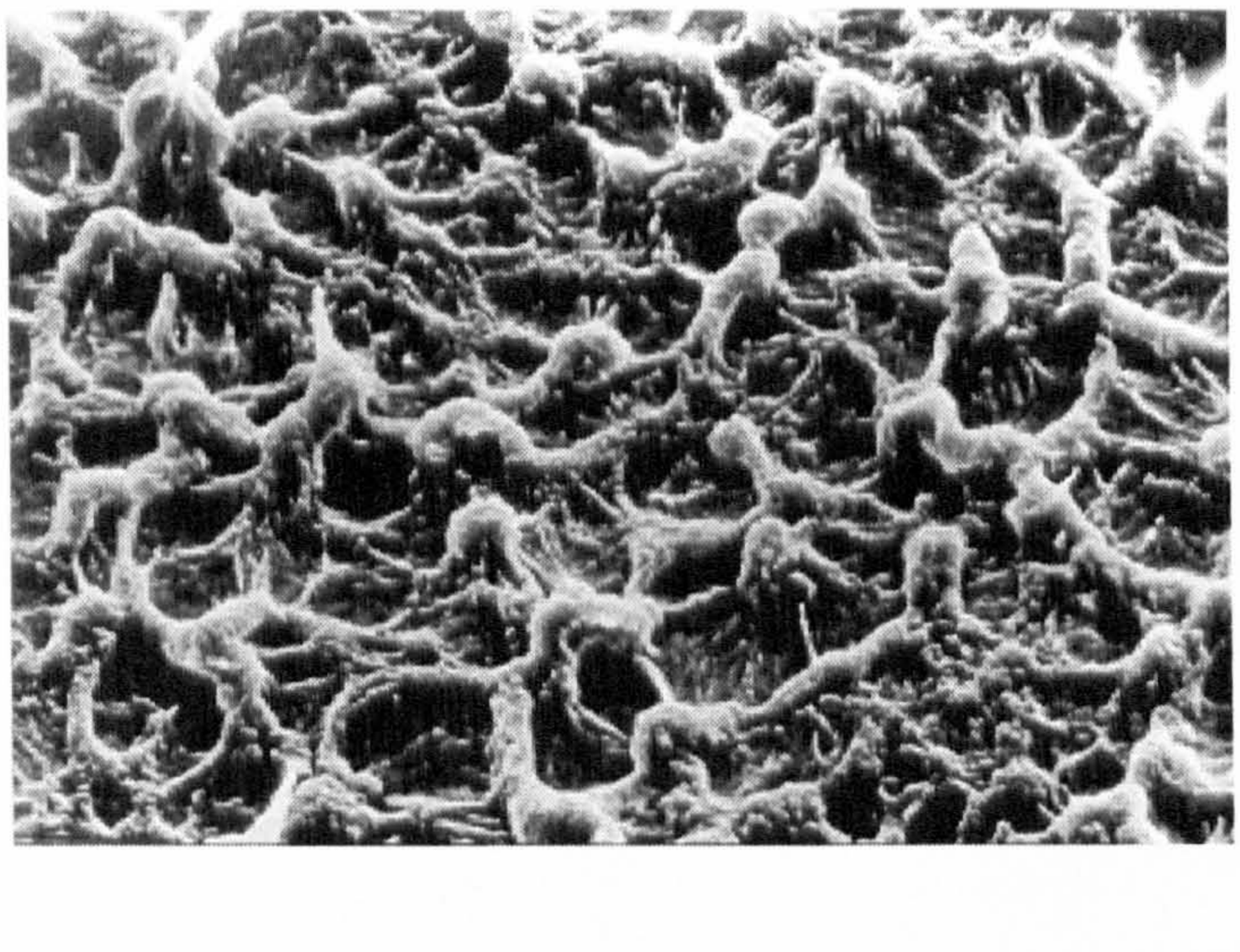

Figure 7.15. High magnification SEM micrograph of the HDPE Eltex brittle failure.

The fatigue test was developed as a tool to rank the three aged and unaged pipe resins samples in terms of

their resistance to slow crack propagation. A comparison of the fracture surfaces of a field and fatigue failed specimens unmistakably shows dissimilarity. The fatigue fracture surface of field failure had a more fibrous nature as clearly visible in Figure 7.16.

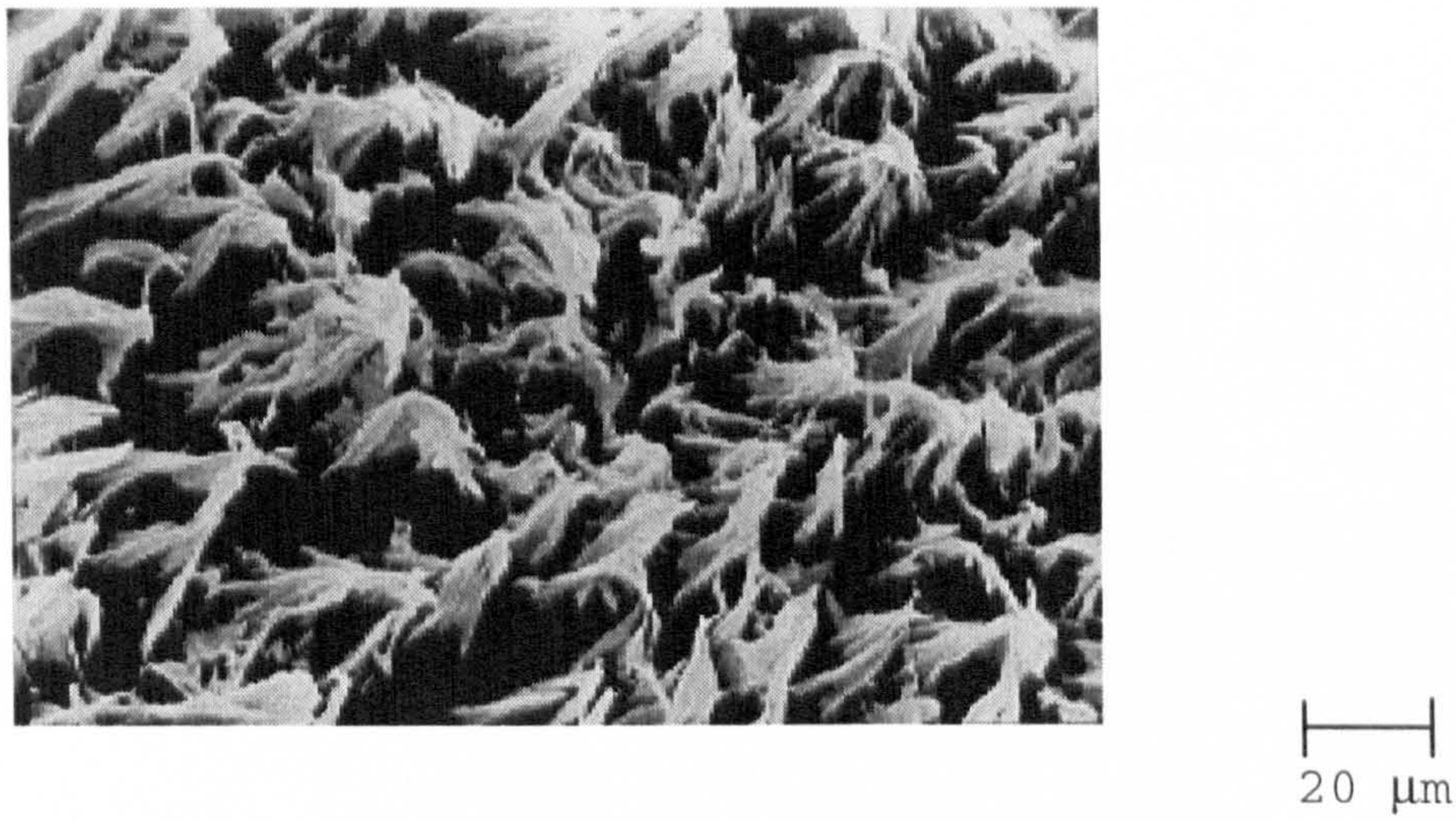

Figure 7.16. Predominately brittle type fracture observed for a field failure Aldyl-A pipe sample.

The main discrepancy between the two conditions, dynamic and static conditions, could be related to the applied stresses as illustrated in Figure 7.17.

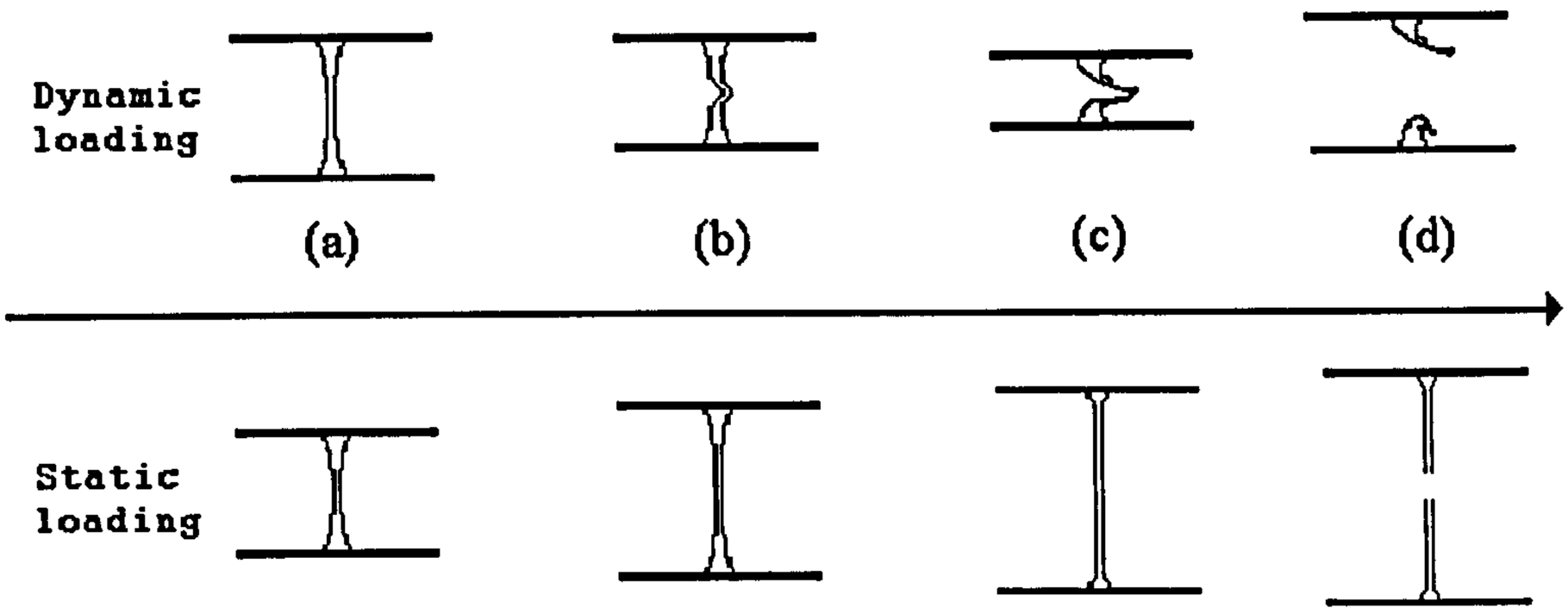

Figure 7.17. Schematic illustration of a fibril under dynamic loading (stress ratio of R=0.1) and under static loading conditions. The sequence of the failure process for the fibril under dynamic loading is as follow: (a) the fibril being stretched under a maximum stress level; (b) the fibril under localised compression stresses; (c) the fibril being crushed under minimum stress level; and (d) fibril failure with the repetition of the maximum stress level. In the static loading conditions, a fibril extension until failure.

In Figure 7.17, the most important factors that produced fibril fracture were the magnitudes of the maximum and minimum stress levels in the dynamic loading conditions. When the maximum tensile stress was applied, the fibrils were damaged by a process of stretching and disentanglement of the polymer chains. When the minimum stress was applied the fibrils are damaged by flexural loading. Even when the fatigue minimum stress was positive there was the possibility of local compression stresses within the fibrils due to the previously mentioned elongation of the fibrils. This stretching and bending is thought to crush and twist the fibrils during the fatigue test leading to a rapid failure of the specimen. In-service, the stresses are usually static causing only excessive elongation and the fibrils are damaged by disentanglement up to failure. However, Strebel et al. [1991] reported that the method of fatigue loading and crack plane orientation greatly affect the similarity between the static and dynamic loading circumstances. They suggested that the sample geometry

influenced the microscopic features of the fracture surfaces. They produced from a fatigue loaded trapezoid shaped sample a fracture surface with a striking similarity to that of a field-failure fracture surface. The similarity was startling especially considering that the crack in the field-failed pipe could have propagated for several years, whereas the trapezoid sample failure was created in three days.

7.2.6. Crack Propagation Analysis

To study crack propagation from another viewpoint, SEN specimens with a pre-set crack were removed from the fatigue test. Thin sections normal to the crack plane and parallel to the crack propagation direction were microtomed from the centre of the specimen. Figure 7.18 shows a fatigue fractured film when viewed in a polarised light microscope. The main crack growth is in a plane perpendicular to the applied stresses. In the work of Reynolds et al. [1993] the stress-whitening similar to that seen in Figure 7.18 was described as an interaction of shear bands with the elastic/plastic boundary. These shear bands intersect to cause intense strain concentrations. The intersection lines could develop into two sets of discrete secondary cracks both at approximately 45° to the plane of the main crack.

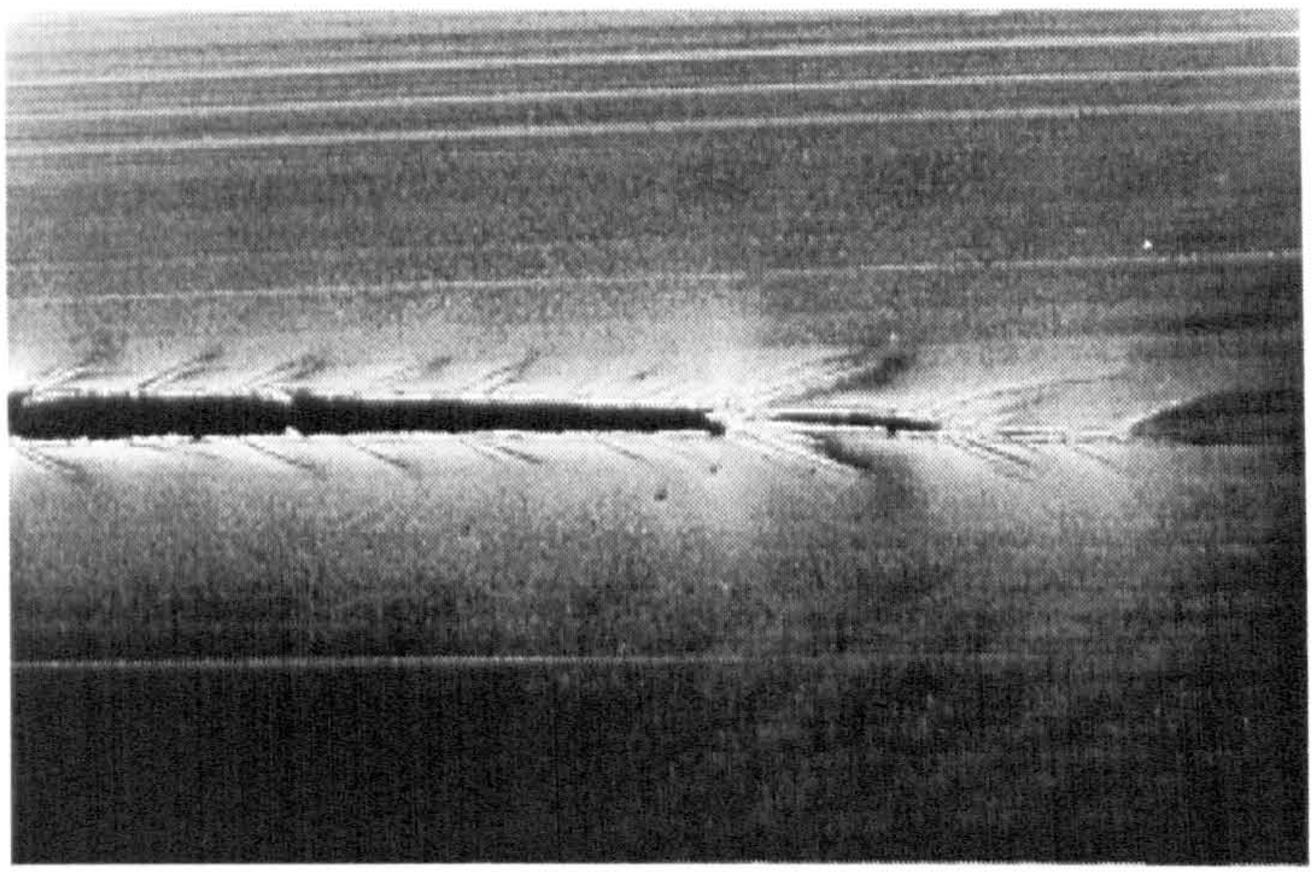

Figure 7.18. A microtomed Rigidex film detailing the propagation of a crack, secondary cracks, crack arrest and a process zone ahead of the crack tip. The SEN specimen was prepared from a Rigidex plaque.

Upon entering the ductile regime at a crack length greater than 5 mm as shown in Figure 7.18, the length and number of side crazes increases and the spacing of the side crazes becomes irregular. These side crazes and the root craze constitute the damage zone which preceded the perpendicular crack. The side crazes were found to have a microstructure similar to the root craze as shown in Figure 7.19. The irreversible deformation process in the from of crazes was limited to the crack tip region.

Figure 7.19. Micrograph showing the process zone and the formation of crazes before the crack front gives way.

Although morphologically a craze is different from a crack, it bears a number of similarities and can be considered a flaw once introduced in a material [Nimmer and Woods, 1991]. The crazes constitute the damage mechanisms associated with brittle failure. The damage mechanism within the root craze is a combination of fibrillation and continuous material yielding. The existence of varying degrees of these features throughout the craze results in an extremely complex craze microstructure. The voids which occupy the spaces between the yielded material could have connected to form larger voids or holes.

The crack damage shown in Figures 7.18 and 7.19 is representative of what was occurring throughout the majority of the SEN specimens made from Rigidex resin and a schematic illustration is shown in Figure 7.20.

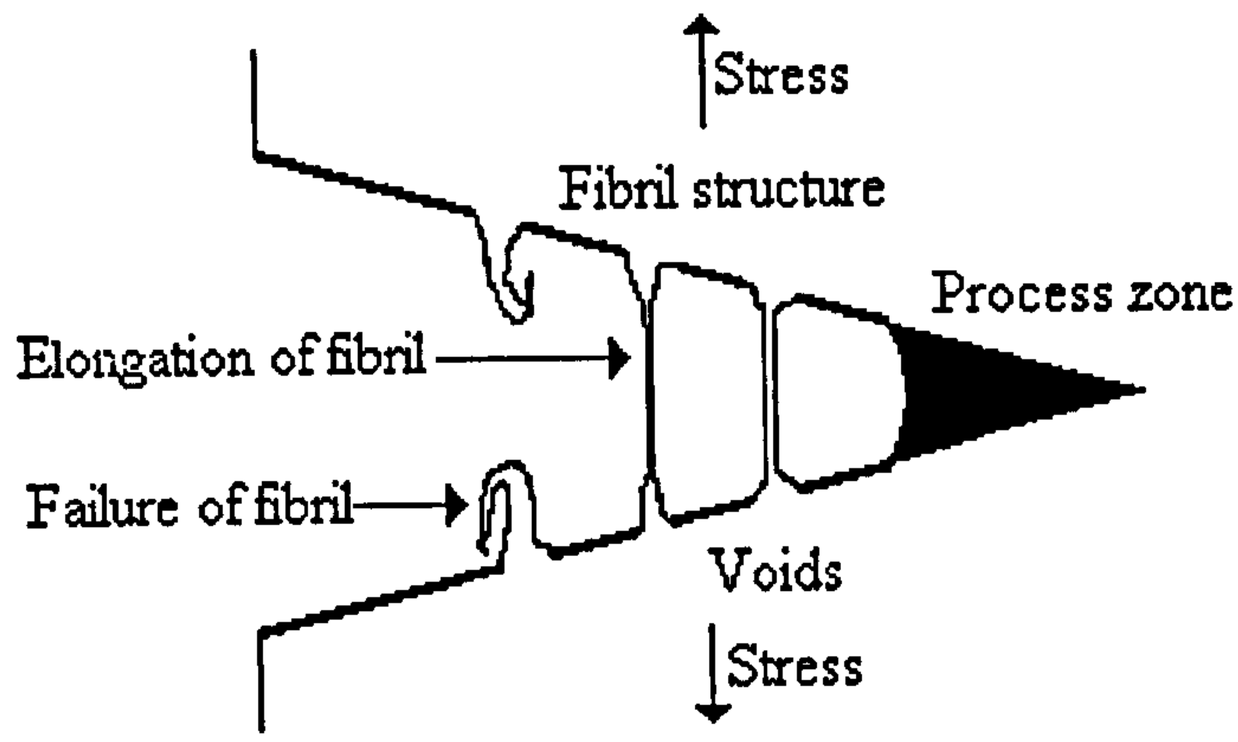

Figure 7.20. Proposed fatigue fracture mechanism.

The crack growth mechanism which occurred in Rigidex resin during the fatigue test could be summarised as follows: Immediately after loading the specimen, a craze forms at the root of the notch. At a certain stress concentration, the craze grows larger and bridging fibrils appear (yield zone). The drawing of the fibrils results in the formation of highly oriented material. The degree of orientation of the polymer tie molecules increases as the voids expanded. Fracture initiates by the rupture of the bridging fibrils linking the voids. The voids connect with opposing voids and form a gap. At the crack tip, the craze forms and from there the process repeats itself. This pattern is the basic mechanism that governs the resistance to fatigue crack growth. In other words, is the rate of disentanglement and crushing of the molecules in the fibrils of the crazes up to failure of the fibrils.

A recent publication by Zhou et al. [1996] found that the resistance to crack growth under fatigue loading conditions was directly linked to the molecular structure such as branching and molecular weight. They suggested that the introduction of side branches increased the plasticity of the material. More importantly, they

predicted that by increasing the molecular weight, the number of chains that linked the crystalline regions increased. Furthermore, the entanglements in the material between the crystalline regions also increased. The Eltex resin was designed with a similar formula: high molecular weight and an average of 3 branches every 1000 carbon backbone atom.

Evidence of a different behaviour for HDPE Eltex resin is shown in Figure 7.21. The crack tip did not travel in a straight line and had a tendency to branch as indicated by the arrows.

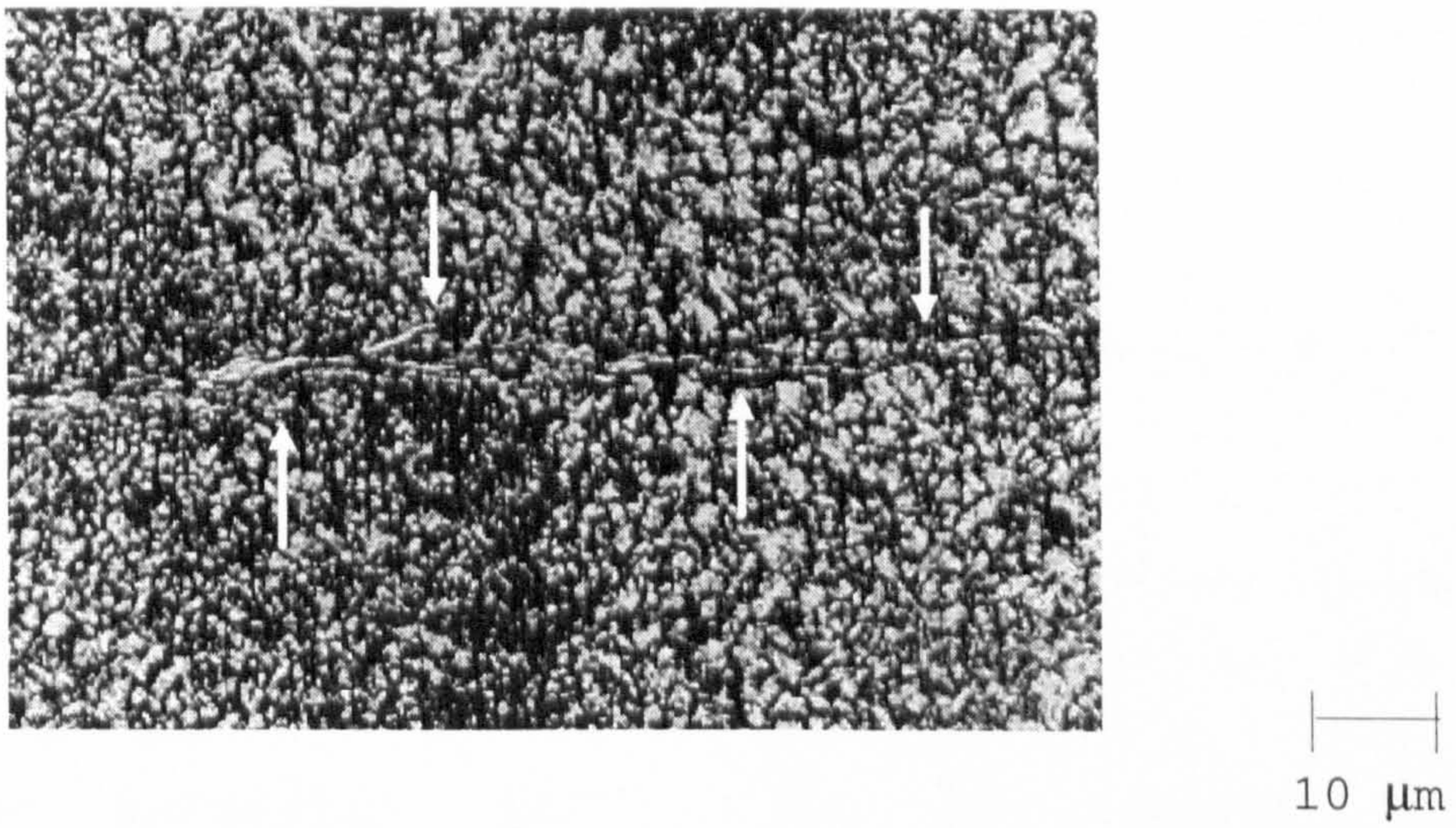

Figure 7.21. Micrograph showing main crack and crack branching in Eltex pipe resin under cross-polar microscope.

As described earlier, each brittle band occurred by the following processes: (i) void nucleation, (ii) void growth and (iii) coalescence of voids. The material adjacent to these nucleation sites must be able to be deformed in order for the void to grow and as suggested by Lu et al. [1995] the deformability of the material is governed by the degree of order and thickness of the crystalline regions. Therefore, it could be argued that in the case of HDPE Eltex resin the voids could have

initiated and grown in the amorphous region. Here, the resistance to void growth was determined by the deformability of these regions, tie chains across the amorphous regions and physical entanglements within them. Inevitably the growing voids reached the crystalline lamellae. The stress was then transferred to the lamellae and their deformability also influenced the crack propagation process. The crystals acted as anchors to the motion of the tie molecules under the action of stress. This meant the crack had to navigate through the dense crystalline material causing it not to travel in a straight line but with a tendency to branch. Gedde et al. [1983] reported on a similar observation. They studied fractography of fatigue fractured PE samples with different spherultic sizes by means of SEM and polarised light microscopy. They suggested that a fracture preferentially develops along a weakest link path defined by regions of segregated low molecular weight material. The segregated material is to a considerable extent accumulated in the spherulite boundaries.

In general, under a given set of loading conditions, some pipe materials will have a characteristic to resist slow crack growth better than others. This is due to a fundamental mechanism which is the rate of disentanglement of the molecules in the fibrils of the craze at the crack tip. The details of the disentanglement process at the molecular level was difficult to determine. But, the strength of the crystals is also equally important.

Since the resistance of the polymer to slow crack growth would be expected to influence the service life of a given PE resin system, SEN specimens prepared from aged and unaged pipe samples were tested using the specified fatigue method.

7.3. Fatigue Data

The fatigue test data are summarised in Tables 7.1 to 7.3.

Table 7.1. Fatigue data for pipe samples made from the Aldyl-A resin aged in the specified environments for one year.

Sample	Cycle to failure (cycles)
Virgin 125-pipe	201014 (45662)
125-pipe aged in water at 23°C	195263 (42098)
125-pipe aged in an air circulating oven at 80°C	145247 (37767)
125-pipe aged in water at 80°C	155256 (44984)
125-pipe aged in a vacuum-oven at 80°C	147325 (36348)
125-pipe from site age=17 years	113356 (37457)
125-pipe from site age=24 years (resin 5044)	92015 (37359)
8"pipe from site age=17 years	105214 (37870)
125-pipe (tan) from site age=24 years (resin 5044)	80366 (39247)

Standard deviation in parenthesis.

Table 7.2. Fatigue data for pipe and plaque samples made from the Rigidex resin aged in the specified environments for one year.

Sample	Cycle to failure (cycles)
Virgin 125-pipe	620325 (49563)
125-pipe aged in water at 23°C	600254 (46670)
125-pipe aged in an air circulating oven at 80°C	509398 (54519)
125-pipe aged in water at 80°C	522369 (46557)
125-pipe aged in a vacuum-oven at 80°C	508765 (40876)
125-pipe site sample laid in 1981 excavated 1995, age=15 years	584887 (37266)
Virgin 180-pipe	662077 (55535)
180-pipe aged in water at 23°C	658741 (39068)
180-pipe aged in an air circulating oven at 80°C	495056 (45564)
180-pipe aged in water at 80°C	543243 (47027)
180-pipe aged in a vacuum-oven at 80°C	526784 (44654)
Virgin Rigidex plaque	453686 (51098)
Plaque aged in water at 23°C	446422 (43465)
Plaque aged in an air circulating oven at 80°C	314452 (45778)
Plaque aged in water at 80°C	332458 (49546)
Plaque aged in vacuum-oven at 80°C	316543 (47543)

Standard deviation in parenthesis.

Table 7.3. Fatigue data for pipe samples made from the Eltex resin aged in the specified environments for one year.

Sample	Cycle to failure (Cycles)
Virgin 180-pipe	897258 (56673)
180-pipe aged in water at 23°C	880811 (52948)
180-pipe aged in an air circulating oven at 80°C	532277 (53832)
180-pipe aged in water at 80°C	640998 (57547)
180-pipe aged in a vacuum-oven at 80°C	635656 (54255)

Standard deviation in parenthesis.

With reference to Tables 7.1 to 7.3, to clarify the various complicated behaviours observed for the three polymer resins, each of the ageing conditions is discussed in a separate section.

7.3.1. Ageing in Water at 23°C

There were no significant changes in cycles to failure for the Aldyl A, Rigidex and Eltex samples presented in Tables 7.1, 7.2 and 7.3, respectively.

7.3.2. Ageing in an Air Circulating Oven at 80°C

With reference to the Aldyl A data summarised in Table 7.1, major changes were recorded in the cycles to failure for all the samples which were thermally aged at 80°C. For example, there was a reduction of 27% in the fatigue lifetime of the Aldyl A sample aged in an air circulating oven for one year at 80°C.

With reference to the Rigidex data presented in Table 7.2, this also showed a reduction in their fatigue life. For instance, the reductions were 18% for the 125-pipe, 25% for the 180-pipe and 31% for the plaque sample. The effect of crystallinity on fatigue crack propagation in PEs is again evident from these results. The fatigue lifetime of SEN specimen made from the same material was lower for samples with a high crystallinity.

Although the unaged Eltex pipe sample presented in Table 7.3 had the highest fatigue life, when thermally aged for one year, a reduction of 40% was recorded. This deterioration in the fatigue life for the Eltex resin is much higher than the reduction observed for both the Aldyl A and Rigidex resins.

7.3.3. Ageing in Water at 80°C

With reference to the Aldyl A data summarised in Table 7.1, the fatigue test results of the pipe samples for this ageing conditions were similar to that of all the thermally aged samples. A 23% reduction in the fatigue life of the Aldyl A sample was recorded.

With reference to the Rigidex data summarised in Table 7.2, a reduction of 16% in cycle to failure was recorded for the aged 125-pipe, 31% for the aged 180-pipe and 27% for the aged plaque Rigidex samples.

With reference to the Eltex data presented in Table 7.3, the fatigue life of the sample was reduced by 29%.

7.3.4. Ageing in a Vacuum at 80°C

With reference to the Aldyl A data summarised in Table 7.1, similar results were also recorded in this thermal environment. The aged Aldyl A sample showed a reduction of 26 % in its fatigue life.

With reference to the Rigidex data summarised in Table 7.2, the aged resin samples showed a reduction of 18% for the 125-pipe, 25% for the 180-pipe and 30% for the plaque sample.

With reference to the Eltex data presented in Table 7.3, the aged sample showed a reduction of 29% in its fatigue life time.

7.3.5. Samples Aged In-Service

The Aldyl A samples which were aged under site conditions (see Table 7.1) showed a marked reduction in their fatigue lifetimes. The 17 years old aged 125-pipe showed a 43% reduction. The 24 years 125-pipe made from the 5044 pipe resin showed a 54% reduction in its fatigue life when compared to the virgin samples made from the 5046 resin. A 47% reduction was recorded for the 8" pipe which was aged in-service for 17 years. A reduction of 60% was recorded for the 24 years old 125-pipe (resin 5044).

There was only one Rigidex 125-pipe sample which was aged in-service for 15 years (see Table 7.2). The fatigue lifetime of this sample showed a reduction of 6%.

7.4. The Effect of Ageing on Dynamic Mechanical Properties

7.4.1. Fracture Toughness

An attempt was made to measure the fatigue fracture toughness (J-integral) using the method developed by Strebel et al. [1992(a)], mentioned in chapter 3. Figure 7.22 shows the fracture toughness as a function of the change in crack length (a). The SEN specimens were prepared from unaged, in-service aged for 15 years and oven aged at 80°C for one year using Rigidex 125-pipes. The J-integral (J_{1c}) was determined from the intercept of the J-delta / (a) curves.

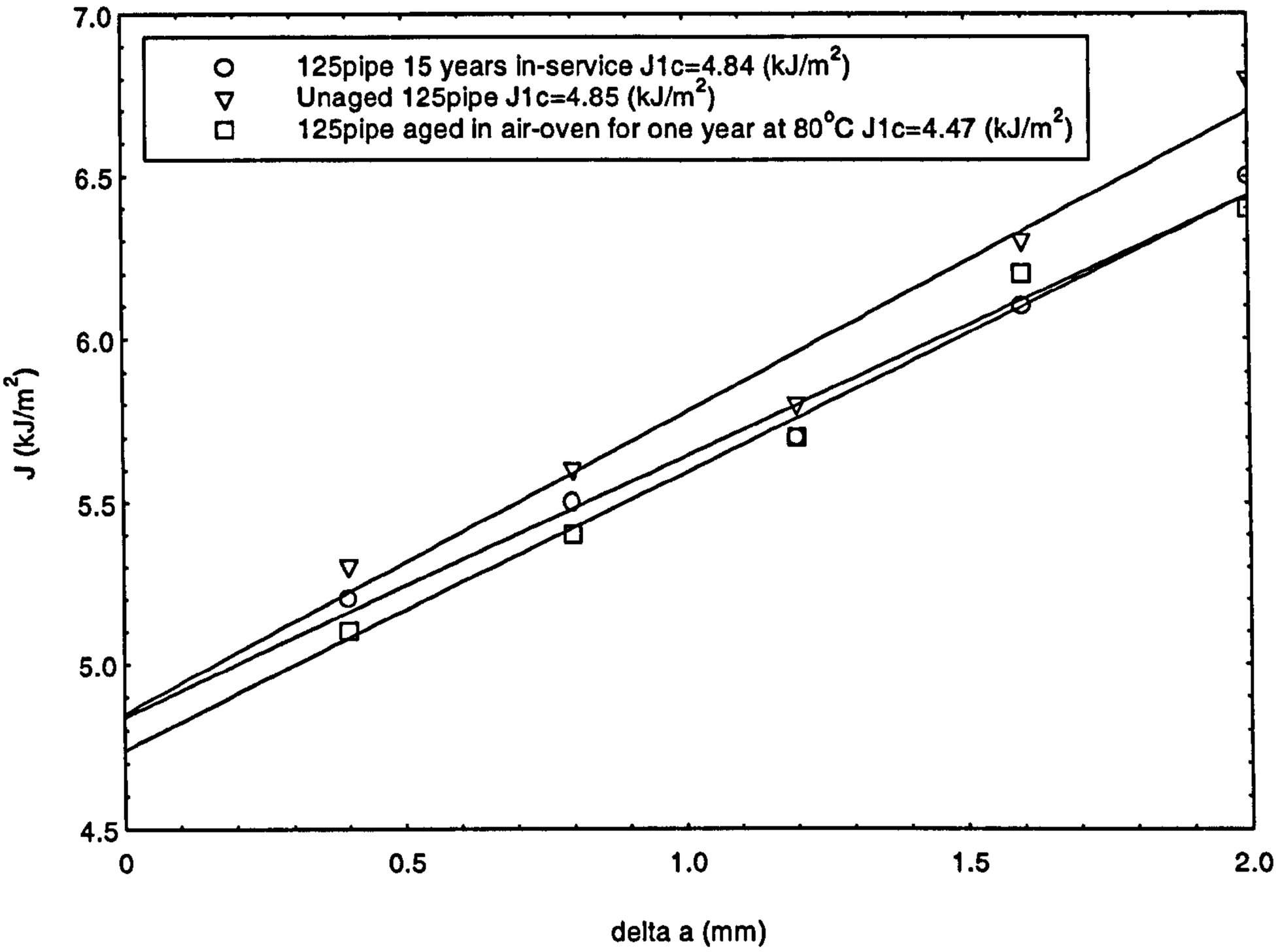

Figure 7.22. The fracture toughness (J) as a function of delta crack length (a) for the three Rigidex 125-pipe samples.

Several attempts have been made to measure the J_{1c} at crack initiation of polymers using the ASTM standard method [ASTM D 2837 1988] which utilises a three point bending set-up. Under plain strain conditions, typical values obtained from this test method for HDPE were between 0.2 to 2.5 kJm^{-2} [Narisawa, 1987; Swei et al., 1991; Hashemi and Williams, 1986]. Only Strebel et al. [1992(a);(b)] reported a J_{1c} value of 1.4 and 4.25 kJm^{-2} for a HDPE and MDPE respectively using the fatigue method. These vales are in a good agreement with J_{1c} values presented in Figure 7.22. However, the J_{1c} values for the three pipe samples were very similar to each other. This was attributed to the hysteresis loops generated during the fatigue experiments to calculate J_{1c} which were highly distorted and had to be averaged. The accuracy of this technique is highly dependent on the

performance of the fatigue machine. The sinusoidal wave generated by the machine was not a precise sine-wave. The Instron model 8032 servo-hydraulic machine used in this experiment had no waveform control. In addition to this, localised plane stress conditions mentioned by Rimnac et al. [1988] could have existed at the crack tip for the three samples. The existence of such localised stress conditions was related to another serious problem with the fatigue machine used in this investigation which was the absence of amplitude control. This meant that once the compliance of the specimen changed, corrective action could not be taken to maintain the required stress amplitude.

7.4.2. Fatigue Lifetime

A more direct method to rank the three pipe resin materials is to simply obtain the fatigue lifetime for the SEN specimens using the developed fatigue test. Change in the physical structure of PE pipe samples was the only effect detected during the laboratory accelerated ageing conditions: Thermal ageing caused an increase in the crystallinity of PE pipe samples. The Figure 7.23. represents the fatigue lifetime (taken from Tables 7.1 to 7.3) for the Rigidex resin in the form of 125-pipes, 180-pipes and plaques aged at the specified ageing environments. Each bar represent an average of six SEN specimens.

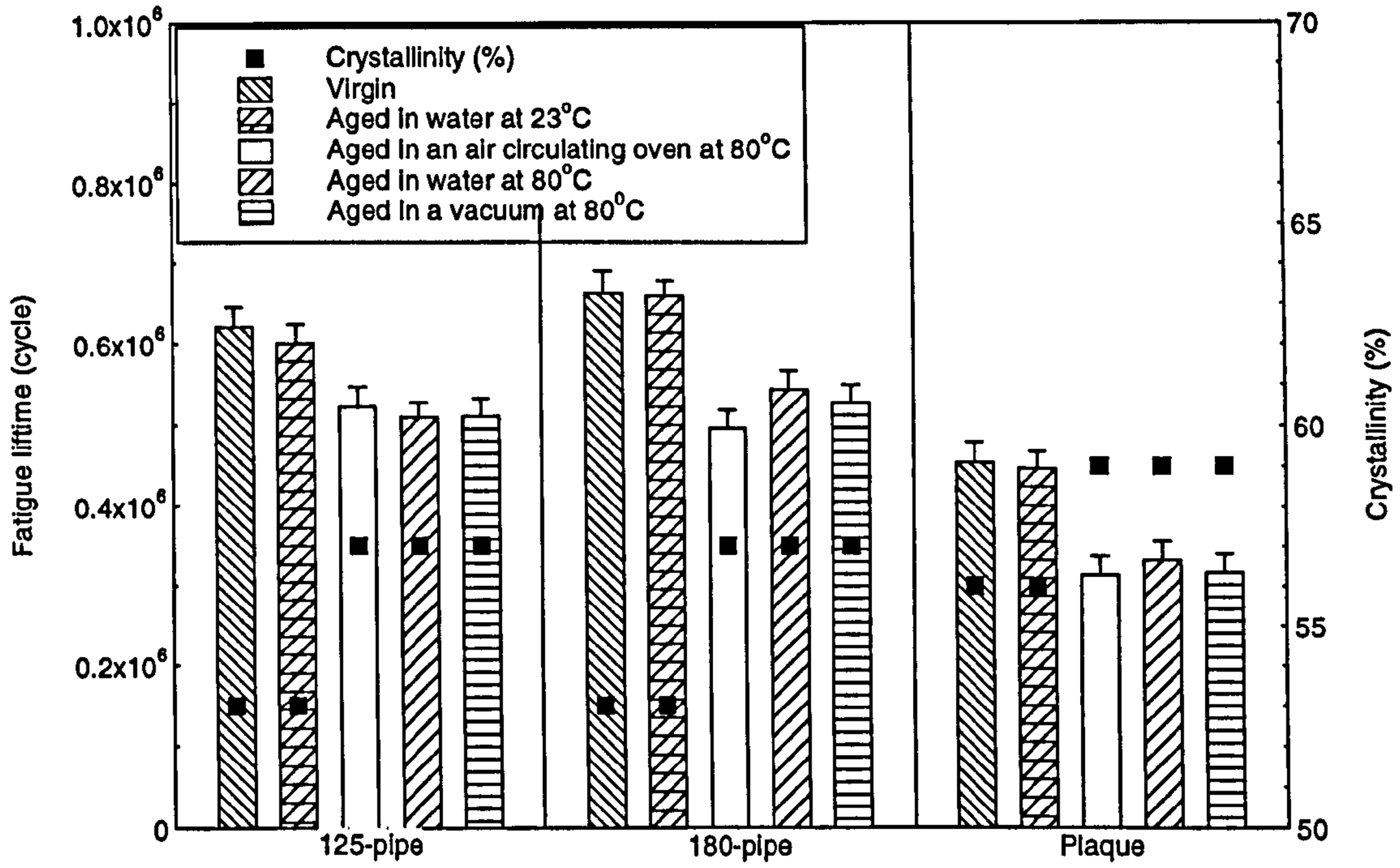

Figure 7.23. The fatigue lifetimes for the Rigidex 125-pipe, 180-pipe and plaque aged in the specified environments plotted along with their average pipe wall crystallinity.

With reference to Figure 7.23, the fatigue lifetimes for the unaged 125-pipe and 180-pipe specimens are very close together. It is also apparent that these specimens showed the same trend in their fatigue lifetimes with respect to the ageing environments. This was attributed to the crystallinities of these samples which were identical. The fatigue lifetime for the unaged plaque specimens were shorter than the unaged pipe samples. This can be related to their average crystallinity which was slightly higher than the pipe samples. Upon thermal ageing, the crystallinity of the plaque samples increased to 59%. This resulted in a very short fatigue lifetime of about $3x10^5$. This is in a good agreement with the fatigue lifetime of an unaged specimen which was prepared from the same resin with the same crystallinity as shown in Figure 7.5.

The fatigue lifetimes and crystallinity for the three pipe resin samples used in this study which were aged in the specified environments are presented in Figure 7.24.

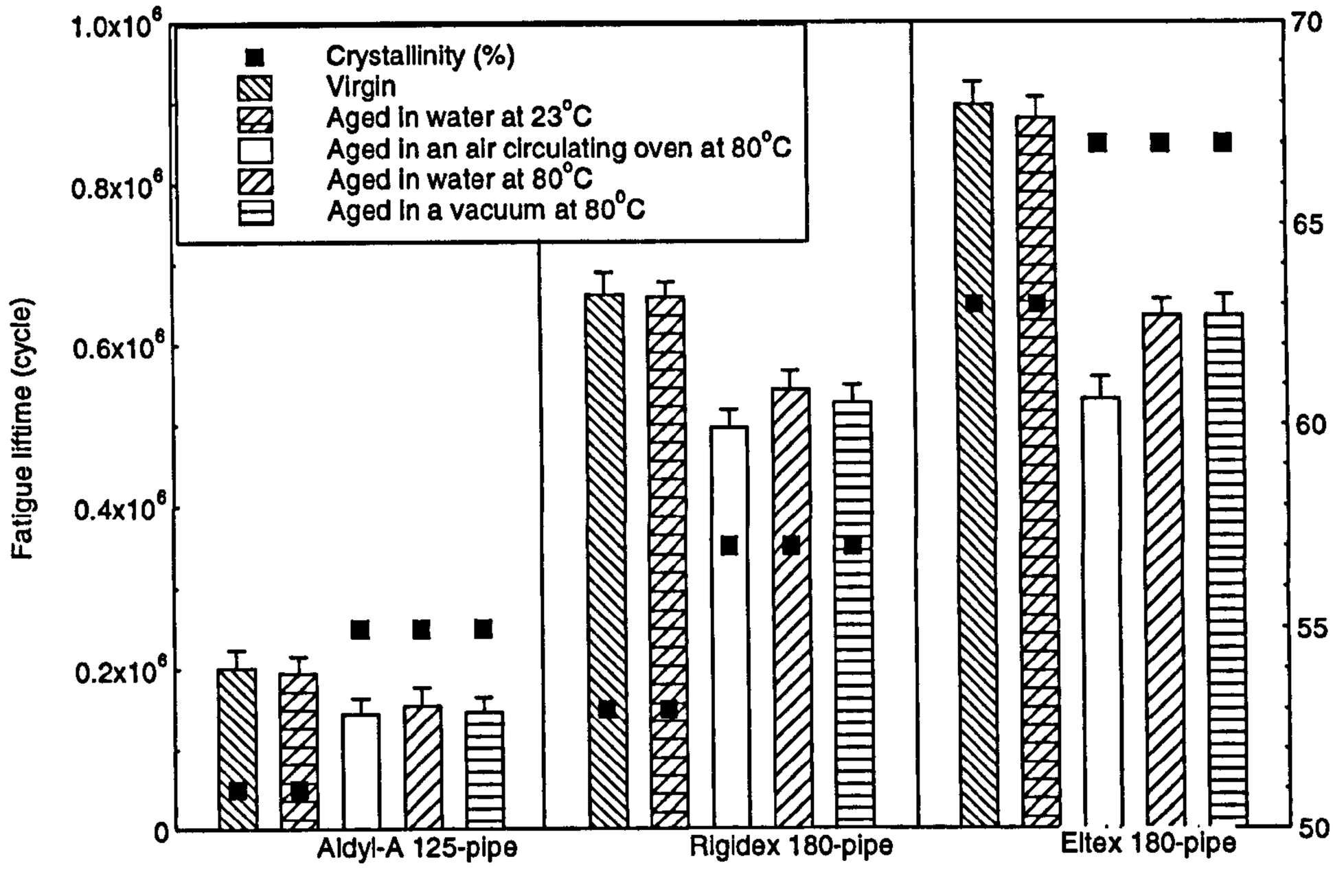

Figure 7.24. The fatigue lifetimes for the Aldyl-A, Rigidex and Eltex pipe resin samples aged in the specified environments along with their correspondent crystallinity.

It is apparent from Figure 7.24 that the resistance to fatigue crack growth for the virgin Aldyl-A pipe resin material is inferior to both the virgin Rigidex and Eltex specimens. It also clear that when aged at 80°C environment for one year further reduction was seen. The long fatigue lifetime recorded for the virgin Eltex pipe sample is a good indication of the high resistance of the material to fatigue crack growth. However, when aged in the air circulating oven for one at 80°C the fatigue lifetime is seen to decrease significantly to the same level as the Rigidex pipe sample aged in similar conditions.

In general, since there was no chemical degradation detected in all the aged samples used in this study it is appropriate to concluded that the thermal ageing for one year resulted in an increase in the crystallinity of the aged specimens which in turn led to a reduction in their fatigue lifetime. It is also possible to conclude that at a given crystallinity each resin system showed unique dynamic mechanical properties. This can be attributed to other resin parameters which are molecular weight, molecular weight distribution, branch density and branch length. These parameters have profound effect on the tie molecules and the spherulites size in the polymer. These factors determine the fatigue lifetime of the PE resin [Runt and Jacq, 1989; Botsis et al., 1996; Pecorini and Hertzberg, 1993; Yeh et al., 1994].

CHAPTER

EIGHT

CHAPTER EIGHT

CONCLUSIONS AND SUGGESTIONS FOR FUTURE WORK

8.1. Conclusions

The OIT test was a useful tool for the condition assessment programme. However, it was found that the OIT value was greatly influenced by the oxygen gas flow rate and the sample mass. The gas flow rate was easily controlled, but it was difficult to precisely cut 12 mg each time an OIT sample was prepared. A small variation in sample mass was believed to contribute to a noticeable scatter in the OIT data. The difficulty in pinpointing the onset of oxidation along the OIT traces also contributed to the observed scatter.

An OIT test temperature of 200°C which was selected using the Arrhenius relationship was found suitable for the aged and unaged polymer samples used in this study.

The OIT test provided only limited information on the oxidative stability of the PE samples tested. It served as an indicator of the thermal stability for the aged and unaged PE samples. However, it does not provide quantitative information on the relative concentrations of individual additives as a function of ageing. Therefore, this technique had to be coupled with HPLC analysis to provide quantitative information on the relative concentrations of additives in the polymer with the various ageing environment. HPLC analysis revealed that both Irganox 1076 and Chimassorb 81 used in Rigidex pipe resin migrated from the middle section to the surface during ageing when aged at 80°C in an air circulating oven. In the case of the Rigidex pipe sample aged in the vacuum oven, it was found that the Chimassorb 81 concentration decreased in the surface, middle and bore regions of the pipe. This was attributed to the volatility of the additive. Under the same ageing

conditions, the concentration of Irganox 1076 decreased slightly and there was no detectable reduction in the concentration of Santonox R. The HPLC analysis provided conclusive evidence for the additives leaching to the water bath where the Rigidex resin samples were aged.

The use of HPLC analyses and the highly accurate results obtained from this technique would not have been possible without the successful development of a procedure to extract the additives from the PE resins. The microwave extraction method developed in this study ensured high recovery rates of the additives. This in turn made it easy to interpret the OIT data and relate it to the behaviour of individual additives during ageing.

Most of the OIT traces for the Rigidex and Eltex resin samples showed a convoluted double exothermic peak. But, the Aldyl A (5046) resin samples showed only one exothermic peak. However, a different behaviour was observed for the Aldyl A pipe sample made from 5044 resin (obtained from site) and the Aldyl A pipe sample (made from 5046 resin) which were aged in water for one year at 23°C. The OIT traces for these samples showed the appearance of a separate and premature exothermic peak along with the usual major exotherm. The premature peak was attributed to cross-linking of the polymer during the OIT test at 200°C. However, further analysis on this was not possible because there was no information available on the additive system used in any of the Aldyl A resins.

The virgin Eltex resin samples gave higher OIT values than the Rigidex resin. This was related to the fact that most of the additives used in the Eltex resin had higher melting points than the additives used in the Rigidex resin. This difference gives rise to the volatility of the Rigidex additives and therefore, upon exposure to heat the additives loss increased from the OIT sample which resulted in low OIT values.

Chemical degradation was not detected in PE pipe samples during the specified ageing environments using FTIR spectroscopy. However, the sensitivity of the FTIR instrument used in this study was questioned due to variations in humidity and temperature at different testing times during the course of this project. It is conceivable to postulate from the FTIR results that no major chemical degradation process was detected in any of the aged pipe samples.

In general, ageing at ambient temperature had no significant effect on the additive concentrations within the pipe materials. But thermal ageing environments at 80°C had a marked effect on the profile of the additive concentrations across the pipe wall. This was explained in terms of several mechanisms working together.

A linear relationship was obtained between the density of PE samples measured via the density column and the corresponding crystallinity measured via DSC. This was also the case for the thermally-aged PE pipe samples. The density was found to increase during thermal ageing.

The degree of crystallinity was found to be at the lowest at the surface regions for all the PE pipes investigated in this study. This was due to the differential cooling rates experienced across the pipe wall during its manufacture. The highest density corresponded to the region next to the inner surface of pipes. Upon thermal ageing it was also found that the rate of crystallinity increase was the highest at the pipe outer surface. However, the degree of crystallinity became the highest near the pipe bore after ageing at 80°C for one year. Examination of DSC traces of thermally aged samples showed no evidence of the peak melting point shifting to higher temperatures. However, there was a noticeable peak appearing at approximately 90°C with thermal ageing at

80°C. This behaviour was explained in terms of two possibilities:

(i) the first possibility is that there was a molten fraction of the polymer at 80°C which recrystallised with ageing and which had exactly the kinetics of primary crystallisation i.e., reorganisation of the molten material to form thicker and thicker lamellae until they display an endothermic peak at approximately 90°C;

(ii) the second possibility could be that the order in the interface region between the crystalline and the amorphous phases increased with thermal ageing. This interface region had a melting point just between 80 to 90°C.

Of course, it also possible that both mechanisms could be taking place concurrently during thermal ageing.

In this study the increased crystallinity observed for thermally aged samples was not related to any chemical modification process of the polymer such as chain scission. It was simply attributed to the thermal energy which caused rearrangement in the system over a long period of time. This behaviour is part of an overall physical ageing phenomenon explained in this study.

The use of a dumb-bell type sample with a thickness of 70 μm as a micro-tensile test sample was not possible because of the occurrence of multiple yield points in the stress-strain traces. As an alternative, a rectangular sample was used as a micro-tensile specimen and was shown to be very effective in reflecting the same trends as that observed for the macro-tensile test. It is proposed that this negates the need to excavate large sections of pipe sample for the purpose of the condition assessment of PE pipelines.

PE polymer was shown to be a very sensitive to the strain rate. A detailed study was undertaken into ways of notching the fatigue specimens. It was demonstrated that the use of a thin sharp blade was crucial in obtaining repeatable fatigue data.

The increase in the degree of crystallinity of thermally aged samples mentioned earlier raised the question of the validity of the hydrostatic test at 80°C. The so called knee and the steep curve termed the brittle failure region usually seen in the hydrostatic test results then arguably could be related to the increase in the degree of crystallinity of the pipe sample during thermal testing. The increase in crystallinity had a marked effect on the static and dynamic mechanical properties of the material. The tensile data showed that the modulus and the stress at yield increased and the elongation at break decreased for all the thermally aged samples. In addition to this, the fatigue fracture toughness of thermally aged samples was also found to decrease because of the thermal conditions employed. This result was clearly reflected in the cycles to failure data which decreased with increasing the degree of crystallinity. The residual stress measurements also confirmed that the physical structure of the pipe samples had changed during thermal ageing.

Naturally aged pipe samples from service also showed a noticeable increase in the degree of crystallinity. Again this was reflected in a significant reduction in the fatigue cycles to failure. This behaviour was attributed to the physical ageing phenomenon which is still not fully understood.

A ductile-brittle transition was evident in the fractured SEN specimens. Eltex pipe resin samples showed different fracture growth and surface fracture features than the Rigidex resin samples. This behaviour was linked to the

major differences in the characteristics of the two materials such as the molecular weight, molecular weight distribution and branch density which give rise to unique microstructural properties.

A fatigue fracture propagation mechanism was explained in terms of a process zone at the crack tip at which nucleation of crazes occurs and eventually transformation of these crazes to individual growing voids lapping. At a certain stage of the SEN specimen fatigue life, the growing voids connect together to form the brittle zone. The transformation process of a craze to a void in the fatigue test occurred as a result of bending, crunching and stretching of the fibrilar structure to form voids. This failure mechanism lead to accelerated failure. Fracture surfaces of samples that failed in-service did not show the same features as the fatigue fractured SEN specimens. The process leading to this type of failure was explained in terms of stretching or elongating the fibrilar structure within the crazes.

The achievements of this study can be summarised as follows: (i) reliable test methods that can detect physical and chemical ageing in polyethylene pipes were established; (ii) the effect of laboratory ageing mechanisms on the integrity of pipe materials were elucidated and (iii) procedures for monitoring and rapid inspection for buried polyethylene pipes has been developed using OIT value, HPLC analysis, carbonyl index, crystallinity measurement, macro- and micro-tensile and fatigue testing.

8.2. Suggestions for Future Work

Oxidative stability

An important factor which was not examined as a possible contributing factor which could have influenced the OIT test is the sample surface area. The surface area of an OIT sample is directly exposed to oxygen and an increase in this area would increase the possibility of thermal

oxidation. Also, there is the probability of an increase in additives loss as the surface area increases due to volatility. In order to investigate this several OIT samples having, as much as possible, similar shape and mass should be prepared. Each sample should then be sliced in a controllable manner in order to increase the surface area from one sample to another.

With reference to section 4.4, where presence of a minor exothermic (first) peak was observed in the OIT traces, further work should be carried out to investigate if the delay in the major (second) exothermic peak was directly related to the process of cross-linking. In addition to this it is necessary to establish if this cross-linking was due to an increase in vinyl groups and what role the vinyl groups play in the degradation process.

The possibility that the additives could have reacted directly with oxygen or water during ageing should be investigated. NMR analysis should be carried out on aged and unaged pure additives in the same specified ageing conditions. The probability of additives chemically reacting with the polymer chains during the specified ageing conditions should also be explored using NMR analysis.

It was uncertain how the solubility of additives could have influenced their diffusion and volatility mechanisms during the specified ageing conditions. In order to understand these mechanisms an investigation should be carried out to study the solubility of additives in the three polymer resins in air and water at 23°C and 80°C. The samples tested should also have a wide range of crystallinity.

The use of HPLC analysis in this study proved to be a powerful method in determining the additives concentrations in aged and unaged Rigidex resin samples.

Moreover, the success of this method was due to the advances made in the extractability procedure developed using the microwave method. Therefore, it is imperative to continue to progress this work to reach an optimum procedure to obtain even higher recovery rates of additives. Eltex and Aldyl resins should also be included in this work.

Although, the HPLC analysis yielded good results the minimum time it took to produce such results was about two hours. This was due to the need to filter the PE specimen as part of the extraction procedure. It would be preferable to find a faster method for the condition assessment programme. The application of UV spectroscopy to monitor the depletion of additives should also be considered.

The outcome of the specified ageing environments did not produce any detectable levels of oxidation using FTIR spectroscopy. To understand the effect of oxidation on pipe performance the following is suggested:

(i) increase the ageing temperature of the air-oven experiment to above 80°C but not more than 115°C. Samples should include PE materials free from additives;

(ii) as the PE pipe are usually stored out doors prior to installation, it is important to investigate the photoxidative stability of PE pipe resins and to find out what detrimental effect this would have on the performance of the pipe;

Preliminary work (not reported in this study) showed that the microwave method can be used to solvent etch PE samples yielding high quality microstructural details when observed using polarised light microscopy. Further work is needed to optimise this procedure and then it might be used to study the effect of oxidation on the

might be used to study the effect of oxidation on the spherulitic structure. Also, it would be interesting to investigate if the etched surfaces can be examined using TEM by a replica procedure.

Physical ageing

It was proposed that the physical ageing phenomenon could lead to an decrease in the free volume in the polymer system due to an increase in crystallinity. To investigate further this phenomenon and its effect on the integrity of PE pipes the following techniques can be used to detect and measure the free volume:

(i) Positron annihilation spectroscopy: This method can be used to measure directly both free volume and the distribution of free volume by monitoring the ortho-positonium which is an electron-positron state with parallel spins which has a mean lifetime of 142 ns in vacuum. This state is concentrated in the free volume 'holes' within the polymer and its lifetime is proportional to the hole size. In condensed matter, the lifetime of this state is considerably reduced because it can pick off and annihilate an electron with anti-parallel spin;

(ii) Small angle x-ray scattering (SAXS): Indirectly to give an insight on the free volume by monitoring structural changes due to lamellae thickening which may occur during ageing; and

(iii) Micro-Indentation test: The plastic and elastic properties of the near-surface region of PE pipe samples can be measured by a sub-microindentation technique. From slow loading and unloading tests, values of plasticity indices and Young's moduli can be derived. The sensitivity of such techniques can be very high and reach measurements representing nano-scale levels. The results can yield valuable information on the plasticity of the

volume concept. This test if proven successful can be modified and used on site as a NDT technique to detect the loss of ductility due to physical or chemical ageing.

Thermal ageing was shown to increase the polymer crystallinity in the polymer. It is possible that this could lead to a tensioning of the entangled polymer chains in the amorphous phase. Raman spectroscopy can be used to measure the backbone chain C-C stretch at 1063cm^{-1} which can be interpreted as internal stresses exerted by the extended lamellae layers upon increasing crystallinity during thermal ageing.

Physical ageing studies should also include welded sections and the effect of this phenomenon on the weld mechanical properties.

Mechanical properties

The fatigue test was established to characterise the relative resistance to crack initiation and growth for virgin and aged samples. To capitalise on this test further investigations are needed in the following areas:

(i) the condition assessment study was hindered by the inability to carry out routine inspections of in-service pipes to monitor their integrity. It is envisaged that the success of this test and indeed this programme is highly dependent on the availability of pipe samples from site;

(ii) generation of S-N curves for two types of pipe size namely, 125 and 180 mm OD SDR11 at different temperatures;

(iii) one of the most sensitive experimental variables found in the fatigue test was the method of notching. The possibility of preparing a compression moulded SEN sample prenotched is highly desirable and may eliminate any

notch sensitivity. Moreover, the prenotched fatigue samples are likely to be reproducible. However, a disadvantage in this method would be the sharpness of the notch. The existing method used in this study can be further modified;

(iv) the effect of crack front length, sample width, stress ratio, compressive stresses, annealing at different temperatures including ageing at sub-zero temperatures, fluctuating temperatures and UV radiation on fatigue properties should be investigated; and

(v) the surfaces of fatigue fractured SEN samples were examined using SEM. The fracture surface was beam damaged at high magnifications. A replica technique can be used to obtain high magnification SEM micrographs or a cold stage SEM which can be advantageous in this matter.

Samples with a wide range of crystallinity should be prepared in order to investigate the effect of crystallinity on the mechanical properties. This should be carried out for all the three polymer resins investigated in this study.

Different test methods should be considered for the fatigue test namely, three point bending, arc-shape samples and whole pipe sections. These sample shapes should be designed to restrain the amount of plasticity at the crack tip and to ensure that plane strain conditions prevail.

The microtome blade created scratches along the micro-tensile film samples. The scratches influenced the elongation to break and the failure behaviour. The maximum thickness that could be produced using this equipment was 70 micrometres. It is suggested that the microtomy equipment should be modified to include a cold

stage sample holder with capability of cutting thick samples.

REFERENCES

Ahlstrand L (1995), Oxygen Induction Time - What Does it Actually Tell Us About Thermal Stability? ANTEC 95, Vol.3, 87-91.

Alferink F and Wolters M (1991), The Effect of Material and Installation Quality on The Lifetime of Buried PE Pipes, 12th Plastic Fuel Gas Pipe Symposium, Boston, 272-284.

Allen N, Marshall G, Moore L and Kotecha J (1988), Oxidation Processes in Blue Water Pipe, Polymer Degradation and Stability, Vol.20, 315-324.

Allen N, Moore L, Marshall G, Vasiliou C and Kotecha J (1990), Diffusion and Extractability Characteristics of Antioxidants in Blue PE Water Pipe: A DSC and Radiolabelling Study, Polymer Degradation and Stability, Vol.27, 145-157.

Annual Book of ASTM Standards 08/04/317 (1988), ASTM, Philadelphia.

Audouin D (1994), Role of Oxygen Diffusion in Polymer Ageing: Kinetic and Mechanical Aspects, J. of Materials Science, Vol.29, 569-583.

Barham P and Keller A (1989), The Initial Stages of Crystallistation of PE from the Melt, J. of Polymer Physics: Part B: Polymer Physics, Vol.27, 1029-1042.

Barker M (1980), Fatigue Properties of HDPE Pipe Systems, Journal of Materials Science Letters, Vol.15, 265.

Barker M, Bowman J and Bevis M (1983), The Performance and Causes of Failure of Polyethylene Pipes Subjected To Constant and Fluctuating Internal-Pressure Loadings, Journal of Materials Science, Vol.18, 1095-1118.

Barry D and Delatycki O (1989), The Strain Rate Dependency of Fracture in PE: Fracture Initiation, Journal of Applied Polymer Science, Vol.38, 339-350.

Barry D and Delatycki O (1992), The Effect of Molecular Structure and Polymer Morphology on The Fracture Resistance of HDPE, Polymer, Vol.33, 1261-1265.

Battiste D, Bulter J, Cross J and McDanial M (1981), Infrared Spectrometric Determination of Catalysts Used in The Production of HDPE, Analytical Chemistry, Vol.53, 2232-2234.

Bezprozvannykh A, Kronfeld A, Logvinov A, Loginova N, Volf L (1986), Certain Rheological Properties of Ftoroplast-50 Melts and Their Influence on Fiber Formation, Journal of Applied Chemistry of the USSR (English translation of Zhurnal Prikladnoi Khimii), Vol.59, No.4 pt 2, 881-884.

Bharel R, Anand RC, Choudhary V and Varma IK (1992), Performance Evaluation of Antioxidants in Polyethylene By DSC, Polymer Degradation and Stability, Vol.38, 107-112.

Bhatnager A and Broutman L (1985), Effect of Residual Stresses on Performance of Plyethylene Pipe, 9th Plastic Fuel Gas Pipe Symposium, New Orleans, 101-115.

Billingham N and Calvert P (1980), in "Developments in Polymer Stabilization", Ed. by Scott G, Applied Science, London, 139.

Bjorklund I (1996), Future Use of Plastic Pipes - Forecast on 40 Years Experience in Nordic Countries, Plastics, Rubber and Composites Processing and Applications, Vol.25, 364-367.

Blacker R, Vaughan A and Bassett D (1995), Thermal Processing, Morphology and Electrical Strength of PE, IEEE International Conference on Conduction and Breakdown in Solid Dielectrics, Piscataway, NJ, USA, 214-218.

Boast R and Latoszynski P (1985), Comparison of DSC and HPLC As Techniques For Analysis of Stabilisers in PE, Royal Australian Chemical Inst., Polymer Div., Parkville Polymer 85: An International Symposium on Characterization and Analysis of Polymers - Preprints, Melbourne, 11-14 March, 165-167.

Botsis J, Oerter G and Friedrich K (1996), Fatigue Fracture in Polypropylene With Different Spherulitic Sizes, Annual Technical Conference - ANTEC, Conference Proceedings, Vol.3, 3294-3300.

Brady J and Thomas E (1988), Effect of Short-Chain Branching on The Morphology of LLDPE-Oriented Thin Films, J. of Polymer Science, Part B: Polymer Physics, Vol.26, 2385-2398.

Bradley S and Bradley W (1995), Study of Slow Crack Growth in Polyethylene, ANTEC 95, Vol.2, 1930-1931.

Bragaw C (1979), The Validity of Fracture Mechanics For The Design of Polyethylene Piping Systems, 4th International Conference on Deformation, Yield and Fracture of Polymers, Cambridge, Vol.1, 2-5.

Bratnagar A and Broutman L (1985), ANTEC 85, 545.

British Gas specification manual PL2-Part:1 (1994).

Brooks N, Duckett R and Ward I (1992), Investigation into Double Yield Points in PE, Polymer, Vol.33, 1872.

Broutman L and Bhatnager A (1985), Effect of Residual Stresses on Performance of PE Pipe, Conference Proceedings, 9th Plastic Fuel Gas Pipe Symposium, New Orleans, LA, USA, 101-115.

Broutman L (1986), Ageing of Plastic Pipes Used For Distribution, Annual Report 1984-1985, Gas Research Institute.

Brown N, Kamei E and Ward I (1983), The Influence of Morphology and Molecular Weight on Ductile-Brittle Transitions in Polyethylene, International Gas Research Conference, London, 214-223.

Brown N (1992), International Round Robin Study of A Fatigue Test Approach To The Ranking of PE Piping Material, 12th Plastic Fuel Gas Pipe Symposium, Boston, 446-454.

Brown N and Lu X (1995), A Fundamental Theory For Slow Crack Growth in PE, Polymer, Vol.36, 543-548.

Bubeck R and Baker M (1982), Influnce of Branch Length on The Deformation and Microstructure of PE, Polymer, Vol.23, 1680-1684.

Bulinski A, Bamji S, So E and Gubanski S (1995), Diagnostic Measurments of High Voltage Polymeric Cable Insulation, Proceeding of the Symposium on Electrical Insulating Materials, 19-26.

Butler M and Donald A (1997), Deformation of Spherulitic Polyethylene Thin Films, Journal of Materials Science, Vol.32, No.14, 3675-3685.

Calvert P and Billingham N (1979), Loss of Additives From Polymers: A Theoretical Model, J. of Applied Polymer Science, Vol.24, 357-370.

Celement J, Jakeways R and Ward I (1979), Study of the Effects of Annealing on the Mechanical Stiffness and Structure of PE, Polymer, Vol.20, 295-300.

Chan M and Williams J (1981), Plane Strain Fracture Toughness Testing of HDPE, Polymer Engineering and Science, Vol.21, 1019-1026.

Chaoui K, Chudnovsky A and Moet A (1987), Effect of Residual-Stress on Crack-Propagation in MDPE Pipes, Journal of Materials Science, Vol.22, 3873-3879.

Chirinos-Padron A, Hernandez P, Allen N, Vasilion C and Marshall G (1987), Synergism of Antioxidants in HDPE, Polymer Degradation and Stability, Vol.19, 177-189.

Choi S and Broutman L (1983), Residual Stresses in PE Pipe, Annual Technical Conference, Society of Plastics Engineers, Brookfield Centre, CT, USA, 378.

Christison G (1977), Manufacture of HDPE By The Union Carbide Gas Phase Process, Institute of Chemical Engineers symposium Series, 27-37.

Cowie J (1973), "Polymer: Chemistry and Physics of Modern Material", International Textbook Company Limited, UK.

Crist B (1989), Crystallinity and Mechanical Behavior in Model Polyethylenes, Miami Beach, FL, USA, 10-15 Sep Polymer Preprints, Division of Polymer Chemistry, American, Chemical Society, Vol.30, 299-300.

Darras O and Seguela R (1993), Tensile Yield of PE in Relation to Crystal Thickness, J. Polymer Science: Part B: Polymer Physics, Vol.31, 759-766.

Dear J (1991), Study of The Physical Properties of PE Polymers That Affect Crack Initiation and Propagation, Fatigue Fracture Engineering Materials and Structure, Vol.14, 663-678.

Defoor F, Groeninckx G and Reynaers H (1993), Molecular, Thermal and Morphology Characterisation of Narrowly Branched Fractions of 1-Octene LLDPE, Macromolecules, Vol.26, 2575-2582.

Derringer G (1989), Model For Service Life of PE Pipe Exhibiting Ductile-Brittle Transition in Failure Mode, J. Applied Polymer Science, Vol.37, 215-224.

deVries J, Haak L, Prater T, Kaberline S, Gerlock J and Chakel J (1994), Characterisation of Interfacial Chemistries Associated With Polymer Systems By Spatially Resolved Surface Analytical Methodologies, Progress in Organic Coatings, Vol.25, 95-108.

Dimov A and Islam M (1990), Preparation Conditions Affecting The Permeability of PE Microfilteration Membranes, Vol.52, 109-113.

Edward G (1986), Crystallinity of LLDPE and of Blends With HDPE, British Polymer Journal, Vol.18, 88-93.

Egan B and Delatycki O (1995), The Morphology, Chain Structure and Fracture Behaviour of HDPE, Journal of Materials Science, Vol.30, 3307-3318.

ElLaithy W (1997), World's First 4.5 Inch Coiled Tubing Pipeline, Society of Petroleum Engineers (SPE) Richardson, TX, USA, Proceeding of the Middle East Oil Show, Vol.2, 121-126.

Elkoun S, GaucherMiri V and Seguela R (1997), Plastic Behaviour of Homogeneous Ethylene Copolymer From the Metallocene Technology, Polymeric Materials Science and Engineering, Proceeding of the ACS Division, Vol.76, 164.

Eltex product data, Solvay & Cie product data sheet.

Fisch M (1991), in "Modern Plastics Encyclopedia 91", 161.

Foldes N (1993), Transport of Small Molecules in Polyolefins. II Diffusion and Solubility of Irganox 1076 in Ethylene Polymers, Journal of Applied Polymer Science, Vol.48, 1905-1913.

Frank H (1977), Some Oxidation Characteristics of Polypropylene, Journal of Polymer Science, Polymer Symposia, 1976, 311-318.

Gandek T, Hatton T and Reid R (1989), Batch Extraction With Reaction: Phenolic Antioxidant Migration From Polyolefins To Water. 1. Theory, Industrial and Engineering Chemistry Research, J, 1030-1036.

Gebler H (1989), Long-Term Behaviour and Ageing of PE-HD Pipes, Kunststoffe - German Plastics, Vol.79, 34-36.

Gedde U, Terselius B and Jansson J (1981), A Survey of Methods For The Detection of Thermal-Oxidation in HDPE Pipes, Polymer Testing, Vol.2, 211-222.

Gedde U, Eklund S and Jansson J (1983), Microscopic Observations Relating Fracture Morphology to Molecular Weight Segregation in Melt-Crystallised Polyethylene, Polymer Bulletin (Berlin), Vol.9, 90-97.

Graham J, Alamo R and Mandelkern L (1997), Effect of Molecular Weight and Crystallite Structure on Yielding in Ethylene Copolymers, Journal of Polymer Science, Part B: Polymer Physics, Vol.35, No.2, 213-223.

Grassie N and Scott G (1985), Polymer Degradation and Stabilisation, Cambridge University Press, Cambridge.

Greaves D (1983), Evaluation of The Effects of Temperature Changes on Internal Pressure When Pressure Testing Pipe Systems, 38th Annual Conference Reinforced Plastics/Composites, Institute, Society of plastic Industry, RP/C 83:Composite, 4.

Greig J (1988), The Possibility of Assessing The Long Term Prformance of PE Pipes Using A Quality Control Fatigue Test, Presented at the 7th International Conference on Plastic Pipes, Bath, 14/1.

Greig J (1994), PE pipe in the British gas distribution system, Plastic, Rubber and Composites Processing and application, Vol.21, 133-140.

Groff I, Franzese R, Landro L, Pagano M and Genoni M (1996), Characterization of Polypropylene Pipes During Accelerated Aging in Air and Water, Polymer Testing, Vol.15, 347-361.

Grzybowski S and Zubielik P and Kuffel E (1986), Structure Changes in PE Cable Insulation Caused By The Thermal Aging, IEEE International Symposium on Electrical Insulation, Washington, 179-182.

Gugumus F (1994), Critical Stabilizer Concentrations in Oxidizing Polymers, Polymer Degradation and Stability, Vol.46, 123-140.

Gugumus F (1995), Re-examination of The Role of Hydroperoxides in PE and PP: Chemical and Physical Aspects of Hydroperoxides in PE, Polymer Degradation and Stability, Vol.49, 29-50.

Hall M, James and Watkinson K (1978), Process History Links With Thermoplastic Product Performance, SPE Annual Conference, 36th, Pap, Washington, DC, 369-372.

Hagemann H, Snyder R, Peacook A and Mandelkern L (1989), Quantitative Infrared Methods for the Measurement of Crystallinity and its Temperature Dependence: PE, Macromolecules, Vol.22, 3600-3603.

Han J, Miltz J, Harte B and Giacin J (1987), Loss of 2-Tertiary-Butyl-4-Methoxy Phenol (BHA) From HDPE Film, Polymer Engineering and Science, Vol.27, 934.

Hashemi S and Williams J (1986), Fracture Characterazation of Tough Polymers Using The J Method, Polymer Engineering and Science, Vol.26, 760-767.

Howard J (1973), DTA for Control of Stability in Polyolefin Wire and Cable Compounds, Polymer Engineering and Science, Vol.13, 429-434.

Hayashi H and Matsuzawa S (1993), Vaporization Behavior of Antioxidant Additives BHT in Polypropylene By Heating, Journal of Applied Polymer Science, Vol.49, 1825-1833.

Hendra P (1991), Passingham C and Jones SA, The Effect of Cold Treatment on the Relaxation of Low Density PE, European Polymer Journal, Vol.27, 127-134.

Hodgkinson J and Williams J (1983), Deformation Yield and Fracture of Polymers, 351.

Hogan J (1983), Catalysis of The Phillips Petroleum Company, Appl. Ind. Catal., Vol.2, 149-176.

Huang Y and Brown N (1992), Slow Crack Growth in Blends of HDPE and UHMWPE, Polymer, Vol.22, 2989.

Jaafar H and Fernando G (1995), Integrity Assessment of Buried Polyethylene Pipes, Materials Ageing And Component Life Extension Conference, Milan, Italy, 1995.

Jaafar H and Fernando G (1996), Fatigue Fracture Behaviour Of Single Edge Notched Specimens Prepared from Polyethylene Pipes, ECF 11- Mechanism And Mechanics Of Damage And Failure Conference, Poitiers-Futuroscope, France, 1996.

Kadota K, Chudnovsky A, Strebel J and Moet A (1991), Fractographic Analysis of Fatigue Fracture in Polyethylene, in Search of Excellence Annual Technical Conference, ANTEC 91, Vol.3, 2180-2182.

Kadota K, Chum S and Chudnovsky A (1993), Bridging The Polyethylene Lifetime Under Fatigue and Creep Conditions With its Crystallization Behavior, Journal of Applied Polymer Science, Vol.49, 863-875.

Kanninen M, Odonoghue P, Popelar C and Kenner V (1990), A Viscoelastic Fracture-Mechanics Assessment of Slow Crack-Growth in Polyethylene Gas-Distribution Pipe Materials, Engineering Fracture Mechanics, Vol.36, 903-918.

Karlsson K, Assargren C and Gedde U (1990), Thermal Analysis for the Assessment of Antioxidant Content in PE, Polymer Testing, Vol. 9, 421-431.

Kasakevich M, Moet A and Chudnovsky A (1990), Comparative Crack Layer Analysis of Fatigue and Creep Crack-Propagation in HDPE, Polymer, Vol.31, 435-439.

Kennedy_MA, Peacock_AJ, Mandelkern_L (1994), Tensile Properties of Cystalline Polymers: linear polyethylene, Macromolecules, Vol.27, No.19, 5297-5310.

Kim S, Janiszewski J, Skibo M, Manson J and Hertzberg R (1977), Effect of Molecular Weight Distribution on Fatigue Crack Propagation in Polymers, American Chemical Society, Division of Organic Coatings and Plastics Chemistry, Preprints, Vol.38, 317-321.

Kline D and Hansen D (1970), Thermal Conductivity of Polymers, in P. E. Slade, Jr and Jenkins LT (Eds) Thermal Characterization Techniques, Ch. 5, Dekker, New York.

Konar J and Ghosh R (1988), Oxidative Degradation of PE in the Presence of Phase Transfer Catalyst: Part 1 - Infrared Studies, Polymer Degradation and Stability, Vol.21, 263-275.

Korolyov V and Marugin A (1996), Laser Infrared Spectroscopy System for Water Vapour Concentration Control, Proceedings of SPIE - The International Society For Optical Engineering, Vol. 2713, 481-484.

Kryzhanovskii A and Pvanchev S (1990), Synthesis of Linear PE on Supported Ziegler-Natta Catalysts. Review, Polymer Science USSR, Vol.32, 1312-1329.

Kurian J, Chaki T, Nando G and De S (1989), Scanning Electron-Microscope Studies on Tension Fatigue Failure of HDPE filled Natural-Rubber Vulcanizate, International Journal of Fatigue, Vol.11, 129-133.

Kurtz SM, Jewett C, Moalli J, Vogt R and Edidln A (1997), True Ultimate stresses and Fracture Morphology of UHMWPE Upon Tensile Failure, Proceedings of the 1997 Bioengineering Conference, Sunriver, OR, USA, Jun 11-15 1997, American Society of Mechanical Engineers, Bioengineering Division (Publication) BED, 1997, Vol.35, 57-58.

Lassiaz M, Pouyet J and Verdu J (1994), Effect of Photochemical Ageing on The Tensile Properties and Behaviour Law of Unstabilized Film of LDPE, J. of Materials Science, Vol.29, 2177-2181.

Lawrence C and Sumner C (1989), Introduction of Fatigue Loading Into The Routine Testing of Polyethylene Gas Pipe Systems, Fatigue and Fracture of Engineering Materials and Structures, Vol.12, 439-446.

Long Y, Shanks R and Stachuesk Z (1995), Kinetics of Polymer Crystallisation, Progress in Polymer Science, Vol.20, 651-701.

Lu X and Brown N (1990), Transition From Ductile To Slow Crack Growth in A Copolymer of PE, J. of Materials Science, Vol.25, 411-416.

Lu X, Mcghie A and Brown N (1993), The Dependence of Slow Crack Growth in A Linear PE on Test Temperature and Morphology, Journal of Polymer Science: Part B: Polymer Physics, Vol.31, 767-772.

Lu X, Zhou Z and Brown N (1994), The Anisotropy of Slow Crack Growth in PE Pipes, Polymer Engineering and Science, Vol.34, 109.

Lu X, Qian R and Brown N (1995), The Effect of Crystallinity on Fracture and Yielding of PE, Polymer, Vol.36, 4239-4242.

Lustiger A (1983), Analysis of Field Failures Caused By Slow Crack Growth, Proceedings of 8th Plastic Fuel Gas Pipe Symposium.

Lustiger A (1995), Analysis of Field Failure in PE Pipes, ANTEC 95, Vol.3, 3946.

Lustiger A (1996), Understanding Environmental Stress Cracking in Polyethylene, Technical Papers, Regional Technical Conference - Society of Plastics Engineers, Proceedings of the 1996 Society of Plastics Engineers (SPE) Medical Plastics Division, Anaheim, CA, USA, Feb 7, 1-10.

Luston J, Pastusakova V and Vass F (1993), Volatility of Additives From Plymers. Concentration Dependence and Crystallinity Effects, J. of Applied Polymer Science, Vol.48, 219-224.

MacKay G and Pachuta S (1996), Characterisation of Additives and Primers on Polymer Surfaces Using Time-of-Flight Secondary Ion Mass Spectroscopy, Polymer Preprints, Division of Polymer Chemistry, American Chemical Society, Vol.37, 299-300.

Maddams W and Parker S (1989), Vibrational Spectroscopy of The Oxidation of PE I. Fourier Self-Deconvolution of Carbonyl Absorption, Journal of Polymer Science: Part B: Polymer Physics, Vol.27, 1691-1698.

Malaika S, Goonetileka M and Scott G (1991), Migration of 4-Substituted 2-Hydroxy Benzophenones in LDPE: Part I-Diffusion Characteristics, Vol.32, 231-247.

Malik J (1992), Diffusion of Hindered Amine Light Stabilizers in LDPE and Isotactic PP, Polymer Degradation and Stability, Vol.35, 61-66.

Malik J, Stoll K, Cabaton D and Thurmer A (1995), Processing Stabilization of HDPE: A Complete Study of An Additive Package, Polymer Degradation and Stability, Vol.50, 329-336.

Mamoun M (1995), New PE pipe technologies available now and technologies on the horizon, Proceeding of the American Gas Association operating section, Las Vegas, NV, USA, 484-498.

Mandelkern L (1986), The Enthalpy of Fusion of Linear PE, Journal of Physical Chemistry, Vol.72, 309-318.

Mandelkern L, Kennedy M and Peacock AJ (1991), Influence of Microstructure on the Tensile Properties of Crystalline Polymers: An Overview, Annual Technical Conference, ANTEC - Conference Proceedings, 49th Annual Technical Conference -ANTEC '91, Montreal, Que, Can, 05-09 May, Vol.37., 1542.

Marshall G, Hepburn and Gosgrove B (1995), Development of Toughness in Butt Fusion Welds For PE Pressure Pipes, Progress in Rubber and Plastics Technology, Vol.11, 193-210.

Mathot V and Pijpers M (1983), Heat-capacity, Enthalpy and Crystallinity For A Linear PE Obtained By DSC, Journal of Thermal Analysis, Vol.28, 349-358.

McMahon E (1981), Tree Growth Inhibiting Insulation For Power Cable, IEEE Transaction on Electrical Insulation, Vol.EI-16, 304-318.

Moison J (1985), in "Polymer Permeability", Ed. by Comyn J, Elsevier Applied Science, London and New York, 119.

Moller K and Thomas G (1994), An FTIR Solid-State Analysis of the Diffusion of Hindered Phenols in LDPE: The Effect of molecular Size on The Diffusion Coefficient, Vol.51, 895-903.

Monserrat S and Cortes P (1995), Physical Ageing Studies in Semicrystalline Polymers, J. of Materials Science, Vol.30, 1790-1793.

Msuya W and Yue C (1989), The Correlation Between The Lamellar Thickness and The Degree of Crystallinity in Semicrystalline Polymers, J. of Materials Science Letters, Vol.8, 1266-1268.

Munteanu D, Tincul I and Chirila (1981), Stabilization of Polyolefins By Grafting, Materiale Plastice, Elastomeri, Fibre Sintetice, Vol.18, 147-154.

Mruk S (1985), Validating The Hydrostatic Design Basis of Piping Materials, Proceeding of 9th Plastic Fuel Gas Pipe Symposium.

Narisawa I (1987), Fracture and Toughness of Crystalline Polymer Solids, Polymer Engineering Science, Vol.27, 41.

Nichols M and Robertson R (1992), The Origin of Multiple Melting Endotherms in the Thermal Analysis of Polymers, J. of Polymer Science: Part B: Polymer Physics, Vol.30, 305-3-7.

Nimmer R and Woods J (1991), Investigation of Brittle Failure in Ductile, Notch-sensitive Thermoplastics, American Society of Mechanical Engineers, Materials Division, ASME, New York, NY, USA, Vol.29., 129-148.

Norman S, Moore L and Marshall G , Vasiliou C and Kotecha J (1990), Diffusion and Extractability Characteristics of Antioxidants in Blue PE Water Pipe: A DSC and Radiolabelling Study, Polymer Degradation and Stability, Vol.27, 145-157.

Nunes R, Martin J and Johnson J (1982), Influence of Molecular Weight and Molecular Weight Distribution on Mechanical Properties of Polymers, Polymer Engineering and Science, Vol.22, 205-228.

Ogita T, Yamamoto R, Suzuki N, Ozaki F and Matsuo M, (1991), Molecular-Weight dependence of morphology and Mechanical Properties of Ultrahigh-Molecular-Weight Polyethylene gel films, Polymer, Vol.32, No.5, 822-834.

Okada T and Mandelkern L (1967), J. of Polymer Science: Part A-2, Vol.5, 239-262.

Pages P, Carrasco F, Saurina J and Colom X (1996), FTIR and DSC Study of HDPE Structural Changes and Mechanical Properties Variation When Exposed To Weathering Aging During Canadian Winter, J. of Applied Polymer Science, Vol.60, 153-159.

Parmer R and Bowman J (1989), Crack Initiation and Propagation Paths For Brittle Failures in Aligned and Misaligned Pipe Butt Fusion Joints, Polymer Engineering Science, Vol.29, 1396-1405.

Pascaud R, Evans W and McCullagh P (1997), Critical Assessment of Methods for Evaluating J1c for a Medical Grade Ultra High Molecular Weight PE, Polymer Engineering and Science, Vol.37, 11-17.

Phillips P and Vatansever A (1989), Crystallinity in Chemically Crosslinked LDPE. 5. Annealing Behaviour of XLPE-2, Polymer, Vol.30, 710-717.

Pecorini J and Hertzberg W (1993), Fracture Toughness and Fatigue Crack Propagation Behaviour of Annealed PET, Polymer, Vol.34, No.24, 5053-5062.

Platzer N (1983), Branched PE: LDPE & HDPE, Industrial and Engineering Chemistry, Product Research and Development, Vol.22, 158-160.

Popelar C, Kenner V and Wooster J (1991), An Accelerated Method For Establishing The Long-Term Performance of Polyethylene Gas Pipe Materials, Polymer Engineering and Science, Vol.31, 1693-1700.

Prasad K and Grubb DT (1989), Direct Observation of Taut Tie Molecules in HDPE Fibres By Raman Spectroscopy, Vol.27, 381-403.

Qayyum M and White J (1993), Effect of Stabilizers on Residual-Stresses in Weathered Polyethylene, Polymer Degradation and Stability, Vol.39, 199-205.

Ranby B and Rabek J (1975), Photodegradation, Photooxidation and Photostabilization of Polymers, Wiley, London.

Read B, Tomlins P and Dean G (1990), Physical Ageing and Short-Term Creep in Amorphous and Semi-Crystalline Polymers, Polymer, Vol.31, 1204.

Reynolds P and Lawrence C (1993), Mechanisms of Deformation in The Fatigue of PE pipe, J. of Materials Science, Vol.28, 227-2282.

BP Rigidex product data sheet.

Rueda D and Salazar J (1984), Lamellar Diffusion During Heat Treatment in Melt-Crystallized LDPE, J. of Polymer Science: Polymer Physics Edition, Vol.22, 1811-1820.

Rugg F, Smith J, and Bacon R (1954), Journal of Polymer Science, Vol.13, 535.

Runt J and Jacq M (1989), Effect of Cystalline Morphology on Fatigue Crack Propagation in Polyethylene, Journal of Materials Science, Vol.24, No.4, 1421-1428.

Saunders K (1988), Organic Polymer Chemistry, Chapman and Hall, New York, Second Edition, 53.

Scheirs J (1991), Effect of Thermal Oxidation on The Spherulitic Morphology of HDPE, Journal of Polymer Science: Part B: Polymer Physics, Vol.29, 795-804.

Scheirs J, Delatycki O, Bigger S and Billingham N (1991), Staining Techniques For Detecting Localized Oxidation in HDPE Powders and Films, Vol.26, 187-193.

Sebaa M, Servens C and Pouyet J (1992), Natural and Artificial Weathering of LDPE. Calorimetric Analysis, J. of Applied Polymer Science, Vol.45, 1049-1053.

Sehanobish K, Patel R, Croft B, Chum S and Kao C (1994), Effect of Chain Microstructure on Modulus of Olefin Copolymers, Journal of Applied Polymer Science, Vol.51, 887-894.

Severini F, Gallo R, Ipsale S and Del Fanti N (1986), Polymer Degradation and Stability, Vol.14, 341.

Shlyapnikov Yand Torsueva E (1992), Oxidation of Atactic Polypropylene in The Presence of 2,6-di-tert-butyl-4-phenylphenol, polymer Degradation and Stabilisation, Vol.49, 361-364.

Showaib E, Moet A and Sehanobish K, (1995) Effect of Short Chain Branching on The Viscoelastic Behaviour During Fatigue Fracture of MDPE, Polymer Engineering Science, Vol.35, 786-793.

Smith G, Karlsson K and Gedde U (1992), Modeling of Antioxidant Loss From Polyolefins in Hot Water Applications. 1. Model and Application To MDPE Pipes, Vol.32, 658-667.

Stafford T (1994), The British Gas distribution system, Gas Engineering & Management, Vol.34, 257-263.

Strebel J and Moet A (1991), Accelerated Fatigue Fracture Mechanism of Medium Density Polyethylene Pipe Material, Journal of Materials Science, Vol.26 No.20, 5671-5680.

Strebel J and Moet A (1992 (a)), Accelerated Fatigue Fracture of Polyethylene Pipe Material - Crack, International Journal of Fracture, Vol.54, 21-34.

Strebel J and Moet A (1992 (b)), Determining Fracture Toughness of Polyethylene From Fatigue, J. of Materials Science, Vol.27, 2981-2988.

Strebel J and Moet A (1992 (c)), Time dependent Fracture Toughness Measurement For PE, American Society of Mechanical Engineering, AMD, Vol.155, 61-69.

Strebel JJ and Moet A (1993), Plane Strain and Plane Stress Analysis of Fatigue Crack Propagation in Medium Density Polyethylene Pipe Materials, Polymer Engineering and Science, Vol.33, 217.

Struik L (1978), Physical Ageing in Amorphous Polymers and Other Materials, Elsevier, Oxford.

Struik L (1987 (a)), The Mechanical and Physical Ageing of Semicrystalline Polymers:1., Polymer, Vol.28, 1521.

Struik L (1987 (b)), The Mechanical and Physical Ageing of Semicrystalline Polymers:2., Polymer, Vol.28, 1534.

Struik L (1989 (a)), The Mechanical and Physical Ageing of Semicrystalline Polymers:3. Prediction of Long Term Creep From Short Time Tests, Polymer, Vol.30, 799.

Struik L (1989 (b)), The Mechanical and Physical Ageing of Semicrystalline Polymers:4., Polymer, Vol.30, 815.

Sugiura M, Horri M, Hayashi H and Sasayama M (1996), Application of Sepiolite To Prevent Bleeding and Blooming For EPDM Rubber Composition, Applied Clay Science, Vol.11, 89-97.

Swei H, Crist B and Carr S (1991), J Integral Fracture Toughness and Damage Zone Morphology in PE, Vol.32, 1440-1446.

Tatarenko L (1992), The Processes Running During The Induction Period of Inhibiting Oxidation of Polyethylene, Intermolecular Journal of Polymeric Material, Vol.16, 45-54.

Terselius B, Gedde U and Jansson J (1982), Structure and Morphology of Thermally Oxidized HDPE Pipes, Polymer Engineering and Science, Vol.22, 422.

Tidjani A Arnaud R (1993), Photo-oxidation of LLDPE: A Comparison of Photoproducts Formation Under Natural and Accelerated Exposure, Polymer Degradation and Stability, Vol.39, 285-292.

Tincer T, Cimen F and Akay G (1981), Plast. and Rubber Inst., London, Engl., International Conference, Radiation Processing For Plastics and Rubber, Brighton, Sussex, Eng., Vol.1, 33.

Tochacek J and Sedlar J (1993), Effect of Hydrolysability and Structural Features of Phosphite on processing Stability of Isotactic PP, Polymer Degradation and Stability, Vol. 41, 177-184.

Torikai A, Takeuchi A, Nagaya S and Fueki K (1986), Photodegradation of PE: Effect of Crosslinking on The Oxygenated Products and Mechanical Properties, Polymer Photochemistry, Vol.7, 199.

Trankner T, Hedenqvist M and Gedde U (1997), Structure and Strength of A PE Pipe Grade Containing Glass Spheres and Low-Molar_Mass Linear PE, Polymer Engineering Science, Vol.37, 346-354.

Viebke J, Hedenqvist M and Gedde U (1996), Antioxidant Efficiency Loss By Precipitation and Diffusion to Surrounding Media in PE Hot-Water Pipes, Polymer Engineering and Science, Vol.36, 2896-2904.

Vile J, Hendra P and Cudby M (1984), Chain Branching in High Pressure Polymerized PE:2, Polymer, Vol.18, 1173.

Wedgewood A and Seferis J (1983), Structural Characterization of Linear PE By Infrared Spectroscopy, Pure and Applied Chemistry, Vol.55, 873-892.

Weiland M, Daro A and David C (1995), Biodegradation of Thermally Oxidized PE, Polymer Degradation and Stability, Vol.48, 275-289.

Welker R (1996), How To Minimize Gas Piping Turbulence, Gas Industries, Park Ride, Illinois, Vol.40, 3.

Williams J and Osorio A (1981), Model of Fatigue Threshold Effects in Polymers and its Application to Pipe Failure, Fatigue Thresholds, Fundamentals and Engineering Applications, Proceeding of an International Conference, Stockholm, Swed., Vol2., 763-690.

Williams J and Hodgkinson J, (1981) The Determination of Residual Stresses in Plastic Pipe and Their Role in Fracture, Polymer Engineering and Science, Vol.21, 822.

Williams J (1987), Fracture Mechanics of Polymers, Ellis Horwood Ldt., Chichester, England, 2nd Edition.

Wlochowicz A and Eder M (1984), Distribution of Lamella Thickness in Isothermally Crystallized PP and PE by DSC, Polymer, Vol.25, 1268.

Woo L, Ling M and Chan E (1991), Applications of The Oxidative Induction Test To Medical Polymers, ANTEC 91, Vol.3, 1837-1840.

Yeh J and Lin Y (1993), Effect of Notching speed on Dynamic Fatigue Behavior of Polyethylene Terephthalate Polymers, Journal of Materials Science, Vol.28, No.14, 3900-3910.

Yeh J, Chen C and Hong H (1994), Static Fatigue Behaviour of LLDPEs, J. of Materials Science, Vol.29, 4104-4112.

Young J (1989), Introduction To Polymers, Chapman and Hall, London.

Yue C and Msuya W (1990), Changes in Yield in PP of Different Morphology caused by Physical Ageing, J. of Materials Science Letters, Vol.9, 985-988.

Zhou Y and Brown N (1995), Anomalous Fracture Behaviour in PE Under Fatigue and Constant Load, J. of Materials Science, Vol.30, 6065.

Zhou Y, Lu X, Zhou Z and Brown N (1996), Relative Influence of Molecular Structure on Brittle Fracture by Fatigue and Under Constant Load in PEs, Polymer Engineering and Science, Vol.36, 2101-2107.

APPENDIX 1

The design diagram of the custom-made pipe cutting machine.

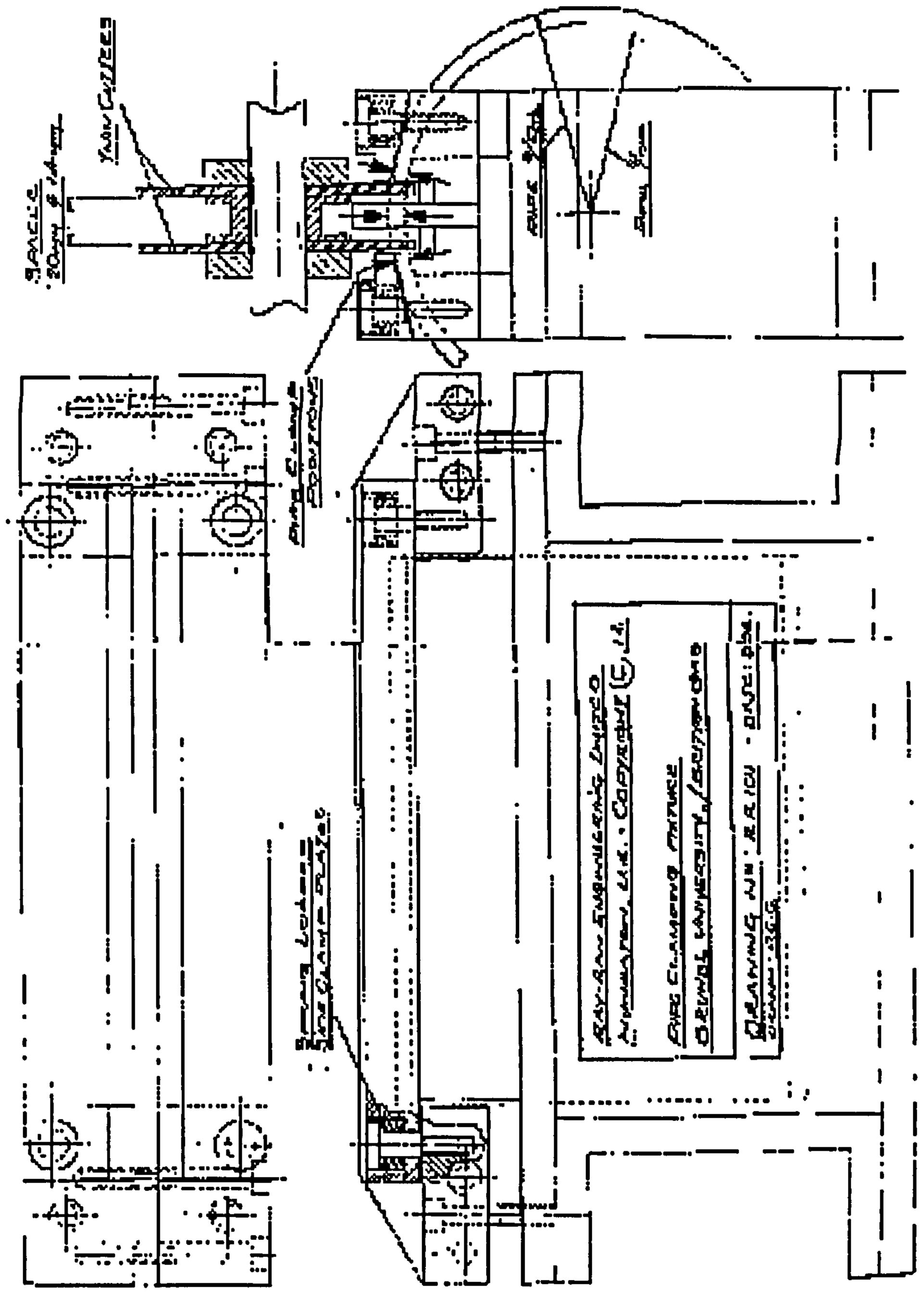

APPENDIX 2

A spectroscopic method was developed to obtain characteristic absorption frequencies for different gas grade PE resins to enable identification. This was necessary because some pipes obtained from site did not always exhibit legible identification marks and visual inspection was not enough. FTIR spectrum for gas grade Neste, Fina, Repsol and BP Rigidex polymers are presented:

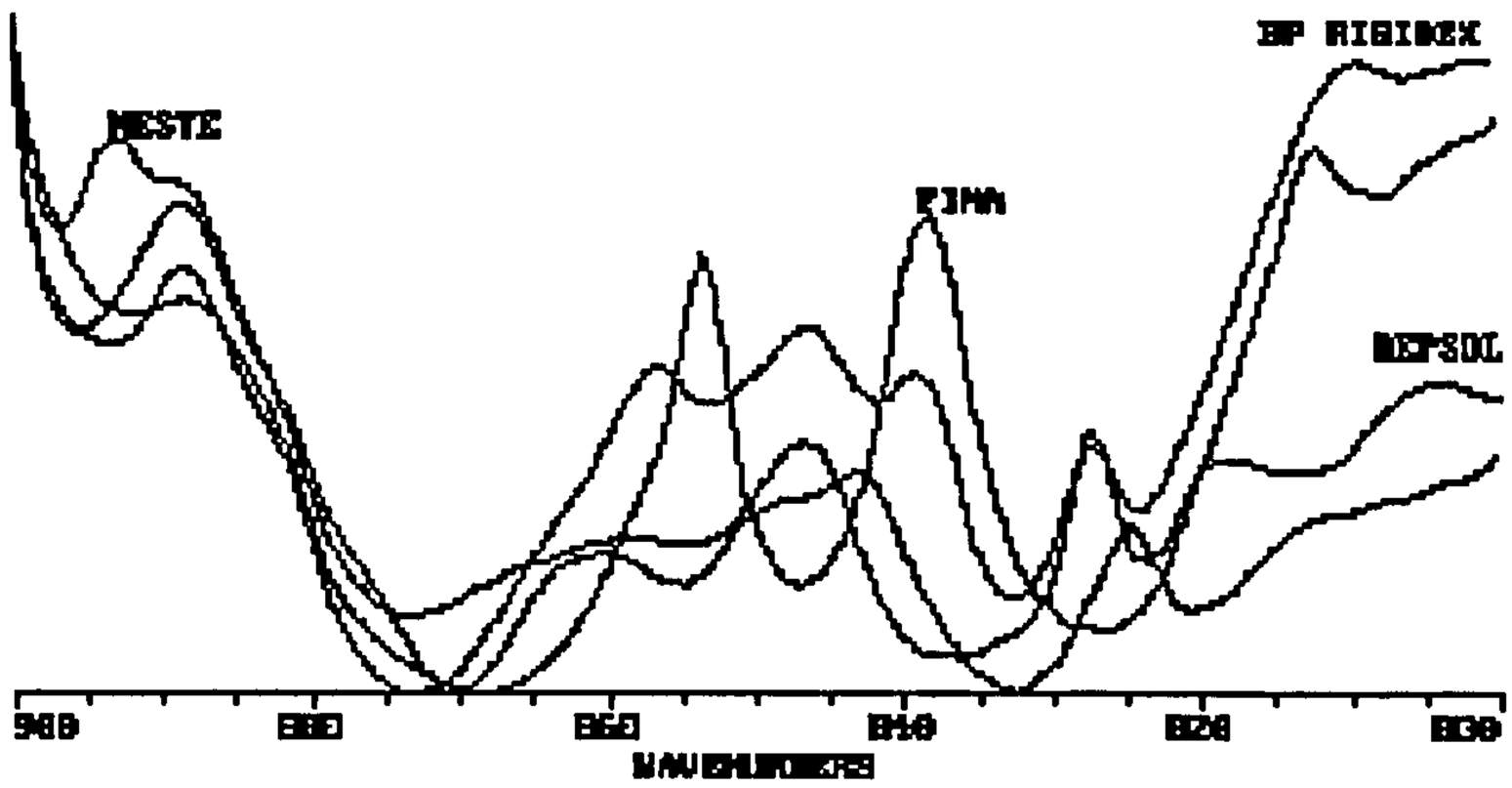

The FTIR spectrum from 900-800 cm^{-1} wavenumbers for gas grade PE manufacture by Neste, Fina, Repsol, British Petroleum.

Although gas grade Neste, Fina, Repsol and BP Rigidex polymers are all resins manufactured employing the Phillips processes, there were significant differences found in the infrared spectrum in the region of 900-800 cm^{-1}. These differences were attributed to the silica-bed composition for different PE manufacturers. Residues in the Phillips process are kept in the resin and not removed.

APPENDIX 3

Index of peak assignments reported in the literature, relevant to PE in different densities.

Vibration	Wavenumber (cm^{-1})
Silica	470
CH_2 rocking amorphous	720
methylene rocking crystalline	722-730
Silica	800
epoxy in the side chain	830
C-H wagging	850-1000
unsaturated vinylidene	890
butyl branches	893
terminal vinyl $-CH=CH_2$	908
vinyls	909
vinyl (hydrocarbon structure)	910, 920
acids	935
trans-vinylene	965
trans-vinylene	990
C-O-C ether	1000-1220
esters, lactones, alcohols	1046
trans-back bone twist$(-CH_2-)_n$ crystalline	1050
oxygenated compounds	1070
CH_2 wagging adjacent to gauche bonds	1078
alcoholic structures, C-O-C	1080
silica SiO_2, lactones	1118
CH_2 rocking	1168
CH_2 wagging crystalline	1176
C-O vibrations in the ester structures	1180
phenol	1180-1295
amorphous CH_2 twisting	1303
amorphous CH_2 torsion	1303-1352
P=O	1320
amorphous CH_2 wagging	1352
amorphous CH_2 wagging	1368
CH_3	1370-1380
carboxylate	1390
CH_2 wagging	1415
methylene scissoring	1420
CH_2 internal standard, C-H deformation	1460
CH_2 deformation	1473
methylene scissoring	1475
carboxylate	1498
conjugated unsaturated groups + COO^-	1520-1680
carboxylate ion	1570-1680
COOH	1595
benzophenone	1630
vinyls C=C stretch end-group	1640-1660
C=C (-CO-CH=CH-)	1680-1690
unsaturated aldehydes	1680
alcohols	1700
ketones C=O srtreching	1710
C=O (-R-CO-OH)	1710-1715
saturated acids	1712
saturated carboxylic acids	1714

ketones (-R-CO-R-)	1715-1720
saturated ketones	1719-1721
saturated carboxylic acids	1723
C=O (-R-CO-H)	1730-1745
saturated aldehydes	1733
C=O (-R-CO-OR)	1735-1745
ester	1735-1740
C=O (-R-CO-OOR)	1763
g-lactone	1782
C=O (-R-CO-OOH)	1785
CH_2 rocking crystalline	1894
$C=C=CH_2$	1900
CH_2 twisting	2016
internal standard	2018
thiol	2560
C-H stretching	2800-2900
C-H aliphatic	2840-2960
phenolic and alcoholic	3100-3500
internal standard	3220
bonded hydroperoxide	3360
alcohols, free hydroperoxide (OH)	3400-3600
Si-OH	3600
phenolic hydroxyl	3650

APPENDIX 4

DSC traces of the three Rigidex additives.